JOÃO PAULO BATISTA MACHADO

INSIGHTS INTO REGULATORY MECHANISMS OF THE NIK-MEDIATED ANTIVIRAL DEFENSE: NEW COMPONENTS AND THE MOLECULAR BASES OF THE DEFENSE

Tese apresentada à Universidade Federal de Viçosa, como parte das exigências do Programa de Pós-Graduação em Bioquímica Aplicada, para obtenção do título de *Doctor Scientiae*.

VIÇOSA
MINAS GERAIS – BRASIL
2015

Ficha catalográfica preparada pela Biblioteca Central da Universidade Federal de Viçosa - Câmpus Viçosa

T
M149i
2015

Machado, João Paulo Batista, 1984-
Insights into regulatory mechanisms of the NIK-mediated antiviral defense : new components and the molecular bases of the defense / João Paulo Batista Machado. – Viçosa, MG, 2015.
x, 189f. : il. (algumas color.) ; 29 cm.

Inclui anexos.
Orientador: Elizabeth Pacheco Batista Fontes.
Tese (doutorado) - Universidade Federal de Viçosa.
Inclui bibliografia.

1. *NSP- Interacting Kinase*. 2. Vírus de plantas. 3. Biologia molecular. 4. Geminivírus - Análise de infectividade. 5. Plantas - Interação de proteína. I. Universidade Federal de Viçosa. Departamento de Bioquímica e Biologia Molecular. Programa de Pós-graduação em Bioquímica aplicada. II. Título.

CDD 22. ed. 572.8

JOÃO PAULO BATISTA MACHADO

INSIGHTS INTO REGULATORY MECHANISMS OF THE NIK-MEDIATED ANTIVIRAL DEFENSE: NEW COMPONENTS AND THE MOLECULAR BASES OF THE DEFENSE

Tese apresentada à Universidade Federal de Viçosa, como parte das exigências do Programa de Pós-Graduação em Bioquímica Aplicada, para obtenção do título de *Doctor Scientiae*.

APROVADA: 20 de julho de 2015.

Marcia Flores da Silva Ferreira	Poliane Alfenas Zerbini
Pedro Augusto Braga dos Reis	Maximiller Dal-Bianco Lamas Costa (Coorientador)

Elizabeth Pacheco Batista Fontes
(Orientadora)

Aos meus amados pais Antonio e
Maria Lucia, aos meus irmãos
Elisangela, Edilâine e Marco Antônio,
e a minha querida sobrinha Estela

DEDICO

AGRADECIMENTOS

Agradeço a Deus, por ter me dado força e perseverança e guiado meus passos para chegar até aqui, por providenciar tudo que sou e que tenho, e por me ensinar a reconhecer, nas coisas simples do dia-a-dia, sua providência divina.

Aos meus pais Antonio e Maria Lucia, meus exemplos de vida. Posso estudar a vida inteira que nunca terei a sabedoria de vocês! Agradeço por sempre me apoiarem e acreditarem em mim. Agradeço também por não cessarem de rezar e interceder por mim. A oração de vocês me fez forte principalmente nos momentos em que o desânimo me fazia fraco.

Aos meus irmãos Elisangela, Edilâine e Marco Antônio, por me incentivarem em cada nova etapa da minha vida. Tenho muito orgulho de vocês!

À professora Elizabeth, exemplo de dedicação e competência profissional, pela orientação e pelas inúmeras oportunidades de aprendizado oferecidas durante estes nove anos que passei em seu laboratório. Agradeço também pela oportunidade de desenvolver este projeto, que permitiu meu crescimento profissional, e por permitir que em seu laboratório eu pudesse dar os primeiros passos na pesquisa.

À Universidade Federal de Viçosa, por todas as oportunidades de estudo oferecidas durante toda minha vida acadêmica.

Ao Conselho Nacional de Desenvolvimento Científico e Tecnológico (CNPq) pelo apoio financeiro.

À minha namorada Analice, pela companhia, parceria, amizade, apoio e compreensão em todos os momentos, principalmente nesta fase final da minha tese. Agradeço pelos valiosos conselhos que sempre vinham em momentos oportunos.

Aos amigos Pedro, Pato, Claudinha, Priscila, Maiana, Cris, Lucas, Giselle, Iara, Bianca, Janaína, por me incentivarem durante todos os momentos. Obrigado

por aturarem minhas reclamações, minha chatice e meu mau humor, e por todos os momentos divertidos que passamos durante este tempo.

Ao estudante de iniciação científica Marcos, que além de um estagiário, foi um amigo. Agradeço por toda ajuda na condução dos experimentos realizados nos primeiros anos do meu doutorado.

Aos integrantes do Laboratório de Biologia Molecular de Plantas, os antigos e os atuais, pela prazerosa convivência durante estes anos e por tornarem cada dia de trabalho uma oportunidade única de aprendizado.

À Marlene, à Gláucia e ao Eduardo, pela presteza.

E a todos que passaram pela minha vida durante a realização deste trabalho e que deixaram sua contribuição para a concretização do mesmo.

ÍNDICE

RESUMO

MACHADO, João Paulo Batista, D.Sc., Universidade Federal de Viçosa, julho de 2015. **Introspecções sobre os mecanismos regulatórios da via de sinalização antiviral mediada por NIK: novos componentes e bases moleculares da defesa**. Orientadora: Elizabeth Pacheco Batista Fontes. Coorientadores: Anésia Aparecida dos Santos e Maximiller Dal-Bianco Lamas Costa.

A proteína NIK (*NSP-interacting kinase*), identificada por interagir com a proteína NSP (*nuclear shuttle protein*) de geminivírus, apresenta características estruturais, bioquímicas e biológicas condizentes com um autêntico receptor cinase envolvido na resposta de defesa à infecção por geminivírus. A ativação deste receptor imune resulta na fosforilação da proteína ribossomal L10 (RPL10) e na subsequente relocação nuclear desta proteína ribossomal. Apesar dos avanços obtidos com a identificação de RPL10, outras conexões moleculares que ligam a ativação de NIK à resposta antiviral ainda são desconhecidas, bem como a natureza deste mecanismo de defesa. Nesta investigação, foi identificado um novo componente efetor *downstream* da via de sinalização mediada por NIK, um fator de transcrição denominado LIMYB (*L10-Interacting Myb domain-containing protein*), isolado pela sua capacidade de interagir com RPL10 pelo sistema de duplo híbrido em leveduras. Ensaios de co-imunoprecipitação e de complementação de fluorescência bimolecular (BiFC) mostraram que o complexo RPL10-LIMYB ocorre estavelmente na planta, mais precisamente no núcleo das células vegetais. Estudos de caracterização funcional mostraram que LIMYB atua como um autêntico fator de transcrição, ligando-se ao promotor e inibindo a expressão de genes de proteínas ribossomais. Estes resultados sugerem que o mecanismo de defesa antiviral mediado por NIK baseia-se na supressão da tradução do hospedeiro. Para examinar esta hipótese, inicialmente foi avaliado os níveis de tradução em linhagens de tomate superexpressando um mutante superativo de *At*NIK1 (T474D). Os resultados mostraram que as linhagens transgênicas apresentaram menor acúmulo de proteínas recentemente sintetizadas quando comparadas com plantas WT. Posteriormente, as linhagens de tomate superexpressando T474D foram infectadas com duas espécies de begomovírus altamente divergentes, ToYSV (*Tomato yellow spot virus*) e ToSRV (*Tomato severe rugose virus*). As linhagens transgênicas apresentaram sintomas atenuados ou foram assintomáticas. Estas observações foram associadas com um atraso na infecção viral, com taxas de infecção menores e com a redução no acúmulo de DNA viral em folhas sistêmicas infectadas. Apesar

do fenótipo de tolerância exibido pelas linhagens superexpressando T474D e dos menores índices de síntese proteica, estas linhagens não apresentaram diferenças no desenvolvimento, no desempenho fisiológico e nas características horticulturais quando comparadas com plantas WT ou com linhagens superexpressando *At*NIK1. Finalmente, foi determinado se a redução nos níveis de tradução global do hospedeiro causado pela superexpressão de T474D poderia prejudicar a síntese de proteínas virais. Para isto, frações polissomais foram isoladas a partir de linhagens WT e T474D infectadas com ToYSV e a presença de mRNA viral foi examinada nestas frações. Os resultados mostraram uma menor associação do mRNA que codifica a proteína do capsídeo viral nas frações de polissomos de linhagens T474D quando comparadas àquelas de linhagens não transformadas. Coletivamente, estes resultados indicam que begomovírus não são capazes de manter altos níveis de tradução de mRNA virais nas linhagens superexpressando o mutante T474D, indicando que a supressão global da síntese de proteínas, identificada nestes genótipos, pode proteger eficientemente as células contra a infecção por estes vírus. Entretanto, estudos da variação global na expressão gênica de plantas *nik1* alelos nulos mostraram que a perda da função de *NIK1* promoveu a indução de componentes do *hub* principal da sinalização a brassinosteróide e de *hubs* envolvidos na sinalização ao ácido salicílico e na imunidade antibacteriana. Estes resultados sugerem que NIK1 pode funcionar como um regulador negativo em vias de sinalização de desenvolvimento e imunidade, apesar de sua propriedade antiviral.

ABSTRACT

MACHADO, João Paulo Batista, D.Sc., Universidade Federal de Viçosa, July, 2015. **Insights into regulatory mechanisms of the NIK-mediated antiviral defense: new components and the molecular bases of the defense**. Adviser: Elizabeth Pacheco Batista Fontes. Co-advisers: Anésia Aparecida dos Santos and Maximiller Dal-Bianco Lamas Costa.

The NSP-interacting kinase (NIK) protein, identified through interaction with the geminivirus nuclear shuttle protein (NSP), displays structural, biochemical and biological characteristics consistent with an authentic receptor kinase involved in defense response against geminivirus infection. The activation of this immune receptor leads to phosphorilation of the ribosomal protein L10 (RPL10) and in the subsequent nuclear relocation of this ribosomal protein. Apart from the identification of RPL10 as a downtream component of the defense signaling, others molecular connections that link the NIK activation to the antiviral response, as well as the nature of this defense mechanism, remain to be determined. In this investigation, a new downstream effector component of the NIK-mediated signaling pathway, a transcription fator designated LIMYB (L10-Interacting Myb domain-containing protein), was identified by its capacity to interact with RPL10 through yeast two-hybrid system. Co-immunoprecipitation and bimolecular fluorescence complementation assays showed that RPL10-LIMYB complex occurs stably in the plant, specifically in the nucleus of plant cells. Functional characterization studies showed that LIMYB acts as an authentic transcription fator, binding to and inhibiting expression of ribosomal protein promoters. These results suggest that NIK-mediated antiviral defense mechanism is based on host translation suppression. To examine this hypothesis, the translation levels in tomato lines overexpressing the constitutively active mutant of *At*NIK1 (T474D) was initially assessed. The results demonstrated that transgenic lines had lower accumulation of newly synthesized proteins when comparated to WT plants. Subsequently, T474D-overexpressing tomato lines were infected with two highly divergent begomovirus species, ToYSV (*Tomato yellow spot virus*) and ToSRV (*Tomato severe rugose virus*). The transgenic lines either displayed attenuated symptons or were asymptomatic. These findings were associated with delay in viral infections, lower infection rates and reduction in viral DNA accumulation in systemically infected leaves. Despite the tolerance phenotype and lower rates of protein synthesis displayed by T474D-overexpressing lines, no difference in the development, physiological performance and horticultural traits was observed

between T474D-overexpressing and WT or *At*NIK1-overexpressing lines. Finally, whether the reduction in overall levels of host translation caused by overexpression of T474D could affect the viral proteins synthesis was examined. For this purpose, polysomal fractions were isolated from WT and T474D lines infected with ToYSV and examined for the presence of viral mRNA. The results showed lower association of mRNA encoding viral capsid protein at the polysomes fractions of T474D lines when comparated to that of untransformed lines. Collectively, these results indicate that begomovirus are not able to maintain high levels of viral mRNA translation into T474D-overexpressing lines, indicating that the global suppression of the protein synthesis identified in these genotypes may efficiently protect cells against infection by these virus. However, studies of global changes in gene expression of *nik1* null alleles revealed that loss of *NIK1* function promoted induction of components of the main brassinosteroid signaling hub and of hubs involved in salicylic acid signaling and antibacterial immunity. These results suggest that NIK1 may function as a negative regulator in development and immunity signaling pathways, despite its antiviral property.

INTRODUÇÃO GERAL

As plantas, devido a sua natureza séssil, estão constantemente submetidas a condições externas adversas, como por exemplo, seca, calor, salinidade, frio, ataque de predadores e infecções por patógenos, que afetam negativamente o seu crescimento e desenvolvimento, resultando em perdas consideráveis na produtividade em condições de campo. Dentre os fatores bióticos, infecções por geminivírus merecem destaque, pois limitam severamente a produção de uma variedade de sistemas de cultivo por todo o mundo. No Brasil, a incidência de doenças causadas por geminivírus em tomateiros tem aumentado drasticamente nas últimas duas décadas, tornando-se uma das principais ameaças para o seu cultivo.

Os métodos convencionais de controle da propagação de geminivírus que se baseiam no combate ao inseto vetor pela utilização de inseticidas têm sido mal-sucedidos em atenuar o impacto da infecção viral. Deste modo, o desenvolvimento de genótipos resistentes por meio de engenharia genética representa um método mais confiável e eficaz no manejo de doenças causadas por estes vírus. Considerando a ocorrência de infecções mistas e as altas taxas de mutação e recombinação que permitem aos geminivírus se adaptarem rapidamente a novos hospedeiros e ambientes, torna-se essencial que as estratégias empregadas tenham caráter geral, capazes de atingir diversos componentes deste grupo viral. Diante disto, um melhor entendimento das interações geminivírus-hospedeiro e seu efeito na infecção viral são cruciais para o desenvolvimento de uma metodologia efetiva no controle da indução de doenças causadas por estes vírus.

Dentro desse contexto, as proteínas NIKs (*NSP-interacting kinase*) de soja, tomate e Arabidopsis foram identificadas por interagir com a proteína NSP (*nuclear shuttle protein*) de diferentes begomovírus, pertencentes ao gênero *Begomovirus* da família *Geminiviridae* (Fontes *et al*., 2004; Mariano *et al*., 2004; Sakamoto *et al*.,

2012). NIKs são proteínas localizadas na membrana plasmática que apresentam uma série de propriedades estruturais, bioquímicas e biológicas características de autênticos receptores Ser/Thr cinase que medeiam a transdução de sinal através da membrana plasmática (Carvalho *et al*., 2008c; Fontes *et al*., 2004, Santos *et al*., 2009). A interação de NSP com a alça de ativação de NIK inibe a sua atividade cinase, e a perda da função do gene *NIK* ou mutações que comprometem a capacidade de autofosforilação deste receptor aumentam a suscetibilidade à infecção por geminivírus (Fontes *et al*., 2004; Santos *et al*., 2009). Por outro lado, a superexpressão de NIK em Arabidopsis ou tomateiros atenua o desenvolvimento de sintomas e atrasa a infecção viral (Carvalho *et al*., 2008c; Fontes *et al*., 2004). Progressos no entendimento molecular que conecta a ativação do receptor imune NIK à resposta antiviral foram obtidos com a identificação da proteína ribossomal L10 (RPL10) como componente *downstream* desta via de sinalização (Rocha *et al*., 2008). A ativação de NIK resulta na fosforilação de RPL10 e no redirecionamento da proteína ribossomal para o núcleo onde pode atuar montando uma resposta de defesa antiviral. Em células infectadas, a localização nuclear de RPL10 mediada por NIK é bloqueada, resultando no acúmulo da proteína ribossomal em corpos puntiformes dispersos no citoplasma (Carvalho *et al*., 2008c). Coletivamente, estes resultados sugerem que NIK esteja envolvida em uma via de resposta de defesa antiviral, e que esta via pode ser um alvo molecular em potencial para conferir tolerância a diferentes begomovírus.

NIK pertence à família de receptores-*like* cinases (RLK) contendo repetições ricas em leucina (LRR) em seu domínio extracelular. Considerando a identidade de sequência, o número de cópias e a disposição dos motivos LRR, as proteínas NIK (NIK1, NIK2 e NIK3) foram classificadas dentro da subfamília LRRII-RLK (Zhang *et al*., 2006). Esta subfamília é composta ainda por proteínas envolvidas no desenvolvimento e defesa, e por proteínas cujas funções são desconhecidas. O membro mais bem estudado desta subfamília é BAK1/AtSERK3 (*BRI1-associated*

kinase 1/*SOMATIC EMBRYOGENESIS RECEPTOR KINASE 3*), que desempenha uma função importante na imunidade inata de plantas contra patógenos, atuando como coreceptor de diversos receptores que reconhecem padrões (PRR) moleculares associados a patógenos (PAMP), induzindo PTI (*PAMP-triggered immunity*). Apesar da similaridade estrutural verificada entre NIK e BAK1, o mecanismo de defesa antiviral mediado por NIK diverge daquele induzido por BAK1, não se encaixando no modelo elicitor-receptor de resistência. Além da sua função na imunidade inata, BAK1 contribui para o desenvolvimento da planta por meio da sua interação com BRI1 (*BRASSINOSTEROID INSENSITIVE 1*), um LRR-RLK que reconhece o fitohôrmonio brassinosteróide. Uma vez que os componentes SERK da subfamília LRRII-RLK são encontrados em associação dependente de estímulo com LRR-RLK que se ligam a ligantes, é razoável pressupor que NIK, por integrar esta subfamília, participe também de outras vias de sinalização mediadas por LRR-RLKs ainda não identificados.

A ativação do receptor imune NIK resulta na indução de uma resposta de defesa antiviral. Apesar do conhecimento obtido com a identificação de RPL10 como membro integrante desta via de sinalização, componentes nucleares efetores *downstream* não foram identificados e diversas lacunas, como a natureza do mecanismo da resposta de defesa, ainda estão presentes. Deste modo, esta investigação teve como objetivo principal a identificação e elucidação da via de sinalização mediada por NIK1 que leva à tolerância a geminivírus. Este objetivo é explorado principalmente no segundo capítulo, cujos resultados apresentados colaboraram para publicações em Nature (Zorzatto *et al*., 2015) e Plant Biotechnology Journal (Brustolini *et al*., 2015) e em cujos manuscritos o autor dessa tese de doutorado compartilha a primeira autoria. O terceiro capítulo, publicado em BioEssays (Machado *et al*., 2015), descreve o estado da arte do mecanismo de sinalização antiviral mediado por NIK, bem como uma possível participação deste receptor como um regulador negativo em vias de sinalização imune e de

desenvolvimento. O primeiro capítulo refere-se a um levantamento bibliográfico sobre geminivírus e suas interações com fatores do hospedeiro, bem como uma revisão sobre sistema imune de plantas.

CAPÍTULO I

REVISÃO DE LITERATURA

Geminivírus

A família *Geminiviridae* constitui um grupo de vírus de plantas de grande importância econômica, pois infectam culturas agronômicas relevantes (Moffat, 1999). Muitas das doenças causadas por estes vírus representam uma ameaça séria para a segurança alimentar de países em desenvolvimento nas regiões tropicais e subtropicais do mundo (Rey *et al*., 2012; Rybicki e Pietersen, 1999). Na América latina, que apresenta uma das maiores diversidades e distribuição de geminivírus transmitidos por mosca branca, a produção de alimentos básicos é altamente afetada (Morales, 2006). A produção de tomate no Brasil é reduzida em até 100% em algumas regiões devido à infecção por geminivírus (Fernandes *et al*., 2008; Ribeiro *et al*., 2003).

Geminivírus são vírus de DNA fita simples (ssDNA) circular, compostos por um ou dois componentes genômicos encapsulados individualmente em uma partícula icosaédrica geminada. Até o momento, sete gêneros foram reconhecidos dentro da família *Geminiviridae*: *Mastrevirus*, *Eragrovirus*, *Becurtovirus*, *Curtovirus, Topocuvirus*, *Turncurtovirus e Begomovirus* (Varsani *et al*., 2014), que podem ser diferenciados de acordo com o tipo de inseto vetor do vírus, gama de hospedeiros (monocotiledôneas ou dicotiledôneas), organização genômica e relacionamento filogenético (Brown *et al*., 2012; Varasani *et al*., 2014). Dentre os gêneros de geminivírus, o *Begomovirus* possui o maior número de representantes e inclui vírus transmitidos pela mosca branca *Bemisia tabaci* para várias espécies de dicotiledôneas (Fauquet *et al*., 2008). Os begomovírus podem ser bipartidos,

possuindo dois componentes genômicos, ou monopartidos, com apenas um componente de DNA, mas com dois genes adicionais, ambos codificando proteínas envolvidas no movimento do vírus (Rojas *et al*., 2001). A maioria dos begomovírus encontrados no Brasil é bipartida, ou seja, possui dois componentes genômicos denominados DNA-A e DNA-B (Ribeiro *et al*., 2003).

Os dois componentes genômicos de begomovírus compartilham pouca identidade de sequência, com exceção de uma região de aproximadamente 200 nucleotídeos com identidade tipicamente maior que 85%, conhecida como região comum (CR; Briddon *et al*., 2010). A CR abriga uma estrutura em grampo, que contém, dentro do *loop*, uma sequência de nove nucleotídeos (TAATATTAC) que define a origem de replicação do DNA, e sequências repetidas (conhecidas como iterons), que são reconhecidas pela proteína viral Rep (*replication-associated protein*) e requeridas para a replicação viral (Argüello-Astorga e Ruiz-Medrano, 2001; Hanley-Bowdoin *et al*., 2000). A CR funciona na manutenção da integridade do genoma dividido, garantindo que a replicação de ambos componentes possa ser iniciada pela proteína Rep (Fontes *et al*., 1994). O reconhecimento por Rep é considerado específico do vírus (Argüello-Astorga *et al*., 1994); no entanto, em alguns casos, a proteína Rep codificada pelo DNA-A de um determinado vírus reconhece o DNA-B de um vírus diferente, resultanto em um fenômeno conhecido como pseudorecombinação (Rojas *et al*., 2005).

O ciclo de replicação de geminivírus inclui um primeiro estágio no qual o DNA genômico fita simples (ssDNA) é convertido a fita dupla (dsDNA), um processo realizado por DNA polimerases do hospedeiro. O dsDNA produzido é transcrito pela RNA polimerase II do hospedeiro, permitindo a síntese da proteína Rep. Esta proteína inicia a replicação viral, que ocorre por uma combinação de replicação por círculo rolante e replicação dependente de recombinação (Jeske *et al*., 2001; Preiss e Jeske, 2003). O ssDNA circular nascente pode ser convertido em dsDNA para

entrar novamente no ciclo de replicação ou pode ser empacotado em vírions, após a síntese da proteína CP (*coat protein*).

Devido ao pequeno tamanho de seu genoma, geminivírus codificam de quatro a oito proteínas, algumas das quais evoluíram para proteínas multifuncionais que, juntamente com a presença de genes sobrepostos, contribuem para a economia genética apresentada por estes vírus (Fondong, 2013). O DNA-A da maioria dos begomovírus contém cinco genes, um na fita de sentido viral (*AV1*) e quatro na fita de sentido complementar (*AC1*, *AC2*, *AC3* e *AC4*), que codificam para as funções requeridas na replicação do DNA viral, no controle da expressão gênica, na supressão das defesas do hospedeiro e na encapsidação (Rojas *et al*., 2005). O gene *AV1* codifica a proteína CP, a única proteína estrutural de geminivírus (Stanley e Gay, 1983). Além do empacotamento do genoma viral, a proteína CP está associada com a transmissão pelo inseto vetor (Briddon *et al*., 1990). Sequências importantes para a transmissão pelo inseto vetor têm sido mapeadas na parte central da proteína CP (Hohnle *et al*., 2001; Noris *et al*., 1998). Além disso, CP interage com a chaperonina GroEL de *Arsenophonus* e *Hamiltonella*, bactérias endossimbiontes encontradas no intestino médio de *B. tabaci*, e com HSP16 (*heat shock protein 16*), codificada pela mosca branca, presumivelmente para proteger os vírions de proteólise rápida na hemolinfa do inseto vetor (Gottlieb *et al*., 2010; Ohnesorge e Bejarano, 2009; Rana *et al*., 2012).

A proteína Rep, codificada pelo gene *AC1*, é conservada em sequência, posição e função (Hanley-Bowdoin *et al*., 2004) e consiste na única proteína essencial para o processo de replicação (Elmer *et al*., 1998; Fontes *et al*., 1994). Essa proteína se liga especificamente ao intermediário dsDNA durante o reconhecimento da origem de replicação viral e cliva o motivo em grampo que se localiza na região intergênica, dentro da CR, para iniciar a replicação via círculo rolante (Heyraud-Nitschke *et al*., 1995). Rep possui também a atividade de ligase, unindo as extremidades do grampo após a terminação da replicação (Fontes *et al*.,

1994; Heyraud-Nitschke *et al*., 1995). Além da replicação, tem sido demonstrado que a proteína Rep de alguns geminivírus, incluindo os do gênero *Begomovirus*, está envolvida na regulação de genes virais, reprimindo a expressão de genes de sentido complementar (Eagle *et al*., 1994). Estudos mais recentes têm sugerido que a proteína Rep apresenta também atividade supressora do silenciamento gênico (Rodríguez-Negrete *et al*., 2013).

A proteína TrAP (*transcriptional activator protein*), codificada pelo gene *AC2*, ativa a transcrição dos genes de sentido viral, *AV1* e *BV1* (Rojas *et al*., 2005; Shivaprasad *et al*., 2005). TrAP não se liga especificamente ao dsDNA (Hartitz *et al*., 1999). Portanto, acredita-se que esta proteína seja direcionada para as regiões promotoras responsivas por meio de interações com proteínas celulares (Hartitz *et al*., 1999; Lacatus e Sunter, 2009). Resultados que fortalecem esta hipótese foram fornecidos em trabalhos onde a proteína de Arabidopsis PEAPOD2 (*At*PPD2), também conhecida como *At*TIFY4B, interagiu com sequências promotoras dos genes *AV1* de CaLCuV (*Cabbage leaf curl virus*) e de TGMV (*Tomato golden mosaic virus*; Lacatus e Sunter, 2009), e *BV1* de TGMV (Berger e Sunter 2013). A expressão de TIFY4B aumenta em resposta à infecção viral e correlaciona com o nível aumentado de mRNA de *AV1* (Chung e Sunter, 2014). Isto implica que TrAP pode influenciar também a expressão de genes do hospedeiro por meio de suas interações. TrAP atua também como um fator de patogenicidade, comprometendo a funcionalidade de CSN (*COP9 signalosome*), um complexo protéico que atua na via ubiquitina-proteassomo e que regula diversos processos celulares (Lozano-Durán *et al*., 2011a). Além disto, TrAP pode atuar na supressão do silenciamento gênico (Buchmann *et al*., 2009; Trinks *et al*., 2005; Wang *et al*., 2003; Zhang *et al*., 2011).

O gene *AC3* codifica a proteína REn (*replication enhancer protein*), uma proteína que, embora não seja essencial para a replicação, aumenta o acúmulo do DNA viral e o desenvolvimento dos sintomas em plantas infectadas (Hanley-Bowdoin *et al*., 2000; Settlage *et al*., 2001). Além disto, a proteína REn de ToLCKeV (*Tomato*

leaf curl Kerala virus) interage com Rep e reforça a atividade ATPase mediada por Rep (Pasumarthy *et al*., 2010), confirmando assim o seu papel na replicação do DNA viral. A proteína AC4, codificada pelo gene *AC4*, possui a capacidade de suprimir o silenciamento de RNA (Chellappan *et al*., 2005).

O DNA-B contém dois genes, *BV1* na fita de sentido viral e *BC1* na fita de sentido complementar, que codificam as proteínas de movimento NSP (*nuclear shuttle protein*) e MP (*movement protein*), respectivamente (Hanley-Bowdoin *et al*., 2000). Estas proteínas estão envolvidas com o movimento do vírus durante a infecção e afetam a patogenicidade viral (Rojas *et al*., 2005; Zhou *et al*., 2007).

As proteínas MP e NSP são as únicas proteínas consideradas de movimento, uma vez que mutações que inativam os genes correspondentes levam à perda completa de infectividade em plantas, sem causar qualquer efeito aparente na replicação do genoma viral (Lazarowitz, 1992). Estudos bioquímicos, moleculares e celulares têm mostrado que NSP se liga ao DNA viral fita simples e o transporta do núcleo para o citoplasma, na forma de um complexo NSP-DNA viral, ao passo que MP facilita o movimento célula-a-célula por meio de sua interação cooperativa com NSP de begomovírus bipartidos (Hehnle *et al*., 2004; Lazarowitz e Beachy, 1999; Pascal *et al*., 1994; Rojas *et al*., 1998; Sanderfoot e Lazarowitz, 1995, 1996). Evidências que NSP se liga ao DNA viral de um modo independente de sequência tem sido mostrado para SqLCV (*Squash leaf curl virus*; Pascal *et al*., 1994), BDMV (*Bean dwarf mosaic virus*; Rojas *et al*., 1998) e AbMV (*Abutilon mosaic virus*; Hehnle *et al*., 2004). Para se movimentar célula-a-célula e a longas distâncias, o complexo NSP-DNA viral é retido pela MP no citoplasma e redirecionado através da parede celular para uma célula adjacente não infectada, onde NSP direciona o genoma viral para o núcleo para novos ciclos de replicação (Hehnle *et al*., 2004; Pascal *et al*., 1994; Sanderfoot e Lazarowitz, 1995; Zhang *et al*., 2001). Resultados recentes têm sugerido que a cooperação MP-NSP, levando à exportação do DNA viral nascente, segue um modelo de transporte "*couple-skating*" (Frischmuth *et al*., 2007; Hehnle *et*

al., 2004; Zhang *et al*., 2001), no qual MP se liga ao complexo NSP-DNA na face citoplasmática da membrana plasmática ou vesículas microssomais e permite a transferência para uma célula adjacente (Kleinow *et al*., 2009b). Plantas transgênicas expressando MP apresentam sintomas típicos de infecção, enquanto que aquelas expressando NSP possuem aparência normal (Ingham *et al*., 1995; Pascal *et al*., 1993). Além disso, NSP e MP diferem quanto à localização subcelular. Em plantas infectadas, NSP localiza-se no núcleo (Pascal *et al*., 1994; Sanderfoot e Lazarowitz, 1995) e MP encontra-se na membrana plasmática (Pascal *et al*., 1993).

Os begomovírus estão associados com duas classes de satélites, denominadas alfassatélites e betassatélites (Briddon e Stanley, 2006). Os betassatélites são capazes de reforçar a eficiência de infecção, o acúmulo e os sintomas do vírus auxiliar (Jyothsna *et al*., 2013; Patil e Fauquet, 2010; Saeed *et al*., 2005), provavelmente devido a atividade supressora do silenciamento de βC1, proteína codificada por estes satélites (Cui *et al*., 2005). Os alfassatélites, também denominados DNA 1, codificam sua própria proteína Rep, que desencadeia sua replicação independente do vírus auxiliar. Entretanto, os alfassatélites dependem do begomovírus auxiliar para sua infecção sistêmica e transmissão pelo inseto vetor (Nawaz-ul-Rehman e Fauquet, 2009). Em alguns casos, alfassatélites suprimem os sintomas virais (Patil e Fauquet, 2010), em outros, suprimem a atividade de silenciamento gênico (Nawaz-ul-Rehman *et al*., 2010). Os betassatélites ocorrem apenas no Velho Mundo, e a grande maioria tem sido identificada em associação com begomovírus monopartidos (Briddon e Stanley, 2006). Os alfassatélites, por sua vez, além de se associarem com begomovírus monopartidos associados com betassatélites no Velho Mundo (Nawaz-ul-Rehman e Fauquet, 2009), também podem se associar com begomovírus ocorrendo no Novo Mundo (Jeske *et al*., 2014; Paprotka *et al*., 2010; Romay *et al*., 2010).

Interação geminivírus-hospedeiro

Por apresentar uma capacidade codificante limitante, os geminivírus dependem extensivamente das maquinarias celulares do hospedeiro e interagem com um grande número de proteínas de plantas durante o processo de infecção viral (Hanley-Bowdoin *et al*., 2013). Geminivírus reprogramam o ciclo celular de células infectadas para induzir a replicação do genoma viral, alteram o padrão de expressão gênica, inibem as vias de morte celular, alteram o tráfego de macromoléculas e interferem com a sinalização celular e *turnover* de proteínas para redirecionar ou bloquear as defesas do hospedeiro e a sinalização hormonal (Hanley-Bowdoin *et al*., 2013).

Geminivírus infectam tipicamente células totalmente diferenciadas, que já saíram do ciclo de divisão celular e que apresentam quantidades insignificantes de enzimas envolvidas na replicação do DNA (Nagar *et al*., 1995). Portanto, estes vírus devem criar um ambiente celular favorável à replicação por meio de interações complexas entre fatores virais e fatores do hospedeiro (Desvoyes *et al*., 2006). Uma vez que a proteína viral Rep consiste em um fator chave para replicação viral, é provável que ela tenha um papel fundamental no recrutamento e montagem do replissomo viral, um complexo que inclui proteínas virais e fatores do hospedeiro envolvidos na replicação do DNA, reparo e outras funções nucleares (Hanley-Bowdoin *et al*., 2013). É provável que a proteína REn, que aumenta o acúmulo de DNA viral e interage com Rep e fatores de replicação do hospedeiro (Settlage *et al*., 2005), também faça parte do replissomo viral. Tanto Rep quanto REn se ligam a PCNA (*proliferating cell nuclear antigen*; Bagewadi *et al*., 2004; Castillo *et al*., 2003), cujo acúmulo em células vegetais diferenciadas é induzido após infecção por geminivírus (Nagar *et al*., 1995). PCNA forma um anel trimérico ao redor do DNA, atuando como um grampo deslizante que aumenta a processividade da DNA polimerase e modula a interação de outras proteínas com o DNA. De fato, PCNA

interage com diversas proteínas envolvidas em processos celulares importantes, como a replicação e reparo do DNA e regulação do ciclo celular (Maga e Hubscher, 2003). Também crítica para a replicação do DNA viral é a interação entre Rep e RFC (*replication factor C*), que forma um complexo com PCNA antes da ligação à extremidade 3' do DNA e que catalisa o carregamento de PCNA na junção oligonucleotídeo iniciador-molde (Gomes *et al*., 2001; Luque *et al*., 2002). Rep interage também com RPA (*replication protein A*; Singh *et al*., 2007), uma proteína chave no recrutamento de proteínas importantes do aparato de replicação, tais como DNA polimerase α, RFC e PCNA (Loor *et al*., 1997). Estudos mais recentes têm investigado a funcionalidade de RPA na estabilização da estrutura em grampo, alvo da atuação de Rep no início do processo de replicação (Singh *et al*., 2007). Além disto, Rep interage com RAD54 e RAD51, proteínas envolvidas no processo de recombinação homóloga (Kaliappan *et al*., 2012; Suyal *et al*., 2013a). Apesar destas interações indicarem uma possível participação de RAD54 e RAD51 na replicação viral dependente de recombinação, estudos mais recentes utilizando linhagens de Arabidopsis *rad54* alelos nulos demosntraram especificamente que RAD54 não é essencial para o processo de replicação viral (Richter *et al*., 2015). Tem sido demonstrado que o dsDNA de geminivírus forma minicromossomos por meio da associação com nucleossomos (Pilartz e Jeske, 2003). Rep interage com a histona H3, e esta interação pode estar envolvida no deslocamento dos nucleossomos do DNA viral, o que permitiria o acesso da maquinaria de replicação e transcrição (Kong e Hanley-Bowdoin, 2002).

Rep se liga ainda com GRIMP (*geminivirus Rep-interacting motor protein*; Kong e Hanley-Bowdoin, 2002), uma cinesina mitótica, e com MCM2 (*minichromosome maintenance protein 2*; Suyal *et al*., 2013b), uma subunidade do complexo MCM, que funciona como uma possível helicase em eucariotos (Bochman e Schwacha, 2008). Assim como outros fatores do hospedeiro, GRIMP também é induzida após a infecção por geminivírus. Cinesinas são proteínas motoras que se

ligam ao aparato do fuso mitótico, e, portanto, Rep poderia impedir a progressão do ciclo celular para a fase mitótica e favorecer a ocorrência de endociclos por meio da interação com GRIMP (Desvoyes *et al*., 2006; Kong e Hanley-Bowdoin, 2002). Plantas de Arabidopsis *mcm2* alelos nulos apresentam uma redução na eficiência da replicação de MYMIV (*Mungbean yellow mosaic India virus*; Suyal *et al*., 2013b). No entanto, o mecanismo pelo qual MCM2 influencia a replicação de MYMIV não é conhecido. Além disto, o papel de todo o complexo MCM na replicação de geminivírus continua a ser investigado (Rizvi *et al*., 2015).

A interação de Rep com duas serina/treonina cinases proximamente relacionadas, denominadas GRIK1 (*geminivirus Rep-interacting kinase1*) e GRIK2, representa outro nível de interação entre fatores do hospedeiro e fatores virais (Kong e Hanley-Bowdoin, 2002; Shen e Hanley-Bowdoin, 2006). GRIKs são proteínas cinases que se ligam à subunidade catalítica de SNRK1 (*SNF1-related protein kinase 1*) e fosforilam um resíduo de treonina presente em seu *loop* de ativação. A fosforilação mediada por GRIKs resulta na ativação da atividade cinase de SNRK1 (Shen *et al*., 2009). SNRK1 desempenha um papel central na coordenação do balanço energético e metabolismo de nutrientes, promovendo o catabolismo celular e inibindo a síntese macromolecular em resposta à limitação de nutrientes (Baena-Gonzalez *et al*., 2007). Além disto, SNRK1 interage com a proteína TrAP e com a proteína βC1 de betassatélites (Hao *et al*., 2003; Shen *et al*., 2011). A interação TrAP-SNRK1 leva à inativação da proteína cinase (Hao *et al*., 2003), enquanto a interação βC1-SNRK1 resulta na fosforilação da proteína viral, atrasando o estabelecimento da infecção viral (Shen *et al*., 2011). Em um trabalho mais recente, Shen *et al*. (2014) mostraram que a proteína viral TrAP também é alvo de fosforilação por SNRK1. A forma fosfomimética de TrAP apresentou um atraso no surgimento de sintomas e no acúmulo de DNA viral durante infecção de Arabidopsis por CaLCuV (Shen *et al*., 2014). O papel de GRIK e SNRK1 durante o processo de infecção ainda não está claro. Provavelmente, as proteínas cinases GRIKs desencadeiam uma cascata de

sinalização por meio de diversos mecanismos, como por exemplo, a fosforilação de SNRK1, levando a uma resposta de defesa por meio da ativação da maquinaria metabólica (Shen e Hanley-Bowdoin, 2006).

Geminivírus alteram o controle transcricional do hospedeiro para induzir a produção da maquinaria de síntese do DNA do hospedeiro (Hanley-Bowdoin, *et al*., 2004). Análise do transcriptoma de Arabidopsis infectada com CaLCuV mostrou que a infecção por geminivírus altera a expressão de genes associados ao ciclo celular, ativando preferencialmente genes que são expressos durante a fase S e G2 do ciclo celular e inibindo genes que são ativos nas fases G1 e M (Ascencio-Ibáñez *et al*., 2008). Um conjunto limitado de genes do ciclo celular central, associados com a reentrada no ciclo celular, com a fase G1 tardia, com a fase S e com a fase G2 inicial, apresentou um aumento no nível de expressão, enquanto que genes do ciclo celular central ligados a fase G1 inicial e G2 tardia apresentaram os níveis de transcritos reduzidos (Ascencio-Ibáñez *et al*., 2008). A análise do transcriptoma realizada por Ascencio-Ibáñez *et al*. (2008) mostrou também que a infecção por geminivírus estimula a expressão de genes do hospedeiro associados ao estresse genotóxico, incluindo genes que codificam proteínas envolvidas no reparo e recombinação do DNA. A ativação de genes do ciclo celular central e de genes envolvidos no reparo do DNA durante a infecção por CaLCuV é consistente com a utilização dos mecanismos de replicação por círculo rolante e de replicação dependente de recombinação para amplificação do genoma de geminivírus (Jeske *et al*., 2001).

A proteína RBR (*retinoblastoma-related protein*) consiste em um regulador chave do ciclo celular em plantas. Esta proteína interage com o fator de transcrição E2F, inibindo a expressão de genes que codificam proteínas envolvidas na replicação do DNA do hospedeiro (Argüello-Astorga *et al*., 2004). Durante o ciclo celular normal, RBR é regulado por fosforilação, desestabilizando sua ligação com E2F, o que permite a transcrição de genes alvo deste transfator durante a fase G1 tardia. Inativação de RBR para permitir a entrada na fase S representa uma característica

conservada de vírus de DNA que infectam plantas e animais (Hanley-Bowdoin *et al*., 2013). Deste modo, a interação entre Rep e RBR interfere com a interação entre RBR e E2F, liberando o fator de transcrição para ativar a expressão de genes necessários para a replicação do DNA, incluindo PCNA (Argüello-Astorga *et al*., 2004; Egelkrout *et al*., 2001; Kong *et al*., 2000). A interação REn-RBR pode também estar envolvida na liberação de RBR da inibição em folhas terminalmente diferenciadas (Settlage *et al*., 2001). REn interage também com *Sl*NAC1 (*Solanum lycopersicum NAC1*; Selth *et al*., 2005). Os níveis de *Sl*NAC1 são maiores em células infectadas com ToLCV (*Tomato leaf curl virus*), sugerindo que NAC1 esteja envolvido na replicação do DNA viral, possivelmente por meio da interação com REn (Selth *et al*., 2005).

Geminivírus alteram a maquinaria de ubiquitinação para obterem uma infecção completa. A modificação de proteínas pela ligação de ubiquitina e ubiquitina-*like* representa eventos de modificações pós-traducionais que modulam a função da proteína e regulam muitos processos na planta, incluindo desenvolvimento, ciclo celular e resposta a estresse biótico e abiótico (Castro *et al*., 2012; Marino *et al*., 2006). O complexo SCF (*SKP1, CUL1/CDC53, F box proteins*) E3 ligase parece ser um alvo importante durante a infecção por geminivírus, uma vez que proteínas virais sequestram ou interferem com a função deste complexo (Lozano-Durán *et al*., 2011a, 2011b). Estudos realizados por Lozano-Durán *et al*. (2011b) mostraram que a infecção por TYLCSV (*Tomato yellow leaf curl Sardinia virus*) é comprometida quando há o silenciamento de ASK2 (*S-phase kinase-associated protein 1*) e CSN3 (*COP9 signalosome 3*). ASK2 pertence a uma família gênica que codifica proteínas SKP1-*like* em Arabidopsis, podendo ser montadas em diferentes complexos SCF, e que desempenham importante papel em um grande número de processos celulares (Liu *et al*., 2004; Umezawa *et al*., 2004). A proteína CSN3 é uma das oito subunidades do complexo CSN (*COP9 signalosome*). Este complexo atua derrubilando o componente culina, regulando, deste modo, a atividade do complexo CRL (*Cullin RING ligases*), incluindo o complexo SCF (Hotton e Callis, 2008). A proteína TrAP de

geminivírus também interfere com a atividade de derrubilação do complexo CSN sobre Culina 1, por meio da sua interação com CSN5A (*COP9 signalosome 5A*), a subunidade catalítica do complexo CSN (Lozano-Durán *et al*., 2011a). A interação TrAP-CSN altera processos celulares regulados pelos complexos SCF, incluindo a sinalização ao jasmonato (Lozano-Durán *et al*., 2011a). Além disto, tem sido demonstrado que a interação entre a proteína βC1, codificada pelo betassatélite associado com CLCuMV (*Cotton leaf curl Multan virus*), e uma enzima E2 ubiquitina conjugadora de tomateiros, denominada *Sl*UBC3, é necessária para a indução dos sintomas específicos causados pelo betassatélite, possivelmente por meio da perturbação da via ubiquitina-proteassomo (Eini *et al*., 2009). Considerando que os complexos SCF ligases são reguladores chave de muitos processos celulares, a capacidade de geminivírus em sequestrar estes complexos representa uma estratégia poderosa para modulação das funções do hospedeiro (Hanley-Bowdoin *et al*., 2013)

A infecção viral pode levar também a alterações do padrão de sumoilação de fatores celulares. Rep se liga a enzima E2 conjugadora de SUMO (SCE1) por meio de resíduos de lisina (K68 e K96) localizados em sua região N-terminal. Mutações que alteram a associação de Rep com SCE1 resultam na redução ou eliminação da infectividade do vírus, bem como na redução do acúmulo viral, sugerindo que a interação Rep-SCE1 é necessária para a replicação do DNA viral (Castillo *et al*., 2004; Lozano-Durán *et al*., 2011b). A expressão ectópica de Rep não altera o padrão geral de sumoilação das proteínas da planta; no entanto, a detecção de alterações específicas indica que Rep modifica o estado de sumoilação de algumas proteínas do hospedeiro, criando um ambiente mais favorável para a replicação viral (Lozano-Durán *et al*., 2011b).

Interações de fatores do hospedeiro com as proteínas de movimento MP e NSP

Para o estabelecimento de uma infecção produtiva, os geminivírus devem replicar-se no núcleo das células, mover-se célula-a-célula e, finalmente, mover-se por toda a planta via transporte mediado pelo floema. Neste processo, os geminivírus precisam transpor duas barreiras distintas, impostas pelo envelope nuclear e pela parede celular, para assim infectar a planta de forma sistêmica (Rojas *et al*., 2005). Considerando a importante função de NSP no transporte do vírus na planta, acredita-se que essa proteína interaja com proteínas do hospedeiro nos diversos compartimentos celulares (Lazarowitz e Beachy, 1999). Da mesma forma, o transporte célula-a-célula de geminivírus representa um mecanismo com vários passos, no qual a proteína MP tem que mediar uma série de funções distintas: (i) ligação ao complexo DNA/NSP, (ii) direcionamento e modificação do plasmodesma, (iii) passagem através do plasmodesma e (iv) liberação do substrato transportado após a transferência ser completada (Lucas, 2006). Durante estes processos, uma série de interações de MP com proteínas do hospedeiro são esperadas. Deste modo, para entender melhor os mecanismos do movimento inter e intracelular dos vírus, vários grupos têm buscado identificar as proteínas do hospedeiro que podem estar envolvidas nestes processos, baseando-se na sua habilidade de ligação às proteínas de movimento viral (Oparka, 2004).

A identificação de três sítios de fosforilação na porção C-terminal da proteína MP de AbMV, que apresentam um impacto no desenvolvimento dos sintomas e/ou no acúmulo do DNA viral (Kleinow *et al*., 2009a), indica uma possível regulação de diversas funções de MP por proteínas cinases do hospedeiro ainda desconhecidas. A chaperone cpHSC70-1 de Arabidopsis, uma proteína de choque térmico cognata de 70 kDa (cpHSC70-1) codificada no núcleo e direcionada para os plastídeos, interage com o domínio N-terminal de MP de AbMV por meio do sistema de duplo

híbrido em leveduras (Krenz *et al*., 2010). A interação entre estas proteínas foi avaliada *in vivo*, e estudos, utilizando linhagens de *Nicotiana benthamiana* silenciadas para esta chaperone, sugerem um envolvimento de cpHSC70 no ciclo de infecção do AbMV (Krenz *et al*., 2010). Outra proteína, uma sinaptotagmina (SYTA), foi identificada também pelo sistema de duplo híbrido em leveduras, utilizando a proteína MP de CaLCuV como isca (Lewis e Lazarowitz, 2010). A interação entre SYTA e MP de CaLCuV e de TMV (*Tobacco mosaic virus*), um vírus não relacionado, foi confirmada *in vitro*. Estudos com linhagens *knockdown* para SYTA, bem como a utilização de uma forma dominante negativa da mesma, mostraram que esta proteína regula tanto a reciclagem de endossomos quanto a atividade de MP no movimento viral célula-a-célula (Lewis e Lazarowitz, 2010). Para determinar se SYTA tem um papel central na regulação do tráfego célula-a-célula de um número mais amplo de vírus, Uchiyama *et al*. (2014) estenderam os estudos utilizando vírus de plantas que empregam diferentes estratégias de movimento. Os resultados mostraram que a infecção sistêmica e o tráfego célula-a-célula das proteínas de movimento do potivírus TuMV (*Turnip mosaic virus*) e o do tobamovírus TVCV (*Turnip vein clearing virus*) foram atrasadas em mutantes *syta-1 knockdown*. Em contraste, a infecção sistêmica do caulimovírus CaMV (*Cauliflower mosaic virus*) não foi inibida em *syta-1*. O fato de MP de diferentes vírus interagirem com SYTA sugere que essa proteína seja um regulador chave de movimento intercelular de vírus de planta, sendo necessária para a habilidade de diversas MPs em alterarem o plasmodesma e mediar à propagação célula-a-célula (Uchiyama *et al*., 2014). Ensaios de *Gel overlay* e de co-imunoprecipitação, *in vitro* e *in vivo*, mostraram interação de H3 com MP e NSP de BDMV, bem como com CPs de diferentes geminivírus (Zhou *et al*., 2011). H3, expressa transientemente em protoplastos de *Nicotiana tabacum* e em folhas de *N. benthamiana*, co-localizou com NSP no núcleo, e na presença de MP foi redirecionada para a periferia celular e plasmodesmas. Complexos formados de H3, NSP, MP e DNA viral foram recuperados por co-imunopreciptação de folhas de *N.*

benthamiana expressando transientemente H3. Os resultados suportam um modelo no qual H3 faz parte de um complexo de movimento que é estruturado no núcleo e transferido para a periferia celular e plasmodesmas (Zhou *et al*., 2011).

A proteína NSP codificada por CaLCuV interage diretamente com a proteína NSI (*nuclear shuttle protein interactor*) de Arabidopsis, uma acetiltransferase nuclear (McGarry *et al*., 2003) capaz de acetilar as histonas H2A e H3 *in vitro*, bem como a proteína capsidial viral. Apesar da interação, a proteína NSP não serve como substrato para esta acetiltransferase (McGarry *et al*., 2003). Entretanto, foi mostrado que NSP pode inibir a atividade de NSI por interferir com a sua montagem em complexos ativos, sugerindo um mecanismo no qual NSP possa recrutar NSI para regular a exportação nuclear do genoma viral (Carvalho *et al*., 2006).

Florentino *et al*. (2006) identificaram uma proteína de *Arabidopsis*, denominada NsAK (*NSP-associated Kinase*), capaz de interagir especificamente com NSP de CaLCuV. NsAK pertence à famíia de receptores do tipo serina/ treonina cinases (RLK, *receptor-like kinase*) classificada como PERK-*like*. Foi demonstrado que NSP funciona como substrato de NsAK e que a perda de função desta cinase reduz a eficiência de infecção e atenua o desenvolvimento de sintomas. Isto indica que NsAK atua como um contribuidor positivo para a infecção de geminivírus podendo atuar na regulação da função de NSP.

Outra proteína de Arabidopsis foi identificada por interagir, *in vitro* e *in vivo*, com a proteína NSP de geminivírus (Carvalho *et al*., 2008a). Esta proteína, denominada NIG (*NSP-interacting GTPase*), se localiza no citoplasma, com um evidente acúmulo ao redor do envelope nuclear em células vegetais, apresenta ligação específica a GTP e possui atividade de GTPase intrínseca (Carvalho *et al*., 2008a). A co-expressão transiente de NIG e NSP em folhas de tabaco resulta no redirecionamento da proteína viral do núcleo para o citoplasma. Além disso, a superexpressão de NIG em plantas transgênicas acarreta em um aumento da suscetibilidade à infecção por geminivírus (Carvalho *et al*., 2008a). Diante disto, foi

proposto um modelo, no qual NIG se ligaria à NSP no lado citoplasmático do complexo poro nuclear e facilitaria o transporte intracelular do complexo DNA-NSP do envelope nuclear para a periferia celular, onde ocorreria sua substituição por MP (Carvalho *et al*., 2008b).

A interação entre membros da família LRR-RLK (*leucine rich-repeat - receptor-like kinase*), denominados NIK (*NSP-interacting kinase*), e NSP de geminivírus é conservada entre homólogos de NIK de diferentes espécies hospedeiras e NSP de diferentes geminivírus (Mariano *et al*., 2004). NIKs são proteínas cinases autênticas, com propriedades bioquímicas de receptores de sinalização. A ligação de NSP ao *loop* de ativação (A-loop) de NIK suprime sua atividade cinase, impedindo a autofosforilação de resíduos de treonina regulatórios, que, de outra forma, levariam à ativação do receptor (Fontes *et al*., 2004). Da mesma forma, mutações no A-loop de NIK, que impedem a sua autofosforilação, prejudicam a capacidade de NIK em elicitar a resposta de defesa contra geminivírus (Santos *et al*., 2009). Além de ser inibida por NSP, a perda da função do gene *NIK* aumenta a suscetibilidade à infecção por geminivírus, e a superexpressão de NIK1 de Arabidopsis em plantas de tomate atenua o desenvolvimento de sintomas e atrasa a infecção por ToYSV (*Tomato yellow spot virus*). Estes resultados sugerem que NIK esteja envolvida em resposta de defesa antiviral (Fontes *et al*., 2004). Progressos recentes no sentido de elucidar a sinalização antiviral mediada por NIK inclui a identificação da proteína ribossomal L10 (RPL10) como um efetor *downstream* na via (Carvalho *et al*., 2008c; Rocha *et al*., 2008). A fosforilação de RPL10 por NIK promove a translocação da proteína ribossomal para o núcleo, onde ela pode funcionar na montagem de uma resposta de defesa que afeta negativamente a infecção viral (Carvalho *et al*., 2008c).

Sistema imune de plantas

A interação dinâmica entre patógeno e planta hospedeira resulta de milhões de anos de co-evolução. Esta luta é geralmente descrita em termos de uma “corrida armamentista”, um termo apropriado, considerando o investimento necessário e o significando para ambos os lados (Malinovsky *et al*., 2014). O objetivo da planta é manter-se saudável e fértil, já a estratégia dos patógenos varia. Microrganismos biotróficos e hemibiotróficos dependem do hospedeiro vivo e inconsciente de sua presença, pelo menos até estágios mais avançados da infecção. Por sua vez, os microrganismos necrotróficos vivem e se alimentam de células mortas, podendo, portanto, utilizar uma estratégia de ataque mais forte (Davidsson *et al*., 2013).

A linha de frente do sistema de defesa de plantas consiste de barreiras físicas e químicas, tais como cutícula, parede celular, e compostos antimicrobianos produzidos constitutivamente. Para penetrar esta barreira física, patógenos tem evoluído um arsenal de enzimas que degradam a parede celular e que são fatores de virulência chaves (Davidsson *et al*., 2013; Nuhse, 2012). Os agentes patogênicos que conseguem romper estas barreiras físicas e químicas pré-formadas, tem de enfrentar, em seguida, o sistema imunológico da planta, sistema de vigilância elaborado, no qual sentinelas moleculares operam para ativar as respostas de resistência (Jones e Dangl, 2006).

Entre os mecanismos pelos quais as plantas respondem a patógenos, a resposta imune inata é um dos mais importantes e emprega um sistema de percepção em dois níveis (Dodds e Rathjen, 2010). O primeiro deles é mediado por PRRs (*pattern recognition receptors*) localizados na superfície celular e que desencadeiam a imunidade induzida por PAMP (PTI; *PAMP-triggered immunity*). O segundo nível envolve receptores imunes intracelulares que reconhecem, direta ou indiretamente, efetores de virulência secretados no interior da célula do hospedeiro

pelo patógeno, induzindo, deste modo, a imunidade induzida por efetores (ETI; *effector-triggered immunity*; Jones e Dangl, 2006).

Imunidade induzida por PAMP (PTI)

PTI baseia-se na percepção do patógeno por meio do reconhecimento de PAMPs (*pathogen-associated molecular patterns*) por PRRs. PAMPs são moléculas derivadas do patógeno, essenciais para estes organismos, mas que podem ser reconhecidas pelas plantas. PAMPs incluem proteínas, como por exemplo, flagelina e fator de elongação Tu (EFTu); carboidratos, entre eles quitina; lipopolissacarídeos, entre outros (Macho e Zipfel, 2014). As plantas são capazes também de detectar DAMPs (*damage-associated molecular patterns*), produtos de degradação resultantes da ação de patógenos invasores ou peptídeos endógenos que são liberados pelas plantas decorrente do ataque por patógeno (Boller e Felix, 2009). O reconhecimento de DAMPs também desencadeia resposta imune similar à resposta PTI (Yamaguchi e Huffaker, 2011). PRRs são, geralmente, RLKs ligados à membrana plasmática, ou RLPs (*receptor-like proteins*) com domínio extracelular que permite a percepção de PAMPs (Bohm *et al*., 2014). Poucos pares PRR/PAMPs têm sido reconhecidos, entre eles FLS2 (*flagellin-sensitive 2*), que reconhece o N-terminal de flagelina, representado pelos vinte e dois aminoácidos do epítopo fls22 de *Pseudomonas aeruginosa* (Gomez-Gomez e Boller, 2000) e EFR (*EF-Tu receptor*), que percebe o fator de elongação Tu por meio de um epítopo com dezoito resíduos de aminoácidos, denominado elf18 de *Escherichia coli* (Zipfel *et al*., 2006). A percepção de PAMP resulta na formação de complexos receptores imunes e em diferentes reações de autofosforilação e transfosforilação envolvendo estes receptores, processos necessários para o desencadeamento da sinalização intracelular (Macho e Zipfel, 2014). Além disto, plantas apresentam RLCKs (*receptor-*

like cytoplasmic kinases), que se associam funcionalmente e/ou fisicamente com RLKs para transmitir a sinalização intracelular por meio de eventos de fosforilações (Lin *et al*., 2013)

Após a detecção do patógeno por PRRs, plantas são capazes de induzir numerosos mecanismos de defesa, incluindo fechamento estomático para limitar a entrada de bactéria (Sawinski *et al*., 2013); influxo de íons Ca^{2+} extracelular para o citosol, onde atua como mensageiro secundário sendo percebido por sensores de ligação a Ca^{2+} que podem mediar à transdução de sinal *downstream* (Ranf *et al*., 2011); produção e secreção de compostos antimicrobianos incluindo fitoalexinas, entre eles a camalexina (Ahuja *et al*., 2012); produção de espécies reativas de oxigênio (ROS), que possui efeito tóxico sobre patógenos (O'Brien *et al*., 2012) e deposição de calose, que forma uma barreira química e física contra a invasão de agentes patogênicos (Underwood, 2012). A indução destes mecanismos de defesa baseia-se numa rede complexa de vias de sinalização.

Além dos eventos de autofosforilação e transfosforilação de complexos receptores imunes, outras proteínas cinases são rapidamente ativadas após a percepção de PAMP. A maioria delas pertence às famílias de proteínas cinases CDPK (*calcium-dependent protein kinases*) e MAPK (*mitogen-activated protein kinases*), e são elementos chave que permitem a regulação de um grande número de proteínas alvo, como por exemplo, fatores de transcrição, enzimas metabólicas, proteínas de membrana plasmática e proteínas do citoesqueleto (Rayapuram *et al*., 2014). Durante PTI, CDPKs atuam como sensores de Ca^{2+} e dependem destes íons para sua ativação. Algumas CDPKs são ativadas transientemente após tratamento com flg22, entre elas CPK4, CPK5, CPK6 e CPK11 (Boudsocq e Sheen, 2013). CPK4/5/6/11 estão envolvidas na explosão oxidativa e na reprogramação transcricional mediada por fls22 e na resistência induzida por fls22 para o patógeno bacteriano *Pseudomonas syringae* (Boudsocq e Sheen, 2013; Romeis e Herde, 2014). Vários substratos de CDPK foram identificados, como por exemplo ACS2 (*1-*

aminocyclopropane-1-carboxylic acid synthase), uma enzima limitante na síntese de etileno (ET; Boudsocq e Sheen, 2013; Kamiyoshihara *et al*., 2010; Schulz *et al*., 2013) e RBOHD (*respiratory burst oxidase homolog D*), uma NADPH localizada na membrana plasmática, responsável pela explosão oxidativa induzida por PAMP (Dubiella *et al*., 2013; Ranf *et al*., 2011).

As cascatas de sinalização MAPK também funcionam na transmissão de sinal, traduzindo um estímulo extracelular em respostas apropriadas, por meio de fosforilações diferenciais. Nestas cascatas de sinalização, MAP-cinase-cinase-cinase (MAPKKKs) fosforilam MAP-cinase-cinase (MAPKKs), que por sua vez fosforilam MAP-cinase (MAPKs; Rasmussen *et al*., 2012). Quase a metade dos substratos de MAPK são fatores transcricionais, o que destaca o envolvimento de MAPKs na reprogramação transcricional que ocorre durante a defesa (Mao *et al*., 2011; Meng *et al*., 2013). Um exemplo da ligação entre a transdução de sinal e a implementação de mecanismos de defesa induzidos pela PTI consiste na cascata de MAPK ativando a produção e secreção de compostos antimicrobianos. MAPK3, MAPK4 e MAPK6 fosforilam o fator de transcrição WRKY33 (Andreasson *et al*., 2005; Mao *et al*., 2011). Análises genéticas mostraram que WRKY33 é essencial para a biossíntese de calamexina, uma fitoalexina, após a infecção por diferentes patógenos e após a sinalização MPK3/MPK6 (Mao *et al*., 2011; Qiu *et al*., 2008). Além disto, tem sido demonstrado que WRKY33 controla a biossíntese de camalexina por meio da sua interação com MPK4. WRKY33 forma um complexo nuclear com MPK4 e MKS1 (Qiu *et al*., 2008). Após a infecção por bactéria, a fosforilação de MKS1 por MPK4 induz a liberação do complexo MKS1-WRKY33, que ativa, então, a expressão do gene *PAD3* (*phytoalexin deficient 3*), envolvido no último passo da biossíntese de calamexina (Andreasson *et al*., 2005; Mao *et al*., 2011; Qiu *et al*., 2008).

Os fitohormônios, entre eles ácido salicílico (SA), ácido jasmônico (JA) e ET, constituem outra classe importante de moléculas sinalizadoras envolvidas na regulação de respostas de defesa de plantas a patógenos. A sinalização do SA está

geralmente envolvida na defesa contra patógenos biotróficos e hemibiotróficos, enquanto que a sinalização do JA e ET são geralmente importantes contra patógenos necrotróficos (Glazebrook, 2005). As sínteses de SA, JA, e ET são acionadas após a percepção de PAMP, e uma vez produzidos, estes fitohormômios são reconhecidos pelos seus receptores, que transmitem diferentes sinalizações e respostas imunes (Alazem e Lin, 2014). Estes hormônios que regulam as vias de defesa da planta possuem efeitos antagônicos. Por exemplo, a indução da via de sinalização do SA pode reprimir a via do JA/ET, enquanto que a indução da via JA/ET reprime a expressão de certos genes *downstream* da via de sinalização do SA (Alazem e Lin, 2014). Em particular, evidências crescentes indicam que ET está proximamente associado com a via de sinalização de PTI. Por exemplo, a ativação de MPK6 por flg22 estabiliza ACS2 e ACS6, enzimas limitantes para a síntese de ET (Liu e Zhang, 2004). ET exerce sua regulação nas respostas de defesa por meio de EIN3 (*Ethylene insensitive 3*) e EIL1 (*EIN3-like 1*), dois fatores de transcrição relacionados (Guo e Ecker, 2003), que, por exemplo, regulam positivamente a transcrição de FLS2 (Boutrot *et al.,* 2010; Mersmann *et al*., 2010). EIN3/EIL1 também regulam negativamente a imunidade dependente de SA, ligando-se a região promotora de *SID2* (*Salicylic acid induction deficient 2*), que controla a biossíntese de SA (Chen *et al*., 2009).

Imunidade induzida por efetores (ETI)

As respostas desencadeadas pela PTI normalmente evitam que micróbios não adaptados infectem o hospedeiro, representando uma importante barreira contra o desenvolvimento de doenças. Por sua vez, patógenos apresentam uma notável propensão a se adaptar a determinados genótipos hospedeiros, evoluindo um conjunto de fatores de virulência, conhecidos como efetores, dos quais alguns são

enviados para dentro da célula do hospedeiro para interferirem com a PTI, amenizando a defesa basal (Cui *et al*., 2015). Os efeitos causados pelos efetores impulsionaram a coevolução da interação hospedeiro-patógeno, e as plantas, como uma forma de contra defesa, desenvolveram proteínas de resistência (R) que reconhecem alguns dos efetores e ativam a defesa da planta. Efetores que são reconhecidos por uma proteína R correspondente são chamados de proteínas de avirulência (Avr; Alfano e Collmer, 1997), enquanto que o patógeno que transporta esta proteína Avr, que desencadeia a resistência da planta, é denominado de avirulento. A detecção de efetores liberados por um patógeno avirulento induzirá uma resposta de resistência vigorosa, denominada ETI, que interrompe o crescimento do patógeno (Jacob *et al*., 2013; Jones e Dangl, 2006). ETI reintegra e amplifica a reprogramação transcricional basal e as defesas antimicrobianas desencadeada pela PTI, e está geralmente associada com morte celular localizada, denominada resposta hipersensível (HR; Jones e Dangl, 2006).

A maioria das proteínas R são receptores intracelulares NB-LRR (*nucleotide binding-leucine rich repeat*), que são subclassificados de acordo com a variabilidade do seu domínio N-terminal em CC-NB-LRR (*coiled-coil-NB-LRR*) ou TIR-NB-LRR (*toll/interleukin 1 receptor-like-NB-LRR*). Estas proteínas receptoras funcionam como interruptores moleculares que alternam entre uma forma fechada inativa e uma forma aberta ativa. A forma inativa se liga ao ADP, com o domínio N-terminal, TIR ou CC, e o domínio C-terminal, LRR, cooperando para inibir estereoquimicamente o domínio NB e a consequente troca de ADP por ATP. Após a indução, as proteínas R passam por modificações conformacionais que expõem o domínio NB, antes oculto por interações intramoleculares, levando à troca de ADP por ATP e a consequente ativação da proteína R, que inicia a sinalização ETI (Cui *et al*., 2015; Griebel *et al*., 2014). Em resposta à infecção por patógenos, proteínas R induzem respostas fisiológicas locais dramáticas, incluindo explosão oxidativa, produção e acúmulo de SA e expressão de genes relacionados à patogenicidade (PR) e morte celular

programada (PCD), ao custo de alterar processos fisiológicos normais (Wu *et al*., 2015). Portanto, vários mecanismos do hospedeiro devem atuam para restringir a expressão de genes R e evitar ativação inapropriada de proteínas R (Gloggnitzer *et al*., 2014; Palma *et al*., 2010; Staiger *et al*., 2013).

O primeiro passo para ativar a ETI após infecção por um patógeno avirulento consiste no reconhecimento das proteínas Avr que foram liberadas no interior das células do hospedeiro. As plantas desenvolveram mecanismos distintos de reconhecer efetores. O modelo de interação direta, ou gene por gene, preconiza que pares complementares de genes da planta hospedeira e do patógeno determinam a especificidade de resistência à doença (Flor, 1971). Uma interpretação molecular do modelo gene por gene em termos de reconhecimento proteína R-efetor é que interação específica entre o receptor e seu efetor cognato desencadeia resistência. De fato, apenas alguns casos de reconhecimento direto têm sido demonstrados (Catanzariti *et al*., 2010; Cesari *et al*., 2013; Deslandes *et al*., 2003; Jia *et al*., 2000).

Em outras respostas de resistência desencadeada por efetores, variações de um modelo de reconhecimento indireto do efetor explicam mais satisfatoriamente os resultados de interação molecular (Collier e Moffett, 2009; Takken e Goverse, 2012). Neste modelo de interação indireta, ou modelo guarda, o receptor é ativado indiretamente por efetores do patógeno, que modificam fatores do hospedeiro ligados a proteínas R e monitorados (ou guardados) por elas (Collier e Moffett, 2009; Takken e Goverse, 2012). Uma vez ativadas, as proteínas R desencadeiam uma variedade de respostas, como por exemplo, explosão oxidativa, influxo de Ca^{2+}, cascatas de MAPK, recrutamento de fatores de transcrição, reprogramação transcricional resultando na expressão de genes de defesa e produção de fitohormônios (Wu *et al*., 2015). As mudanças transcricionais causadas pela ETI se sobrepõem consideravelmente aquelas causadas pela PTI (Navarro *et al*., 2004). Esta observação sugere que a mesma maquinaria central é utilizada por diferentes

receptores para reprogramar transcricionalmente as células. Apesar das respostas causadas pela PTI e ETI, tais como produção de ROS, influxo de Ca^{2+} e ativação de MAPK, serem qualitativamente similares, na ETI elas são amplificadas, ou possuem maior duração do que na PTI (Gao *et al*., 2013; Tsuda e Katagiri, 2010). Deste modo, a sinalização da ETI durante a infecção por patógeno parece operar impulsionando a rede de resposta imune basal desencadeada pela PTI, mas emitindo respostas mais fortes e/ou mais duradouras (Cui *et al*., 2015). Uma possibilidade diferente, mas não exclusiva, é que a sinalização desencadeada na ETI opera desfazendo os efeitos repressores do sistema de resposta PTI. Durante PTI, um equilíbrio é normalmente atingido entre ativação de reguladores positivos e negativos da imunidade a fim de manter o crescimento da planta e não reagir de forma exagerada a micróbios inofensivos (Bohm *et al*., 2014). Ao contrário, efetores são assinaturas claras da presença de patógeno, e, portanto, durante ETI, as plantas podem relaxar os freios da regulação negativa da PTI, resultando em respostas imunes mais fortes (Cui *et al*., 2015). Diante disto, é sugerido um modelo em que o papel central das proteínas R ativadas consiste em remover, direta ou indiretamente, as restrições no programa transcricional da PTI, amplificando, assim, a resistência (Cui *et al*., 2015).

A característica marcante da ETI consiste na indução rápida de PCD no local de infecção, um processo de liberação de proteínas antibacterianas vacuolares no apoplasto, resultante da fusão entre a membrana do vacúolo e a membrana plasmática. O objetivo principal da resposta hipersensitiva (HR) consiste em isolar e impedir a proliferação do patógeno invasor (Wu *et al*., 2014). Esta estratégia de defesa é eficaz contra patógenos virais, bacterianos, fúngicos, bem como contra oomiceto e nematóides, que se alimentam de células vegetais vivas. Em Arabidopsis, a PCD está sob a regulação do SA, NPR1 (*nonexpresser of PR genes 1*), um supressor da morte celular, e de NPR3 e NPR4, receptores do SA. Baixos níveis de SA suprimem a morte celular, enquanto que o acúmulo de SA induz este processo. NPR3 e NPR4 interagem com NPR1 e Cullina 3 E3 ligase e funcionam como

proteínas adaptadoras para facilitar a poliubiquitinação e subsequente degradação de NPR1 pelo proteassomo 26S (Fu *et al*., 2012). NPR4 tem uma elevada afinidade por SA, enquanto que NPR3 possui uma baixa afinidade por este hormônio. Altos níveis de SA no centro da zona de morte celular interrompe a interação entre NPR1 e NPR4, mas favorece a interação entre NPR1 e NPR3. Então, NPR3 promove a degradação de NPR1 a um nível que não é suficiente para suprimir a morte celular. Em células vizinhas, o nível intermediário de SA desfaz a interação NPR1-NPR4, mas não é alto o suficiente para promover a interação NPR1-NPR3. Como resultado, NPR3 e NPR4 não podem mediar a degradação de NPR1. Assim, o alto nível de NPR1 nas células vizinhas suprime a propagação da morte celular e interage com fatores transcricionais para ativar as respostas de defesa da planta (Fu *et al*., 2012).

Agentes patogênicos diferentes (vírus, bactéria, fungo, por exemplo) codificam diversas proteínas Avr, possuem diferentes elicitores e utilizam estratégias de infecção distintas; entretanto, alteram, de forma similar, o estado metabólico, fisiológico e celular do hospedeiro. Apesar da diversidade, os inúmeros efetores injetados pelos patógenos no interior da célula para promover virulência podem alvejar poucos *hubs* conservados na rede de sinalização que controlam a defesa da planta, metabolismo e sinalização (Pritchard e Birch, 2011). De fato, um estudo recente que utilizou o sistema de duplo híbrido para identificar interações físicas entre proteínas de Arabidopsis relacionadas à imunidade (incluindo 30 proteínas R) e efetores de dois patógenos evolutivamente separados, mostrou que efetores patogênicos podem convergir para um conjunto limitado de proteínas do hospedeiro que são *hubs* altamente interconectados com funções reguladoras importantes na sinalização imune de plantas (Mukhtar *et al*., 2011).

Resistência sistêmica adquirida (SAR)

Patógenos avirulentos desencadeiam não apenas respostas de defesa local, mas também induzem respostas de defesa sistêmica em tecidos distantes do local da infecção, afim de proteger o restante da planta de infecções secundárias (Durrant e Dong, 2004). O estabelecimento desta imunidade sistêmica mais duradoura, chamada resistência sistêmica adquirida (SAR), envolve o transporte de várias moléculas sinal, como por exemplo, SA, MeSA (ácido metil-salicílico), AzA (ácido azeláico), G3P (gliceraldeído-3-fosfato) e DA (*dehydroabietinal*) do sítio de infecção inicial para toda a planta (Chanda *et al*., 2011; Chaturvedi *et al*., 2012; Metraux *et al*., 1990; Park *et al*., 2007). A percepção destes sinais em tecidos sistêmicos conduz ao acúmulo de SA, que conduz a reprogramação transcricional de diversos genes, incluindo aqueles que codificam proteínas PR (van Loon *et al*., 2005; Park *et al*., 2007). Esta reprogramação transcricional é altamente dependente do fator de transcrição NPR1, que além de ativar a expressão de inúmeros genes relacionados a imunidade (tais como os genes *PR*) e de genes que codificam fatores de transcrição que iniciam cascatas adicionais de transcrição, também suprime genes envolvidos em processos celulares básicos, como a fotossíntese, privilegiando, assim, resposta imune ao custo do crescimento da planta (Sugano *et al*., 2010; Wang *et al*., 2006). NPR1 também participa na sobreposição entre as vias de defesa dependentes de JA e SA, facilitando o estabelecimento de respostas imunes adequadas, dependentes da natureza do patógeno e do estágio da infecção (Spoel *et al*., 2003). A memória imune conferida pela SAR em plantas pode durar de semanas a meses, e possivelmente até mesmo durante todo o período de crescimento da planta (Fu e Dong, 2013)

Defesas mediadas por RNAi

O silenciamento de RNA consiste em um mecanismo de regulação gênica com implicações fundamentais em muitos processos biológicos. Este mecanismo é induzido pela presença de RNA fita dupla (dsRNA), que é processado por diferentes ribonucleases, denominadas Dicer-*like* (DCL) em plantas, em pequenos RNAs (21-24 nucleotídeos), que são incorporados em complexos de silenciamento citoplasmático induzido por RNA (RISC), cujo componente catalítico chave corresponde a um membro da família de proteínas argonauta (AGO). Estes complexos, guiados pela especificidade de sequência dos pequenos RNAs (sRNAs), medeiam inibição transcricional, clivagem do transcrito, metilação do DNA, ou alguma combinação destes processos, dependendo das proteínas AGO e dos pequenos RNAs que eles contêm (Kamthan *et al*., 2015). Plantas possuem três vias de silenciamento caracterizadas: (i) a via de silenciamento pós-transcricional ou citoplasmática (PTGS), resultando na degradação de um mRNA complementar alvo; (ii) a via de microRNA (miRNA) desencadeada por precursores de miRNA especificados por genes não codificadores de proteínas; (iii) silenciamento gênico transcricional e heterocromático (TGS) mediado pela metilação de histonas e DNA, direcionada por pequenos RNAs de interferência (siRNA; Kamthan *et al*., 2015).

O silenciamento de RNA, além de sua função no controle da expressão gênica, constitui um mecanismo de defesa que plantas e outros eucariotos utilizam para proteger seus genomas de ácidos nucléicos invasores, tais como vírus, transposons e transgenes (Incarbone e Dunoyer, 2013). A maioria dos vírus que infectam plantas possuem genoma de RNA, que comumente possui elementos de estrutura secundária em fita dupla e/ou produzem intermediários de dsRNA por meio da atividade de RNA polimerases dependentes de RNA (RDRs) durante os passos de replicação (Qi *et al*., 2009). Estes dsRNAs virais são processados principalmente por DCL4 ou DCL2, produzindo pequenos RNAs derivados do vírus (vsRNA) com 21

ou 22 nucleotídeos de extensão, respectivamente (Blevins *et al*., 2006). Os vsRNAs são subsequentemente recrutados, principalmente por AGO1 e AGO2, para direcionar PTGS de RNAs virais como parte de RISCs antivirais (Harvey *et al*., 2011; Zhang *et al*., 2006).

A infecção por vírus de DNA, como por exemplo geminivírus, também produz dsRNA por meio de transcrição convergente bidirecional (Aregger *et al*., 2012). Em plantas infectadas com vírus de DNA, são produzidas também grandes quantidades de vsRNAs com 24 nucleotídeos de extensão, que direcionam o TGS por meio de metilação do DNA direcionada por RNA (RdDM; Blevins *et al*., 2006). A produção de siRNA heterocromático de 24-nt envolve a RNA polimerase IV, que produz transcritos fita simples a partir do genoma viral (Huang *et al*., 2009). Estes RNAs de fita simples (ssRNAs) são convertidos em dsRNA por meio da atividade de RDR2, e subsequentemente clivados por DCL3, produzindo siRNAs de 24-nt de extensão. Estes siRNA são incorporados em complexos RISC e funcionam como guias para metilação de citosinas e condensação da cromatina de episssomos virais nucleares e minicromossomos, principalmente por meio da atividade de AGO4 (Raja *et al*., 2008; Yadav e Chattopadhyay, 2011). A correlação inversa entre o nível de DNA viral metilado e a severidade dos sintomas virais sugere que a defesa de plantas contra vírus de DNA depende também da via de RdDM (Incarbone e Dunoyer, 2013).

Para lidar com a elevada taxa de replicação e movimento do vírus, as plantas têm evoluído também meios para amplificar a resposta de silenciamento antiviral. Isto ocorre por meio da produção de vsRNAs secundários, que, diferentemente dos vsRNAs primários, são produzidos por meio da atividade de RDRs celulares, que convertem ssRNA em novos substratos dsRNA para processamento por DCLs (Donaire *et al*., 2008; Wang *et al*., 2011). Em Arabidopsis, RDR1, RDR6 e, em menor contribuição, RDR2 estão envolvidas neste passo de amplificação de acúmulo de vsRNA (Qu, 2010; Wang *et al*., 2010). Além disto, o sinal de silenciamento de RNA antiviral pode também se propagar a partir do local de iniciação para os tecidos

circundantes, primeiramente por meio dos plasmodesmas, e, em seguida, pelo floema, semelhante a SAR (Palauqui *et al*., 1997). Em plantas, a natureza dos ácidos nucléicos de silenciamento móvel que transmite a especificidade de sequência foi inequivocamente atribuída a siRNA (Molnar *et al*., 2010). Este aspecto autônomo do silenciamento de RNA representa uma arma sistêmica desta reação antiviral, em que a transmissão de vsRNAs móveis à frente da infecção antecipa o silenciamento antiviral em células que ainda não foram infectadas. Consequentemente, replicação ou movimento de patógenos nestas células são atrasados ou impedidos (Havelda *et al*., 2003).

Embora o silenciamento de RNA tenha evoluído para ser uma potencial estratégia de defesa antiviral, a maioria dos vírus codificam pelo menos uma proteína supressora do silenciamento, que compromete a via de silenciamento de RNA da planta hospedeira, neutralizando as respostas antivirais da planta (Bisaro, 2006). Supressores virais do silenciamento (VRS) interferem com a via de siRNA em diferentes pontos e por meio de diversos mecanismos, incluindo prejuízos na biossíntese de siRNA, defeitos na incorporação de siRNA no complexo RISC, degradação de AGO, aprisionamento de siRNA e supressão da amplificação de siRNA (Burgyán e Havelda, 2011).

Infecções por geminivirus estão associadas com quantidades abundantes de siRNAs com 24 nt de comprimento, que direcionam a metilação do DNA (Akbergenov *et al*., 2006). Entretanto, esta defesa antiviral pode ser suprimida por proteínas codificadas por geminivírus e por satélites associados a geminivírus (Buchmann *et al*., 2009; Yang *et al*., 2011). A proteína TrAP se liga e inibe ADK (*adenosine kinase*), enzima necessária para a síntese de SAM (*S-adenenosylmethionine*), que fornece o grupo metil para a metilação do DNA (Wang *et al*., 2005). A proteína C2 de um curtovírus interage com SAMDC1 (*S-adenosylmethionine decarboxylase 1*), enzima que catalisa a conversão de SAM para a forma descarboxilada (dcSAM; Zhang *et al*., 2011). A interação C2-SAMDC1 atenua a degradação de SAMDC1 mediada pelo

proteassomo, o que aumenta a razão dsSAM/SAM suficientemente para inibir a metilação do DNA de BSCTV (*Beet severe curly top virus*; Zhang *et al*., 2011). Adicionalmente, tem sido mostrado que a proteína βC1 também interfere no ciclo de metilação, inibindo a atividade de SAHH (*S-adenosyl homocysteine hydrolase*), uma enzima do ciclo de metilação necessária para a síntese de SAM, molécula doadora de grupos metil (Yang *et al*., 2011). Geminivírus prejudicam a metilação do DNA também por meio da redução da expressão de DNA metiltransferases. A proteína Rep apresenta atividade supressora do TGS reprimindo a expressão de MET1 (*Methyltransferase* 1) e CMT3 (*Chromomethylase* 3), DNA metiltransferases responsáveis pela manutenção da metilação simétrica (Rodríguez-Negrete *et al*., 2013). Mais recentemente, a proteína AC5 de MYMIV foi relacionada com a supressão do TGS, reprimindo a expressão de DRM2 (*Domains rearranged methyltransferase 2*; Li *et al*., 2015), uma DNA metiltransferase que está envolvida no estabelecimento e manutenção da metilação assimétrica em sítios CHH (onde H = A, C ou T; Law e Jacobsen, 2010).

Além da supressão do TGS, proteínas virais interferem também na via de PTGS em diferentes etapas, como produção de siRNA, carregamento de siRNA no complexo efetor, e expressão de proteínas envolvidas na via relacionada ao silenciamento gênico (Burgyán e Havelda, 2011; Diaz-Pendon e Ding, 2008; Raja *et al*., 2010;). Resultados de perfil transcricional em protoplastos de Arabidopsis transfectados com TrAP de ACMV (*African cassava mosaic virus*) ou de MYMV (*Mungbean yellow mosaic virus*) sugeriram que esta proteína viral pode suprimir o silenciamento gênico por meio da ativação da expressão de uma proteína celular, WEL1 (*Werner exonuclease-like 1 protein*), que pode funcionar como um regulador negativo endógeno do sistema (Trinks *et al*., 2005). Além disso, TrAP induz a expressão e interage com uma calmodulina-*like* (At-rgsCaM) de Arabidopsis (Chung *et al*., 2014), relacionada a reguladores conhecidos do silenciamento de RNA em tomate e *N. tabacum* (Anandalakshmi *et al*., 2000). Da mesma forma, a atividade

supressora viral do silenciamento de RNA de βC1, codificada pelo DNA satélite de TYLCCNV (*Tomato yellow leaf curl China virus*), é dependente de uma calmodulina-*like* de *N. benthamiana*, Nb-rgsCaM. A indução de Nb-rgsCaM por βC1 resultou na supressão do silenciamento de RNA, provavelmente por meio da redução dos níveis de mRNA de RDR6 (Li *et al*., 2014). Estes resultados demonstram que a supressão do PTGS realizado por βC1 é mediado por meio de supressores endógenos do hospedeiro de silenciamento de RNA (ESR). Já a proteína AC4 de ACMV e de vírus *East African cassava mosaic virus* (EACMV)-*like* suprime o PTGS (Fondong *et al*., 2007; Vanitharani *et al*., 2004) pela ligação a miRNA e a siRNA (Chellappan *et al*., 2005). A proteína AC5 de MYMIV, além do envolvimento na supressão do TGS citado acima, atua também suprimindo o PTGS induzido por ssRNA, mas não o PTGS induzido por dsRNA, indicando que esta proteína viral pode suprimir a formação de dsRNA, sem interferir com a ação de siRNAs (Li *et al*., 2015).

Referências bibliográficas

Ahuja, I., Kissen, R., Bones, A.M. (2012) Phytoalexins in defense against pathogens. *Trends Plant Sci*, 17, 73-90.

Akbergenov, R., Si-Ammour, A., Blevins, T., Amin, I., Kutter, C., Vanderschuren, H., Zhang, P., Gruissem, W., Meins, F. Jr., Hohn, T., Pooggin, M.M. (2006) Molecular characterization of geminivirus-derived small RNAs in different plant species. *Nucleic Acids Res*, 34, 462-471.

Alazem, M., Lin, N-S. (2014) Roles of plant hormones in the regulation of host–virus interactions. *Mol Plant Pathol*, 16, 529-540.

Alfano, J.R., Collmer, A. (1997) The type III (Hrp) secretion pathway of plant pathogenic bacteria: trafficking harpins, Avr proteins, and death. *J Bacteriol*, 179, 5655-5662.

Amin, I., Patil, B.L., Briddon, R.W., Mansoor, S., Fauquet, C.M. (2011) A common set of developmental miRNAs are upregulated in Nicotiana benthamiana by diverse begomoviruses. *Virol J*, 8, 143.

Anandalakshmi, R., Marathe, R., Ge, X., Herr Jr., J.M., Mau, C., Mallory, A., Pruss, G., Bowman, L., Vance, V.B. (2000) A calmodulin-related protein that suppresses posttranscriptional gene silencing in plants. *Science*, 290, 142-144.

Andreasson, E., Jenkins, T., Brodersen, P., Thorgrimsen, S., Petersen, N.H., Zhu, S., Qiu, J.L., Micheelsen, P., Rocher, A., Petersen, M., Newman, M-A., Nielses, H.B., Hirt, H., Somssich, I., Mattsson, O., Mundy, J. (2005) The MAP kinase substrate MKS1 is a regulator of plant defense responses. *EMBO J*, 24, 2579-2589.

Aregger, M., Borah, B.K., Seguin, J., Rajeswaran, R., Gubaeva, E.G., Zvereva, A.S., Windels, D., Vazquez, F., Blevins, T., Farinelli, L., Pooggin, M.M. (2012) Primary and secondary siRNAs in geminivirus-induced gene silencing. *PLoS Pathog*, 8, e1002941.

Argüello-Astorga, G., Herrera-Estrella, L., Rivera-Bustamante, R. (1994) Experimental and theoretical definition of geminivirus origin of replication. *Plant Mole Biol*, 26, 553-556.

Argüello-Astorga, G., Lopez-Ochoa, L., Kong, L.J., Orozco, B.M., Settlage, S.B., Hanley-Bowdoin, L. (2004) A novel motif in geminiviral replication proteins interacts with the plant retinoblastoma related protein. *J Virol*, 78, 4817-4826.

Argüello-Astorga, G.R., Ruiz-Medrano, R. (2001) An iteron-related domain is associated to motif 1 in the replication proteins of geminiviruses: identification of potential interacting amino acid-base pairs by a comparative approach. *Arch Virol*, 146, 1465-1485.

Ascencio-Ibáñez, J.T., Sozzani, R., Lee, T-J., Chu, T-M., Wolfinger, R.D., Cella, R., Hanley-Bowdoin, L. (2008) Global Analysis of Arabidopsis Gene Expression Uncovers a Complex Array of Changes Impacting Pathogen Response and Cell Cycle during Geminivirus Infection. *Plant Physiol*, 148, 436-454.

Baena-Gonzalez, E., Rolland, F., Thevelein, J.M., Sheen, J. (2007) A central integrator of transcription networks in plant stress and energy signalling. *Nature*, 448, 938-942.

Bagewadi, B., Chen, S., Lal, S.K., Choudhury, N.R., Mukherjee, S.K. (2004) PCNA interacts with Indian mung bean yellow mosaic virus rep and downregulates Rep activity. *J Virol*, 78, 11890-11903.

Berger, M.R., Sunter, G. (2013) Identification of sequences required for AL2-mediated activation of the *Tomato golden mosaic virus-yellow vein* BR1 promoter. *J Gen Virol*, 94, 1398-1406.

Bisaro, D.M. (2006) Silencing suppression by geminivirus proteins. *Virology*, 344, 158-168.

Blevins, T., Rajeswaran, R., Shivaprasad, P.V., Beknazariants, D., Si-Ammour, A., Park, H.S., Vazquez, F., Robertson, D., Meins, F.Jr., Hohn, T., Pooggin, M.M. (2006) Four plant Dicers mediate viral small RNA biogenesis and DNA virus induced silencing. *Nucleic Acids Res*, 34, 6233-6246.

Bochman, M.L., Schwacha, A. (2008) The MCM2-7 complex has *in vitro* helicase activity. *Mol Cell*, 31, 287-293.

Bohm, H., Albert, I., Fan, L., Reinhard, A., Nurnberger, T. (2014) Immune receptor complexes at the plant cell surface. *Curr Opin Plant Biol*, 20, 47-54.

Boller, T., Felix, G. (2009) A renaissance of elicitors: perception of microbe-associated molecular patterns and danger signals by pattern-recognition receptors. *Annu Rev Plant Biol*, 60, 379-406.

Boudsocq, M., Sheen, J. (2013) CDPKs in immune and stress signaling. *Trends Plant Sci*, 18, 30-40.

Boutrot, F., Segonzac, C., Chang, K.N., Qiau, H., Ecker, J.R., Zipfel, C., Rathjen, J.P. (2010) Direct transcriptional control of the Arabidopsis immune receptor FLS2 by the ethylene-dependent transcription factors EIN3 and EIL1. *Proc Natl Acad Sci USA*, 107, 14502-14507.

Briddon, R.W., Patil, B.L., Bagewadi, B., Nawaz-ul-Rehman, M.S., Fauquet, C.M. (2010) Distinct evolutionary histories of the DNA-A and DNA-B components of bipartite begomoviruses. *BMC Evol Biol*, 10, 97.

Briddon, R.W., Pinner, M.S., Stanley, J., Markham, P.G. (1990) Geminivirus coat protein replacement alters insect specificity. *Virology*, 177, 85-94.

Briddon, R.W., Stanley, J. (2006) Subviral agents associated with plant single-stranded DNA viruses. *Virology*, 344, 198-210.

Brown, J.K., Fauquet, C.M., Briddon, R.W., Zerbini, F.M., Moriones, E., Navas-Castillo, J. (2012) Family Geminiviridae. In *Virus Taxonomy 9th Report of the International committee on taxonomy of viruses*. Edited by King, A.M.Q., Adams, M.J., Carstens, E.B., Lefkowitz, E.J. Elsevier Academic Press, London, 351-373.

Buchmann, R.C., Asad, S., Wolf, J.N., Mohannath, G., Bisaro, D.M. (2009) Geminivirus AL2 and L2 proteins suppress transcriptional gene silencing and cause genome-wide reductions in cytosine methylation. *J Virol*, 83, 5005-5013.

Burgyán, J., Havelda, Z. (2011) Viral suppressors of RNA silencing. *Trends Plant Sci*, 16, 265-272.

Carvalho, C.M., Fontenelle, M.R., Florentino, L.H., Santos, A.A., Zerbini, F.M., Fontes, E.P.B. (2008a) A novel nucleocytoplasmic traffic GTPase identified as a functional target of the bipartite geminivirus nuclear shuttle protein. *Plant J*, 5, 869-80.

Carvalho, C.M., Machado, J.P.B., Zerbini, F.M., Fontes, E.P.B. (2008b) NSP-interacting GTPase: A cytosolic protein as cofactor for nuclear shuttle proteins. *Plant Signal Behav*, 3, 752-754.

Carvalho, C.M., Santos, A.A., Pires, S.R., Rocha, C.S., Saraiva, D.I., Machado, J.P.B., Mattos, E.C., Fietto, L.G., Fontes, E.P.B. (2008c) Regulated Nuclear Trafficking of rpL10A Mediated by NIK1 Represents a Defense Strategy of Plant Cells against Virus. *PLoS Pathog*, 4, e1000247.

Carvalho, M.F., Turgeon, R., Lazarowitz, S.G. (2006) The Geminivirus Nuclear Shuttle Protein NSP Inhibits the Activity of AtNSI, a Vascular-Expressed Arabidopsis Acetyltransferase Regulated with the Sink-to-Source Transition. *Plant Physiol*, 140, 1317-1330.

Castillo, A.G., Collinet, D., Deret, S., Kashoggi, A., Bejarano, E.R. (2003) Dual interaction of plant PCNA with geminivirus replication accessory protein (Ren) and viral replication protein (Rep). *Virology*, 312, 381-394.

Castillo, A.G., Kong, L.J., Hanley-Bowdoin, L., Bejarano, E.R. (2004) Interaction between a geminivirus replication protein and the plant sumoylation system. *J Virol*, 78, 2758-2769.

Castro, P.H., Tavares, R.M., Bejarano, E.R., Azevedo, H. (2012) SUMO, a heavyweight player in plant abiotic stress responses. *Cell Mol Life Sci*, 69, 3269-3283.

Catanzariti, A.M., Dodds, P.N., Ve T., Kobe, B., Ellis, J.G., Staskawicz, B.J. (2010) The AvrM effector from flax rust has a structured C-terminal domain and interacts directly with the M resistance protein. *Mol Plant-Microbe Interact*, 23, 49-57.

Cesari, S., Thilliez, G., Ribot, C., Chalvon, V., Michel, C., Jauneau, A., Rivas, S., Alaux, L., Kanzaki, H., Okuyama, Y., Morel, J-B., Fournier, E., Tharreau, D., Terauchi, R., Kroj, T. (2013) The rice resistance protein pair RGA4/RGA5 recognizes the *Magnaporthe oryzae* effectors AVR-Pia and AVR1-CO39 by direct binding. *Plant Cell*, 25, 1463-1481.

Chanda, B., Xia, Y., Mandal, M.K., Yu, K., Sekine, K.T., Gao, Q.M., Selote, D., Hu, Y., Stromberg, A., Navarre, D., Kachroo, A., Kachroo, P. (2011) Glycerol-3-phosphate is a critical mobile inducer of systemic immunity in plants. *Nat Genet*, 43, 421-27.

Chapman, E.J., Prokhnevsky, A. I., Gopinath, K., Dolja, V. V., Carrington, J.C. (2004) Viral RNA silencing suppressors inhibit the microRNA pathway at an intermediate step. *Genes Dev*, 18, 1179-1186.

Chaturvedi, R., Venables, B., Petros, R.A., Nalam, V., Li, M., Wang, X., Takemoto, L.J., Shah, J. (2012) An abietane diterpenoid is a potente activator of systemic acquired resistance. *Plant J*, 71, 161-72.

Chellappan, P., Vanitharani, R., Fauquet, C.M. (2005) MicroRNA-binding viral protein interferes with Arabidopsis development. *Proc Natl Acad Sci USA*, 102, 10381-10386.

Chen, H., Xue, L., Chintamannani, S., Germain, H., Lin, H., Cui, H., Cai, R., Zuo, J., Tang, X., Li, X., Guo, H., Zhou, J.M. (2009) ETHYLENE INSENSITIVE3 and ETHYLENE INSENSITIVE3-LIKE1 repress SALICYLIC ACID INDUCTION DEFICIENT2 expression to negatively regulate plant innate immunity in Arabidopsis. *Plant Cell*, 21, 2527-2540.

Chung, H.Y., Lacatus, G., Sunter, G. (2014) Geminivirus AL2 protein induces expression of, and interacts with, a calmodulin-like gene, an endogenous regulator of gene silencing. *Virology*, 460, 108-118.

Chung, H.Y., Sunter, G. (2014) Interaction between the transcription factor AtTIFY4B and begomovirus AL2 protein impacts pathogenicity. *Plant Mol Biol*, 86, 185-200.

Collier, S.M., Moffett, P. (2009) NB-LRRs work a “bait and switch” on pathogens. *Trends Plant Sci*, 14, 521-529.

Cui, H., Tsuda, K., Parker, J.E. (2015) Effector-Triggered Immunity: From Pathogen Perception to Robust Defense. *Annu Rev Plant Biol*, 66, 487-511.

Cui, X., Li, G., Wang, D., Hu, D., Zhou, X. (2005) A begomovirus DNAβ-encoded protein binds DNA, functions as a suppressor of RNA silencing, and targets the cell nucleus. *J Virol*, 79, 10764-10775.

Davidsson, P.R., Kariola, T., Niemi, O., Palva, E.T. (2013) Pathogenicity of and plant immunity to soft rot pectobacteria. *Front Plant Sci*, 4, 191.

Deslandes, L., Olivier, J., Peeters, N., Feng, D.X., Khounlotham, M., Boucher, C., Somssich, I., Genin, S., Marco, Y. (2003) Physical interaction between RRS1-R, a protein conferring resistance to bacterial wilt, and PopP2, a type III effector targeted to the plant nucleus. *Proc Natl Acad Sci USA*, 100, 8024-8029.

Desvoyes, B., Ramirez-Parra, E., Xie, Q., Chua, N.H., Gutierrez, C. (2006) Cell type-specific role of the retinoblastoma/E2F pathway during Arabidopsis leaf development. *Plant Physiol*, 140, 67-80.

Diaz-Pendon, J.A., Ding, S.W. (2008) Direct and indirect roles of viral suppressors of rna silencing in pathogenesis. *Annu Rev Phytopathol*, 46, 303-326.

Dodds, P.N., Rathjen, J.P. (2010) Plant immunity: towards an integrated view of plant-pathogen interactions. *Nat Rev Genet*, 11, 539-548.

Donaire, L., Barajas, D., Martínez-García, B., Martínez-Priego, L., Pagán, I., Llave, C. (2008) Structural and genetic requirements for the biogenesis of *Tobacco rattle virus*-derived small interfering RNAs. *J Virol*, 82, 5167-5177.

Dubiella, U., Seybold, H., Durian, G., Komander, E., Lassig, R., Witte, C.P., Schulze, W.X., Romeis, T. (2013) Calcium-dependent protein kinase/NADPH oxidase

activation circuit is required for rapid defense signal propagation. *Proc Natl Acad Sci USA*, 110, 8744-8749.

Durrant, W.E., Dong, X. (2004) Systemic acquired resistance. *Annu Rev Phytopathol*, 42, 185-209.

Eagle, P.A., Orozco, B.M., Hanley-Bowdoin, L. (1994) A DNA sequence required for geminivirus replication also mediates transcriptional regulation. *Plant Cell*, 6, 1157-1170.

Egelkrout, E.M., Robertson, D., Hanley-Bowdoin, L. (2001) Proliferating cell nuclear antigen transcription is repressed through an E2F consensus element and activated by geminivirus infection in mature leaves. *Plant Cell*, 13, 1437-1452.

Eini, O., Dogra, S., Selth, L.A., Dry, I.B., Randles, J.W., Rezaian, M.A. (2009) Interaction with a host ubiquitin-conjugating enzyme is required for the pathogenicity of a geminiviral DNA βsatellite. *Mol Plant Microbe Interact*, 22, 737-746.

Elmer, J.S., Brand, L., Sunter, G., Gardiner, W., Bisaro, D.M., Rogers, S.G. (1998) Genetic analysis of the tomato golden mosaic virus II. The product of the AL1 coding sequence is required for replication. *Nucleic Acids Resort*, 16, 7043-7060.

Fauquet, C.M., Briddon, R.W., Brown, J.K., Moriones, E., Stanley, J., Zerbini, M., Zhou, X. (2008) Geminivirus strain demarcation and nomenclature. *Arch Virol*, 153, 783-821.

Fernandes, F.R., de Albuquerque, L.C., de Britto Giordano, L., Boiteux, L.S., de Avila, A.C., Inoue-Nagata, A.K. (2008) Diversity and prevalence of Brazilian bipartite *Begomovirus* species associated to tomatoes. *Virus Genes*, 36, 251-258.

Finnegan, E.J., Matzke, M.A. (2003) The small RNA world. *J Cell Sci*, 116, 4689-4693.

Flor, H.H. (1971) Current status of the gene-for-gene concept. *Annu Ver Phytopathol*, 9, 275-296.

Florentino, L.H., Santos, A.A., Fontenelle, M.R., Pinheiro, G.L., Zerbini, F.M., Baracat-Pereira, M.C., Fontes, E.P.B. (2006) A PERK-Like receptor kinase interacts with the geminivirus nuclear shuttle protein and potentiates viral infection. *J Virol*, 80, 6648-6656.

Fondong, V.N. (2013) Geminivirus protein structure and function. *Mol Plant Pathol*, 14, 635-649.

Fondong, V.N., Reddy, R.V., Lu, C., Hankoua, B., Felton, C., Czymmek, K., Achenjang, F. (2007) The consensus N-myristoylation motif of a geminivirus AC4 protein is required for membrane binding and pathogenicity. *Mol Plant–Microbe Interact*, 20, 380-391.

Fontes, E.P.B., Eagle, P.A., Sipe, P.S., Luckow, V.A., Hanley-Bowdoin, L. (1994) Interaction between a geminivirus replication protein and origin DNA is essential for viral replication. *J Biol Chem*, 269, 8459-8465.

Fontes, E.P.B., Santos, A.A., Luz, D.F., Waclawovsky, A.J., Chory, J. (2004) The geminivirus nuclear shuttle protein is a virulence factor that suppresses transmembrane receptor kinase activity. *Genes Dev*, 18, 2545-2556.

Frischmuth, S., Wege, C., Hulser, D., Jeske, H. (2007) The movement protein BC1 promotes redirection of the nuclear shuttle protein BV1 of Abutilon mosaic geminivirus to the plasma membrane in fission yeast. *Protoplasma*, 230, 117-123.

Fu, Z.Q., Dong, X. (2013) Systemic Acquired Resistance: Turning Local Infection into Global Defense. *Annu Rev Plant Biol*, 64, 839-863.

Fu, Z.Q., Yan, S., Saleh, A., Wang, W., Ruble, J., Oka, N., Mohan, R., Spoel, S.H., Tada, Y., Zheng, N., Dong, X. (2012) NPR3 and NPR4 are receptors for the immune signal salicylic acid in plants. *Nature*, 486, 228-232.

Gao, X., Chen, X., Lin, W., Chen, S., Lu, D., Niu, Y., Li, L., Cheng, C., McCormack, M., Sheen, J., Shan, L., He, P. (2013) Bifurcation of Arabidopsis NLR immune signaling via Ca^{2+}-dependent protein kinases. *PLoS Pathog*, 9, e1003127.

Glazebrook, J. (2005) Contrasting mechanisms of defense against biotrophic and necrotrophic pathogens. *Annu Rev Phytopathol*, 43, 205-227.

Gloggnitzer, J., Akimcheva, S., Srinivasan, A., Kusenda, B., Riehs, N., Stampfl, H., Bautor, J., Dekrout, B., Jonak, C., Jiménez-Gómez, J.M., Parker, J.E., Riha, K. (2014) Nonsense-mediated mRNA decay modulates immune receptor levels to regulate plant antibacterial defense. *Cell Host Microbe*, 16, 376-390.

Gomes, X.V., Schmidt, S.L., Burgers, P.M. (2001) ATP utilization by yeast replication factor C. II. Multiple stepwise ATP binding events are required to load proliferating cell nuclear antigen onto primed DNA. *J Biol Chem*, 276, 34776-34783.

Gomez-Gomez, L., Boller, T. (2000) FLS2: an LRR receptor-like kinase involved in the perception of the bacterial elicitor flagellin in Arabidopsis. *Mol Cell*, 5, 1003-1011.

Gottlieb, Y., Zchori-Fein, E., Mozes-Daube, N., Kontsedalov, S., Skaljac, M., Brumin, M., Sobol, I., Czosnek, H., Vavre, F., Fleury, F., Ghanim, M. (2010) The transmission efficiency of *Tomato yellow leaf curl virus* by the whitefly *Bemisia tabaci* is correlated with the presence of a specific symbiotic bacterium species. *J Virol*, 84, 9310-9317.

Griebel, T., Maekawa, T., Parker, J.E. (2014) NOD-like receptor cooperativity in effector-triggered immunity. *Trends Immunol*, 35, 562-570.

Guo, H.W., Ecker, J.R. (2003) Plant responses to ethylene gas are mediated by SCF (EBF1/EBF2)-dependent proteolysis of EIN3 transcription factor. *Cell*, 115, 667-677.

Hanley-Bowdoin, L., Bejarano, E.R., Robertson, D., Mansoor, S. (2013) Geminiviruses: masters at redirecting and reprogramming plant processes. *Nat Rev Microbiol*, 11, 777-788.

Hanley-Bowdoin, L., Settlage, S.B., Orozco, B.M., Nagar, S., Robertson, D. (2000) Geminiviruses: models for plant DNA replication, transcription, and cell cycle regulation. *Crit Rev Biochem Mol Biol*, 35, 105-140.

Hanley-Bowdoin, L., Settlage, S.B., Robertson, D. (2004) Reprogramming plant gene expression: a prerequisite to geminivirus DNA replication. *Mol Plant Pathol*, 5, 149-156.

Hao, L., Wang, H., Sunter, G., Bisaro, D.M. (2003) Geminivirus AL2 and L2 proteins interact with and inactivate SNF1 kinase. *Plant Cell*, 15, 1034-1048.

Hartitz, M.D., Sunter, G., Bisaro, D.M. (1999) The geminivirus transactivator (TrAP) is a zinc-binding phosphoprotein with an acidic activation domain. *Virology*, 263, 1-14.

Harvey, J.J., Lewsey, M.G., Patel, K., Westwood, J., Heimstädt, S., Carr, J.P., Baulcombe, D.C. (2011) An antiviral defense role of AGO2 in plants. *PLoS ONE*, 6, e14639.

Havelda, Z., Hornyik, C., Crescenzi, A., Burgyán, J. (2003) In situ characterization of *Cymbidium ringspot tombusvirus* infection-Induced posttranscriptional gene silencing in *Nicotiana benthamiana*. *J Virol*, 77, 6082-6086.

Hehnle, S., Wege, C., Jeske, H. (2004) Interaction of DNA with the movement proteins of geminiviruses revisited. *J Virol*, 78, 7698-7706.

Höhnle, M., Hofer, P., Bedford, I.D., Briddon, R.W., Markham, P.G., Frischmuth, T. (2001) Exchange of three amino acids in the coat protein results in eficiente whitefly transmission of a nontransmissible *Abutilon mosaic virus* isolate. *Virology,* 290, 164-171.

Hotton, S.K., Callis, J. (2008) Regulation of cullin RING ligases. *Annu Rev Plant Biol*, 59, 467-489.

Huang, L., Jones, A.M., Searle, I., Patel, K., Vogler, H., Hubner, N.C., Baulcombe, D.C. (2009) An atypical RNA polymerase involved in RNA silencing shares small subunits with RNA polymerase II. *Nat Struct Mol Biol*, 16, 91-93.

Incarbone, M., Dunoyer, P. (2013) RNA silencing and its suppression: novel insights from in planta analyses. *Trends Plant Sci*, 18, 382-392.

Ingham, D.J., Pascal, E., Lazarowitz, S.G. (1995) Both bipartite geminivirus movement proteins define viral host range, but only BL1 determines viral pathogenicity. *Virology*, 207, 191-204.

Jacob, F., Vernaldi, S., Maekawa, T. (2013) Evolution and conservation of plant NLR functions. *Front Immunol*, 4, 297.

Jeske, H., Kober, S., Schäfer, B., Strohmeier, S., (2014) Circomics of Cuban geminiviruses reveals the first alpha-satellite DNA in the Caribbean. *Virus Genes*, 49, 312-324.

Jeske, H., Lutgemeier, M., Preisz, W. (2001) DNA forms indicate rolling circle and recombination-dependent replication of *Abutilon mosaic virus*. *EMBO J*, 20, 6158-6167.

Jia, Y., McAdams, S.A., Bryan, G.T., Hershey, H.P., Valent, B. (2000) Direct interaction of resistance gene and avirulence gene products confers rice blast resistance. *EMBO J*, 19, 4004-4014.

Jones, J.D., Dangl, J.L. (2006) The plant immune system. *Nature*, 444, 323-329.

Jyothsna, P., Haq, Q.M., Singh, P., Sumiya, K.V., Praveen, S., Rawat, R., Briddon, R.W. and Malathi, V.G. (2013) Infection of *Tomato leaf curl New Delhi virus* (ToLCNDV), a bipartite begomovirus with betasatellites, results in enhanced level of helper virus components and antagonistic interaction between DNA B and betasatellites. *Appl Microbiol Biotechnol*, 97, 5457-5471.

Kaliappan, K., Choudhury, N.R., Suyal, G., Mukherjee, S.K. (2012) A novel role for RAD54: this host protein modulates geminiviral DNA replication. *FASEB J*, 26, 1142-1160.

Kamiyoshihara, Y., Iwata, M., Fukaya, T., Tatsuki, M., Mori, H. (2010) Turnover of LeACS2, a wound-inducible 1-aminocyclopropane-1-carboxylic acid synthase in tomato, is regulated by phosphorylation/dephosphorylation. *Plant J*, 64,140-150.

Kamthan, A., Chaudhuri, A., Kamthan, M., Datta, A. (2015) Small RNAs in plants: recent development and application for crop improvement. *Front Plant Sci*, 6, 208.

Kasschau, K. D., Xie, Z., Allen, E., Llave, C., Chapman, E. J., Krizan, K. A., Carrington, J. C. (2003) P1/HC-Pro, a viral suppressor of RNA silencing, interferes with Arabidopsis development and miRNA function. *Dev Cell*, 4, 205-217.

Kleinow, T., Nischang, M., Beck, A., Kratzer, U., Tanwir, F., Preiss, W., Kepp, G., Jeske, H. (2009a) Three C-terminal phosphorylation sites in the *Abutilon mosaic virus* movement protein affect symptom development and viral DNA accumulation. *Virology*, 390, 89-101.

Kleinow, T., Tanwir, F., Kocher, C., Krenz, B., Wege, C., Jeske, H. (2009b) Expression dynamics and ultrastructural localization of epitope-tagged Abutilon mosaic virus nuclear shuttle and movement proteins in *Nicotiana benthamiana* cells. *Virology*, 391, 212-220.

Kong, L-J., Hanley-Bowdoin, L. (2002) A geminivirus replication protein interacts with a protein kinase and a motor protein that display different expression patterns during plant development and infection. *Plant Cell*, 14, 1817-1832.

Kong, L-J., Orozco, B.M., Roe, J.R., Nagar, S., Ou, S., Feiler, H.S., Durfee, T., Miller, A.B., Gruissem, W., Robertson, D., Hanley-Bowdoin, L. (2000) A geminivirus replication protein interacts with the retinoblastoma protein through a novel domain to determine symptoms and tissue specificity of infection in plants. *EMBO J*, 19, 3485-3495.

Krenz, B., Windeisen, V., Wege, C., Jeske, H., Kleinow, T. (2010) A plastid-targeted heat shock cognate 70 kDa protein interacts with the Abutilon mosaic virus movement protein. *Virology*, 401, 6-17.

Lacatus, G., Sunter, G. (2009) The Arabidopsis PEAPOD2 transcription fator interacts with geminivirus AL2 protein and the coat protein promoter. *Virology*, 392, 196-202.

Law, J.A., Jacobsen, S.E. (2010) Establishing, maintaining and modifying DNA methylation patterns in plants and animals. *Nat Rev Genet*, 11, 204-220.

Lazarowitz, S.G. (1992) Geminiviruses: genomes structure and gene function. *Crit Rev Plant Sci*, 11, 327-349.

Lazarowitz, S.G., Beachy, R.N. (1999) Viral movement proteins as probes for intracellular and intercellular trafficking in plants. *Plant Cell*, 11, 535-548.

Lewis, J.D., Lazarowitz, S.G. (2010) Arabidopsis synaptotagmin SYTA regulates endocytosis and virus movement protein cell-to-cell transport. *Proc Nat Acad Sci USA*, 107, 2491-2496.

Li, F., Huang, C., Li , Z., Zhou, X. (2014) Suppression of RNA Silencing by a Plant DNA Virus Satellite Requires a Host Calmodulin-Like Protein to Repress *RDR6* Expression. *PLoS Pathog*, 10, e1003921.

Li, F., Xu, X., Huang, C., Gu, Z., Cao, L., Hu, T., Ding, M., Li, Z., Zhou, X. (2015) The AC5 protein encoded by *Mungbean yellow mosaic India virus* is a pathogenicity determinant that suppresses RNA silencing-based antiviral defenses. *New Phytol*, doi: http://dx.doi.org/10.1111/nph.13473.

Lin, W., Ma, X., Shan, L., He, P. (2013) Big roles of small kinases: the complex functions of receptor-like cytoplasmic kinases in plant immunity and development. *J Integr Plant Biol*, 55, 1188-1197.

Liu, F., Ni, W., Griffith, M.E., Huang, Z., Chang, C., Peng, W., Ma, H., Xie, D. (2004) The ASK1 and ASK2 genes are essential for Arabidopsis early development. *Plant Cell*, 16, 5-20.

Liu, Y., Zhang, S. (2004) Phosphorylation of 1-aminocyclopropane-1-carboxylic acid synthase by MPK6, a stress-responsive mitogen-activated protein kinase, induces ethylene biosynthesis in Arabidopsis. *Plant Cell*, 16, 3386-3399.

Loor, G., Zhang, S., Zhang, P., Toomey, N.L., Lee, M.Y.W. (1997) Identification of DNA replication and cell cycle proteins that interact with PCNA. *Nucleic Acids Res*, 25, 5041-5046.

Lozano-Durán, R., Rosas-Díaz, T., Gusmaroli, G., Luna, A.P., Taconnat, L., Deng, X.W., Bejarano, E.R. (2011a) Geminiviruses subvert ubiquitination by altering CSN-mediated derubylation of SCF E3 ligase complexes and inhibit jasmonate signaling in *Arabidopsis thaliana*. *Plant Cell*, 23, 1014-1032.

Lozano-Durán, R., Rosas-Díaz, T., Luna, A.P., Bejarano, E.R. (2011b) Identification of Host Genes Involved in Geminivirus Infection Using a Reverse Genetics Approach. *PLoS ONE*, 6, e22383.

Luque, A., Sanz-Burgos, A.P., Ramirez-Parra, E., Castellano, M.M., Gutierrez, C. (2002) Interaction of geminivirus Rep protein with replication factor C and its potential role during geminivirus DNA replication. *Virology*, 302, 83-94.

Macho, A.P., Zipfel, C. (2014) Plant PRRs and the activation of innate immune signaling. *Mol Cell*, 54, 263-272.

Maga, G., Hubscher, U. (2003) Proliferating cell nuclear antigen (PCNA): a dancer with many partners. *J Cell Sci*, 116, 3051-3060.

Malinovsky, F.G., Fangel, J.U., Willats, W.G.T. (2014) The role of the cell wall in plant immunity. *Front Plant Sci*, 5,178.

Mao, G., Meng, X., Liu, Y., Zheng, Z., Chen, Z., Zhang, S. (2011) Phosphorylation of a WRKY transcription factor by two pathogenresponsive MAPKs drives phytoalexin biosynthesis in Arabidopsis. *Plant Cell*, 23,1639-1653.

Mariano, A.C., Andrade, M.O., Santos, A.A., Carolino, S.M.B., Oliveira, M.L., Baracat-Pereira, M.C., Brommonshenkel, S.H., Fontes, E.P.B. (2004) Identification of a novel receptor-like protein kinase that interacts with a geminivirus nuclear shuttle protein. *Virology*, 318, 24-31.

Marino, D., Peeters, N., Rivas, S. (2012) Ubiquitination during plant immune signaling. *Plant Physiol*, 160, 15-27.

McGarry, R.C., Barron, Y.D., Carvalho, M.F., Hill, J.E., Gold, D., Cheung, E., Kraus, W.L., Lazarowitz, S.G. (2003) A novel Arabidopsis acetyltransferase interacts with the geminivirus movement protein NSP. *Plant Cell*, 15, 1605-1618.

Meng, X., Zhang, S. (2013) MAPK cascades in plant disease resistance signaling. *Annu Rev Phytopathol*, 51, 245-266.

Mersmann, S., Bourdais, G., Rietz, S., Robatzek, S. (2010) Ethylene signaling regulates accumulation of the FLS2 receptor and is required for the oxidative burst contributing to plant immunity. *Plant Physiol*, 154, 391-400.

Metraux, J.P., Signer, H., Ryals, J., Ward, E., Wyss-Benz, M., Gaudin, J., Raschdorf, K., Schmid, E., Blum, W., Inverardi, B. (1990) Increase in salicylic acid at the onset of systemic acquired resistance in cucumber. *Science*, 250, 1004-1006.

Moffat, A.C. (1999) Plant pathology-geminiviruses emerge as serious crop threat. *Science*, 286, 1835-1835.

Molnar, A., Melnyk, C.W., Bassett, A., Hardcastle, T.J., Dunn, R., Baulcombe, D.C. (2010) Small silencing RNAs in plants are mobile and direct epigenetic modification in recipient cells. *Science*, 328, 872-875.

Morales, F.J. (2006) History and current distribution of begomoviruses in Latin America. *Adv Virus Res*, 67, 127-162.

Mukhtar, M.S., Carvunis, A.R., Dreze, M., Epple, P., Steinbrenner, J., Moore, J., Tasan, M., Galli, M., Hao, T., Nishimura, M.T., Pevzner, S.J., Donovan, S.E., Ghamsari, L., Santhanam, B., Romero, V., Poulin, M.M., Gebreab, F., Gutierrez, B.J., Tam, S., Monachello, D., Boxem, M., Harbort, C.J., McDonald, N., Gai, L., Chen, H., He, Y., European Union Effectoromics Consortium, Vandenhaute, J., Roth, F.P., Hill, D.E., Ecker, J.R., Vidal, M., Beynon, J., Braun, P., Dangl, J.L. (2011) Independently evolved virulence effectors converge onto hubs in a plant imune system network. *Science*, 333, 596-601.

Nagar, S., Pedersen, T.J., Carrick, K.M., Hanley-Bowdoin, L., Robertson, D. (1995) A geminivirus induces expression of a host DNA synthesis protein in terminally differentiated plant cells. *Plant Cell*, 7, 705-719.

Naqvi, A.R., Choudhury, N.R., Mukherjee, S.K., Haq, Q.M. (2011) In silico analysis reveals that several tomato microRNA/microRNA* sequences exhibit propensity to

bind to *Tomato leaf curl virus* (ToLCV) associated genomes and most of their encoded open reading frames (ORFs). *Plant Physiol Biochem*, 49, 13-17.

Navarro, L., Zipfel, C., Rowland, O., Keller, I., Robatzek, S., Boller, T., Jones, J.D. (2004) The transcriptional innate immune response to flg22. Interplay and overlap with Avr gene-dependent defense responses and bacterial pathogenesis. *Plant Physiol*, 135, 1113-1128.

Nawaz-ul-Rehman, M.S., Fauquet, C.M. (2009) Evolution of geminiviruses and their satellites. *FEBS Lett*, 583, 1825-1832.

Nawaz-ul-Rehman, M.S., Nahid, N., Mansoor, S., Briddon, R.W., Fauquet, C.M. (2010) Post-transcriptional gene silencing suppressor activity of two nonpathogenic alphasatellites associated with a begomovirus. *Virology*, 405, 300-308.

Nitschke, F., Schumacher, S., Laufs, J., Schaefer, S., Schell, J., Gronenborn, B. (1995) Determination of the origin cleavage and joining domain of geminivirus Rep proteins. *Nucleic Acids Res*, 23, 910-916.

Noris, E., Vaira, A.M., Caciagli, P., Masenga, V., Gronenborn, B., Accotto, G.P. (1998) Amino acids in the capsid protein of *Tomato yellow leaf curl virus* that are crucial for systemic infection, particle formation, and insect transmission. *J Virol*, 72, 10050-10057.

Nuhse, T.S. (2012) Cell wall integrity signaling and innate immunity in plants. *Front Plant Sci*, 3, 280.

O'Brien, J.A., Daudi, A., Butt, V.S., Bolwell, G.P. (2012) Reactive oxygen species and their role in plant defence and cell wall metabolism. *Planta*, 236, 765-779.

Ohnesorge, S., Bejarano, E.R. (2009) Begomovirus coat protein interacts with a small heat-shock protein of its transmission vector (*Bemisia tabaci*). *Insect Mol Biol*, 18, 693-703.

Palauqui, J-C., Elmayan, T., Pollien, J-M., Vaucheret, H. (1997) Systemic acquired silencing: transgene-specific post-transcriptional silencing is transmitted by grafting from silenced stocks to non-silenced scions. *EMBO J*, 16, 4738-4745.

Palma, K., Thorgrimsen, S., Malinovsky, F.G., Fiil, B.K., Nielsen, H.B., Brodersen, P., Hofius, D., Petersen, M., Mundy, J. (2010) Autoimmunity in Arabidopsis acd11 is mediated by epigenetic regulation of an immune receptor. *PLoS Pathog*, 6, e1001137.

Paprotka, T., Metzler, V., Jeske, H. (2010) The first DNA 1-like α satellites in association with New World begomoviruses in natural infections. *Virology*, 404, 148-157.

Park, S.W., Kaimoyo, E., Kumar, D., Mosher, S., Klessig, D.F. (2007) Methyl salicylate is a critical mobile signal for plant systemic acquired resistance. *Science*, 318, 113-116.

Pascal, E., Goodlove, P.E., Wu, L.C., Lazarowitz, S.G. (1993) Transgenic tobacco plants expressing the geminivirus BL1 protein exhibit symptoms of viral disease. *Plant Cell*, 5, 795-807.

Pascal, E., Sanderfoot, A.A., Ward, B.M., Medville, R., Turgeon, R., Lazarowitz, S.G. (1994) The geminivirus BR1 movement protein binds single-stranded DNA and localizes to the cell nucleus. *Plant Cell*, 6, 995-1006.

Pasumarthy, K.K., Choudhury, N.R., Mukherjee, S.K. (2010) *Tomato leaf curl Kerala virus* (ToLCKeV) AC3 protein forms a higher order oligomer and enhances ATPase activity of replication initiator protein (Rep/AC1). *Virol J*, 7, 128.

Patil, B.L., Fauquet, C.M. (2010) Differential interaction between cassava mosaic geminiviruses and geminivirus satellites. *J Gen Virol*, 91, 1871-1882.

Pilartz, M., Jeske, H. (2003) Mapping of Abutilon Mosaic Geminivirus Minichromosomes. *J Virol*, 77, 10808-10818.

Preiss, W., Jeske, H., (2003) Multitasking in replication is common among geminiviruses. *J Virol*, 77, 2972-2980.

Pritchard, L., Birch, P.A. (2011) Systems biology perspective on plant–microbe interactions: biochemical and structural targets of pathogen effectors. *Plant Sci*, 180, 584-603.

Qi, X., Bao, F.S., Xie, Z. (2009) Small RNA deep sequencing reveals role for *Arabidopsis thaliana* RNA-dependent RNA polymerases in viral siRNA biogenesis. *PLoS ONE*, 4, e4971.

Qiu, J.L., Fiil, B.K., Petersen, K., Nielsen, H.B., Botanga, C.J., Thorgrimsen, S., Palma, K., Suarez-Rodriguez, M.C., SandbechClausen, S., Lichota, J., Brodersen, P., Grasser, K.D., Mattsson, O., Glazebrook, J., Mundy, J., Petersen, M. (2008) Arabidopsis MAP kinase 4 regulates gene expression through transcription factor release in the nucleus. *EMBO J*, 27, 2214-2221.

Qu, F. (2010) Antiviral role of plant-encoded RNA-dependent RNA polymerases revisited with deep sequencing of small interfering RNAs of virus origin. *Mol Plant Microbe Interact*, 23, 1248-1252.

Raja, P., Sanville, B.C., Buchmann, R.C., Bisaro, D.M. (2008) Viral genome methylation as an epigenetic defense against geminiviruses. *J Virol*, 82, 8997-9007.

Raja, P., Wolf, J.N., Bisaro, D.M. (2010) RNA silencing directed against geminiviruses: post-transcriptional and epigenetic components. *Biochim Biophys Acta*, 1799, 337-351.

Rana, V.S., Singh, S.T., Priya, N.G., Kumar, J., Rajagopal, R. (2012) *Arsenophonus* GroEL interacts with CLCuV and is localized in midgut and salivary gland of whitefly *B. tabaci*. *PLoS ONE*, 7, e42168.

Ranf, S., Eschen-Lippold, L., Pecher, P., Lee, J., Scheel, D. (2011) Interplay between calcium signalling and early signalling elements during defence responses to microbe- or damage-associated molecular patterns. *Plant J*, 68, 100-113.

Rasmussen, M.W., Roux, M., Petersen, M., Mundy, J. (2012) MAP kinase cascades in Arabidopsis innate immunity. *Front Plant Sci*, 3, 169.

Rayapuram, N., Bonhomme, L., Bigeard, J., Haddadou, K., Przybylski, C., Hirt, H., Pflieger, D. (2014) Identification of novel PAM-Ptriggered phosphorylation and

dephosphorylation events in *Arabidopsis thaliana* by quantitative phosphoproteomic analysis. *J Proteome Res*, 13, 2137-2151.

Rey, M.E.C., Ndunguru, J., Berrie, L.C., Paximadis, M., Berry, S., Cossa, N., Nuaila, V.N., Mabasa, K.G., Abraham, N., Rybicki, E.P., Martin, D., Pieterson, G., Esterhuizen, L.L. (2012) Diversity of dicotyledenous-infecting geminiviruses and their associated DNA molecules in Southern Africa, including the South-west Indian ocean islands. *Viruses*, 4, 1753-1791.

Ribeiro, S.G., Ambrozevicius, L.P., Avila, A.C., Bezerra, I.C., Calegario, R.F., Fernandes, J.J., Lima, M.F., de Mello, R.N., Rocha, H., Zerbini, F.M. (2003) Distribution and genetic diversity of tomato-infecting begomoviruses in Brazil. *Arch Virol*, 148, 281-295.

Richter, K.S., Ende, L., Jeske, H. (2015) Rad54 is not essential for any geminiviral replication mode *in planta*. *Plant Mol Biol*, 87, 193-202.

Rizvi, I., Choudhury, N.R., Tuteja, N. (2015) Insights into the functional characteristics of geminivirus rolling-circle replication initiator protein and its interaction with host factors affecting viral DNA replication. *Arch Virol*, 160, 375-387.

Rocha, C.S., Santos, A.A., Machado, J.P.B., Fontes, E.P.B. (2008) The ribosomal protein L10/QM-like protein is a component of the NIK-mediated antiviral signaling. *Virology*, 380, 165-169.

Rodríguez-Negrete, E., Lozano-Durán, R., Piedra-Aguilera, A., Cruzado, L., Bejarano, E.R., Castillo, A.G. (2013) Geminivirus Rep protein interferes with the plant DNA methylation machinery and suppresses transcriptional gene silencing. *New Phytol*, 199, 464-475.

Rojas, M.R., Hagen, C., Lucas, W.J., Gilbertson, R.L. (2005) Exploiting chinks in the plant's armor: evolution and emergence of geminiviruses. *Annu Rev Phytopathol*, 43, 361-394.

Rojas, M.R., Jiang, H., Salati, R., Xoconostle-Cazares, B., Sudarshana, M.R., Lucas, W.J., Gilbertson, R.L. (2001) Functional analysis of proteins involved in movement of the monopartite begomovirus,Tomato yellow leaf curl virus. *Virology*, 291, 110-125.

Rojas, M.R., Noueiry, A.O., Lucas, W.J., Gilbertson, R.L. (1998) Bean dwarf mosaic geminivirus movement proteins recognize DNA in a form- and size specific manner. *Cell*, 95, 105-113.

Romay, G., Chirinos, D., Geraud-Pouey, F., Desbiez, C. (2010) Association of an atypical alphasatellite with a bipartite New World begomovirus. *Arch Virol*, 155, 1843-1847.

Romeis, T., Herde, M. (2014) From local to global: CDPKs in systemic defense signaling upon microbial and herbivore attack. *Curr Opin Plant Biol*, 20, 1-10.

Rybicki, E.P., Pietersen, G. (1999) Plant virus disease problems i the developing world. *Adv Virus Res*, 53, 127-127.

Saeed, M., Behjatnia, A., Mansoor, S., Zafar, Y., Hasnain, S., Rezaian, A. (2005) A single complementary-sense transcript of a geminiviral DNA beta satellite is determinant of pathogenicity. *Mol Plant Microbe Interact*, 18, 7-14.

Sánchez-Durán, M.A., Dallas, M.B., Ascencio-Ibañez, J.T., Reyes, M.I., Arroyo-Mateos, M., Ruiz-Albert, J., Hanley-Bowdoin, L., Bejarano, E.R. (2011) Interaction between geminivirus replication protein and the SUMO-conjugating enzyme is required for viral infection. *J Virol*, 85, 9789-9800.

Sanderfoot, A.A., Lazarowitz, S.G. (1995) Cooperation in viral movement: the geminivirus BL1 movement protein interacts with BR1 and redirects it from the nucleus to the cell periphery. *Plant Cell*, 7, 1185-1194.

Sanderfoot, A.A., Lazarowitz, S.G. (1996) Getting it together in plant virus movement: cooperative interactions between bipartite geminivirus movement proteins. *Trends Cell Biol*, 6, 353-358.

Santos, A.A., Carvalho, C.M., Florentino, L.H., Ramos, H.J.O., Fontes, E.P.B. (2009) Conserved Threonine Residues within the A-Loop of the Receptor NIK Differentially Regulate the Kinase Function Required for Antiviral Signaling. *PLoS ONE*, 4, e5781.

Sawinski, K., Mersmann, S., Robatzek, S., Bohmer, M. (2013) Guarding the green: pathways to stomatal immunity. *Mol Plant Microbe Interact*, 26, 626-632.

Schulz, P., Herde, M., Romeis, T. (2013) Calcium-dependent protein kinases: hubs in plant stress signaling and development. *Plant Physiol*, 163, 523-530.

Selth, L.A., Dogra, S.C., Rasheed, M.S., Healy, H., Randles, J.W., Rezaian, M.A. (2005) A NAC domain protein interacts with *Tomato leaf curl virus* replication accessory protein and enhances viral replication. *Plant Cell*, 17, 311-325.

Settlage, S.B., Miller, A.B., Gruissem, W., Hanley-Bowdoin, L. (2001) Dual interaction of a geminivirus replication accessory factor with a viral replication protein and a plant cell cycle regulator. *Virology*, 279, 570-576.

Settlage, S.B., See, R.G., Hanley-Bowdoin, L. (2005) Geminivirus C3 protein: replication enhancement and protein interactions. *J Virol*, 79, 9885-9895.

Shen, Q., Liu, Z., Song, F., Xie, Q., Hanley-Bowdoin, L., Zhou, X. (2011) Tomato SlSnRK1 protein interacts with and phosphorylates betaC1, a pathogenesis protein encoded by a geminivirus beta-satellite. *Plant Physiol*, 157, 1394-1406.

Shen, W., Dallas, M.B., Goshe, M.B., Hanley-Bowdoin, L. (2014) SnRK1 Phosphorylation of AL2 Delays *Cabbage leaf curl virus* Infection in Arabidopsis. *J Virol*, 88, 10598-10612.

Shen, W., Hanley-Bowdoin, L. (2006) Geminivirus infection up-regulates the expression of two Arabidopsis protein kinases related to yeast SNF1- and mammalian AMPK-activating kinases. *Plant Physiol*, 142, 1642-1655.

Shen, W., Reyes, M.I., Hanley-Bowdoin, L. (2009) Arabidopsis protein kinases GRIK1 and GRIK2 specifically activate SnRK1 by phosphorylating its activation loop. *Plant Physiol*, 150, 996-1005.

Shivaprasad, P.V., Akbergenov, R., Trinks, D., Rajeswaran, R., Veluthambi, K., Hohn, T., Pooggin, M.M. (2005) Promoters, transcripts, and regulatory proteins of Mungbean yellow mosaic geminivirus. *J Virol*, 79, 8149-8163.

Singh, D.K., Islam, M.N., Choudhury, N.R., Karjee, S., Mukherjee, S.K. (2007) The 32 kDa subunit of replication protein A (RPA) participates in the DNA replication of *Mung bean yellow mosaic India virus* (MYMIV) by interacting with the viral Rep protein. *Nucleic Acids Res*, 35, 755-770.

Spoel, S.H., Koornneef, A., Claessens, S.M., Korzelius, J.P., van Pelt, J.A., Mueller, M.J., Buchala, A.J., Métraux, J.P., Brown, R., Kazan, K., van Loon, L.C., Dong, X., Pieterse, C.M. (2003) NPR1 modulates cross-talk between salicylate- and jasmonate-dependent defense pathways through a novel function in the cytosol. *Plant Cell*, 15, 760-770.

Staiger, D., Korneli, C., Lummer, M., Navarro, L. (2013) Emerging role for RNA-based regulation in plant immunity. *New Phytol*, 197, 394-404.

Stanley, J., Gay, M.R. (1983) Nucleotide sequence of *Cassava latent virus* DNA. *Nature*, 301, 260-262.

Sugano, S., Jiang, C.J., Miyazawa, S., Masumoto, C., Yazawa, K., Hayashi, N., Shimono, M., Nakayama, A., Miyao, M., Takatsuji, H. (2010) Role of OsNPR1 in rice defense program as revealed by genome-wide expression analysis. *Plant Mol Biol*, 74, 549-562.

Suyal, G., Mukherjee, S.K., Choudhury, N.R. (2013a) The host fator RAD51 is involved in *mungbean yellow mosaic India virus* (MYMIV) DNA replication. *Arch Virol*, 158, 1931-1941.

Suyal, G., Mukherjee, S.K., Srivastava, P.S., Choudhury, N.R. (2013b) *Arabidopsis thaliana* MCM2 plays role(s) in *mungbean yellow mosaic India virus* (MYMIV) DNA replication. *Arch Virol*, 158, 981–992.

Takken, F.L., Goverse, A. (2012) How to build a pathogen detector: structural basis of NB-LRR function. *Curr Opin Plant Biol*, 15, 375-384.

Trinks, D., Rajeswaran, R., Shivaprasad, P.V., Akbergenov, R., Oakeley, E.J., Veluthambi, K., Hohn, T., Pooggin, M.M. (2005) Suppression of RNA silencing by a geminivirus nuclear protein, AC2, correlates with transactivation of host genes. *J Virol*, 79, 2517-2527.

Tsuda, K., Katagiri, F. (2010) Comparing signaling mechanisms engaged in pattern-triggered and effectortriggered immunity. *Curr Opin Plant Biol*, 13, 459-465.

Uchiyama, A., Shimada-Beltran, H., Levy, A., Zheng, J.Y., Javia, P.A., Lazarowitz, S.G. (2014) The Arabidopsis synaptotagmin SYTA regulates the cell-to-cell movement of diverse plant viroses. *Front Plant Sci*, 5, 584.

Umezawa, T., Yoshida, R., Maruyama, K., Yamaguchi-Shinozaki, K., Shinozaki, K. (2004) SRK2C, a SNF1-related protein kinase 2, improves drought tolerance by controlling stress-responsive gene expression in Arabidopsis thaliana. *Proc Natl Acad Sci* USA, 101, 17306-17311.

Underwood, W. (2012) The plant cell wall: a dynamic barrier against pathogen invasion. *Front Plant Sci*, 3, 85.

van Loon, L.C., Rep, M., Pieterse, C.M.J. (2005) Significance of inducible defense-related proteins in infected plants. *Annu Rev Phytopathol*, 44, 135-162.

Vanitharani, R., Chellappan, P., Pita, J.S., Fauquet, C.M. (2004) Differential roles of AC2 and AC4 of cassava geminiviruses in mediating synergism and suppression of posttranscriptional gene silencing. *J Virol*, 78, 9487-9498.

Varsani, A., Navas-Castillo, J., Moriones, E., Hernández-Zepeda, C., Idris, A., Brown, J.K., Zerbini, F.M., Martin, D.P. (2014) Establishment of three new genera in the family *Geminiviridae*: *Becurtovirus*, *Eragrovirus* and *Turncurtovirus*. *Arch Virol*, 159, 2193-2203.

Wang, D., Amornsiripanitch, N., Dong, X. (2006) A genomic approach to identify regulatory nodes in the transcriptional network of systemic acquired resistance in plants. *PLoS Pathog*, 2, e123.

Wang, H., Buckley, K.J., Yang, X., Buchmann, R.C., Bisaro, D.M. (2005) Adenosine kinase inhibition and suppression of RNA silencing by geminivirus AL2 and L2 proteins. *J Virol*, 79, 7410-7418.

Wang, H., Hao, L., Shung, C.Y., Sunter, G., Bisaro, D.M. (2003) Adenosine kinase is inactivated by geminivirus AL2 and l2 proteins. *Plant Cell*, 15, 3020-3032.

Wang, X-B., Jovel, J., Udomporn, P., Wang, Y., Wu, Q., Li, W-X., Gasciolli, V., Vaucheret, H., Dinga, S-W. (2011) The 21-nucleotide, but not 22-nucleotide, viral secondary small interfering RNAs direct potent antiviral defense by two cooperative argonautes in *Arabidopsis thaliana*. *Plant cell*, 23, 1625-1638.

Wang, X-B., Wu, Q., Ito, T., Cillo, F., Li, W.X., Chen, X., Yu, J.L., Ding, S.W. (2010) RNAi-mediated viral immunity requires amplification of virus-derived siRNAs in *Arabidopsis thaliana*. *Proc Natl Acad Sci USA,* 107, 484-489.

Wu, L., Chen, H., Curtis, C., Fu, Z.Q. (2015) Go in for the kill. *Virulence*, 5, 710-721.

Yadav, R.K., Chattopadhyay, D. (2011) Enhanced viral intergenic region-specific short interfering RNA accumulation and DNA methylation correlates with resistance against a geminivirus. *Mol Plant Microbe Interact*, 24, 1189-1197.

Yamaguchi, Y., Pearce, G., Ryan, C.A. (2006) The cell surface leucine-rich repeat receptor for AtPep1, an endogenous peptide elicitor in Arabidopsis, is functional in transgenic tobacco cells. *Proc Natl Acad Sci USA*, 103, 10104-10109.

Yang, X., Xie, Y., Raja, P., Li, S., Wolf, J.N., Shen, Q., Bisaro, D.M., Zhou, X. (2011) Suppression of methylation-mediated transcriptional gene silencing by βC1-SAHH protein interaction during geminivirus-betasatellite infection. *PLoS Pathog*, 7, e1002329.

Zhang, S.C., Wege, C., Jeske, H. (2001) Movement proteins (BC1 and BV1) of Abutilon mosaic geminivirus are cotransported in and between cells of sink but not of source leaves as detected by green fluorescent protein tagging. *Virology*, 290, 249-260.

Zhang, X., Yuan, Y.R., Pei, Y., Lin, S.S., Tuschl, T., Patel, D.J., Chua, N.H. (2006) Cucumber mosaic virus-encoded 2b supressor inhibits Arabidopsis Argonaute1 cleavage activity to counter plant defense. *Genes Dev*, 20, 3255-3268.

Zhang, Z., Chen, H., Huang, X., Xia, R., Zhao, Q., Lai, J., Teng, K., Li, Y., Liang, L., Du, Q., Zhou, X., Guo, H., Xie, Q. (2011) BSCTV C2 attenuates the degradation of SAMDC1 to suppress DNA methylation-mediated gene silencing in Arabidopsis. *Plant Cell*, 23, 273-288.

Zhou, Y., Rojas, M.R., Park, M-R., Seo, Y-S., Lucas, W.J., Gilbertson, R.L. (2011) Histone H3 interacts and co-localizes with the nuclear shuttle protein and movement protein of a geminivirus. *J Virol*, 85, 11821-11832.

Zhou, Y.C., Garrido-Ramirez, E.R., Sudarshana, M.R., Yendluri, S., Gilbertson, R.L. (2007) The N-terminus of the begomovirus nuclear shuttle protein (BV1) determines virulence or avirulence in Phaseolus vulgaris. *Mol Plant Microbe Interact*, 20, 1523-1534.

Zipfel, C., Kunze, G., Chinchilla, D., Caniard, A., Jones, J.D., Boller, T., Felix, G. (2006) Perception of the bacterial PAMP EF-Tu by the receptor EFR restricts Agrobacterium-mediated transformation. *Cell*, 125, 749-760.

CHAPTER II

DOWSTREAM EVENTS IN THE NIK-MEDIATED DEFENSE ASSOCIATED WITH RESISTANCE TO BEGOMOVIRUS

The results of this chapter were split in two published papers, presented as supplementary material:

1. Zorzatto, C.*, Machado, J.P.B.*, Lopes, K.V.G., Nascimento, K.J.T., Pereira, W.A., Brustolini, O.J.B., Reis, P.A.B., Calil, I.P., Deguchi, M., Sachetto-Martins, G., Gouveia, B.C., Loriato, V.A.P., Silva, M.A.C., Silva, F.F., Santos, A.A., Chory, J., Fontes, E.P.B. (*equal contribution). 2015. NIK1-mediated translation suppression functions as a plant antiviral immunity mechanism. Nature 520, 679-682.

2. Brustolini, O.J.B.*, Machado, J.P.B.*, Condori-Apfata, J.A., Coco, D., Deguchi, M., Loriato, V.A.P., Pereira, W.A., Alfenas-Zerbini, P., Zerbini, F.M., Inoue-Nagata, A.K., Santos, A.A., Chory, J., Silva, F.F., Fontes, E.P.B**.** (*equal contribution). 2015. Sustained NIK-mediated antiviral signalling confers broad-spectrum tolerance to begomoviruses in cultivated plants. Plant Biotechnology Journal DOI: 10.1111/pbi.12349.

DOWSTREAM EVENTS IN THE NIK-MEDIATED DEFENSE ASSOCIATED WITH RESISTANCE TO BEGOMOVIRUS

Abstract

Begomovirus-associated epidemics currently threaten tomato production worldwide due to the emergence of highly pathogenic virus species and the proliferation of a whitefly Middle East-Asia Minor 1 vector that is adapted to tomato. The NIK (nuclear shuttle protein (NSP)-interacting kinase)-mediated antiviral signaling pathway was identified as a virulence target of the begomovirus NSP. Here, this layer of plant innate defense was further characterized by identifying a Myb-domain-containing transcription fator, LIMYB (L10-Interacting Myb domain-containing protein), as a downstream effector of the antiviral signaling. LIMYB was isolated through yeast two-hybrid screening using RPL10 as a bait, a previously characterized component of the NIK-mediated defense response. The interaction between RPL10 and LYMIB was also found to occur *in planta*, specifically in the nucleus of the plant cell, as judged by bimolecular fluorescence complementation assays. The *in vivo* LIMYB-RPL10 interaction was further confirmed by co-immunoprecipitation experiments. The results obtained in this investigation demonstrated further that LIMYB acts as an authentic transcription factor binding to and inhibiting ribosomal protein gene promoters, suggesting that global translational inhibition may be an antiviral defense mechanism. To generate an efficient defence against begomovirus, the activity of the immune defence receptor NIK was modulated in tomato plants. Replacement of threonine at position 474 within the kinase activation loop by aspartate (T474D) promoted the constitutive activation of NIK-mediated defences, resulting in suppression of global translation. Consistent with these findings, transgenic lines harbouring the hyperactive T474D mutant were tolerant to the tomato-infecting begomoviruses ToYSV and ToSRV. This phenotype was associated

with reduced loading of coat protein viral mRNA in actively translating polysomes, lower infection efficiency and reduced accumulation of viral DNA in systemic leaves. Collectively, the results of this investigation indicate that the NIK-mediated suppression of translation functions as an antiviral immunity mechanism in plants.

Introduction

Begomoviruses (whitefly-transmitted geminiviruses) cause severe diseases of high economic impact in a variety of agriculturally relevant crops in tropical and subtropical areas (Rojas *et al*., 2005). Current climate changes are expected to further alter the whitefly distribution across the globe, posing a major threat to agriculture worldwide. The threat is particularly strongly for tomato plants, which are inflicted by a variety of emergente species of tomato-infecting begomoviruses. Previous attempts to develop pathogen-derived resistance using begomovirus DNA sequences in transgenic plants have failed to achieve immunity, resistance or tolerance, even though a delay of infection and/or attenuation of symptoms were frequently observed (Day *et al*., 1991; Hashmi *et al*., 2011; Hong and Stanley, 1996; Kunik *et al*., 1994; Lin *et al*., 2012; Noris *et al*., 1996; Stanley *et al*., 1991). The only exception was a single common bean transgenic line expressing a siRNA that targets the replication protein from BGMV (*Bean golden mosaic virus*), which has been shown to be immune to this begomovirus (Aragão and Faria, 2009). However, it has been extremely difficult to engineer broad-spectrum resistance against tomato-infecting begomoviruses through a similar RNA silencing strategy (Lucioli *et al*., 2008). One explanation for the failure of siRNA tomato transgenic lines to resist begomovirus infection is the emergence of new species of tomato-infecting begomoviruses that evolve rapidly through recombination or pseudo-recombination, which produces divergent genome sequences, giving the virus an advantage over its host's recognition system

(Albuquerque *et al*., 2012; Castillo-Urquiza *et al*., 2008; Galvão *et al*., 2003). More recently, transgenic tomato lines expressing peptide aptamers, which bind efficiently to and inhibit the begomovirus replication protein (Rep), have been shown to display enhanced tolerance to *Tomato yellow leaf curl virus* or *Tomato mottle virus* (Reyes *et al*., 2013). Thus, the Rep-binding peptide octamers may serve as an eficiente strategy for engineering transgenic tomato plants that are resistant to diverse begomoviruses. Likewise, expression of the single-stranded DNA binding protein virE2 from Agrobacterium in tobacco has been shown to reduce *Mungbean yellow mosaic virus* DNA accumulation, although the spectrum of the resistance has not been established (Sunitha *et al*., 2011).

Begomoviruses are single-stranded DNA viruses with a monopartite or bipartite genome configuration. For the bipartite begomoviruses, the proteins required for replication (Rep and REn), transactivation of viral genes (TrAP), the suppression of RNAi defence functions (TrAP and AC4) and encapsidation of viral DNA (CP) are encoded by the DNA-A component, whereas the nuclear shuttle protein (NSP) and intercellular movement protein (MP) are encoded by DNA-B (Rojas *et al*., 2005). NSP facilitates the traffic of viral DNA from the nucleus to the cytoplasm and acts in concert with MP to move the viral DNA to the adjacent, uninfected cells. The mechanistic model for viral DNA intracelular trafficking holds that NSP binds to newly replicated viral DNA in the nuclei of infected cells and utilizes the nuclear export machinery to move the viral DNA to the cytoplasm (Carvalho *et al*., 2008a,b; Gafni and Epel, 2002). Consistent with this model, NSP contains a HIVRev-like or TFIIA-like leucine-rich nuclear export signal (NES) that can be functionally replaced by TFIIIA NES in both nuclear export and infectivity (Ward and Lazarowitz, 1999). NSP is found within the nuclei of transfected plant, insect and yeast cells, but is relocated to the cell periphery when co-expressed with viral movement protein (MP, Carvalho *et al*., 2008b; Sanderfoot and Lazarowitz, 1995, 1996; Sanderfoot *et al*., 1996; Zhang *et al*.,2001). The fundamental role of NSP in virus movement predicts that this viral protein may

interact with host factors in different subcellular compartments. Accordingly, NSP has been shown to interact with an *Arabidopsis thaliana* nuclear acetylase, designated nuclear shuttle protein interactor (*At*NSI) and a cytosolic GTPase that facilitates the release of the viral DNA-NSP complex from the nuclear pores to the cytosol, designated NIG (NSP-interacting GTPase). NSP also interacts with plasma membrane receptor-like kinases, designated NsAKs (NSP-activating kinases) from Arabidopsis and NIKs (NSP-interacting kinases) from tomato, soybean and Arabidopsis (Carvalho *et al*., 2008b; Florentino *et al*., 2006; Mariano *et al*., 2004; McGarry *et al*., 2003). In Arabidopsis, NSP interacts with three members of the LRR-receptor-like kinase (RLK) family, NIK1, NIK2 and NIK3, which have been shown to be authentic serine/threonine kinases with biochemical properties consistent with a receptor signalling function (Fontes *et al*., 2004).

NIK was discovered as a component of the antiviral plant immune system (Carvalho *et al*., 2008c; Fontes *et al*., 2004). The viral NSP binds to the kinase domain of NIK to suppress its activity and increase begomovirus pathogenicity (Fontes *et al*., 2004). The current model for NIK activation holds that upon begomovirus infection, NIK oligomerizes and transphosphorylates the kinase domain on a key threonine residue at position 474 (T474; Carvalho *et al*., 2008c; Rocha *et al*., 2008; Santos *et al*., 2009). This phosphorylation-dependent activation of NIK leads to the phosphorylation of a downstream component, the ribosomal protein L10A (RPL10), which in turn translocates to the nucleus, where it may function to mount a defence response that negatively impacts virus infection (Carvalho *et al*., 2008c). To counteract this mechanism, the viral NSP binds to the kinase domain of NIK and prevents phosphorylation of T474, leading to the suppression of the kinase activity and establishing an environment that is more favourable to begomovirus infection. Accordingly, the loss of NIK function enhances the susceptibility of *nik* null alleles to begomovirus infection, whereas the overexpression of Arabidopsis (*At*) NIK1 in begomovirus-infected tobacco leaves titrates the virally produced NSP inhibitor and

the molar excess of NIK overcomes NSP-mediated inhibition (Santos *et al*., 2010). Likewise, enhanced accumulation of *At*NIK1 in tomato plants attenuates begomovirus infection. However, the effectiveness of the NIK-mediated signalling pathway against begomovirus infection is limited because the viral NSP functions as a NIK suppressor and because activation of the pathway seems to be dependent on the onset of infection.

Apart from the identification of RPL10 as a downstream effector in NIK1-mediated antiviral immunity (Carvalho *et al*., 2008c; Rocha *et al*., 2008), mechanistic knowledge of the signalling pathway is lacking, and the molecular nature of the defence response remains unclear. It has been previously shown that replacing a threonine residue at position 474 with an aspartic acid residue (T474D, a phosphomimic) leads to hyperactivation of the kinase activity and an enhanced capacity to relocate RPL10 to the nucleus (Santos *et al*., 2009). Furthermore, recent studies have shown that mock-inoculated T474D-overexpressing lines shows a constitutively infected wild-type transcriptome (Brustolini *et al*., 2015; Zorzatto *et al*., 2015), and that ectopic expression of T474D downregulates ribosomal genes and other components of the protein synthesis machinery (Zorzatto *et al*., 2015). To gain insights in NIK-mediated antiviral signaling, the yeast two-hybrid system was used to search for nuclear RPL10 partners and a transcription factor, designated LIMYB (L10-Interacting Myb domain-containing protein), was isolated in this study. Furthermore, LIMYB was shown to bind to and suppresses the expression of ribosomal protein gene promoters, supporting the notion that the inhibition of host translation observed in the T474D lines may be an effective mechanism exploited by plant cells to fight begomovirus infection. To further confirm this hypothesis, tomato lines overexpressing a gain-of-function mutant from Arabidopsis were challenged with two highly divergent begomovirus, *Tomato yellow spot virus* (ToYSV) and *Tomato severe rugose virus* (ToSRV). The results demonstrated that the antiviral signaling activity of a constitutively activated receptor NIK from the cruciferous plant *Arabidopsis thaliana*

is retained after its transfer to the solanaceous plant tomato (*Solanum lycopersicum*), making the transgenic tomato lines more resistant to different species of begomovirus.

Results

Identification and isolation of a RPL10 partner, designated LIMYB (L10-Interacting Myb domain-containing protein)

The activation of the receptor kinase NIK1 leads to phosphorylation of RPL10, which results in translocation of the ribosomal protein to the nucleus where it may function to directly mount an antiviral defense response (Carvalho *et al*., 2008c). Because RPL10 plays an important role in plant defense response as a downstream effector of NIK1 signaling, the identification of downstream targets of RPL10 is crucial to decipher this layer of innate defense and to elucidate the underlying mechanism of the NIK-mediated defense. To identify potential cellular targets of RPL10 yeast two-hybrid screens were peroformed with an Arabidopis cDNA library cloned in a pAD-GAL4 vector derivative (pEXP-AD502) and RPL10 fused in-frame to the GAL4 DNA binding domain sequence, as a bait. From 9.4×10^5 independent double transformants screened, one candidate displaying histidine prototrophy and *lacZ* expression on X-gal indicator plates was selected for further testing, followed by retransformation of the yeast modified strain, AH109 pBD-RPL10, with the library rescued plasmid. The interaction previously identified was confirmed by monitoring the growth of double transformants on medium lacking histidine and supplemented with 10 mM 3AT (Figure 1A) and by detecting the β-galactosidase activity in nylon membrane (Figure 1B). The intensity of this interaction was further confirmed by measuring levels of β-galactosidase activity in yeast protein extracts (Figure 1C). The isolated cDNA-encoded product interacted specifically with RPL10, because the

reporters genes *HIS3* and *lacZ* were not activated in co-transformed yeast cells with pBD-RPL10 plus pAD or pBD plus pAD (Figure 1). Yeast co-transformed with pBD-NIK1 and pAD-RPL10 was used as a positive control (Rocha *et al*., 2008). Sequencing analysis of the recovered plasmids showed that the double-transformant, which was able to transactivate reporter genes in the two-hybrid assay, harboured a full-length cDNA corresponding to the locus AT5G05800. The deduced AT5G05800-encoded protein contains 449 amino acid residues (calculated Mr 52690, pI 6.3075), and exhibits two Myb/SANT-like DNA-binding domain (residues 7–100 and 169–263; InterPro database IPR024752; Figure 2A), a structural feature of a possible transcription factor. Because of this structural feature and the ability to bind to RPL10, this transfator was designated LIMYB (L10-Interacting Myb domain-containing protein).

In order to understand the evolutionary relationship of LIMYB with other MYB-domain containing proteins in Arabidopsis and to gather information to facilitate the prediction of their function, a phylogenetic analysis with MYB family sequence retrieved from the Agris database was conducted (http://arabidopsis.med.ohio-state.edu; Figure 2B). LIMYB is most closely related to AT3G11290 (50,93% identity), AT2G19220 (41,50% identity) and AT3G11310 (36,59% edentity), which are deduced proteins of unknown function, but as LIMYB-like proteins, exhibit two Myb/SANT-like DNA-binding domain in similar regions, one at the N-terminus and another in the central region (AT3G11290, residues 7–93 and 167–261; AT2G19220, residues 7–92 and 164–261; AT3G11310, residues 8–95 and 175–274).

LIMYB interacts with RPL10 in vivo and displays overlapping expression profiles with RPL10 and NIK1

In order to examine whether the interaction between RPL10 and LIMYB identified through yeast two-hybrid system also occurs in plant, it was performed co-immunoprecipitation assays and bimolecular fluorescence complementation (BiFC) analysis (Figure 3). In the co-immunoprecipitation assays, *Nicotiana benthamiana* leaves were first agroinoculated with 35S::LIMYB–GFP and 35S::RPL10-6HA or 35S::CSN5A fused to GFP or HA. The CSN5A fusion was used as unrelated protein. The complexes formed between these proteins were isolated from whole-cell protein extracts of transfected cells using anti-HA (Figure 3A) or anti-GFP (Figue 3B) antibody.

The anti-HA antibody was used to isolate immunocomplexes formed with RPL10-6HA or CSN5A-6HA from extracts of leaves co-transfected with these chimeric proteins and LIMYB-GFP. The presence of LIMYB-GFP was analysed by western blotting of the immunocomplexes using anti-GFP antibody (Co-IP; Figure 3A). Both LIMYB-GFP (Co-IP) and RPL10-6HA (IP) were co-immunoprecipated using anti-HA, demonstrating previous association of the proteins. However, LIMYB-GFP was not co-immunoprecipitated with the CSN5A-6HA, demonstrating the specific association of LIMYB-GFP with RPL10-6HA fusions (Figure 3A). Likewise, in the reciprocal experiment, an anti-GFP antibody was capable of co-immunoprecipitating RPL10-6HA (Co-IP) previously associated with LIMYB-GFP (IP) from co-transfected extracts (Figure 3B). However, RPL10 was not detected in protein complexes formed with CSN5A-GFP and isolates with anti-GFP antibody. Moreover, in both experiments, co-immunoprecipitation with the reciprocal antibody showed no cross-reaction, indicating antibody specificity for the respective target protein (Figure 3A and 3B).

The *in vivo* interaction between RPL10 and LIMYB was further confirmed using BiFC assays (Figure 3C). This technique, in addition to detecting the interaction between candidate proteins *in planta*, allows us to identify the cellular compartment where the interaction occurs. Initially, RPL10 and LIMYB were fused to non-

fluorescent fragments (NE and CE) from fluorescent yellow protein (YFP) and the DNA constructs were used to agroinoculate *N. benthamiana* leaves. Examination by confocal microscopy revealed that the formation of an RPL10-LIMYB complex occurred in the nuclei of transfected cells independent of the orientation of the RPL10 and LIMYB fusions (NE, N-terminus or CE, C-termminus of YFP; Figure 3C), and that the reconstituted fluorescent signal was much higher than that of the negative controls, combinations of the protein fusions with empty vectors (Figure 3D). This result is consistent with a possible nuclear function for the RPL10-LIMYB complex.

Genetic and biochemical evidence indicates that RPL10 plays critical role in the defense strategy as a downstream component of the NIK1-mediated signaling pathway (Carvalho *et al*., 2008c). Interaction with RPL10 suggests that LIMYB may also participate in this pathway of antiviral signaling. A first evidence supporting this hypothesis was obtained by analysis of spatial expression of *LIMYB*, *RPL10* and *NIK1* promoters. Immunohistochemical assays using transgenic lines harboring the β-glucuronidase (GUS) reporter gene from the *LIMYB*, *RPL10* and *NIK1* promoters showed that all three genes were ubiquitously expressed in all seedling tissues (Figure 4). WT seedlings did not show color after GUS activity, indicating specificity for the transformed plants (Figure 4). These results demonstrated overlapping expression profiles between NIK1, RPL10 and LIMYB, indicating a possible functional relationship between these proteins.

LIMYB and RPL10 transactivate promoters of ribosomal protein genes

The replacement of the threonine residue at position 474 within the activation-loop domain of the imune receptor NIK1 by an aspartate residue (T474D mutant) has been previously shown to result in a constitutively actived mutant NIK, which is more effective at redirecting RPL10 to the nucleus (Carvalho *et al*., 2008c; Santos *et al*,

2009). In addition, analysis of global variation in gene expression in Arabidopsis lines overexpressing the T474D mutant revealed that the ectopic expression of the hyperactive mutant NIK1 promotes downregulation in the expression of ribosomal genes and other components of the protein synthesis machinery (Zorzatto *et al*., 2015). In mammals, global translational inhibition is a critical part of the antiviral cellular response that blocks viral protein synthesis, effectively dampening virus production (Unterholzner and Bowie, 2008; Williams, 1999). Because LIMYB interacts with RPL10 in the nucleus of plant cells and exhibits structural characteristics consistent with a transcription factor, it is reasonable to assume that LIMYB plays a role in regulating the expression of translational-machinery-related genes, participating in the signal transduction pathway mediated by NIK1. To examine this hypothesis, firstly, the level of transcript accumulation of five ribosomal protein genes (*S13a*, *S25*, *L4/L1*, *L13* and *L28e*) was evaluated in *LIMYB*-overexpressing lines. These rihosomal protein genes were selected among the differentially expressed genes found in Arabidopsis lines overexpressing the T474D mutant (Zorzatto *et al*., 2015). *LIMYB* overexpression downregulated the expression of the selected ribosomal genes (Figure 5A). Conversely, in the *limyb-32* line, a T-DNA insertion mutant in the *LIMYB* gene, the same ribosomal protein genes were upregulated (Figure 5B). Therefore, loss of LIMYB function releaves the repression, promoting the induction of the ribosomal protein genes.

Because RPL10 functions in NIK1-mediated antiviral signalling and interacts with LIMYB, it was examined whether RPL10 also controls the expression of ribosomal genes. In *RPL10*-overexpressing lines, in which an RPL10-YFP fusion was forced into the nucleus by introducing a nuclear localization signal into the RPL10 construct, the expression of ribosomal genes also was downregulated (Figure 5C).

The presence of two DNA-binding domains in the sequence of LIMYB prompted us to examine whether the suppression in the expression of ribosomal protein genes was due to LIMYB binding to the promoter region of these genes. To

this end, chromatin immunoprecipitation (ChiP) experiments from Arabidopsis lines overexpressing LIMYB-GFP were performed. A fragment of 150 base pairs from RPL18 promoter was amplified from the precipitated DNA of *LIMYB*-expressing tissues but not of wild-type tissues (Figure 5D). ChIP-qPCR showed that the 150-bp promoter fragment (-908 to -755) was significantly enriched in samples precipitated by anti-green fluorescent protein (GFP) antibody but not in samples pulled down from wild-type lines (Figure 5E). These results suggested that LIMYB may function as a DNA-binding protein that associates with ribosomal promoters *in vivo*.

To provide further evidence for the regulation of ribosomal target genes by LIMYB and RPL10, a luciferase transactivation assay was performed in agroinfiltrated leaves using 2 kb promoter regions of the ribosomal genes *L28e*, *S13a* and ubiquitin, as an unrelated promoter, controlling the expression of the firefly luciferase reporter gene (Figure 5F). The activity of the ribosomal protein gene promoters is monitored by the firefly luciferase activity normalized by the *Renilla* luciferase activity, expressed under the control of the 35S promoter. Consistent with the gene expression profile, LIMYB and RPL10 specifically repressed the *L28e* and *S13A* promoters but not an unrelated ubiquitin promoter (Figure 5F). Collectively, these results indicate that LIMYB and RPL10 function as transcriptional repressors of common ribosomal protein genes and may regulate common target promoters.

Constitutive activation of NIK confers tolerance to begomovirus infection in tomato but does not impair development

The NIK receptor has been hypothesized to mediate an antiviral defense response through a reversible phosphorylation strategy that both initiates a signaling pathway as well as modulates the consequent adaptive response (Santos *et al*., 2009). Previous work had indicated that the NSP begomovirus binding site on NIK

overlaps two kinase sub domains VIb and VIII, preventing activation of the NIK-mediated signaling pathway and creating an intracellular environment that is more favorable to virus proliferation and spread (Fontes *et al*., 2004). More recently, it has been shown that phosphorylation of the Thr-474 residue is crucial for NIK activity, and that the substitution of this residue by aspartic acid (T474D) results in attenuated effect of NSP on inhibition of NIK immune receptor activity (Santos *et al*., 2009). To examine whether the constitutive activation of NIK1 is effective at controlling begomovirus infection in tomato, independent T474D-overexpressing transgenic lines (T474D-6, T474D-5 and T474D-2; Apfata, 2010), a wild-type (untransformed) line and the NIK-overexpressing lines NIK1-4 and NIK1-6 (Carvalho *et al*., 2008c) were inoculated with tandemly repeated ToYSV DNA-A and DNA-B (Andrade *et al*., 2006) using biolistic delivery. The innoculated plants were assayed for symptoms of infection and the accumulation of viral DNA, as detected by PCR and qPCR. The wild-type plants displayed typical symptoms of ToYSV infection, such as leaf curling and yellow spots all over the leaves (>10 spots/cm^2; Figure 6A). Consistent with a previous observation (Carvalho *et al*., 2008c), the NIK-overexpressing line NIK1-4 displayed attenuated symptoms (less accentuated leaf distortion and a lower number of yellow spots per leaf area, < 6 spots/cm^2). The symptoms in the T474D-overexpressing lines, however, were even more attenuated, with few spots per leaf area (varying among the lines) and no visible leaf curling (see T474D-2 and T474D-5 lines, Figure 6A and 6B). The T474D-6 transgenic line displayed typical tolerance to begomoviruses, as it did not develop symptoms (Figure 6A and 6D), but we detected viral DNA accumulation in both inoculated and systemically infected leaves (Figure 6E). The symptomless ToYSV infections of the T474D-6 line were associated with a delayed course of infection (Figure 6F), a lower rate of infection (DPI50, days postinoculation to infect 50% of plants; Figure 6G), and a lower accumulation of viral DNA in the systemically infected leaves, as shown by qPCR (Figure 6H). Likewise, in the T474D-2 and T474D-5 lines, the progress and rate of infection were delayed compared with

those of the wild-type control lines and the NIK1-overexpressing lines (Figure 6F and 6G). In the case of ToYSV, which showed high levels of accumulation in all samples analysed, both the T474D-2 and T474D-6 lines displayed lower viral DNA accumulation levels in the systemically infected leaves, although the high dispersion of the data among the samples prevented us from ascertaining the statistical significance of these findings (Figure 6H). Collectively, these results indicate that the T474D-overexpressing lines are more tolerant to ToYSV infection as compared to *At*NIK1-overexpressing lines and wild-type lines.

Tomatoes are usually infected by a variety of rapidly evolving species of tomato-infecting begomoviruses and engineering broad-spectrum resistance to these viruses in crops constitutes a relevant trait to achieve durable resistance against begomoviruses. These transgenic lines were also challenged with the tomato-infecting begomovirus ToSRV (*Tomato severe rugose virus*), which displays a highly divergent genomic sequence from ToYSV sequence (Albuquerque *et al*., 2012). ToSRV infection caused severe leaf distortion in wild-type leaves but not in the T474D-6 overexpressing line (Figure 7A). In these T474D-overexpressing lines, the viral DNA accumulation in the systemic leaves from ToSRV infections was significantly lower at 14 and 21 DPI ($P < 0.05$; Figure 7B and 7C). These results indicate that the ectopic expression of T474D in tomato confers tolerance to heterologous species of tomato-infecting begomoviruses, which are phylogenetically separated within the two major groups of begomoviruses found in Brazil (Albuquerque *et al*., 2012). The constitutive activation of T474D and its ability to bypass viral NSP inhibition likely account for the tolerance to begomovirus infection displayed by the transgenic lines.

Constitutive activation of defense proteins often results in losses in the development and growth of the plant (Bao and Hua, 2015). To verify possible deleterious effects arising of the T474D-overexpression, the development, overall physiological performance and horticultural traits were monitored in T474D-2, T474D-

5 and T474D-6 tomato transgenic lines. The results showed that T474D-overexpressing lines were similar to those of wild-type plants and *At*NIK1-expressing transgenic lines (NIK1-4) under normal greenhouse conditions (Figures 8 and 9). During the vegetative phase, the transgenic lines and wild-type control displayed similar plant height and biomass accumulation, as measured by shoot and root dry weight (Figures 8A–D). The net CO_2 assimilation rate (*A*), transpiration rate (*E*), stomatal conductance to water vapour (g_s) ratio and internal to ambient CO_2 concentration ratio (C_i/C_a) of fully expanded leaves did not differ significantly among the transgenic lines and wild-type control (Figure 8E–H). Fully ripened tomatoes were harvested and analysed for colour, morphology, total soluble solids (brix) and nutritional quality (Figure 9). The ripe fruits of the transgenic lines were bright red (Figure 9A) and displayed an overall shape (Figure 9A), colour (Figure 9D), size (Figure 9E) and nutritional value (Figure 9C, 9F and 9G) similar to those of the wild-type control. The fruit yield (Figure 9B and 9I) and the overall development of the reproductive phase (Figure 9H and 9I) of the transgenic lines were similar to those of wild-type plants grown under normal greenhouse conditions.

The enhanced tolerance to begomovirus displayed by the T474D-expressing lines may be associated with the translational control branch of the NIK-mediated antiviral responses

Recently, the T474D ectopic expression has been shown to downregulate components of the translational machinery in Arabidopsis, suggesting that the constitutive activation of NIK1 might influence translation (Zorzatto *et al*., 2015). In addition, LIMYB binds and represses the expression of ribosomal genes (Figure 5). To verify that the protein synthesis could be affected by the constitutive activation of *At*NIK in the T474D tomato lines, leaf proteins were labeled *in vivo* with [^{35}S]Met in control plants and T474D overexpression lines (Figure 10A). There was a significant

decrease (25% in T474D-5, 22.5% in T474D-6 and 19.6% in T474D-2; $P < 0.05$) in the amount of newly synthesized protein in T474D-overexpressing leaves compared with the amounts found in wild-type and NIK-overexpressing leaves. It was observed a slight variation in the T474D-mediated inhibition of translation during development, as the reduction of translation was 18.1% (T474D-2), 16.8% (T474D-5) and 15.5% (T474D-6) when the incorporation of [^{35}S]Met into total proteins was measured in 28-day-old leaves (Figure 10B). These results indicate that the gain-of-function mutant T474D from Arabidopsis functions similarly in tomato plants, and that the suppression of translation might underlie at least partially the molecular mechanism involved in NIK-mediated antiviral defences. To verify this hypothesis, it was investigated whether viral RNA transcripts could be detected in actively translating polysome fractions that had been separated from nonpolysomal fractions on sucrose gradients. The polysomal fractions were prepared from infected leaves at 10 DPI, when the accumulation of viral mRNA in transgenic and wild-type leaves was similar (Figure 11B). A significant reduction in the polysome loading of viral mRNA (coat protein mRNA) was observed in systemically infected leaves of the T474D-6-overexpresing line compared to infected wild-type and NIK1-overexpressing leaves (Figure 11A and 11B). These results indicate that the begomovirus was not capable of sustaining high levels of viral mRNA translation in the T474D-6-expressing lines, indicating that suppression of global protein synthesis may effectively protect plant cells against DNA viruses.

Discussion

Begomoviruses are one of the largest and most successful groups of plant viruses and cause severe diseases in major crops worldwide, inflicting significant economic losses in many dicotyledonous crops. The tomato-infecting begomoviruses

have become an even greater threat to tomato cultivation due to the emergence of new species along with the recent introduction into South America of a new biotype of the whitefly vector *Bemisia tabaci*, which colonizes tomato plants with high efficiency (Albuquerque *et al*., 2012; Castillo-Urquiza *et al*., 2008; Galvão *et al*., 2003). Current climate changes are expected to further alter the whitefly distribution across the globe, posing a serious threat to agriculture worldwide. Here, we described a novel strategy to control begomovirus infection. By constitutively activating NIK-mediated antiviral signalling, we succeeded in developing a tolerant tomato crop. Tomatoes are usually inflicted by diverse begomoviruses, making engineered tolerant/resistant lines even more difficult to develop. Importantly, the T474D-overexpressing tomato transgenic lines were tolerant to ToYSV and ToSRV, which display highly divergent genomic sequences and hence are phylogenetically separated within the two major groups of begomoviruses found in Brazil (Albuquerque *et al*., 2012).

The experiments presented here shed light on the response underlying NIK-mediated antiviral defences. The constitutive activation of NIK in the T474D lines was shown to impair global translation, and such activation might constitute an excelente strategy for fighting begomovirus infection in host cells. It was also demonstrated in Arabidopsis that LIMYB, identified by interacting with RPL10 in yeast and *in planta*, functions in NIK1-mediated antiviral signalling. In fact, the loss of *LIMYB* function recapitulated the enhanced begomovirus susceptibility phenotype of the *nik1*-null alleles and prevented the T474D-mediated downregulation of the ribosomal protein genes in the *limyb-32* transgenic lines that stably expressed T474D (Zorzatto *et al*., 2015). Here, it was demonstred that LIMYB acts as a DNA-binding protein that associates to and downregulates ribosomal protein gene promoters. Because begomoviruses rely completely on the plant translation machinery and cannot circumvent host translational regulation, a global repression of translation is expected to significantly affect virus infection, as observed in the T474D-overexpressing lines. In fact, by directly assessing viral transcripts, it was demonstrated that the loading of

coat protein mRNA into actively translating polysomes was significantly reduced in systemic infected leaves of T474D-overexpressing plants compared to WT and NIK1-overexpressing lines. This result indicates that the suppression of global protein synthesis may effectively protect plant cells against DNA viruses.

The current mechanistic model for the activation of the NIK-mediated antiviral signalling pathway holds that upon an unknown stimulus, the NIK LRR extracellular domain undergoes oligomerization with itself or another receptor, allowing the intracellular kinase domains to transphosphorylate and activate one another. The activation of NIK by phosphorylation on the crucial threonine residue at position 474 leads to the regulated relocation of RPL10 to the nucleus (Carvalho *et al*., 2008c; Santos *et al*, 2009) where it interacts to LIMYB to fully down-regulate translation-related genes. The data are consistent with the notion that the gain-of-function mutant T474D can sustain an activated NIK-mediated antiviral response in the absence of the virus, further confirming that phosphorylation on Thr-474 is the crucial event that leads to the activation of the kinase. In fact, comparison between the transcriptomes induced by virus infection in wild-type lines and by ectopic expression of the T474D gain-of-function mutant in transgenic lines indicated that activation of the NIK-mediated signalling pathway triggers a typical response to virus infection (Brustolini *et al*., 2015). In addition, expression of the T474D mutant potentiated the NIK-mediated response, as it would be expected from expression of a constitutively activated defence receptor NIK. Accordingly, the ectopic expression of the T474D gain-of-function mutant was more effective against begomovirus infection than overexpression of the NIK defence receptor in the tomato transgenic lines.

Based on the results, it is clear that the level of translational inhibition mediated by constitutive activation of NIK1 did not impact development in tomato under greenhouse conditions. In the first generation, however, some transgenic lines displayed shorter roots that regained normal biomass and growth in the subsequent generations. As a possible explanation for this phenotype, the T474D-mediated

translation inhibition would have maintained the transgenic lines under a constant perception of stress, which, in turn, promoted acclimation to maintain normal growth under greenhouse conditions. It was also found that T474D-mediated translation inhibition persisted in diferente developmental stages of the transgenic lines but to diferents extents. At later stages of development (28-day-old leaves), it was observed a 7% reduction in the level of translation inhibition compared to that of seedlings. This difference in the efficiency of global translation inhibition mediated by ectopic expression of the T474D mutant receptor may reflect an adjustment of transgenic lines towards adaptation at later stages. However, it is very intriguing that ectopic expression of T474D did not impact tomato development despite 19–25% suppression of global translation at earlier stages of development, but impacted Arbidopsis development (Zorzatto *et al*., 2015). Therefore, the intrinsic capacity to withstand the deleterious effect from the suppression of global translation must be considered in attempts to transfer the T474D-mediated defence strategy to other agronomically relevant crops.

Material and methods

Plasmid constructs

The clones RPL10AST-pDONR201 (pUFV608), RPL10ANS-pDONR201 (pUFV609), RPL10AST-pDONR207 (pUFV900) and RPL10ANS-pDONR207 (pUFV901), which harbour the *RPL10A* coding region either with (ST) or without (NS) a translational stop codon inserted into the entry vectors pDONR201 or pDONR207, have also been previously described (Carvalho *et al*., 2008c). The *RPL10A* coding region was transferred from these entry clones to the yeast expression vectors pDEST32 and pDEST22, generating the clones pBD-RPL10A (pUFV1422) and pAD-

RPL10 (pUFV785) as GAL4 binding domain (BD) or activation domain (AD) fusions. For BiFC, the *RPL10A* coding region was transferred from RPL10ANS-pDONR207 to the vectors SPYNE-GW and SPYCE-GW. The resulting clones, RPL10-SPYNE (pUFV1652) and RPL10-SPYCE (pUFV1653), harboured the *RPL10A* coding region fused to either the N-terminal (NE) region of YFP or the YFP C terminus (CE), respectively, under the control of the 35S promoter. The HA epitope was fused to the RPL10 C terminus using the triple Gateway system, which consisted of recombination between 35S (2×) promoter, previously cloned in the vector pDONR-P4-P1R (pUFV1920), *RPL10* cDNA without a translational stop codon in pDONR201 (pUFV609), HA (6×) epitope, previously insered in the vector pDONR-P2R-P3, and the destination vector pK7m34GW, yielding the clone 2×35S::RPL10-6HA (pUFV1985), which enabled the expression of RPL10 fused in frame to HA under the control of the 2×35S promoter in plants. The clone YFP-NLS-RPL10 (pUFV1719), which harbours a YFP-RPL10 fusion with a nuclear localization signal (NLS) under the control of the 35S promoter, was constructed by first inserting the amplified coding region of *RPL10A* into the *Sac*I site of the pGR vector. The resulting clone, GR-RPL10 (pUFV1680), which contains the *RPL10A* coding region fused to a glucocorticoid receptor (GR) domain with an NLS at the 5' end, was then used as the template for the amplification of the NLS-containing RPL10 fusion with specific primers. The resulting product was inserted by recombination into pDONR207 (pUFV1698) and transferred to 35S-YFP-casseteA-Nos-pCAMBIA1300, generating YFP-NLS-RPL10.

The *LIMYB* cDNA (*AT5G05800*), which was isolated based on its ability to bind to RPL10A in yeast, was amplified by PCR from the cDNA library vector using LIMYB-specific primers, re-amplified with the primers AttB1-Fwd and AttB1-Rvs, and cloned by recombination into the entry vectors pDONR201 and pDONR207. The resulting clones, LIMYBST-pDONR201 (pUFV1377), LIMYBNS-pDONR201 (pUFV1378) and LIMYBNS-pDONR207 (pUFV1656), harbour the *LIMYB* coding region either with (ST) or without (NS) a translational stop codon. The resulting products were then

transferred to different destination vectors for expression in plants (pK7FWG2, SPYNE-GW and SPYCE-GW). The clone LIMYB-GFP (pUFV1395), obtained from LIMYBNS-pDONR201, harboured the LIMYB coding region fused to the GFP N terminus under the control of the 35S promoter. In the clones LIMYB-SPYNE (pUFV1658) and LIMYB-SPYCE (pUFV1657), obtained from LIMYBNS-pDONR207, the LIMYB cDNA was linked to the YFP NE and the YFP CE, respectively, under the control of the 35S promoter.

The *CSN5A* cDNA, used as unrelated construction in co-immunoprecipitation assay, was isolated and inserted into the pDONR201 and pDONR207 to generate entry clones as previously described (Machado, 2011). The *CSN5A* coding region was transferred from these entry clones to the plant expression vectors pK7FWG2, generating CSN5A-GFP (pUFV1447) and to the destination vector pK7m34GW along with 2×35S promoter and the HA tail, yielding the clone 2×35S::CSN5A-6HA (pUFV1947), as described above for RPL10.

The clone NIK1T474D-pK7FWG2 was described previously (Santos *et al*., 2009). This clone harbours a GFP gene fused in frame after the last codon of the respective mutant cDNA under the control of the CaMV 35S promoter. In the mutant cDNA T474D, the threonine residue at position 474 within the activation loop of NIK1 was replaced with na aspartate residue.

For GUS histochemical assay, approximately 2kb of the 5' flanking sequences of *NIK1*, *RPL10A* and *LIMYB* were amplified from Arabidopsis genomic DNA using Taq Platinum and specific oligonucleotides and inserted into the entry vector pCR8/GW/TOPO (Life Techonology). The promoter sequences were then transferred by recombination into the destination vector pMDC162. The resulting clones, pNIK1-MDC162 (pUFV1428), pRPL10A-MDC162 (pUFV1431) and pLIMYB-MDC162 (pUFV1892), harboured the respective promoter sequences of the three genes fused to the β-glucuronidase (GUS) reporter gene.

For luciferase reporter assay, the *RPL28e* and *RPS13A* promoters were isolated from Arabidopsis DNA by PCR and cloned into pDONR-P4-P1R, generating pUFV2431 and pUFV2428, respectively. The clones LUCF-term-pDONR221 (pUFV 2132), that harbours the firefly luciferase cDNA in the entry vector pDON221, 2×35S::RLUCF-pDONR-P2R-P3 (pUFV2131), that contains *Renilla* luciferase cDNA under the control of a 2×35S promoter, and pUb10-pDONR-P4-P1R (pUFV1921), that harbours the ubiquitin promoter, were previously obtained. The *RPL28e*, *RPS13A* and *Ub10* promoters were transferred by triple recombination in to the destination vector pK7m34GW along with LUCF-term and 2×35S-RLUCF, yielding the clones pRPL28e::LUCF-2×35S::RLUCF (pUFV2437), pRPS13A::LUCF-2×35S::RLUCF (pUFV2439) and pUb10::LUCF-2×35S::RLUCF (pUFV2233), that harbour the firefly luciferase cDNA under the control of the *RPL28e*, *RPS13A* or ubiquitin promoters, as well as the *Renilla* luciferase cDNA under the control of a 2×35S promoter.

Yeast two-hybrid screening

The yeast two-hybrid assays were performed as previously described (Florentino *et al*., 2006). The yeast reporter strain AH109 (*MATa, trp1-901, leu2-3, 112, ura3-52, his3-200, gal4Δ, gal80Δ, LYS2::GAL1$_{UAS}$-GAL1$_{TATA}$-HIS3, GAL2$_{UAS}$-GAL2$_{TATA}$-ADE2, URA3::MEL$_{UAS}$-MEL1$_{TATA}$-lacZ*) was transformed sequentially with pBD-RPL10 and 25 µg of cDNA libraries, prepared from mRNA isolated from aerial tissues and fused to the GAL4 activation domain in the pEXAD502 vector, along with 3 mg of salmon sperm carrier DNA, using the lithium acetate/polyethylene glycol method. Transformants were plated on synthetic dropout medium lacking Trp, Leu, and His but supplemented with 10 mM 3-aminotriazole and cultured for 7 days at 28 °C. Approximately 9.4 ×10^5 transformants were obtained, as estimated based on the number of transformants growing on the SD-Leu-Trp plate. The interactions were

further confirmed by monitoring the β-galactosidase activity using 5-bromo-4-chloro-3-indolyl β-D-galactopyranoside (X-gal) or by measuring β-galactosidase activities from yeast extracts with o-nitrophenyl β-D-galactopyranoside (ONPG), as described previously (Uhrig *et al*., 1999).

Phylogenetic analysis

MYB family sequences were retrieved from the Agris database (http://arabidopsis.med.ohio-state.edu). The alignment was performed by Maft aligner software (Katoh and Standley, 2013), and the tree was built by Fasttree (Price *et al*., 2010) software.

Plant material, growth conditions and transformation

The Columbia (Col-0) ecotype of *Arabidopsis thaliana* and *Solanum lycopersicum*, cultivar Moneymaker, were used as the wild-type. Homozygous seeds of the T-DNA insertion *limyb* mutant (Salk_032054C) was obtained from the Arabidopsis Biological Resource Center; T474D-overexpressing tomato lines were previously obtained by Apfata (2010); and the transgenic lines 35S::NIK1-4 and 35S::NIK1-6 have been previously described (Carvalho *et al*., 2008c). Arabidopsis plants were grown in a growth chamber at 22 ºC under long-day conditions (16 h light/8 h dark), whereas tomato plants were grown greenhouse under standardized conditions. The Col-0 ecotype was transformed with pNIK1-MDC162, pRPL10A-MDC162, pLIMYB-MDC162, LIMYB-GFP and YFP-NLS-RPL10 using the floral dip method (Zhang *et al*., 2006). The transformed shoots were selected on MS medium supplemented with hygromycin (10 $mg.L^{-1}$) or kanamycin (100 $mg.L^{-1}$). The selected

transformants were transferred into soil, and the transgenic lines were confirmed using PCR.

Co-immunoprecipitation assay

The co-immunoprecipitation assay was performed using the μMACS Epitope Tag Protein Isolation Kit (MACS/Miltenyi Biotec) according to the manufacturer's instructions. Total protein extracts were prepared from *N. benthamiana* leaves that had been agroinfiltrated with RPL10-6HA and/or LIMYB-GFP, using *Agrobacterium tumefaciens* strain GV3101, as previously described (Carvalho *et al*., 2008c). At 72h after infiltration, 200 mg of leaves were homogenized with 1ml of lysis buffer (50mM Tris-HCl pH 8.0, 1% (v/v) Nonidet P-40) and incubated for 2 h with anti-GFP magnetic beads (MACS/Miltenyi Biotec) at 4 ºC under gentle agitation. After extensive washing of the magnetic beads, the bound proteins were eluted using 50 μL of elution buffer pre-warmed to 95 ºC. The immunoprecipitated proteins were separated by 10% (w/v) SDS-PAGE and immunoblotted with anti-HA (Miltenyi Biotec, catalogue number 130-091-972) or anti-GFP (Miltenyi Biotec, catalogue number 130-091-833) monoclonal antibodies. The reacting antibodies were detected using Signal West Pico Chemiluminescent Substrate (Thermo Scientific) according to the manufacturer's instructions.

Bimolecular fluorescent complementation (BiFC)

Nicotiana benthamiana leaves were agroinfiltrated with the following combinations of recombinant plasmids: LIMYB-SPYNE + RPL10-SPYCE; RPL10-SPYNE + LIMYB-SPYCE; LIMYB-SPYNE + SPYCE empty vector; RPL10-SPYNE + SPYCE empty vector; SPYNE empty vector + LIMYB-SPYCE; SPYNE empty vector

+ RPL10-SPYCE, using *Agrobacterium tumefaciens* strain GV3101, as previously described (Carvalho *et al*., 2008c). After incubation for 72h, the leaf sectors were examined by confocal microscopy. YFP was excited at 514nm using na argon laser, and YFP emission was detected using a 560-615 nm filter.

Histochemical in situ localization of GUS in Arabidopsis seedlings

The histochemical analysis of β-glucuronidase activity was performed as previously described (McCabe *et al*. 1988). The transformed seedlings with pNIK1-pMDC162, pRPL10-pMDC162 and pLIMYB-pMDC162 were embedded in the GUS assay buffer [100 mM NaH_2PO_4.H2O (pH 7.0), 0.5 mM $K_4Fe(CN)_6.3H_2O$, 10 mM $Na_2EDTA.2H_2O$, 0.1% (v/v) Triton X-100] containing 5-bromo-4-chloro-3-indolyl-b-D-glucuronide (X-Gluc; McCabe *et al*., 1988) and incubated at 37 ºC in the dark for 16 h. Pigments were extracted from stained tissues with methanol:acetone (3:1). The image of the stained seedlings was obtained by a digital camera attached to a stereomicroscope.

RT-PCR and real time RT-PCR analyses

Total RNA was extracted from Arabidopsis leaves using TRIzol (Life Technology). Reverse transcription (RT)-PCR assays were performed with 2 µg of total RNA, 0.5 µM of poly-dT and 1U of M-MLV reverse transcriptase (Invitrogen Life Technologies), as previously described (Delú-Filho *et al*., 2000). For gene expression analysis by qRT-PCR, gene-specific primers were designed using Primer Express 3.0 (Life Technologies). Real-time RT-PCR assays were performed on an ABI7500 instrument (Life Technologies) using the SYBR Green PCR Master Mix (Life Technologies). The amplification reactions were performed as follows: 2 min at 50 ºC,

10 min at 95 ºC and 40 cycles of 94 ºC for 15 s and 60 ºC for 1 min. Actin was used as an endogenous control to normalize all values in the real-time RT-PCR assays. Gene expression was quantified using the $2^{-\Delta Ct}$ method. The fold variation of gene expression was quantified using the comparative Ct method: $2^{-(\Delta CtTreatment - \Delta CtControl)}$.

Chromatin immunoprecipitation (ChIP) assay

The ChIP assay was performed using a chromatin immunoprecipitation assay kit (Imprint ChIP kit; Sigma) following the manufacturer's instructions. Briefly, protoplasts were obtained from LIMYB-GFP–overexpressing lines, the proteins bound to DNA were crosslinked with 1% formaldehyde, and cells were subsequently resuspended in the lysis buffer, followed by sonication. The protein extracts were incubated with antibody against GFP, human RNA polymerase II, or normal mouse IgG. Immunocomplexes were extensively washed, and the DNA was recovered by using a chromatography column and eluted in 50 µL of 10 mM Tris-HCl, pH 8.5. The DNA was used as a template for PCR amplification with sets of primers corresponding to the -908 bp to -755 bp *RPL18A* promoter fragment (5'-gttgaaagcctaatgccacat-3' and 5'-ctctgtttctccttcaatgac-3'). As a negative control, PCR was carried out with DNA immunoprecipted from Col-0.

Luciferase reporter gene assay

Nicotiana benthamiana leaves were agroinfiltrated with *A. tumefaciens* GV3101 strains carrying the DNA constructs pRPL28e::LUCF-2×35S::RLUCF; pRPS13A::LUCF-2×35S::RLUCF and pUb10::LUCF-2×35S::RLUCF alone or co-infiltred with *A. tumefaciens* GV3101 strains carrying RPL10-GFP or LIMYB-GFP.

Forty-eight hours after infiltration, 200 mg of leaf tissue was harvested for total protein extraction. Luciferase activity was assayed with the Dual-Luciferase Reporter Assay System (Promega) according to the manufacturer's instructions.

Infectivity assays

For the infectivity assays, it was used T2 transgenic plants harboring the T474D mutante gene construct, which were derived from three independently regenerated kanamycin-resistant plants (35S::T474D-2, 35S::T474D-5, 35S::T474D-6), previously obtained by Apfata (2010). It was also used the previously described transgenic lines expressing *At*NIK1 under the control of the CaMV 35S promoter, 35S::NIK1-4 and 35S::NIK1-6 (Carvalho *et al*., 2008c). The transgenic and wild-type lines were infected at the six-leaf stage with either ToYSV-[MG-Bi2] or ToSRV by biolistic delivery using tandemly repeated viral DNA-A and DNA-B and a microprojectile bombardment model PDS-1000/He accelerator (BIORAD) at 900 psi. In each experiment, 20 plants of each line were inoculated with 2 µg of tandemly repeated DNA-A plus DNA-B per plant and grown in a greenhouse under natural conditions of light, 70% relative humidity and approximately equal day and night lengths. Total nucleic acid was extracted from the systemically infected leaves (young leaves), and viral DNA was detected by PCR using DNA-A and DNA-B begomovirus-specific primers (PBL1v2040, gcctctgcagcartgrtckatcttcataca, and PCRC1, ctagctgcagcatatttacrarwatgcca, or PAL1v1978, gcatctgcaggcccacatygtcttyccngt, and PAR1c496, aatactgcagggcttyctrtacatrgg) at 10 days post-infection.

Quantitation of viral DNA in infected plants

Viral DNA accumulation was measured by quantitative PCR (qPCR). The reactions were prepared in a final volume of 10 µl using the Fast SYBR Green Master Mix (Life Technology) according to the manufacturer's instructions and analyzed on a 7500 Real Time PCR System (Life Technology). Virus-specific primers were designed using Primer Express 3.0 (Life Technology) and tested by conventional PCR using plasmids containing the complete DNA-A of each virus (10^6 copies per reaction). The following primer sequences were used: ToSRVFwd, 5'-cacgtgcccacatcgtctt-3', and ToSRVRev, 5'-ggccggaacgacctatta-3', or ToYSVFwd, 5'-ccacgattttaaagctgcattct-3', and ToYSVRev, 5'-caatcctggtgagggagtcagt-3'. For viral DNA quantitation, standard curves were prepared using serial dilutions of these clones (10^0 to 10^6 copies of viral genome per reaction). The genomic unit refers to one copy of the DNA-A of ToYSV or ToSRV. Standard curves were obtained by regression analysis of the Ct values of each of the three replicates of a given dilution in relation to the log of the amount of DNA in each dilution. For the absolute quantitation of the number of viral DNA molecules in the different treatments, 100 ng of total DNA from the infected plants was used in the qPCR reactions containing virus-specific primers. Each sample was analyzed in triplicate from at least two biological replicates.

Physiological measurements of tomato transgenic lines

Photosynthetic CO_2 assimilation (A), transpiration rate (E), and stomatal conductance (g_s) measurements were performed with a portable open-flow gas exchange system (LICOR 6400, Li-COR, Lincoln, Nebraska, USA) under ambient CO_2 concentrations (370 ± 10 µmol mol^{-1}) and temperature conditions under artificial, saturating PAR (1,000 µmol photons m^{-2} s^{-1} at the leaf level).

Estimation of total carotenoids, lycopene, and β-carotene

Total carotenoids from fully ripened tomato fruits were extracted with cold acetone and petroleum ether, as described by Rodriguez-Amaya *et al*. (1976). The extract (30 µL) was separated by HPLC using reversed phase C18 column (Phenomenex Gemini, 250 mm x 4,6 mm, 5 µm) and a C18 guard column (Phenomenex ODS, 4 mm x 3 mm) on a Shimadzu, SCL 10AT VP HPLC system coupled to a DAD detector (Shimadzu, SPD-M10A) and operating at a flow rate of 1.7 mL/min. The mobile phase buffer used was methanol:ethyl acetate:acetonitrile (70:20:10, v/v/v). The chromatograms were obtained at 450 nm and integrated using the software Multi System Class Vp 6.12. Lycopene and β-carotene were quantified from HPLC profile by using a purified lycopene standard (Sigma Chemical) and a β-carotene standard purified from carrots.

In vivo labeling of leaf proteins

Tomato seedlings (300 mg) were incubated with 1 mL of nutriente solution containing 50 µg.mL^{-1} chloramphenicol and 20 µCi of [^{35}S]methionine (EasyTag Protein Labeling Mix, [^{35}S]-, 2 mCi (74MBq), Perkin Elmer) for 3 h at room temperature. To quantitate incorporation of [^{35}S]methionine into protein, aliquots of protein extracts were placed in 10% (w/v) TCA and incubated on ice for 30 min. The samples were filtered onto glass microfiber filters and the filters were washed three times with 5 ml of cold 5% (w/v) TCA and two times with 5 ml of 95% ethanol. After drying, the filters were counted with a scintillation counter.

Polysome fractionation

Polysomes were fractionated over sucrose gradients as described (Wang *et al*., 2003). Briefly, 500 mg of 15-day-old tomato seedlings were ground in liquid nitrogen and 1 mL of extraction buffer (0.2 M Tris-HCl, pH 8.0, 50 mM KCl, 25 mM $MgCl_2$, 1% Triton X-100, 400 units/mL of RNasin and 50 mg/mL of cycloheximide). After centrifuging for 10 min, the supernatant was loaded onto a 10-mL 15% to 50% sucrose gradient and spun in a Beckman SW41Ti rotor at 135,000 g for 3.5 h. Fractions were collected manually from the bottom, and total RNA was extracted with phenol/chloroform/isoamyl alcohol, precipitated with isopropanol, and treated with DNase I. The specific transcripts were amplified from RNA of T474D, NIK1 and wilt-type infected lines using qRT-PCR.

References

Albuquerque, L.C., Varsani, A., Fernandes, F.R., Pinheiro, B., Martin, D.P., de Tarso, O.F.P., Lemos, T.O. and Inoue-Nagata, A.K. (2012) Further characterization of tomato-infecting begomoviruses in Brazil. *Arch Virol*, 157, 747–752.

Andrade, E.C., Manhani, G.G., Alfenas, P.F., Calegario, R.F., Fontes, E.P.B. and Zerbini, F.M. (2006) Tomato yellow spot virus, a tomato-infecting begomovirus from Brazil with a closer relationship to viruses from Sida sp., forms pseudorecombinants with begomoviruses from tomato but not from Sida. *J Gen Virol*, 87, 3687–3696.

Apfata, J.A.C. (2010) Análise funcional da via de sinalizacão antiviral mediada por NIK em tomateiro. Dissertação em Fisiologia Vegetal – Universidade Federal de Viçosa, Viçosa. 53 f.

Aragão, F.J. and Faria, J.C. (2009) First transgenic geminivirus-resistant plant in the field. *Nat Biotechnol*, 27, 1086–1088.

Bao, Z. and Hua, J. (2015) Linking the Cell Cycle with Innate Immunity in Arabidopsis. *Mol Plant*, doi: http://dx.doi.org/10.1016/j.molp.2015.03.013.

Brustolini, O.J.B., Machado, J.P.B., Condori-Apfata, J.A., Coco, D., Deguchi, M., Loriato, V.A.P., Pereira, W.A., Alfenas-Zerbini, P., Zerbini, F.M., Inoue-Nagata, A.K., Santos, A.A., Chory, J., Silva, F.F. and Fontes, E.P.B. (2015) Sustained NIK-mediated antiviral signalling confers broad-spectrum tolerance to begomoviruses in cultivated plants. *Plant Biotechnol J*, doi: http://dx.doi.org/10.1111/pbi.12349.

Carvalho, C.M., Machado, J.P.B., Zerbini, F.M. and Fontes, E.B.P. (2008a) NSPInteracting GTPase: a cytosolic protein as cofactor for nuclear shuttle proteins. *Plant Signal Behav*, 3, 752–754.

Carvalho, C.M., Fontenelle, M.R., Florentino, L.H., Santos, A.A., Zerbini, F.M. and Fontes, E.P.B. (2008b) A novel nucleocytoplasmic traffic GTPase identified as a functional target of the bipartite geminivirus nuclear shuttle protein. *Plant J*, 55, 869–880.

Carvalho, C.M., Santos, A.A., Pires, S.R., Rocha, C.S., Saraiva, D.I., Machado, J.P., Mattos, E.C., Fietto, L.G. and Fontes, E.P.B. (2008c) Regulated nuclear trafficking of rpL10A mediated by NIK1 represents a defense strategy of plant cells against virus. *PLoS Pathog*, 4, e1000247.

Castillo-Urquiza, G.P., Beserra, J.E. Jr, Bruckner, F.P., Lima, A.T., Varsani, A., Alfenas-Zerbini, P. and Zerbini, F.M. (2008) Six novel begomoviruses infecting tomato and associated weeds in Southeastern Brazil. *Arch Virol*, 153, 1985–1989.

Day, A.G., Bejarano, E.R., Buck, K.W., Burrell, M. and Lichtenstein, C.P. (1991) Expression of an antisense viral gene in transgenic tobacco confers resistance to the DNA virus tomato golden mosaic virus. *Proc Natl Acad Sci USA*, 88, 6721–6725.

Delú-Filho, N., Pirovani, C.P., Pedra, J.H.F., Matrangolo, F.S.V., Macedo, J.N.A., Otoni, W.C. and Fontes, E.P.B (2000) A sucrose binding protein homologue from soybean affects sucrose uptake in transgenic tobacco suspension-cultured cells. *Plant Physiol Bioch*, 38, 353–361.

Florentino, L.H., Santos, A.A., Fontenelle, M.R., Pinheiro, G.L., Zerbini, F.M., Baracat-Pereira, M.C. and Fontes, E.P.B. (2006) A PERK-like receptor kinase interacts with the geminivirus nuclear shuttle protein and potentiates viral infection. *J Virol*, 80, 6648–6656.

Fontes, E.P.B., Santos, A.A., Luz, D.F., Waclawovsky, A.J. and Chory, J. (2004) The geminivirus NSP acts as virulence factor to suppress an innate transmembrane receptor kinase-mediated defense signaling. *Gene Dev*, 18, 2545–2556.

Gafni, Y. and Epel, B.L. (2002) The role of host and viral proteins in intra- and intercellular trafficking of geminiviruses. *Physiol Mol Plant Pathol*, 60, 231–241.

Galvão, R.M., Mariano, A.C., Luz, D.F., Alfenas, P.F., Andrade, E.C., Zerbini, F.M., Almeida, M.R. and Fontes, E.P.B. (2003) A naturally occurring recombinant DNA-A of a typical bipartite begomovirus does not require the cognate DNA-B to infect *Nicotiana benthamiana* systemically. *J Gen Virol*, 84, 715–726.

Hashmi, J.A., Zafar, Y., Arshad, M., Mansoor, S. and Asad, S. (2011) Engineering cotton (*Gossypium hirsutum* L.) for resistance to cotton leaf curl disease using viral truncated AC1 DNA sequences. *Virus Genes*, 42, 286–296.

Hong, Y. and Stanley, J. (1996) Virus resistance in Nicotiana benthamiana conferred by African cassava mosaic virus replication-associated protein (AC1) transgene. *Mol Plant Microbe Interact*, 9, 219–225.

Institute of medicine (IOM-US) (2001) Food and Nutrition Board. In *Standing committee on the scientific evaluation of dietary reference intakes. Dietary reference intakes for vitamin A, vitamin K, arsenic, boron, chromium, copper, iodine, iron, manganese, molybdenum, nickel, silicon, vanadium, and zinc*. Washington, DC: National Academy Press.

Katoh, K. and Standley, D.M. (2013) MAFFT multiple sequence alignment software version 7: improvements in performance and usability. *Mol Biol Evol*, 30, 772–780.

Kunik, T., Salomon, R., Zamir, D., Navot, N., Zeidan, M., Michelson, I., Gafni, Y. and Czosnek, H. (1994) Transgenic tomato plants expressing the tomato yellow leaf curl virus capsid protein are resistant to the virus. *Biotechnology*, 12, 500–504.

Lin, C.Y., Tsai, W.S., Ku, H.M. and Jan, F.J. (2012) Evaluation of DNA fragments covering the entire genome of a monopartite *begomovirus* for induction of viral resistance in transgenic plants via gene silencing. *Transgenic Res*, 21, 231–241.

Lucioli, A., Sallustio, D.E., Barboni, D., Berardi, A., Papacchioli, V., Tavazza, R. and Tavazza, M. (2008) A cautionary note on pathogen-derived sequences. *Nat Biotechnol*, 26, 617–619.

Machado, J.P.B. (2011) Identificação e caracterização de alvos celulares da proteína NIG (NSP-Interacting GTPase). Dissertação de Mestrado em Bioquímica Agrícola – Universidade Federal de Viçosa, Viçosa. 74 f.

Mariano, A.C., Andrade, M.O., Santos, A.A., Carolino, S.M.B., Oliveira, M.L., Baracat-Pereira, M.C., Brommonshenkel, S.H. and Fontes, E.P.B. (2004) Identification of a novel receptor-like protein kinase that interacts with a geminivirus nuclear shuttle protein. *Virology*, 318, 24–31.

McCabe, D.E., Swain, W.F., Martinell, B.J. and Christou, P. (1988) Stable transformation of soybean (*Glycine max*) by particle bombardment. *Biotechnology*, 6, 923–926.

McGarry, R.C., Barron, Y.D., Carvalho, M.F., Hill, J.E., Gold, D., Cheung, E., Kraus, W.L. and Lazarowitz, S.G. (2003) A novel Arabidopsis acetyltransferase interacts with the geminivirus movement protein NSP. *Plant Cell*, 15, 1605–1618.

Noris, E., Accotto, G.P., Tavazza, R., Brunetti, A., Crespi, S. and Tavazza, M. (1996) Resistance to tomato yellow leaf curl geminivirus in *Nicotiana benthamiana* plants transformed with a truncated viral C1 gene. *Virology*, 224, 130–138.

Price, M.N., Dehal, P.S. and Arkin, A.P. (2010) FastTree 2 – Approximately maximum-likelihood trees for large alignments. *PLoS ONE*, 5, e9490.

Reyes, M.I., Nash, T.E., Dallas, M.M., Ascencio-Ibáñez, J.T. and Hanley-Bowdoin, L. (2013) Peptide aptamers that bind to geminivirus replication proteins confer a resistance phenotype to TYLCV and ToMoV infection in tomato. *J Virol*, 87, 9691–9706.

Rocha, C.S., Santos, A.A., Machado, J.P.B. and Fontes, E.P.B. (2008) The ribosomal protein L10/QM-like protein is a component of the NIK-mediated antiviral signaling. *Virology*, 380, 165–169.

Rodriguez, D.B., Raymundo, L.C., Lee, T-C., Simpson, K.L. and Chichester, C.O. (1976) Carotenoid pigment changes in ripening *Momordica charantia* fruits. *Ann Bot*, 40, 615–624.

Rojas, M.R., Hagen, C., Lucas, W.J. and Gilbertson, R.L. (2005) Exploiting chinks in the plant's armor: evolution and emergence of geminiviruses. *Annu Rev Phytopathol*, 43, 361–394.

Sanderfoot, A.A. and Lazarowitz, S.G. (1995) Cooperation in viral movement: the geminivirus BL1 movement protein interacts with BR1 and redirects it from the nucleus to the cell periphery. *Plant Cell*, 7, 1185–1194.

Sanderfoot, A.A. and Lazarowitz, S.G. (1996) Getting it together in plant virus movement: cooperative interactions between bipartite geminivirus movement proteins. *Trends Cell Biol*, 6, 353–358.

Sanderfoot, A.A., Ingham, D.J. and Lazarowitz, S.G. (1996) A viral movement protein as a nuclear shuttle: the geminivirus BR1 movement protein contains domains essential for interaction with BL1 and nuclear localization. *Plant Physiol*, 110, 23–33.

Santos, A.A., Carvalho, C.M., Florentino, L.H., Ramos, H.J. and Fontes, E.P.B. (2009) Conserved threonine residues within the A-Loop of the receptor NIK differentially regulate the Kinase function required for antiviral signaling. *PLoS ONE*, 4, e5781.

Santos, A.A., Lopes, K.V.G., Apfta, J.A.C. and Fontes, E.P.B. (2010) NSP-interacting kinase, NIK: a transducer of plant defence signalling. *J Exp Bot*, 61, 3839–3845.

Stanley, J., Frischmuth, T. and Ellwood, S. (1991) Defective viral DNA ameliorates symptoms of geminivirus infection in transgenic plants. *Proc Natl Acad Sci USA*, 87, 6291–6295.

Sunitha, S., Marian, D., Hohn, B. and Veluthambi, K. (2011) Antibegomoviral activity of the agrobacterial virulence protein VirE2. *Virus Genes*, 43, 445–453.

Uhrig, J.F., Soellick, T.-R., Minke, C.J., Philipp, C., Kellmann, J.-W. and Schreier, P.H. (1999) Homotypic interaction and multimerization of nucleocapsid protein of tomato spotted wilt tospovirus: identification and characterization of two interacting domains. *Proc Natl Acad Sci USA*, 96, 55–60.

Unterholzner, L., and Bowie, A.G. (2015) The interplay between viruses and innate immune signaling: Recent insights and therapeutic opportunities. *Biochem Pharmacol*, 75, 589–602.

Wang, W., Scali, M., Vignani, R., Spadafora, A., Sensi, E., Mazzuca, S. and Cresti, M. (2003) Protein extraction for two-dimensional electrophoresis from olive leaf, a plant tissue containing high levels of interfering compounds. *Electrophoresis*, 24, 2369–2375.

Ward, B.M. and Lazarowitz, S.G. (1999) Nuclear export in plants: use of geminivirus movement proteins for a cell-based export assay. *Plant Cell*, 11, 1267–1276.

Williams, B.R.G. (1999) PKR; a sentinel kinase for cellular stress. *Oncogene*, 18, 6112–6120.

Zhang, S.C., Wege, C. and Jeske, H. (2001) Movement proteins (BC1 and BV1) of Abutilon mosaic geminivirus are cotransported in and between cells of sink but not of source leaves as detected by green fluorescent protein tagging. *Virology*, 290, 249–260.

Zhang X, Henriques R, Lin S.S., Niu, Q.W. and Chua, N.H. (2006) Agrobacterium-mediated transformation of *Arabidopsis thaliana* using the floral dip method. *Nat Protoc*, 1, 641–646.

Zorzatto, C., Machado, J.P.B., Lopes, K.V.G., Nascimento, K.J.T., Pereira, W.A., Brustolini, O.J.B., Reis, P.A.B., Calil, I.P., Deguchi, M., Sachetto-Martins, G., Gouveia, B.C., Loriato, V.A.P., Silva, M.A.C., Silva, F.F., Santos, A.A., Chory, J. and Fontes, E.P.B. (2015) NIK1-mediated translation suppression functions as a plant antiviral immunity mechanism. *Nature*, 520, 679–682.

Figures

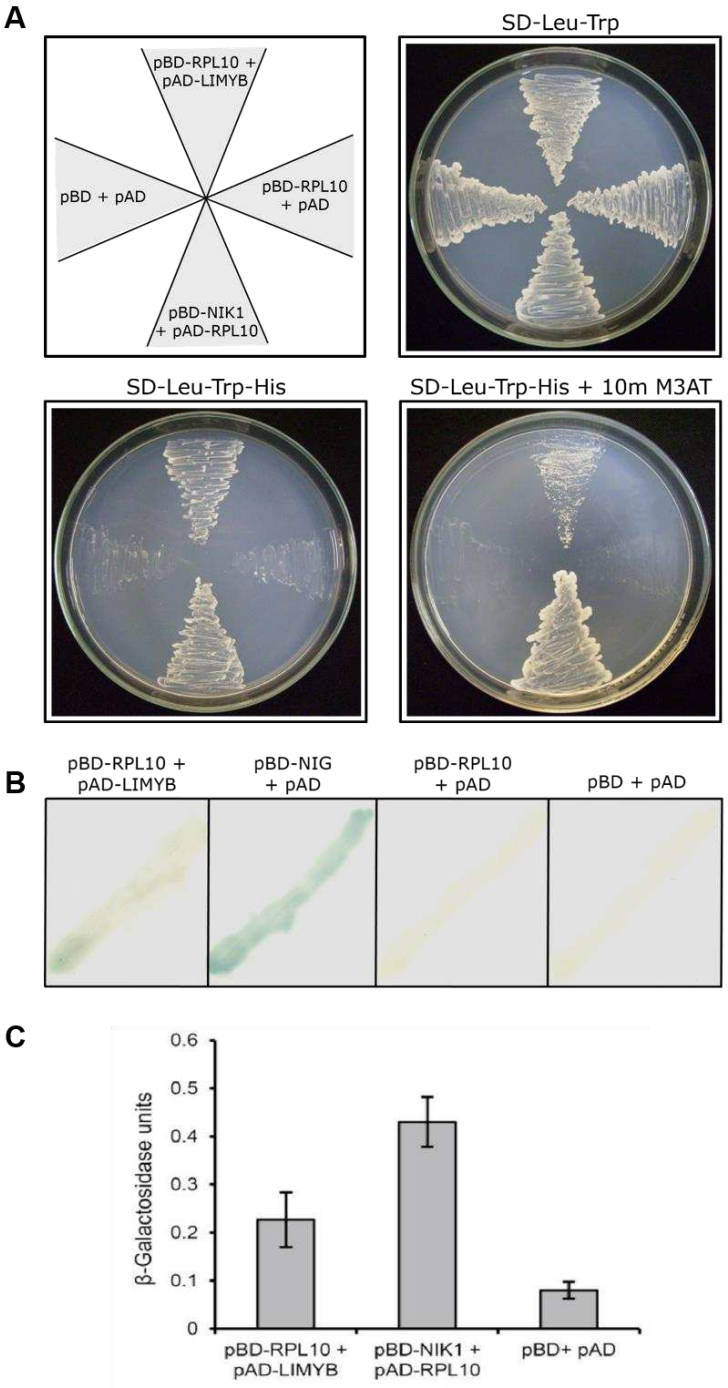

Figure 1: LIMYB interacts with RPL10 in yeast two-hybrid system. (A) LIMYB was expressed in yeast as a GAL4 activation domain (AD) fusion (pAD–LIMYB), and RPL10 was expressed as a GAL4 binding domain (BD) fusion (pBD–RPL10). The interactions between the tested proteins were examined by monitoring His prototrophy. (B–C) Interactions between the indicated proteins were further confirmed by monitoring the β-galactosidase activity, a second reporter gene. (B) Analysis of β-galacatosidase activity in nylon membrane. (C) β-galacatosidase activity was measured in yeast protein extracts. The interaction between pAD–RPL10 and pBD–NIK1 was monitored as a positive control. Means ± 95% confidence intervals (*n* = 3) based on bootstrap resampling replicates of three technical replicates are shown.

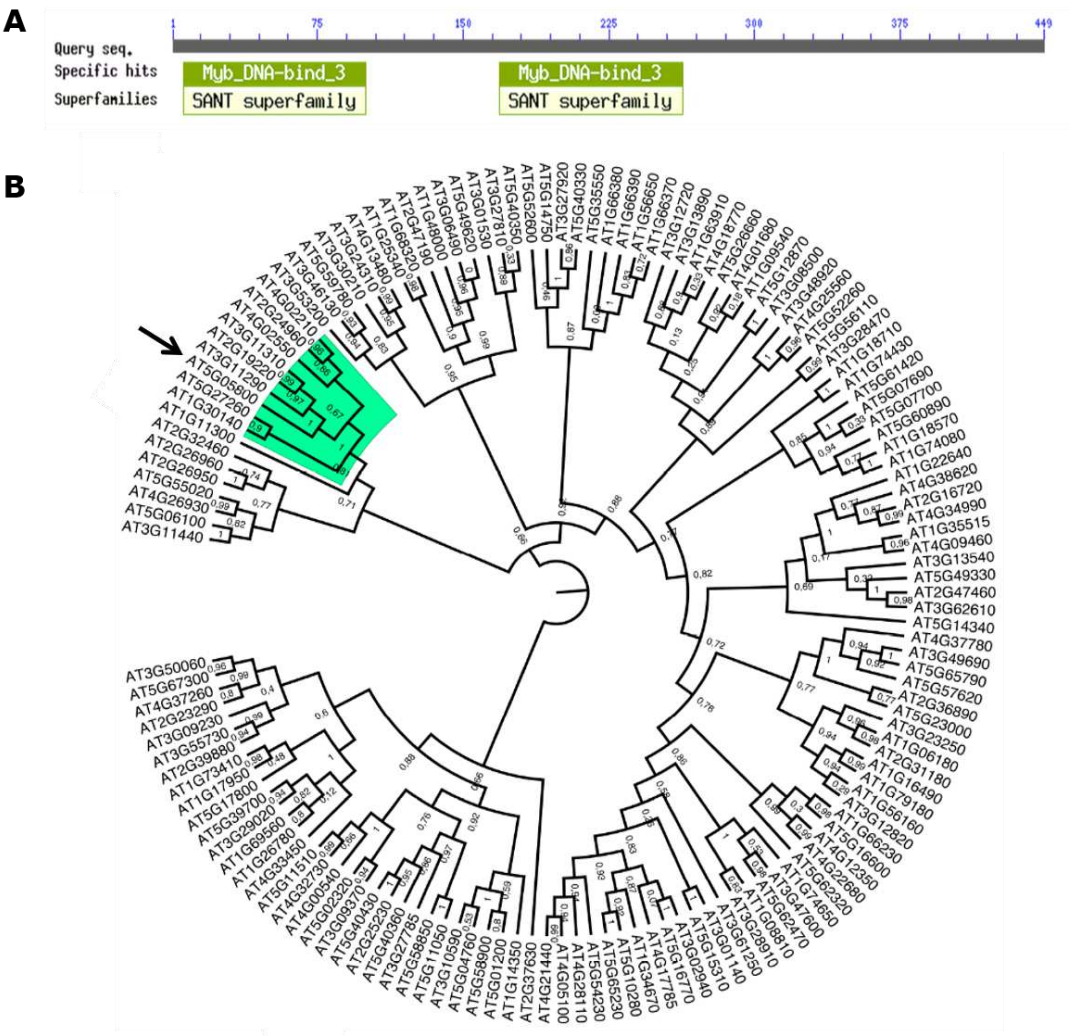

Figure 2: LIMYB belongs to the MYB domain-containing superfamily. (A) LIMYB harbours two MYB domains. The position of these MYB domains is indicated in the schematic representation of the LIMYB primary structure. (B) Dendrogram of MYB domain-containing proteins from Arabidopsis. The MYB family sequences were retrieved from the Agris database (http://arabidopsis.med.ohio-state.edu). The alignment was performed by Maft aligner software using full-length sequences, and the tree was built by Fasttree software (the bootstrap values are indicated close to the branch divisions). The arrow indicates *LIMYB* (*At5g05800*).

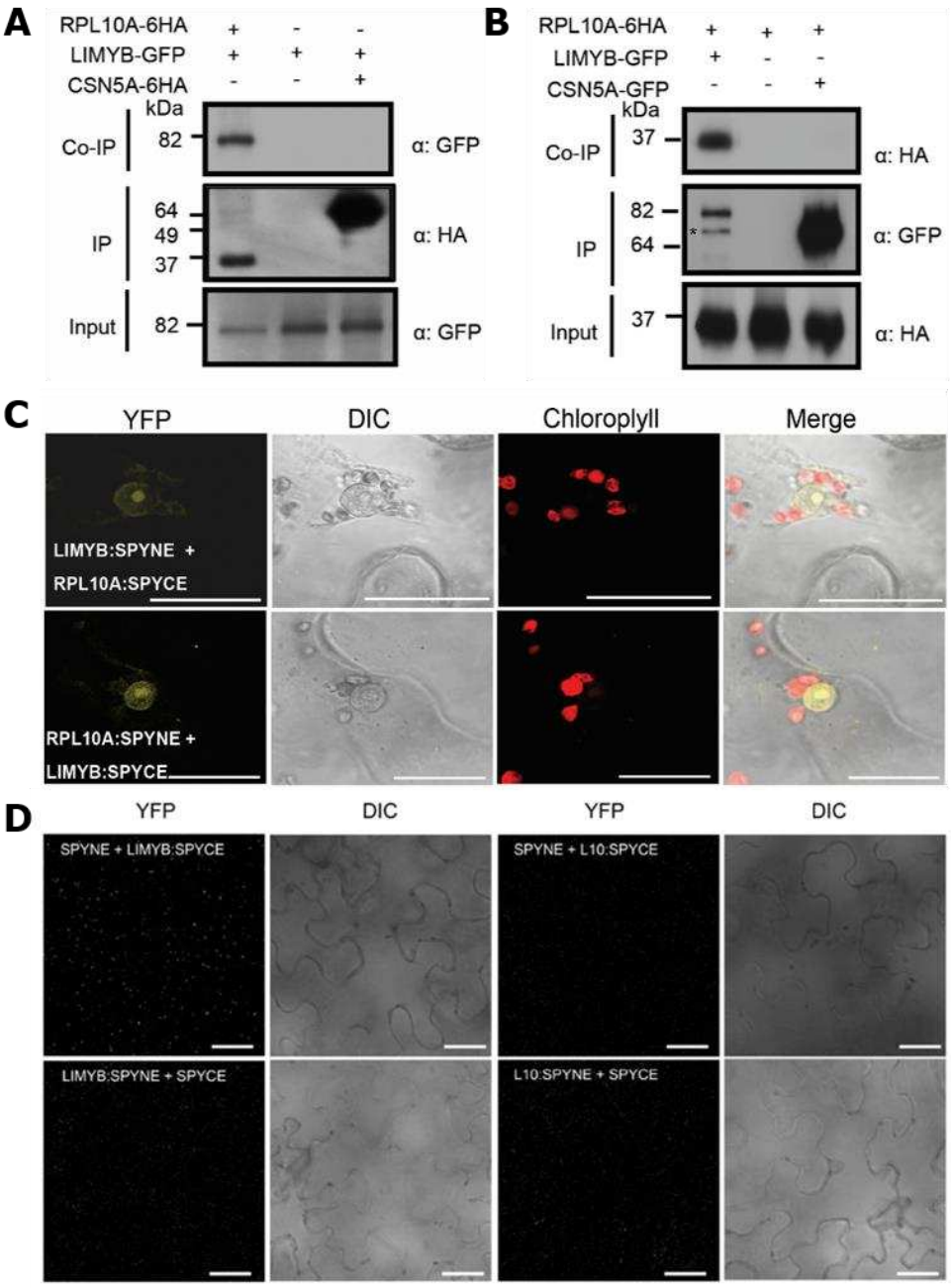

Figure 3: LIMYB interacts with RPL10 in the nucleus. (A) LIMYB and RPL10 interaction *in planta*. The indicated constructs were expressed in *N. benthamiana* leaves, and co-immunoprecipitation (Co-IP) assays were performed using na anti-haemagglutinin (HA) antibody. CSN5A is an unrelated protein used as a negative control. (B) Co-immunoprecipitation assay was performed using an anti-GFP antibody. * Indicates degradation product of LIMYB-GFP. (C) *In vivo* interaction between LIMYB and RPL10 by bimolecular fluorescence complementation (BiFC) analysis. The fluorescence (yellow fluorescent protein (YFP)) images were acquired using *N. benthamiana* leaves co-expressing the 35S::RPL10-SPYNE + 35S::LIMYB-SPYCE and 35S::RPL10-SPYCE + 35S::LIMYB-SPYNE fusion proteins. They are representative samples from three independente biological repeats. Scalebars, 20 µm. DIC, differential interference contrast. (D) The negative controls used in the BiFC analysis. Confocal fluorescent image of SPYNE + LIMYB-SPYCE, LIMYB-SPYNE + SPYCE, SPYNE + RPL10-SPYCE and RPL10-SPYNE + SPYCE, as indicated in the figure. Scale bars, 20 µm.

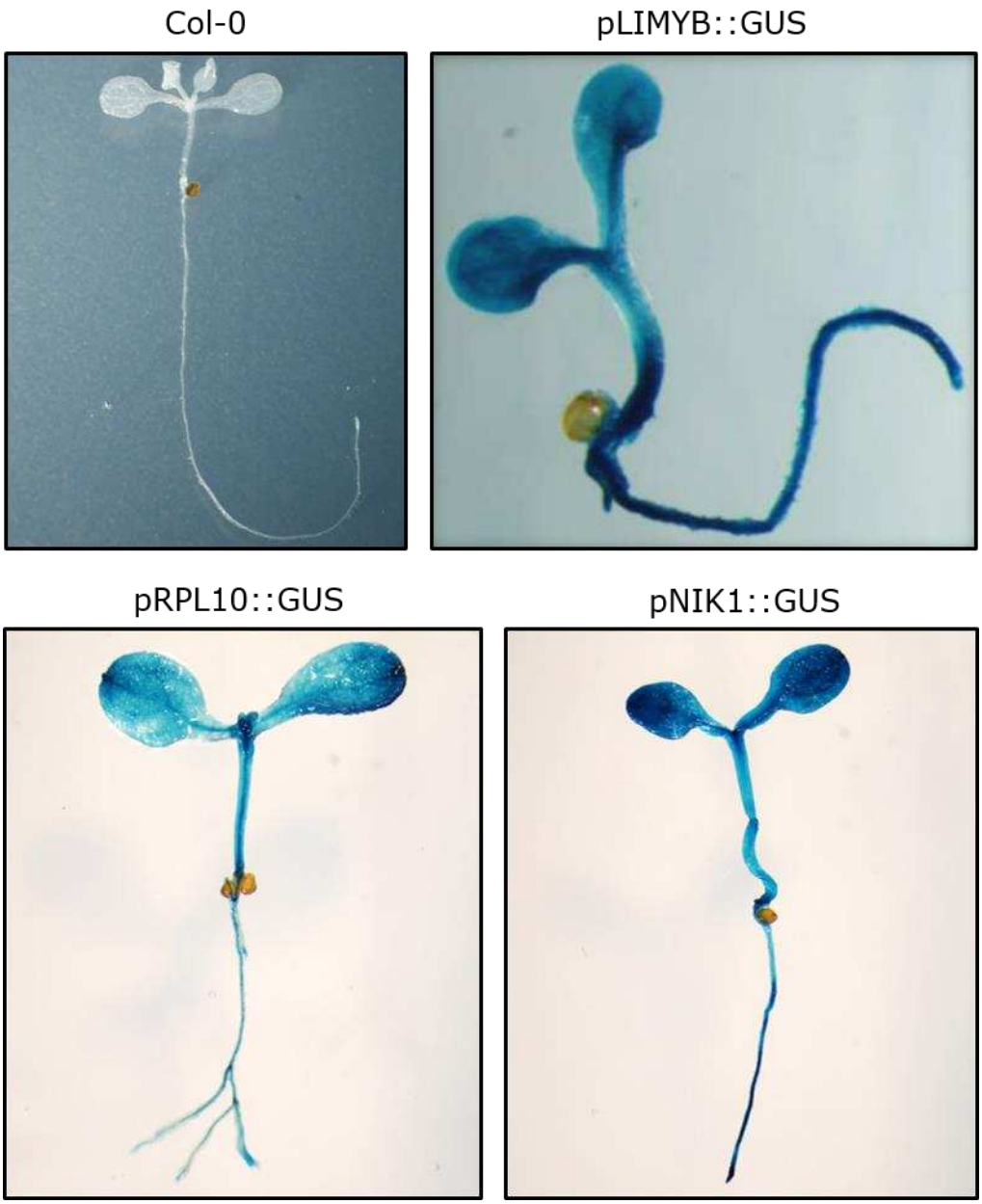

Figure 4: *LIMYB*, *RPL10* and *NIK1* display overlapping expression profiles. pLIMYB::GUS, pRPL10::GUS and pNIK1::GUS are ubiquitously expressed in seedling tissues. GUS reporter gene expression was histochemically monitored in 2-week-old seedling leaves and roots from transgenic lines harbouring a β-glucuronidase (GUS) reporter gene expressed from the *LIMYB*, *RPL10* and *NIK1* promoters. The figure shows representative GUS staining images of three seedlings per genotype. All three genes were ubiquitously expressed in all seedling tissues.

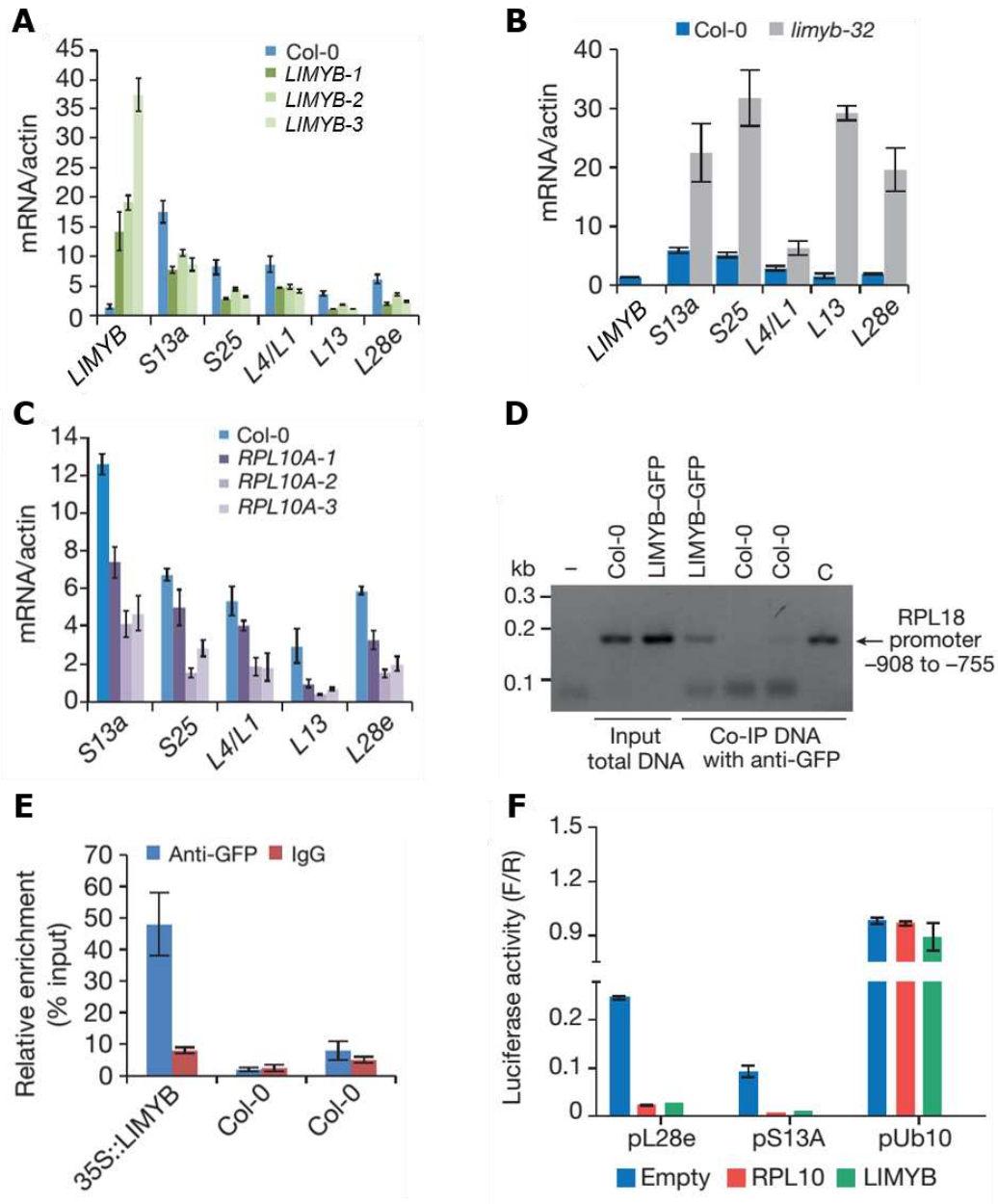

Figure 5: LIMYB links NIK1 activation to the downregulation of RP genes. (A) *LIMYB* overexpression downregulates ribosomal genes. Ribosomal gene expression was monitored by qRT–PCR of RNA from *LIMYB*-overexpressing leaves and Col-0. (B) Induction of ribosomal genes in the *limyb-32* mutant, monitored as in A. (C) RPL10 downregulates ribosomal genes, monitored as in A. (D) LIMYB binds to the *RPL18e* promoter *in vivo*. ChIP assay was performed with *LIMYB–GFP*-expressing leaves or wild type using anti-GFP antibodies. The co-immunoprecipitated (Co-IP) 150-bp fragment of the RPL18 promoter was detected by PCR. C, amplification of the control plasmid. (E) ChIP-qPCR assay of 35S::LIMYB–GFP transgenic and wild-type (Col-0) seedlings. Samples were immunoprecipitated with anti-GFP antibody or IgG antibody. ChIP DNA was quantified with real-time PCR. (F) LIMYB or RPL10 repress the ribosomal promoter. *N. benthamiana* leaves were agroinfiltrated with plasmids carrying the prL28e::luciferase (pL28e), prS23A::luciferase (pS13A) or prUb10::luciferase (pUb10) genes in combination with either the 35S::LIMYB or 35S:RPL10 DNA constructs. Luciferase activity was measured 48 h after agroinfiltration. F/R, firefly luciferase activity to Renilla activity ratio.

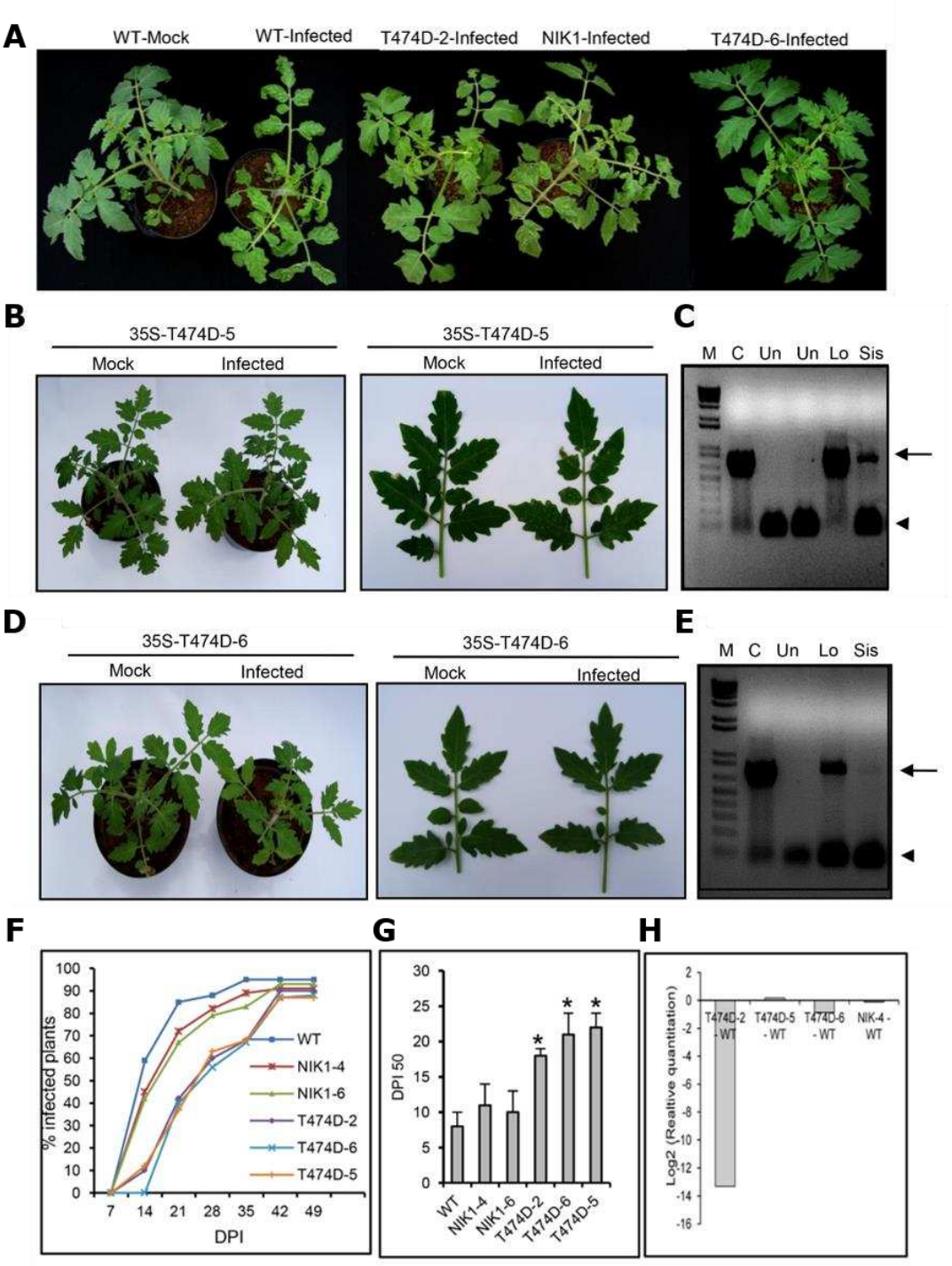

Figure 6: Ectopic expression of T474D in tomato confers tolerance to ToYSV infection. (A) Ectopic expression of T474D in tomato plants attenuates the development of symptoms upon ToYSV infection. Tandemly repeated ToYSV DNA-A and DNA-B sequences were introduced into the indicated lines by biolistic inoculation. Photographs were taken at 21 days postinoculation (DPI). (B) Symptoms associated with ToYSV infection in the 35S::T474D-5 line. Photographs were taken at 21 DPI. (C) Viral DNA accumulation in the infected leaves of the T474-5 line. Viral DNA accumulation was detected by PCR in inoculated ("Lo") and systemic ("Sys") leaves. "Un" indicates mock-inoculated leaves, and "C" indicates leaves with the ToYSV DNA-B-containing plasmid. Arrow - amplified viral DNA-B fragment; arrowheads - primers. (D) and (E) The line 35S-T474D-6 displayed tolerance to ToYSV infection. The T474D-6 line was infected with ToYSV, and photographs were

taken at 21 DPI. Viral DNA accumulation was detected by PCR in inoculated ('Lo') and systemic ('Sys') leaves. (F) The course of infection was delayed in T474D lines. The indicated lines were infected with ToYSV by the biolistic method, and the course of infection was monitored by PCR amplification of viral DNA. In each experiment (three biological replicates), 20 plants of each line were inoculated. Values represent the percentage of systemically infected plants at different DPI. (G) Infection efficiency in T474D-overexpressing lines. The infection efficiency is expressed as the DPI required to infect 50% of the plants (mean ± SD of three replicates). Asterisks indicate significantly different means ($P < 0.05$, Student's *t*-test). (H) Viral DNA accumulation in T474D-overexpressing lines, as determined by quantitative PCR at 28 DPI. The fold variation (± SD, $n = 3$ biological replicates) is shown as log2-scaled copy units of the viral genome. Viral DNA accumulation was determined in systemic leaves at 28 DPI.

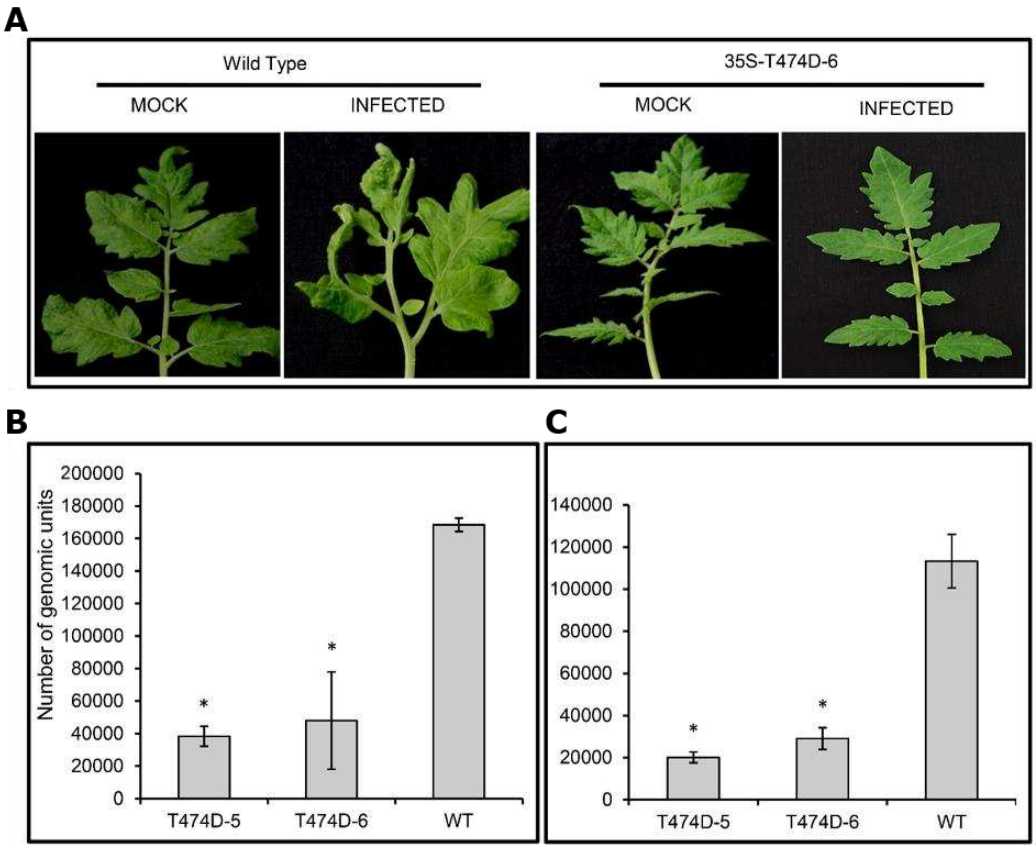

Figure 7: The T474D-6 overexpressing line is also tolerant to ToSRV infection. (A) Symptoms associated with ToSRV infection in the 35S::T474D-6 line. The T474D-6 line was infected with ToSRV, and photographs were taken at 21 DPI. (B) and (C) Viral DNA accumulation in the T474D-6- and T474-5-overexpressing lines at 14 DPI (B) and 28 DPI (C). Prior to performing real-time PCR, infected leaves were diagnosed by standard PCR. Subsequently, total DNA extracted from systemically infected leaves at 14 DPI (B) or 28 DPI (C) was used as a template for quantitative PCR using ToYSV DNA-A-specific primers. The fold variation (± SD, n = 3 biological replicates) is shown as copy units of the viral genome. The asterisks indicate significant differences with $P < 0.05$ according to a Student's t-test.

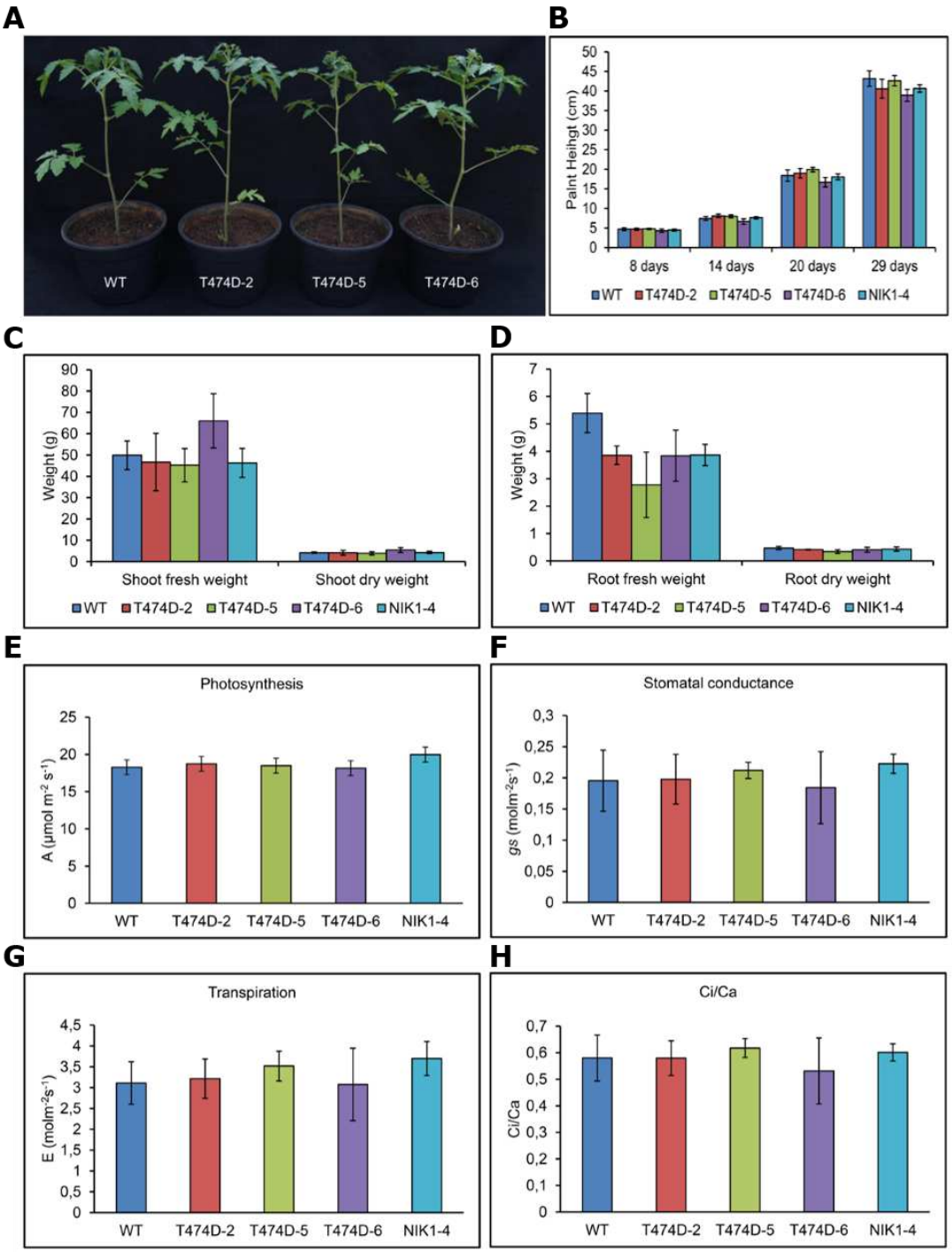

Figure 8: Characterization of the T474D-overexpressing lines during the vegetative phase. (A), (B), (C) and (D) Developmental phenotypes associated with overexpression of the T474D gain-offunction mutant in the R3 generation of tomato transgenic lines. (A) The images are plants of T474D-2, T474D-5, T474D-6 and wild-type lines grown for 30 days under normal greenhouse conditions. The transgenic lines are visibly undistinguishable from the wild-type plant. The indicated day correspond to the period of time after transferring germinated seedlings to the soil. (B) Plant height of wild-type line and T474D-2, T474D-5, T474D-6 and NIK1-4 transgenic lines grown for 8, 14, 20 or 29 days in the greenhouse. The indicated days correspond to the period of time after transferring germinated seedlings to the soil. Values represent the mean ± IC (α = 0,05) of 11 biological replicates and did not differ

between wild-type and transgenic lines in each period of the measurement. (C) Shoot fresh and dry weight and (D) root fresh and dry weight of wild-type and transgenic lines (as indicated) grown for 30 days in greenhouse. Values represent the mean ± IC (α = 0,05) of three biological replicates. (E–H) Physiological measurements of transgenic lines. The net CO_2 assimilation rate (*A*), transpiration rate (*E*),stomatal conductance to water vapor (g_s) and internal-to-ambient CO_2 concentration ratio (C_i/C_a) of fully expanded leaves of wild-type, T474D-2, T474D-5 and T474D-6 transgenic lines were measured by the LI-6400 infrared (IR) gas analyzer at growth irradiance. The error bars represent the confidence interval (α = 0.05) of measurements from five individual plants.

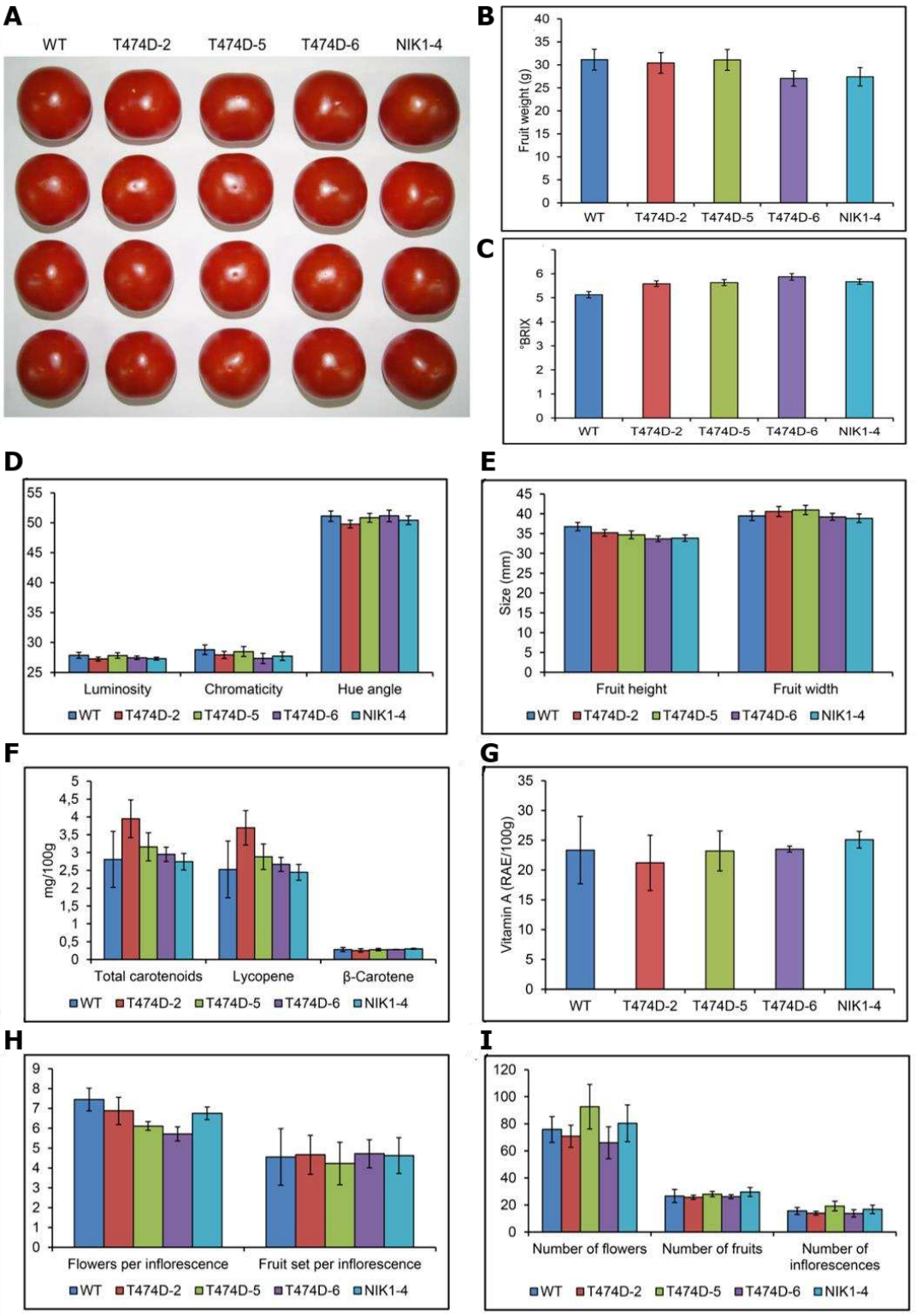

Figure 9: Fruit quality and yield of the T474D-overexpressing lines (A) Morphology and color of fresh ripe tomato fruits from T474D-overexpressing lines. The ripe fruit of the transgenic lines were bright red and were classified as small round, varying in size as indicated in the figure. (B) Fruit weight. Error bars, 95% confidence intervals based on bootstrap resampling replicates from 160 fruits. (C) Content of soluble solids of tomato fruits from T474D–, NIK1–overexpressing lines and wild-type. Fully ripened tomato fruits were also analyzed for total soluble solids (TSS), which were not different between the transgenic lines and wild-type. Total soluble solids were determined using a manual refractometer model ATC103

(BIOBRIX). The tomato sample was squashed manually and about three or four drops were transferred to the refractometer. Results were expressed as degrees of Brix. Error bars, 95% confidence intervals based on bootstrap resampling replicates from 85 fruits. (D) Skin color of tomato fruits. Skin coloration was analyzed according to luminosity (*L*), chromaticity (*C*) and hue angle (*H*) parameters (two readings per fruit), by means of reflectometry in a colorimeter brand KONICA MINOLTA. Values represent the mean ± IC (α = 0,05) of 53 fruits. (E) Fruit Size. Fully ripened tomato fruits were also analyzed for size. Values represent the mean ± IC (α = 0,05) of 160 fruits. (f) Content of carotenoids. Total carotenoids, lycopene and β-carotene were determined by HPLC. Values represent the mean ± IC (α = 0,05, *n* = 3) from three biological replicates. (g) Vitamin A content. The vitamin A contente is expressed as recommended by the Institute of Medicine (2001), in which 1 retinol activity equivalent (RAE) corresponds to 1 µg of retinol, 12 µg of β-carotene and 24 µg of other pro-vitamin carotenoids. Values represent the mean ± IC (α = 0,05, *n* = 3) from three biological replicates. (H) and (I). Developmental and yield performance of wild type and transgenic lines. The number of days to flowering (30-31 days) did not differ among transgenic lines and wild-type control. The number and size of inflorescence as well as fruit yield were measured. Values represent the mean ± IC (α = 0,05) of seven biological replicates.

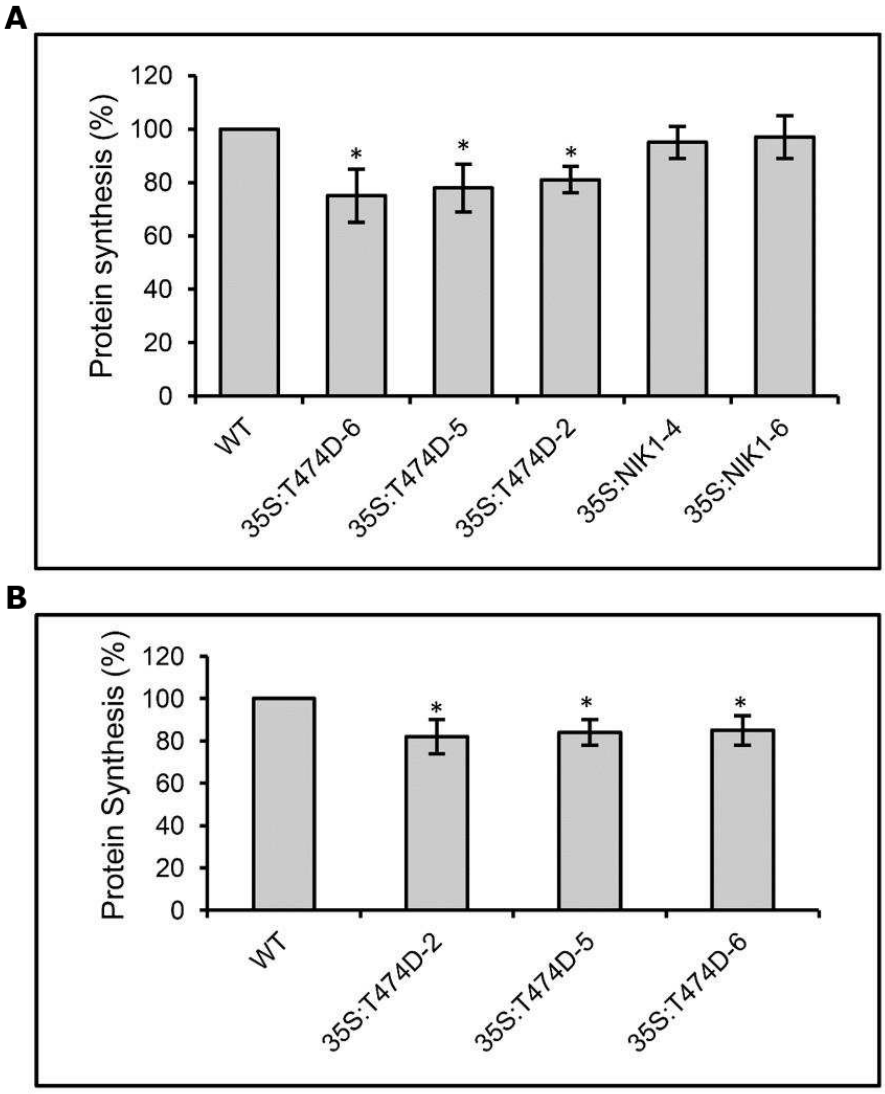

Figure 10: Ectopic expression of the T474D mutant receptor down-regulates global protein synthesis in leaves of tomato plants. Equal fresh weights of tomato leaves (300 mg) of 10 days old (A) and 28 days old (B) were incubated with 50 µg/mL chloramphenicol and 20 µCi of [^{35}S]methionine for 3 h at room temperature. Incorporation of [^{35}S]Met into protein was measured in the TCA-precipitated total protein (mean ± SD, n = 3, P < 0.05) from wild-type and T474D transgenic lines. Asterisks indicate significant differences from the wild-type control (P < 0.05, Student's t-test).

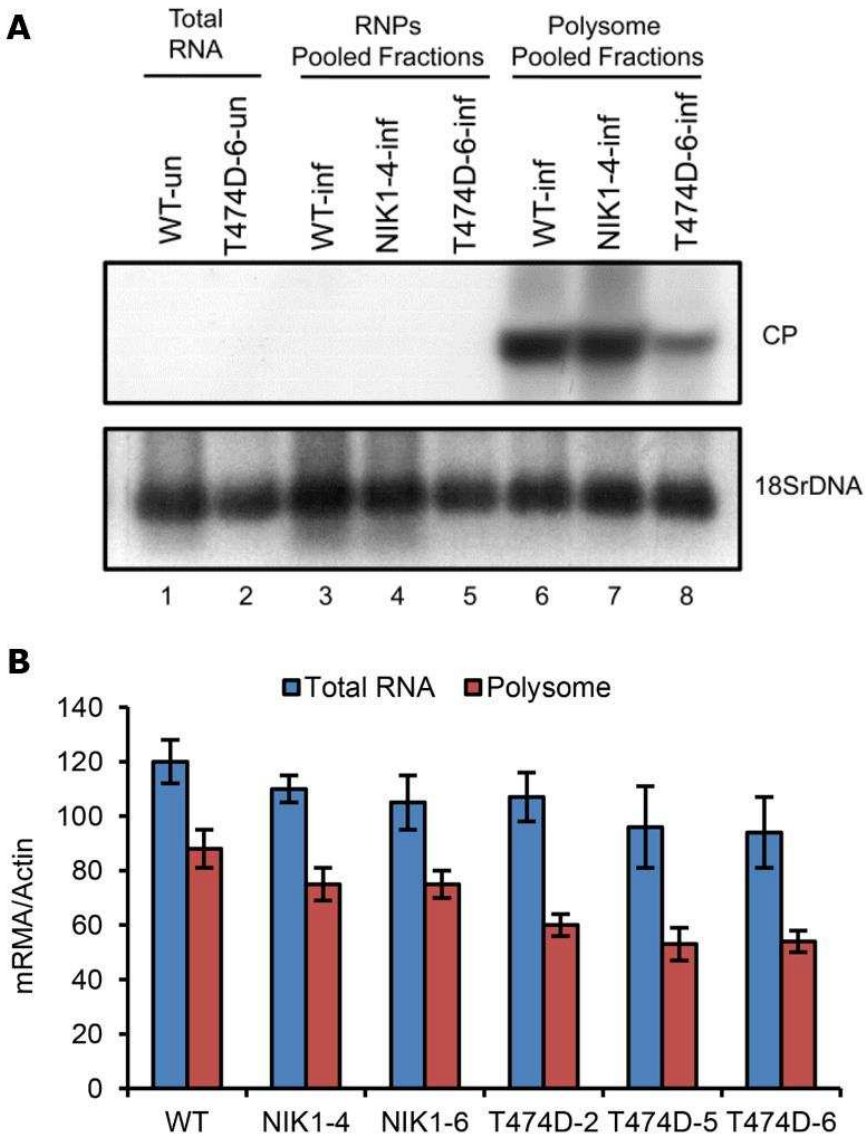

Figure 11: Polysome loading of viral mRNA is reduced in systemically infected leaves in the T474D-6-overexpressing lines. (A) Polysome loading of coat protein (CP) mRNA from ToYSV DNA-A in systemically infected leaves of WT, NIK-overexpressing and T474D-6-overexpressing lines. Polysomes from infected WT, NIK1-4-overexpressing and T474D-6-overexpressing lines were isolated from systemic leaves at 10 days postinoculation with tandem copies of DNA-A and DNA-B of ToYSV. RNPs refer to a 40S-enriched fraction. Polysome-bound RNA from pooledfractions was extracted with phenol/chloroform/isoamyl alcohol, precipitated with isopropanol, blotted and probed with the coat protein DNA (CP) and 18S rDNA. The identity of the polysome-pooled fraction was confirmed by treatment with 25 mM EDTA prior to the sucrose gradiente (data not shown), which releases the mRNA from the polysomes. (B) Quantitation of polysome-associated coat protein viral transcripts in T474D-overexpressing lines by qRT-PCR. Polysomes from infected WT, NIK1-4-overexpressing and T474D-6-overexpressing lines were isolated 10 days postinoculation with infectious ToYSV clones. Polysome-bound RNA from pooled fractions was extracted with phenol/chloroform/isoamyl alcohol, precipitated with isopropanol and quantified by qRT-PCR. Values were normalized to the expression of actin. Error bars represent SD from three measurements.

CHAPTER III

Prospects and Overviews

NIK1, a host factor specialized in antiviral defense or a novel general regulator of plant immunity?

Joao P. B. Machado, Otavio J. B. Brustolini, Giselle C. Mendes, Anésia A. Santos, Elizabeth P. B. Fontes*

Departamento de Bioquímica e Biologia Molecular, BIOAGRO, National Institute of Science and Technology in Plant-Pest Interactions, Universidade Federal de Viçosa, 36571.000, Viçosa, MG, Brazil.

***Corresponding author:**

Elizabeth P B Fontes

Email: bbfontes@ufv.br

Running title: NIK function in plant immunity

Published in BioEssays (DOI 10.1002/bies.201500066)

Abstract

NIK1 is a receptor-like kinase involved in plant antiviral immunity. Although NIK1 is structurally similar to the plant immune factor BAK1, which is a key regulator in plant immunity to bacterial pathogens, the NIK1-mediated defenses do not resemble BAK1 signaling cascades. The underlying mechanism for NIK1 antiviral immunity has recently been uncovered. NIK1 activation mediates the translocation of RPL10 to the nucleus, where it interacts with LIMYB to fully down-regulate translational machinery genes, resulting in translation inhibition of host and viral mRNAs and enhanced tolerance to begomovirus. Therefore, the NIK1 antiviral immunity response culminates in global translation suppression, which represents a new paradigm for plant antiviral defenses. Interestingly, transcriptomic analyses in nik1 mutant suggest that NIK1 may suppress antibacterial immune responses, indicating a possible opposite effect of NIK1 in bacterial and viral infections.

Keywords: begomoviruses; immune receptor; immune responses; NIK1; NSP-interacting kinase; plant antiviral immunity; translation suppression

Abbreviations: ETI, effector-triggered immunity; **LRR-RLK,** leucine-rich repeats receptor-like kinases; **PAMP,** pathogen-associated molecular pattern; **PRR,** pattern recognition receptor; **PTI,** PAMP-triggered immunity; **RLK,** receptor-like kinase; **RP,** ribosomal protein; **SA,** salicylic acid; **Ser,** serine; **Thr,** threonine.

Introduction

Plants depend on their immune system to detect pathogens and activate defenses against invaders. The plant innate immune system employs a perception and defense system at two levels [1]. At the first level of defense, PAMP-triggered immunity (PTI) is mediated by pattern recognition receptors (PRRs), which perceive and recognize pathogen-associated molecular patterns (PAMPs) that are presented by the pathogens [2]. So far, plant PRRs are receptor-like kinases (RLKs) or receptor-like proteins (RLPs) located at the cell surface [3]. The second level, effector-triggered immunity (ETI), involves intracellular immune receptors, designated as resistance proteins (R), which recognize – directly or indirectly – virulence effectors secreted by the pathogens into the host intracellular environment, thereby activating a defense response [4]. Plants use the second level of defense to fight virus [5, 6]. An emerging picture is the capacity of plants to trigger PTI against viruses [7, 8]. Furthermore, the pre-activation of PTI by the elicitor chitosan through interaction with chitin-binding PRRs has also been shown to be effective against viruses [9]. Two kinds of chitin elicitor-binding PRRs have been identified: a RLP, in rice, and a RLK, in Arabidopsis, which share chitin binding-extracellular lysine motifs (LysMs).

The well-characterized co-receptor of the plasma membrane-associated PRRs, designated BRASSINOSTEROID INSENSITIVE1 (BRI1)-associated kinase 1, BAK1, has been shown to be involved in antiviral immunity [7, 8]. Another immune receptor, nuclear shuttle protein (NSP)-interacting kinase 1 (NIK1), which is also located in the plasma membrane and is structurally similar to BAK1, is also involved in antiviral immunity. Nevertheless, we have shown recently that the mechanism underlying the antiviral function of NIK1 is totally different from the classical BAK1-mediated PTI. Here, we discuss the possibility that NIK1 may antagonize PTI by

interacting negatively with the classical mechanism of plant anti-bacterial immunity. If this is the case, NIK1 may function as a negative co-receptor in suppressing translation and the plant immune system through distinct branches of the NIK1-supported signaling pathways.

Like BAK1, NIK1 belongs to subfamily II of the leucine-rich repeats (LRR) receptor-like kinases (RLK)

The RLK superfamily consists of the largest group of plant receptors, comprising more than 600 members in Arabidopsis, tomato and soybean [10-12] and more than 1,000 representatives in rice [13]. Members of the RLK superfamily are involved in development and/or defense responses against a wide range of pathogenic agents [14-16]. RLKs are structurally organized into a receptor configuration with a peptide signal, a transmembrane segment that connects a variable extracellular domain with the capacity to interact with a specific ligand to a cytosolic kinase domain that phosphorylates threonine/serine residues and, in some cases tyrosine residues, on protein substrates [15, 17, 18]. RLK-mediated signaling is frequently initiated by a ligand-dependent dimerization or oligomerization of the receptor. The immune receptor RLKs (PRRs) recognize conserved molecular signatures characteristics of a class of pathogens (PAMPs) or endogenous danger signals released by the host during a wound or pathogenic attack (DAMPs), which function as elicitors. Upon elicitor binding, the PRR undergoes dimerization/oligomerization with a co-receptor [3]. The RLK heterodimers are then auto- or trans-phosphorylated by their cytosolic kinase domains, leading to activation, recognition and phosphorylation of the downstream components of the signaling pathway [19].

The RLK superfamily is divided into approximately 50 families, based on a phylogenetic analysis of the kinase domain, by which the RLKs with structurally

similar extracellular domains were clustered together defining the families [20]. Among them, the largest family comprises RLKs, with a leucine-rich repeat (LRR) extracellular domain that is represented by more than 200 copies in the Arabidopsis genome [12, 21]. The LRR-RLK family is further subdivided into 13 subfamilies based on sequence identity, number (3–26 LRRs) and disposition of the LRR motifs in the extracellular domain. Subfamily II of LRR-RLK (LRRII-RLK) comprises 14 receptors, which possess four complete LRR motifs (with 24 amino acid residues) and a fifth incomplete LRR motif (with 16 amino acid residues), arranged in a unique contiguous block in the extracellular domain [22]. Phylogenetic analysis of this subfamily clustered the 14 components into three distinct clades: (i) antiviral defense receptors, (ii) development and defense receptors and (iii) receptors of unknown function [22].

Subgroup II of the LRRII-RLK subfamily, involved in development and defense, is formed by the five members of the SOMATIC EMBRYOGENESIS RECEPTOR KINASE (SERK1-5) gene family, which play different functions in male sporogenesis, response to brassinosteroids (BRs) and in the control of PTI and cell death [23]. BAK1, also designated AtSERK3, is the best characterized member of this subfamily of receptors. BAK1 functions as a co-receptor of several plasma membrane-tethered ligand-dependent LRR-RLKs and thereby participates actively in distinct signaling pathways. BAK1 contributes to plant development through interactions with BRI1, an LRR-RLK that perceives the signal of the BR phytohormone [24, 25]. The BAK1-BRI1 heterodimerization initiates signaling for BR-induced developmental responses [26]. In addition to participating in BR signaling, BAK1 also plays a role in plant innate immunity against many classes of pathogens as a co-receptor through interactions with flagellin sensing 2 (FLS2) receptor, elongation factor Tu receptor

(EFR) or pep one receptor 1 (PEPR1), which perceive specific PAMPs and trigger PTI [3, 27-30]. The BAK1 positive regulation in plant immunity and in BR signaling is underscored by phosphorylation reactions between the BAK1 co-receptor and the corresponding receptor.

NIK1, NIK2 and NIK3 form a gene family belonging to group I of the LRRII-RLK subfamily, which is involved in antiviral defenses [22]. NIKs were first identified as virulence targets of the NSP of bipartite geminiviruses (begomoviruses) [31]. The NSP-NIK interaction is conserved among begomovirus NSPs and NIK homologs from distinct hosts. NIK homologs from Arabidopsis, tomato and soybean interact with NSP from Cabbage leaf curl virus (CaLCuV) and from tomato-infecting begomoviruses, such as Tomato golden mosaic virus (TGMV), Tomato crinkle leaf yellow virus (TCrLYV) and Tomato yellow spot virus (ToYSV) [11, 31, 32]. These interactions inhibit the NIK kinase activity and prevent the activation of the signal transduction pathway that would trigger an antiviral defense response, creating a host environment enabling begomovirus infection [33, 34].

The NIK1/RPL10 module transduces a defense response to begomoviruses

The transmembrane receptor NIK1 was isolated through two-hybrid screening on account of its capacity to bind to the viral protein NSP, and the interaction of NIK1-NSP was further confirmed by in vitro binding assays [31, 32]. More recently, the interaction between NSP from CaLCuV and NIK1 from Arabidopsis was confirmed in planta through bimolecular fluorescence complementation (BiFC) assays, which located the NIK1-NSP complex in the cell periphery [35]. The NSP-binding site was mapped to an 80 amino acid stretch (positions 422–502) of NIK1 that encompasses

the putative active site for Ser/Thr kinases (subdomain VIb–HrDvKssNxLLD) and the activation loop (subdomain VII–DFGAk/rx, plus subdomain VIII–GtxGyiaPEY) [31].

The viral NSP is encoded by the component B, DNA-B, of bipartite begomoviruses (Geminiviridae family) that also encodes the movement protein (MP), both viral proteins required for systemic infection [36]. A second genomic component, DNA-A, encodes all of the functions required for viral replication, transcriptional activation of viral genes, suppression of siRNA-mediated plant defenses and encapsidation of the viral genomes as single-stranded DNA circles in twinned isometric particles. Begomoviruses replicate their genome in the nuclei of infected plants via rolling circle replication. NSP binds to the nascent viral DNA in the nucleus and facilitates the intracellular trafficking of viral DNA between the nucleus and the cytoplasm, whereas MP potentiates its cell-to-cell movement. In addition to encoding suppressors for siRNA-mediated defenses, begomoviruses enhance their pathogenicity in susceptible hosts through the NSP-mediated suppression of the antiviral activity of the NIK1 receptor [31, 33, 35].

In addition to the virulence function of NSP as an NIK suppressor, several other lines of evidence indicate that NIK1 functions in antiviral defenses. First, loss of NIK1, NIK2, or NIK3 function in Arabidopsis is linked to an enhanced susceptibility phenotype to CaLCuV infection [31, 33, 37]. Second, overexpression of NIK1 from Arabidopsis in tomato plants attenuates symptom development and delays ToYSV infection [38]. Finally, as an authentic defense signal transducer, mutations in the activation loop (A-loop) of NIK1 that block autophosphorylation activity also impair the capacity of NIK1 to elicit a defense response against begomoviruses [33].

As Ser/Thr kinase receptors, NIKs contain all of the 11 conserved subdomains of protein kinases, in addition to specific signatures of serine/threonine kinases in

subdomains VIb and VIII [39]. NIK1 exhibits trans-autophosphorylation activity in vitro and substrate phosphorylation activity in vitro and in vivo [31, 37, 38]. NIK1 is phosphorylated in vitro at the conserved positions Thr-474 and Thr-469, and mutations within the A-loop interfere in the NIK1 capacity of autophosphorylation [33]. Replacement of Thr-474 with alanine strongly inhibits the autophosphorylation activity, whereas replacement of Thr-474 with a phosphomimetic aspartate residue increases autophosphorylation activity and results in the constitutive activation of the NIK1 mutant receptor that it is no longer inhibited by begomovirus NSP [33]. Consistent with these findings, ectopic expression of the Arabidopsis phosphomimetic T474D mutant in tomato transgenic lines confers a higher level of tolerance to tomato-infecting begomoviruses than expression of an intact NIK1 receptor [35]. In contrast, ectopic expression of loss-of-function Thr-474 mutants, such as T474A or the double mutant G4743V/T474A, did not reverse the enhanced susceptibility phenotype of NIK1 knockout lines, demonstrating that Thr-474 autophosphorylation is required to transduce a defense response to begomoviruses [33]. Collectively, these results support the notion that phosphorylation at the essential Thr-474 residue within the A-loop constitutes a key regulatory mechanism for NIK1 activation.

The ribosomal protein L10 (RPL10) was isolated through two-hybrid screening by its capacity to bind to the kinase domain of NIK1 [37], and was biochemically and genetically linked to the NIK1 signaling pathway [33, 37, 38]. RPL10 is localized in the cytoplasm, but is redirected to the nucleus by co-expression with NIK1. Although RPL10 binds to NIK1 in vitro and in vivo, it is not efficiently phosphorylated by NIK1 in vitro and may not serve as a direct NIK1 substrate in vivo. Nevertheless, the nucleocytoplasmic shuttling of RPL10 is regulated by phosphorylation and is dependent on the kinase activity of NIK1. In fact, NIK1 does not relocate a

phosphorylation-deficient mutant of RPL10 to the nucleus [38]. Furthermore, the gain-of-function T474D mutant is more effective at redirecting RPL10 to the nucleus, and inactive mutants of NIK1 fail to change the cytosolic localization of RPL10 [33]. Mutations in the A-loop similarly affect the NIK1 capacity to elicit an antiviral response and to mediate a phosphorylation-dependent nuclear relocalization of the RPL10 downstream component.

The mechanism of NIK1-mediated antiviral defense is underscored by suppression of host global translation: a new paradigm for antiviral defenses in plants

Since the discovery of the NIK1 receptor [32] and the downstream component RPL10 [37], progress towards deciphering this layer of plant defense has been limited for two major reasons. First, the NIK1-mediated antiviral signaling represents a resistance response evolutionarily overcome by a begomovirus virulence strategy. Therefore, in this compatible interaction, triggering the signaling pathway also elicits the side effects of virus infection, because the viral protein NSP suppresses defense to cause disease. Second, the complete lack of knowledge of the critical early events that elicit signaling and transduction from the receptor does not allow us to trigger the pathway in a controlled manner. These difficulties were recently overcome by replacing the NIK1 gene with the constitutively activated T474D mutant in Arabidopsis and analyzing the T474D-induced changes in gene expression as the signature of a sustained NIK1 signaling pathway in the absence of virus infection [40]. Constitutive activation of NIK1 down-regulates components of the translational machinery and, thereby, causes suppression of global translation, decreasing the loading of host mRNAs in actively translating polysomes (PS). Induction of T474D

expression through a dexamethasone-inducible promoter also impairs global translation, which is accompanied by a reduction in PS and monosome (NPS) fractions as well as in the RNA content associated with these fractions in the T474D lines. The transgenic lines ectopically expressing T474D were tolerant to CaLCuV, a phenotype that is associated with a symptomless infection, lower infection efficiency, reduced accumulation of viral DNA in systemic leaves and reduced loading of coat protein viral mRNA in actively translating polysomes. Therefore, begomovirus was not capable of sustaining high levels of viral mRNA translation in the T474D-expressing lines, indicating that suppression of global protein synthesis may effectively protect plant cells against DNA viruses (see also comments by Nicaise [41]). Consistent with this argument, overexpression of T474D in tomato represses ribosomal protein genes, suppresses global protein synthesis, decreases viral mRNA association with polysome fractions, and recapitulates the enhanced resistance phenotype of the Arabidopsis T474D transgenic lines [35]. The T474D-overexpressing tomato transgenic lines were tolerant to ToYSV and Tomato severe rugose virus (ToSRV), which display highly divergent genomic sequences and hence are phylogenetically separated within the two major groups of begomoviruses found in Brazil [42]. These observations demonstrate the potential of a sustained NIK1-mediated defense pathway to confer broad-spectrum tolerance to begomoviruses in distinct plant species.

Recent progress towards elucidation of the molecular bases for the NIK1-mediated suppression of translation includes the isolation of an RPL10-interacting MYB-domain containing transcriptional repressor LIMYB, which acts in concert with RPL10 to fully repress the expression of ribosomal protein (RP) genes, components of the translational machinery [40]. LIMYB and RPL10 interact in the nucleus of transfected cells and coordinately regulate common target promoters. T474D also

down-regulates the expression of the same sub-set of LIMYB-regulated RP genes but requires the LIMYB function to repress RP gene expression. As a downstream component of the NIK1-mediated antiviral signaling and a transcriptional repressor, LIMYB overexpression down-regulates RP genes at the transcriptional level, suppresses translation and enhances tolerance to begomovirus. In contrast, the loss of LIMYB function releases the repression of translation-related genes and increases susceptibility to virus infection. Therefore, LIMYB links NIK1 activation to global translation suppression as an antiviral immunity strategy in plants.

Based on the current data and common features of the LRRII-RLK family, we propose a mechanistic model for a NIK1-mediated defense signaling pathway and its interaction with the begomovirus NSP (Fig. 1). Upon begomovirus infection, the LRR extracellular domain undergoes oligomerization, allowing the intracellular kinase domains to transphosphorylate each other on the crucial Thr-474 residue, causing signaling transducer activation [33]. Alternatively or additionally, NIK1 may serve as a co-receptor that interacts with an unidentified ligand-dependent LRR-RLK receptor in response to virus infection. In this scenario, the phosphorylation-dependent activation of NIK1 leads to the regulated relocation of RPL10 to the nucleus, where it interacts with LIMYB to fully repress translation-related genes [38, 40]. Prolonged down-regulation of translation machinery-related genes causes a suppression of global protein synthesis, reducing the association not only of host mRNAs but also of viral mRNAs with the actively translating polysomes in infected cells. Therefore, this down-regulation of cytosolic translation underlies at least partially the molecular mechanisms involved in NIK1-mediated antiviral defenses. Counteracting the NIK1 activation mechanism, NSP binds to the receptor kinase domain and sterically interferes with phosphorylation of Thr-474 in the A-loop. As a consequence,

phosphorylation of the substrate RPL10 is impaired, and the ribosomal protein is trapped in the cytoplasm during begomovirus infection (see confocal microscopy of fluorescent RPL10 in infected cells, as an insert in Fig. 1 showing punctuate bodies dispersed in the cytoplasm [38]). Therefore, NSP inhibition of NIK1 prevents activation of the NIK1-mediated signaling pathway and suppresses the plant defense response.

NIK may be a general negative co-receptor in signaling pathways: a property that may impact negatively defense against other pathogens

Although NIK1 is structurally similar to BAK1, the mechanism of NIK1-mediated antiviral defense is distinct from the BAK1-mediated PTI. In fact, expression of the constitutively activated NIK1 mutant T474D does not induce PAMP immune response-associated marker genes but rather down-regulates translation-related genes [40]. We took advantage of the nik1 null alleles to examine the global variation of gene expression induced by inactivation of the NIK1 gene and examined the contrast nik1-Col0 from 10 day-old seedlings using the differential gene expression (DGE) method Deseq2 [43]. The differentially expressed (DE) genes were stored using SQL tables at the PostgreSQL relational database (http://inctipp.bioagro.ufv.br/arabidopsisnik0/), which listed the corresponding $\log_2$FC (fold change) and p-value corrected by FDR (q-value) for all DE genes.

RNA-seq data were then analyzed using the eigenvector centrality method [44] to identify up-regulated genes in nik1 that represent relevant protein hubs in the plant-pathogens interactome network based on protein-protein and genetic interactions. By taking the fold change >1.5 as the major criterion for the eigenvector centrality metrics, the nik1 up-regulated genes, which were retrieved from the Arabidopsis pathogens

interactome network database (http://interactome.dfci.harvard.edu/A_thaliana), were classified by gene ontology categories, and are presented in Fig. 2A. Among the differentially expressed genes that represented relevant centralization points from protein-protein and genetic interactions in the biological network, biotic stimuli responsive genes and negative regulators of development largely predominated the up-regulated list. The negative regulators of development were sub-categorized in hubs controlling stem cell differentiation, maintenance and development, flower development, cell differentiation and post-embryonic development (Fig. 2B). This result indicated that NIK1 may also be involved in developmental control with a strong influence in stem cell development as well as floral induction and development. In this developmental category, the up-regulation of major hubs from BR signaling in the nik1 mutant line may also implicate NIK1 as a negative regulator of the BR responses, which would be in marked contrast with the positive role of BAK1 in BRI1 pathway. The antagonistic roles of BAK1 and NIK1 may extend to include the plant immune response. In the nik1 mutant line, the differentially expressed genes encoding important hubs in the biotic stress response are over-represented in the up-regulated list (Fig. 2A and 2B). These include up-regulated hubs functioning in salicylic acid (SA) signaling and in bacteria response (Fig. 2B). In the SA signaling category, relevant marker genes, such as PR1, PR5 and NIM1-INTERACTING 1, are up-regulated in the nik1 mutant lines, and the hubs are represented by genes involved in perception, signaling and SA biosynthesis. In the bacteria response category, relevant up-regulated hubs form a major antibacterial immune response group. Collectively, these results suggest that inactivation of the NIK1 function may relieve repression of some layers of the immune response.

Conclusions and outlook

From recent studies with SERK-like co-receptors, a common theme emerges: the five LRRs-containing receptor-like kinases function as co-receptors for ligand-binding LRR-RLKs in a stimulus-dependent manner. As members of the LRRII-RLK subfamily, NIKs are likely to target LRR-RLK-mediated signaling pathways as well, although LRR-RLK partners of NIKs have yet to be identified. Recently, we have uncovered a translation control branch of the NIK1 signaling that transduces an antiviral signal to protect plants against begomoviruses, one of the largest and most successful groups of plant DNA viruses that collectively infect a variety of relevant crops in tropical and sub-tropical areas. Nevertheless, the transcriptome profiling resulting from inactivation of the NIK1 gene suggests that NIK1 functions as a negative regulator in developmental and immune signaling pathways as co-receptors of different LRR-RLK receptors. If this is the case, the general negative function of the NIK1 co-receptor will pose a problem in targeting NIK1 for begomovirus resistance, because antibacterial immunity-related genes might be down-regulated in these virus resistant lines. The identification of new distinct signaling arms of the NIK1 transducer along with receptor partners of the NIK1 co-receptor will allow us to engineer NIK1-based defense strategies that cover antiviral immunity without compromising plant antibacterial immunity. One such strategy would be to target downstream components of the translational control branch of NIK1 signaling for genetic engineering of begomovirus resistance.

Acknowledgements

This research was financially supported through the following grants from Brazilian Government Agencies: CNPq grants 573600/2008-2, 447578/2014-6 (to E.P.B.F.)

and FAPEMIG grant CBB-APQ-00070-09 (to E.P.B.F.). J.P.B.M. was supported by a CNPq graduate fellowship; O.J.B.B. and G.C.M. were supported by postdoctoral fellowships from CNPq.

The authors have declared no conflicts of interest

References

1. **Dodds PN, Rathjen JP.** 2010. Plant immunity: towards an integrated view of plant-pathogen interactions. Nat Rev Genet **11**: 539–48.

2. **Boller T, Felix G.** 2009. A renaissance of elicitors: perception of microbe-associated molecular patterns and danger signals by pattern-recognition receptors. Annu Rev Plant Biol **60**: 379–406.

3. **Macho AP, Zipfel C.** 2014. Plant PRRs and the activation of innate immune signaling. Mol Cell **54**: 263–72.

4. **Jones JDG, Dangl JL.** 2006. The plant immune system. Nature **444**: 323–9.

5. **Mandadi KK, Scholthof K-BG.** 2013. Plant immune responses against viruses: how does a virus cause disease? Plant Cell **25**: 1489–505.

6. **Nicaise, V.** 2014. Crop immunity against viruses: outcomes and future challenges. Front Plant Sci **5**: 660.

7. **Kørner CJ, Klauser D, Niehl A, Domínguez-Ferreras A,** et al. 2013. The immunity regulator BAK1 contributes to resistance against diverse RNA viruses. Mol Plant Microbe Interact **26**: 1271–80.

8. **Yang H, Gou X, He K, Xi D,** et al. 2010. BAK1 and BKK1 in Arabidopsis thaliana confer reduced susceptibility to turnip crinkle virus. Eur J Plant Pathol **127**: 149–56.

9. **Iriti M, Varoni EM.** 2014. Chitosan-induced antiviral activity and innate immunity in plants. Environ Sci Pollut Res **22**: 2935–44.

10. **Liu P, Wei W, Ouyang S, Zhang J-S,** et al. 2009. Analysis of expressed receptor-like kinases (RLKs) in soybean. J Genet Genomics **36**: 611–9.

11. **Sakamoto T, Deguchi M, Brustolini OJB, Santos AA,** et al. 2012. The tomato RLK superfamily: phylogeny and functional predictions about the role of the LRRII-RLK subfamily in antiviral defense. BMC Plant Biol **12**: 229.

12. **Shiu S-H, Bleecker AB.** 2001. Receptor-like kinases from Arabidopsis form a monophyletic gene family related to animal receptor kinases. Proc Natl Acad Sci USA **98**: 10763–8.

13. **Shiu S-H, Karlowski WM, Pan R, Tzeng Y-H,** et al. 2004. Comparative analysis of the receptor-like kinase family in Arabidopsis and rice. Plant Cell **16**: 1220–34.

14. **Afzal AJ, Wood AJ, Lightfoot DA.** 2008. Plant receptor-like serine threonine kinases: roles in signaling and plant defense. Mol Plant Microbe Interact **21**: 507–17.

15. **Gish LA, Clark SE.** 2011. The RLK/Pelle family of kinases. Plant J **66**: 117–27.

16. **Johnson KL, Ingram GC.** 2005. Sending the right signals: regulating receptor kinase activity. Curr Opin Plant Biol **8**: 648–56.

17. **Lin W, Li B, Lu D, Chen S,** et al. 2014. Tyrosine phosphorylation of protein kinase complex BAK1/BIK1 mediates Arabidopsis innate immunity. Proc Natl Acad Sci USA **111**: 3632–7.

18. **Oh M-H, Wang X, Kota U, Goshe MB,** et al. 2009. Tyrosine phosphorylation of the BRI1 receptor kinase emerges as a component of brassinosteroid signaling in Arabidopsis. Proc Natl Acad Sci USA **106**: 658–63.

19. **Clouse SD.** 2011. Brassinosteroid signal transduction: from receptor kinase activation to transcriptional networks regulating plant development. Plant Cell **23**: 1219–30.

20. **Shiu S-H, Bleecker AB.** 2003. Expansion of the receptor-like kinase/pelle gene family and receptor-like proteins in Arabidopsis. Plant Physiol **132**: 530–43.

21. **Lehti-Shiu MD, Zou C, Hanada K, Shiu S-H.** 2009. Evolutionary history and stress regulation of plant receptor-like kinase/pelle genes. Plant Physiol **150**: 12–26.

22. **Zhang XS, Choi JH, Heinz J, Chetty CS.** 2006. Domain-specific positive selection contributes to the evolution of Arabidopsis leucine-rich repeat receptor-like kinase (LRR RLK) genes. J Mol Evol **63**: 612–21.

23. **Albrecht C, Russinova E, Kemmerling B, Kwaaitaal M,** et al. 2008. Arabidopsis SOMATIC EMBRYOGENESIS RECEPTOR KINASE proteins serve brassinosteroid-dependent and -independent signaling pathways. Plant Physiol **148**: 611–9.

24. **Li J, Wen J, Lease KA, Doke JT,** et al. 2002. BAK1, an Arabidopsis LRR receptor-like protein kinase, interacts with BRI1 and modulates brassinosteroid signaling. Cell **110**: 213–22.

25. **Nam KH, Li J.** 2002. BRI1/BAK1, a receptor kinase pair mediating brassinosteroid signaling. Cell **110**: 203–12.

26. **Bücherl CA, van Esse GW, Kruis A, Luchtenberg J,** et al. 2013. Visualization of BRI1 and BAK1(SERK3) membrane receptor heterooligomers during brassinosteroid signaling. Plant Physiol **162**: 1911–25.

27. **Chinchilla D, Zipfel C, Robatzek S, Kemmerling B,** et al. 2007. A flagellin-induced complex of the receptor FLS2 and BAK1 initiates plant defence. Nature **448**: 497–500.

28. **Heese A, Hann DR, Gimenez-Ibanez S, Jones AME,** et al. 2007. The receptor-like kinase SERK3/BAK1 is a central regulator of innate immunity in plants. Proc Natl Acad Sci USA **104**: 12217–22.

29. **Postel S, Küfner I, Beuter C, Mazzotta S,** et al. 2010. The multifunctional leucine-rich repeat receptor kinase BAK1 is implicated in Arabidopsis development and immunity. Eur J Cell Biol **89**: 169–74.

30. **Roux M, Schwessinger B, Albrecht C, Chinchilla D,** et al. 2011. The Arabidopsis leucine-rich repeat receptor-like kinases BAK1/SERK3 and BKK1/SERK4 are required for innate immunity to hemibiotrophic and biotrophic pathogens. Plant Cell **23**: 2440–55.

31. **Fontes EPB, Santos AA, Luz DF, Waclawovsky AJ,** et al. 2004. The geminivirus nuclear shuttle protein is a virulence factor that suppresses transmembrane receptor kinase activity. Genes Dev **18**: 2545–56.

32. **Mariano AC, Andrade MO, Santos AA, Carolino SMB,** et al. 2004. Identification of a novel receptor-like protein kinase that interacts with a geminivirus nuclear shuttle protein. Virology **318**: 24–31.

33. **Santos AA, Carvalho CM, Florentino LH, Ramos HJO,** et al. 2009. Conserved threonine residues within the A-loop of the receptor NIK differentially regulate the kinase function required for antiviral signaling. PLoS One **4**: e5781.

34. **Santos AA, Lopes KVG, Apfata JAC, Fontes EPB.** 2010. NSP-interacting kinase, NIK: a transducer of plant defence signalling. J Exp Bot **61**: 3839–45.

35. **Brustolini OJB, Machado JPB, Condori-Apfata JA, Coco D,** et al. 2015. Sustained NIK-mediated antiviral signalling confers broad-spectrum tolerance to begomoviruses in cultivated plants. Plant Biotechnol J doi: http://dx.doi.org/10.1111/pbi.12349.

36. **Hanley-Bowdoin L, Bejarano ER, Robertson D, Mansoor S.** 2013. Geminiviruses: masters at redirecting and reprogramming plant processes. Nat Rev Microbiol **11**: 777–88.

37. **Rocha CS, Santos AA, Machado JPB, Fontes EPB.** 2008. The ribosomal protein L10/QM-like protein is a component of the NIK-mediated antiviral signaling. Virology **380**: 165–9.

38. **Carvalho CM, Santos AA, Pires SR, Rocha CS,** et al. 2008. Regulated nuclear trafficking of rpL10A mediated by NIK1 represents a defense strategy of plant cells against virus. PLoS Pathog **4**: e1000247.

39. **Hanks SK, Quinn AM, Hunter T.** 1988. The protein kinase family: conserved features and deduced phylogeny of the catalytic domains. Science **241**: 42–52.

40. **Zorzatto C, Machado JPB, Lopes KVG, Nascimento KJT,** et al. 2015. NIK1-mediated translation suppression functions as a plant antiviral immunity mechanism. Nature **520**: 679–82.

41. **Nicaise V.** 2015. Lost in translation: an antiviral plant defense mechanism revealed. Cell Host Microbe **17**: 417–9.

42. **Albuquerque LC, Varsani A, Fernandes FR, Pinheiro B,** et al. 2012. Further characterization of tomato-infecting begomoviruses in Brazil. Arch Virol **157**: 747–52.

43. **Love MI, Huber W, Anders S.** 2014. Moderated estimation of fold change and dispersion for RNA-Seq data with DESeq2. Genome Biol **15**: 550.

44. **Bonacich P.** 1987. Power and centrality: a family of measures. Am J Sociol **92**: 1170–82.

Figure Legends

Figure 1. Mechanistic model for the NIK1-mediated antiviral signaling pathway. Virus infection-induced oligomerization of the extracellular domain of NIK1 (1a) brings the intracellular kinase domains into proximity and allows them to transphosphorylate Thr-474 and activate one another (2). Alternatively, NIK1 interacts with an unknown ligand-binding LRR-RLK in a stimulus-dependent manner (1b). Although virus infection triggers NIK1-mediated antiviral signaling, the molecular basis of such elicitation is unknown. Upon activation, NIK1 indirectly mediates the RPL10 phosphorylation (3) promoting its translocation to the nucleus (4), where it interacts with LIMYB (5) to down-regulate the expression of translation-related genes (6). Therefore, the propagation of the antiviral signal culminates with suppression of host global protein synthesis (7), which also impairs translation of viral mRNA (8). Conversely, the binding of begomovirus NSP to the NIK1 kinase domain (A-Loop) inhibits autophosphorylation at Thr-474 (9), thereby preventing receptor kinase activation and RPL10 phosphorylation (10). As a consequence, RPL10 is trapped in the cytoplasm of infected cells (11, see the punctuate bodies in the insert), creating an intracellular environment that is more favorable to begomovirus infection. The viral single-stranded DNA replicates via double-stranded DNA intermediates (12) that are transcribed in the nucleus of plant infected cell. NSP binds to nascent viral DNA and facilitates its movement to the cytoplasm in a process that may be mediated by a yet unidentified exportin-like protein (denoted as ? green).

Figure 2. Selected up-regulated genes as major hubs in the plant-pathogens interactome network. **A:** Functional categorization of up-regulated hubs based on biological processes. The pie chart illustrates the distribution of up-regulated genes

that represent relevant hubs across functional categories as defined by the Gene Ontology (GO) Biological process. The numbers represent the percentage of up-regulated genes in nik1 that represent relevant hubs in each category compared to the WT control. **B:** Sub-categorization of interacting up-regulated hubs in nik1 across the functional categorization. The figure was generated by the Cytoscape program, which connected the interacting sub-classes of a biological process. Node size reflects the gene frequency in each functional sub-category. Node color identifies the nodes associated with a given GO biological category from the list of up-regulated genes as in 2A.

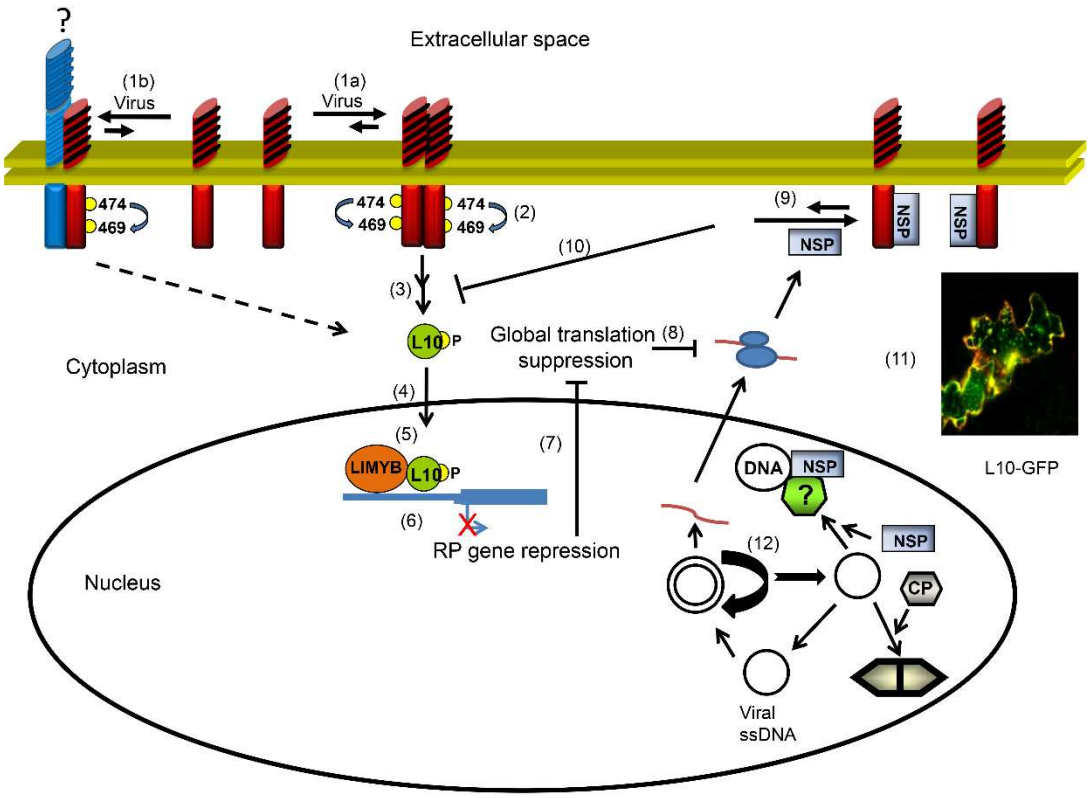

Figure 1. Mechanistic model for the NIK-mediated antiviral signaling pathway.

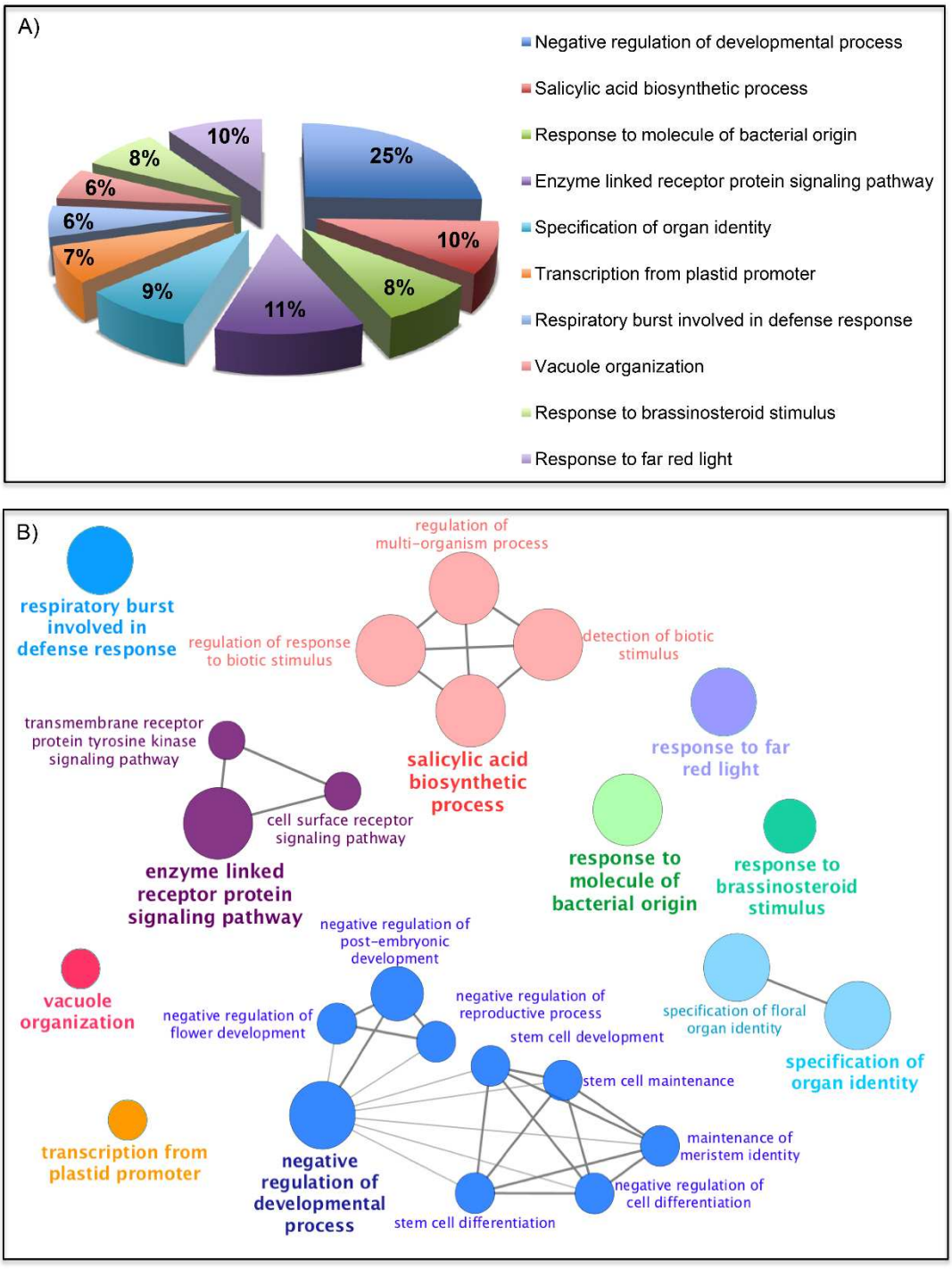

Figure 2. Selected up-regulated genes as major hubs in the plant-pathogens interactome network.

CONCLUSÕES GERAIS

A presente investigação resultou na identificação de um novo componente *downstream* da via de sinalização antiviral mediado por NIK, denominado LIMYB (*L10-Interacting Myb domain-containing protein*), cuja caracterização funcional forneceu indícios sobre o mecanismo da resposta antiviral induzida por este receptor imune. LIMYB foi isolada pela sua capacidade de interagir com RPL10 pelo sistema de duplo híbrido em leveduras. Os resultados obtidos nos ensaios de co-imunoprecipitação e complementação de fluorescência bimolecular (BiFC) mostraram que a interação entre LIMYB e RPL10 ocorre também na planta, mais precisamente no núcleo das células vegetais, sugerindo uma possível função nuclear para o complexo LIMYB-RPL10. De fato, os resultados apresentados nesta investigação mostraram que LIMYB atua como um autêntico fator de transcrição, ligando-se à região promotora e inibindo a expressão de genes ribossomais. Coletivamente, estes resultados sugerem que o mecanismo de resposta antiviral mediada por NIK seja baseado na supressão da tradução do hospedeiro.

A superexpressão do mutante T474D, um mutante superativo de *At*NIK1, em tomateiros confere tolerância a diferentes begomovírus, mas não compromete o desenvolvimento. Ensaios de infecção viral mostraram que linhagens de tomateiros T474D apresentaram sintomas atenuados ou foram assintomáticas quando infectadas com duas espécies divergentes de begomovírus, ToYSV e ToSRV. A atenuação ou ausência de sintomas nas linhagens transgênicas está associada com um atraso na infecção viral, com uma menor taxa de infecção e com um menor acúmulo do DNA viral em folhas infectadas sistemicamente. Apesar do fenótipo de tolerância à infecção por ToYSV e ToSRV, o monitoramento do desenvolvimento, do desempenho fisiológico e de características horticulturais não mostrou diferenças

entre linhagens superexpressando T474D e linhagens WT ou superexpressando *At*NIK1.

A tolerância à begomovírus verificada em linhagens de tomateiros superexpressando o mutante superativo de *At*NIK1 pode estar associada com a redução da tradução global do hospedeiro. Esta conclusão é suportada por ensaios que mostraram que linhagens de tomateiros T474D apresentaram menor acúmulo de proteínas recentemente sintetizadas, quando comparado com os níveis detectados em plantas WT. Além disto, isolamento da fração polissomal a partir de plantas WT e T474D infectadas mostraram que o carregamento do mRNA que codifica a proteína do capsídeo viral foi menor nas linhagens transgênicas. Estes resultados indicaram que a redução da tradução global do hospedeiro verificada nas linhagens T474D também compromete a síntese de proteínas virais, contribuindo para proteção contra a infecção por geminivírus.

NIK1 pode atuar como um regulador negativo em vias de sinalização de desenvolvimento e imunidade. Análise da variação global da expressão gênica induzida pela inativação do gene *NIK1* mostrou que genes responsivos a estímulos bióticos e reguladores negativos do desenvolvimento predominaram entre aqueles cuja expressão foi estimulada, como por exemplo, o *hub* principal da sinalização a brassinosteróide e *hubs* envolvidos na sinalização ao ácido salicílico e na imunidade antibacteriana. Apesar destes resultados indicarem um papel negativo de NIK1 nestas vias de sinalização, estudos adicionais devem ser conduzidos a fim de confirmar os resultados obtidos a partir do perfil de expressão gênica de *nik1* alelos nulos. Além disso, experimentos adicionais devem ser conduzidos para a identificação de possíveis parceiros LRR-RLKs de NIK.

ANEXOS

LETTER

doi:10.1038/nature14171

NIK1-mediated translation suppression functions as a plant antiviral immunity mechanism

Cristiane Zorzatto[1,2]*, João Paulo B. Machado[1,2]*, Kênia V. G. Lopes[1,2], Kelly J. T. Nascimento[1,2], Welison A. Pereira[1,2], Otávio J. B. Brustolini[1,2], Pedro A. B. Reis[1,2], Iara P. Calil[1,2], Michihito Deguchi[1,2], Gilberto Sachetto-Martins[2,3], Bianca C. Gouveia[1,2], Virgílio A. P. Loriato[1,2], Marcos A. C. Silva[2], Fabyano F. Silva[4], Anésia A. Santos[2], Joanne Chory[2,5] & Elizabeth P. B. Fontes[1,2]

Plants and plant pathogens are subject to continuous co-evolutionary pressure for dominance, and the outcomes of these interactions can substantially impact agriculture and food security[1–3]. In virus–plant interactions, one of the major mechanisms for plant antiviral immunity relies on RNA silencing, which is often suppressed by co-evolving virus suppressors, thus enhancing viral pathogenicity in susceptible hosts[1]. In addition, plants use the nucleotide-binding and leucine-rich repeat (NB-LRR) domain-containing resistance proteins, which recognize viral effectors to activate effector-triggered immunity in a defence mechanism similar to that employed in non-viral infections[2,3]. Unlike most eukaryotic organisms, plants are not known to activate mechanisms of host global translation suppression to fight viruses[1,2]. Here we demonstrate in *Arabidopsis* that the constitutive activation of NIK1, a leucine-rich repeat receptor-like kinase (LRR-RLK) identified as a virulence target of the begomovirus nuclear shuttle protein (NSP)[4–6], leads to global translation suppression and translocation of the downstream component RPL10 to the nucleus, where it interacts with a newly identified MYB-like protein, L10-INTERACTING MYB DOMAIN-CONTAINING PROTEIN (LIMYB), to downregulate translational machinery genes fully. LIMYB overexpression represses ribosomal protein genes at the transcriptional level, resulting in protein synthesis inhibition, decreased viral messenger RNA association with polysome fractions and enhanced tolerance to begomovirus. By contrast, the loss of *LIMYB* function releases the repression of translation-related genes and increases susceptibility to virus infection. Therefore, LIMYB links immune receptor LRR-RLK activation to global translation suppression as an antiviral immunity strategy in plants.

NIK1 was first identified as a virulence target of the begomovirus NSP[5,6]. For begomoviruses, a group of single-stranded DNA viruses that infect major crops, the success of infection relies not only on viral suppressors of RNA silencing[4] but also on the viral inhibitor, NSP, of the immune receptor, NIK1 (ref. 5). The NIK1 protein belongs to the same LRR-RLK subfamily as the well-characterized PAMP recognition co-receptor BRI1-ASSOCIATED RECEPTOR KINASE 1 (BAK1)[7,8]. NIK1 is involved in plant antiviral immunity[5], whereas BAK1 is required for plant immunity against bacteria, fungi and oomycetes through its interactions with multiple PAMP-recognition LRR-RLKs[9]. We have previously demonstrated that the activation of NIK1 kinase is induced by the phosphorylation of Thr 474 within the activation (A)-loop[10,11] (Supplementary Discussion 1). Apart from the identification of RPL10 as a downstream effector in NIK1-mediated antiviral immunity[12,13], mechanistic knowledge of the signalling pathway is lacking, and the molecular nature of the defence response remains unclear. In this study, we replaced the normal NIK1 receptor with the NIK1 phosphomimetic gain-of-function mutant T474D[11] in transgenic *Arabidopsis* lines to understand the molecular basis of the NIK1-mediated defence mechanism (Extended Data Fig. 1a–c). Transgenic lines possessing the gain-of-function mutant T474D in the *nik1* knockout background[10] were challenged with infectious clones of the *Arabidopsis*-infecting begomovirus cabbage leaf curl virus (CaLCuV)[10,11]. Then, we compared the virus-induced and T474D-induced transcriptomes at 10 days post-inoculation (dpi). A global cluster analysis of the expressed sequences among the mock-treated and infected wild-type (Col-0), NIK1 and T474D lines (Supplementary Table 1) revealed that the transcriptomes of the infected wild-type and mock-inoculated T474D lines were most closely related; these samples clustered together with a high bootstrap probability and a high approximately unbiased *P* value (Fig. 1a), which suggests that the NIK1-mediated response and the response to begomovirus infection share similar mechanisms. These transcriptomes differed greatly from the NIK1 mock-inoculated transcriptome, indicating that virus infection activates the NIK1-mediated response. Moreover, the gain-of-function T474D mutant might be activated in a constitutive manner that allows it to support a sustained NIK1-mediated response, in contrast with the expression of the intact NIK1 receptor in the *nik1* genetic background. The transcriptome from NIK1-complemented lines clustered with the Col-0 mock-inoculated transcriptome.

We also employed these transgenic lines to assess the T474D-induced global variation in gene expression. Gene enrichment analyses of immune system category genes indicated that ectopic expression of T474D did not activate typical viral defences, such as salicylic acid signalling or virus-induced gene silencing (Supplementary Table 2, Extended Data Fig. 2a, b and Supplementary Discussion 2). Among the differentially expressed genes, we observed an overrepresentation of translational-machinery-related genes, which largely predominated the downregulated gene list (Extended Data Fig. 3a, red spots; Supplementary Tables 2 and 3). Using enrichment analysis, these downregulated genes included ribosomal genes and other components of the protein synthesis machinery. Therefore, T474D ectopic expression downregulates components of the translational machinery, suggesting that the constitutive activation of NIK1 might influence translation. To confirm that protein synthesis was impaired by constitutive activation of NIK1 in the T474D lines, we labelled leaf proteins *in vivo* with [^{35}S]Met in the control and *nik1* plants, as well as in the *NIK1*- (ref. 11), G473V/T474A- (ref. 11) and T474D-expressing lines (Fig. 1b and Extended Data Fig. 3b). The one-proportion statistical test indicated a significant decrease (12.8% for T474D line 4 (T474D-4) and 13% for T474D-6; $P < 0.05$) in the amount of newly synthesized protein in T474D-expressing leaves compared with wild-type and *NIK1*-expressing leaves. We also demonstrated that dexamethasone-inducible T474D expression for 8 h led to a higher inhibition of *de novo* protein synthesis in the transgenic lines (Fig. 1c and Extended Data Fig. 3c–e). In the dexamethasone-inducible lines, the expression of T474D significantly reduced polysome (PS) and monosome (NPS) fractions (12% total reduction) to a similar extent as it

[1]Departamento de Bioquímica e Biologia Molecular, National Institute of Science and Technology in Plant–Pest Interactions, Bioagro, Universidade Federal de Viçosa, 36570.000 Viçosa, Minas Gerais, Brazil. [2]National Institute of Science and Technology in Plant-Pest Interactions, Bioagro, Universidade Federal de Viçosa, 36570.000 Viçosa, Minas Gerais, Brazil. [3]Departamento de Genética, Universidade Federal do Rio de Janeiro, 21944.970 Rio de Janeiro, Brazil. [4]Departamento de Zootecnia, Universidade Federal de Viçosa, 36570.000 Viçosa, Minas Gerais, Brazil. [5]Howard Hughes Medical Institute and Plant Biology Laboratory, The Salk Institute for Biological Studies, La Jolla, California 92037, USA.
*These authors contributed equally to this work.

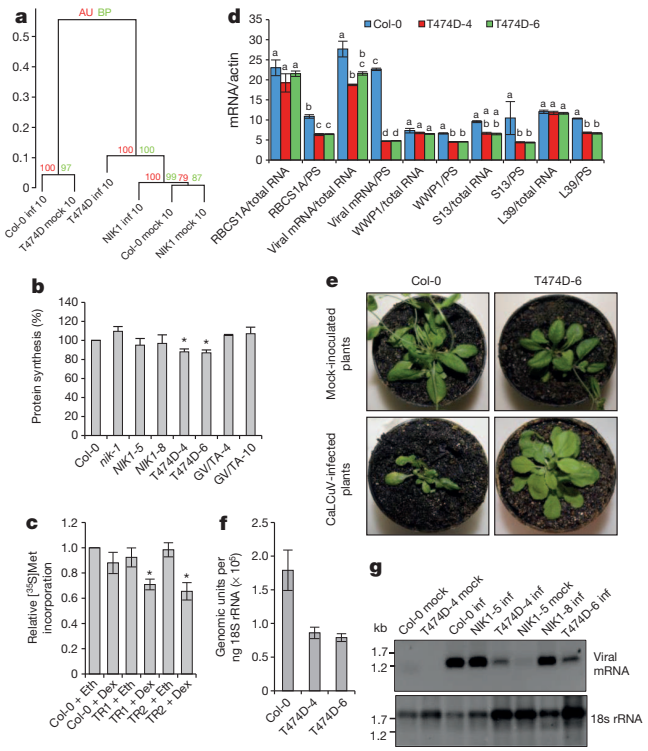

Figure 1 | Constitutive activation of the NIK1 receptor suppresses global host translation and confers tolerance to begomovirus. **a**, Ward hierarchical clustering of the gene expression data from the *Arabidopsis* infection experiments at 10 dpi. The dendrogram provides two types of *P* values: approximately unbiased (AU; red) and bootstrap probability (BP; green). inf, infected plants; mock, mock-inoculated plants. **b**, Global translation suppression by T474D expression. *In vivo* labelling of leaf proteins with [^{35}S]Met was performed in Col-0 and transgenic seedlings. The labelling percentage was also normalized to the leaf chlorophyll content (Extended Data Fig. 1d). Estimated proportion (in %) with respective error bars showing standard error of the mean (s.e.m.) from three independent experiments ($n = 3$). Asterisks indicate that the proportion is significantly ($P < 0.05$) different from 100% using the one-sided (less) chi-squared test. GV/TA, G473V/T474A double-mutant lines. **c**, Inhibition of global translation upon induction of T474D expression. An oestrogen-receptor-based chemical-inducible system was used to induce T474D expression in *Arabidopsis* seedlings, which were treated with 10 μM dexamethasone (Dex) or ethanol (Eth) for 8 h, and then were pulse labelled with L-[^{35}S]Met for 1 h. Tricarboxylic acid (TCA)-precipitable radioactivity in each sample was normalized to Col-0 + ethanol. Estimated proportion with respective error bars showing s.e.m. from three independent experiments ($n = 3$). Asterisks indicate that the proportion is significantly ($^*P < 0.05$) different from 1 using the one-sided (less) chi-squared test. TR1 and TR2 are independently transformed lines harbouring T474D under the control of the dexamethasone-inducible promoter. **d**, Quantitation of total and PS-associated viral replication initiator protein (Rep) and host transcripts by qRT–PCR. The two-way analysis of variance (ANOVA) results were sliced by RNA fractions (total and PS). Different letters indicate significant differences among the RNA levels of the same gene by the TukeyHSD test ($P < 0.01$). mRNA/actin, mRNA of the gene normalized to actin mRNA. **e**, Symptoms associated with CaLCuV infection in wild-type and transgenic lines at 21 dpi. The figure shows representative samples from three independent experiments, each one with ten plants (biological replicates). **f**, Absolute quantitation of CaLCuV genomic units in infected lines at 14 dpi. An 18S ribosomal RNA (rRNA) target was run in parallel for normalizing the template load per reaction. Error bars, 95% confidence intervals based on bootstrap resampling replicates of four independent ($n = 4$) experiments. **g**, PS loading of viral mRNA in systemically infected leaves. PS-bound RNA was probed with viral Rep complementary DNA and 18S rDNA.

reduced PS and NPS RNA (13% reduction; Extended Data Fig. 4a–c). The loading of host mRNA (*RBCS*, *Arabidopsis thaliana* (*At*)*WWP1*, *S13* and *S39* genes) in actively translating PS fractions was significantly reduced in T474D-overexpressing lines compared to the wild-type line, although to a different extent (Fig. 1d, Extended Data Fig. 4d and Supplementary Discussion 3). Therefore, the activation of NIK1 reduces global levels of translation, but the effect may not be the same for all mRNAs. This downregulation of cytosolic translation might at least partially underlie the molecular mechanisms involved in NIK1-mediated antiviral defences.

To examine whether the constitutive activation of NIK1 was effective at controlling begomovirus infection, the transgenic lines were inoculated with CaLCuV DNA-A and DNA-B. The wild-type plants displayed typical symptoms of CaLCuV infection, whereas the symptoms in the T474D-expressing lines were greatly attenuated (Fig. 1e and Extended Data Fig. 5b). The symptomless CaLCuV infections of the T474D-expressing lines were associated with a delayed course of infection (Extended Data Fig. 5a) and a lower accumulation of viral DNA in the systemically infected leaves (Fig. 1f).

Because T474D expression caused downregulation of protein synthesis, we determined whether viral RNA translation was impaired in the T474D-expressing lines. We examined viral RNA transcripts in actively translating PS fractions prepared from infected leaves at 10 dpi (Extended Data Fig. 4e–g), when the total viral mRNA accumulation in the Col-0 and T474D-expressing lines was not very dissimilar (Fig. 1d and Extended Data Fig. 5c). We observed a significant reduction in the PS loading of viral mRNA in the T474D infected leaves compared with the wild-type infected leaves (Fig. 1d, g), indicating that the begomovirus was not capable of sustaining high levels of viral mRNA translation in the T474D-expressing lines.

Our data indicate that the translational suppression induced by NIK1 constitutive activation is associated with the downregulation of translational-machinery-related genes. Hence, NIK1-mediated

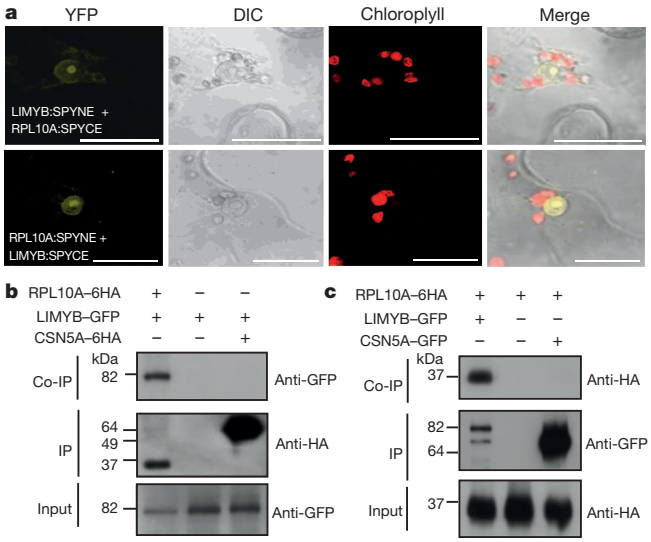

Figure 2 | LIMYB interacts with RPL10 in the nucleus. **a**, *In vivo* interaction between LIMYB and RPL10 by bimolecular fluorescence complementation (BiFC) analysis. The fluorescence (yellow fluorescent protein (YFP)) images were acquired using *Nicotiana tabacum* leaves co-expressing the 35S::RPL10-SPYNE + 35S::LIMYB-SPYCE and 35S::RPL10-SPYCE + 35S::LIMYB-SPYNE fusion proteins. They are representative samples from three independent biological repeats. Scale bars, 20 μm. DIC, differential interference contrast. **b**, LIMYB and RPL10 interaction *in planta*. The indicated constructs were expressed in *N. tabacum* leaves, and co-immunoprecipitation (Co-IP) assays were performed using an anti-haemagglutinin (HA) antibody. CSN5A is an unrelated protein used as a negative control. **c**, Co-immunoprecipitation assay was performed using an anti-GFP antibody.

nucleocytoplasmic trafficking of RPL10 may be linked to the regulation of gene expression. The previously identified extraribosomal functions of RPL10 associated with transcription factor regulation[14–16] may serve as potential targets for assessing this hypothesis. We used the two-hybrid system to search for RPL10 nuclear partners and isolated a MYB-domain-containing transcription factor, which was designated as LIMYB (Extended Data Fig. 6a–e). As a putative transcription factor, LIMYB localized in the nucleus of transiently or stably transformed plant cells (Extended Data Fig. 7a–i) and interacted with RPL10 in the nuclei of plant cells (Fig. 2a and Extended Data Fig. 6f, g). We further demonstrated that RPL10 and LIMYB interact *in vivo* using co-immunoprecipitation assays (Fig. 2b, c).

The function of LIMYB in NIK1-mediated antiviral signalling was examined using several different approaches. We first demonstrated that *LIMYB*, *RPL10* and *NIK1* are co-expressed in several organs (Extended Data Fig. 8). Then, we identified transfer DNA (T-DNA) insertion mutants (*limyb-32* and *limyb-82*) in the *LIMYB* gene (Extended Data Fig. 1e, f). We also prepared *LIMYB*-overexpressing lines (Extended Data Fig. 1g) and determined the LIMYB-induced global variation in gene expression compared to Col-0 leaves. Remarkably, the overexpression of *LIMYB* resulted in a downregulation of translational-machinery-related genes similar to that induced by T474D expression (Extended Data Fig. 1h, red spots). We selected five ribosomal protein (RP) genes to confirm the deep-sequencing results for the *LIMYB*-overexpressing lines by quantitative polymerase chain reaction with reverse transcription (qRT–PCR) (Fig. 3a). *LIMYB* overexpression downregulated the expression of the selected RP genes but not of the unrelated gene (*AtWWP1*; Extended Data Fig. 9c). Conversely, in the *limyb-32* line, the RP genes were upregulated (Fig. 3 and Extended Data Fig. 9a, d). Expression of *LIMYB* in *limyb* lines restored the wild-type expression of the RP genes (Extended Data Fig. 9b). As in the T474D-expressing lines, protein synthesis was slightly but significantly reduced in the *LIMYB*-overexpressing lines (Fig. 3c and Extended Data Fig. 4h). Because RPL10 functions in NIK1-mediated antiviral signalling and interacts with LIMYB, we examined whether RPL10 also controls the expression of RP genes. In *RPL10*-overexpressing lines (Extended Data Fig. 1i, j), the expression of RP genes but not of the unrelated *AtWWP1* gene was downregulated (Fig. 3d and Extended Data Fig. 9e). We then examined whether LIMYB, a putative transcription factor, binds to an RP promoter (RPL18) *in vivo*. We performed chromatin immunoprecipitation (ChIP) experiments

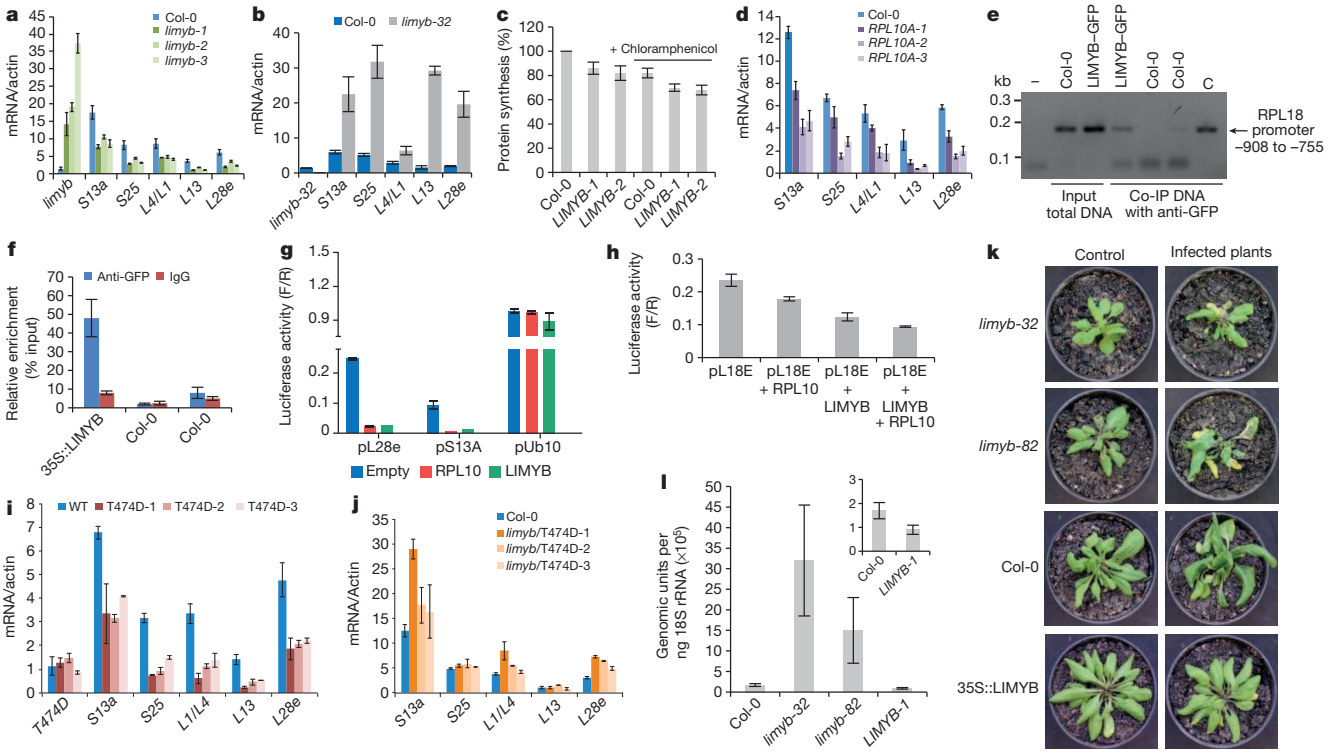

Figure 3 | LIMYB links NIK1 activation to the downregulation of RP genes and confers tolerance to begomovirus. **a**, *LIMYB* overexpression downregulates RP genes. RP gene expression was monitored by qRT–PCR of RNA from *LIMYB*-overexpressing leaves and Col-0. **b**, Induction of RP genes in the *limyb-32* mutant, monitored as in **a**. **c**, *LIMYB* overexpression suppresses global host translation. Col-0 and *LIMYB*-overexpressing seedlings were labelled with [^{35}S]Met in the presence and absence of chloramphenicol, as described in Fig. 1b. **d**, RPL10 downregulates RP genes, monitored as in **a**. **e**, LIMYB binds to the RPL18e promoter *in vivo*. ChIP assay was performed with LIMYB–GFP-expressing leaves or wild type using anti-GFP antibodies. The co-immunoprecipitated (Co-IP) 150-bp fragment of the RPL18 promoter was detected by PCR. C, amplification of the control plasmid. **f**, ChIP-qPCR assay of 35S:LIMYB–GFP transgenic and wild-type (Col-0) seedlings. Samples were immunoprecipitated with anti-GFP antibody or IgG antibody. ChIP DNA was quantified with real-time PCR. **g**, LIMYB or RPL10 repress the RP promoter. *N. benthamiana* leaves were agro-infiltrated with plasmids carrying the prL28e-luciferase (pL28e), prS23A-luciferase (pS13A) or prUb10-luciferase (pUb10) genes in combination with either the *35S::LIMYB* or *35S:RPL10* DNA constructs. Luciferase activity was measured 48 h after agro-infiltration. F/R, firefly luciferase activity to *Renilla* activity ratio. **h**, LIMYB and RPL10 determine the full transcriptional repression of the RP promoter. *N. benthamiana* leaves were agro-infiltrated with the indicated combination of DNA constructs and luciferase activity was measured 48 h after infiltration. **i**, Downregulation of RP genes in T474D-expressing lines, monitored as in **a**. **j**, T474D requires the function of LIMYB to mediate RP gene suppression. The *limyb-32* (*limyb*) mutant was transformed with 35S::T474D, and the expression of RP genes was monitored as described in **a**. **k**, Symptoms associated with CaLCuV infection in Col-0 plants, the *LIMYB*-overexpressing line and *limyb* mutants at 21 dpi. Representative samples from three independent experiments, each one with ten plants (biological replicates). **l**, Absolute quantitation of CaLCuV genomic units in infected *LIMYB*-overexpressing lines and *limyb* mutants. Viral accumulation was determined by quantitative PCR at 14 dpi, as described in Fig. 1f. **a**–**d**, **f**–**j**, **l**, The respective 95% confidence interval limits were estimated based on bootstrap resampling replicates of three independent ($n = 3$) experiments and two technical repeats, except that in **g**, $n = 2$ with two technical repeats.

in which a 150 base pair (bp) RPL18 promoter was amplified from the precipitated DNA of *LIMYB*-expressing tissues but not of wild-type tissues (Fig. 3e). ChIP-qPCR showed that the 150-bp promoter fragment was significantly enriched in samples precipitated by anti-green fluorescent protein (GFP) antibody but not in samples pulled down from wild-type lines (Fig. 3f). These results suggest that LIMYB may function as a DNA-binding protein that associates with RP promoters *in vivo*.

To provide further evidence for the regulation of RP target genes by LIMYB and RPL10, we performed a luciferase transactivation assay in agro-infiltrated leaves. Consistent with the gene expression profile, LIMYB and RPL10 specifically repressed the L28e, S13A and L18E promoters but not an unrelated ubiquitin promoter (Fig. 3g, h). The co-transfection of *Arabidopsis* protoplasts with both LIMYB and RPL10 promoted increased repression of the L18E promoter compared to regulation of the gene reporter by individual expression of the transfactors. Collectively, these results indicate that LIMYB and RPL10 function as transcriptional repressors of common RP genes and that both transfactors are required for full regulation (Fig. 3h). Therefore, LIMYB and RPL10 may coordinately regulate common target promoters.

We also demonstrated that T474D expression downregulated the RP genes (Fig. 3i) but not *AtWWP1* (Extended Data Fig. 9f), confirming the RNA-sequencing data (Extended Data Fig. 3a). As an additional control, we showed that the double-mutant NIK1 G4743V/T474A[12], which does not complement the enhanced susceptibility phenotype of the *nik1*-null alleles (Extended Data Fig. 5a), also does not affect RP genes (Extended Data Fig. 9g). Nevertheless, the loss of *LIMYB* function prevented the T474D-mediated downregulation of the RP genes in both the *limyb-32* transgenic lines that stably expressed T474D (Fig. 3j and Extended Data Fig. 9h, i) and the *limyb-32* protoplasts that transiently expressed T474D (Extended Data Fig. 10). These results genetically link *LIMYB* to the translation suppression portion of the NIK1-mediated antiviral response.

We predicted that if the suppression of host translation was the basis for the begomovirus-tolerant phenotype of the T474D-expressing lines, *LIMYB* overexpression would also be effective against CaLCuV and the loss of *LIMYB* function would further debilitate the plant upon begomovirus infection. Col-0, *limyb-32*, *limyb-82* and *LIMYB*-overexpressing lines were inoculated with infectious clones of CaLCuV DNA-A and DNA-B (Fig. 3k). Both Col-0 and *limyb* lines developed typical CaLCuV symptoms, although to different extents. The disease symptoms varied in severity from extreme stunting and leaf distortion with severe chlorosis in the *limyb-32* and *limyb-82* leaves to mild leaf distortion and moderate chlorosis in Col-0. The course of infection in the *limyb* leaves was accelerated compared to that in the Col-0 plants (Extended Data Fig. 5d) and the *limyb-32* and *limyb-82* systemic leaves accumulated higher levels of viral DNA than Col-0 (Fig. 3l). Therefore, the loss of *LIMYB* function recapitulated the enhanced begomovirus susceptibility phenotype of the *nik1*-null alleles, as would be expected from a downstream component of the NIK1-mediated antiviral defence. By contrast, the *LIMYB*-overexpressing lines did not develop symptoms, displayed delayed infection and accumulated a lower level of viral DNA in their systemic leaves, resembling the tolerant phenotype of the T474D-overexpressing lines. We also found that *LIMYB* overexpression did not induce salicylic-acid-signalling marker genes or typical defence responses to viral infection (Extended Data Fig. 2c and Supplementary Table 2). Collectively, these results further support the notion that the inhibition of host translation observed in the T474D and *LIMYB* lines may be an effective mechanism exploited by plant cells to fight begomovirus infection. Therefore, the demonstration that immune-receptor-mediated defence signalling controls translation in plant cells may represent a new paradigm for antiviral defences in plants (Supplementary Discussion 4).

Online Content Methods, along with any additional Extended Data display items and Source Data, are available in the online version of the paper; references unique to these sections appear only in the online paper.

Received 18 February; accepted 19 December 2014.
Published online 23 February 2015.

1. Pumplin, N. & Voinnet, O. RNA silencing suppression by plant pathogens: defence, counter-defence and counter-counter-defence. *Nature Rev. Microbiol.* **11,** 745–760 (2013).
2. Mandadi, K. K. & Scholthof, K. B. Plant immune responses against viruses: how does a virus cause disease? *Plant Cell* **25,** 1489–1505 (2013).
3. Jones, J. D. & Dangl, J. L. The plant immune system. *Nature* **444,** 323–329 (2006).
4. Hanley-Bowdoin, L., Bejarano, E. R., Robertson, D. & Mansoor, S. Geminiviruses: masters at redirecting and reprogramming plant processes. *Nature Rev. Microbiol.* **11,** 777–788 (2013).
5. Santos, A. A., Lopes, K. V. G., Apfta, J. A. C. & Fontes, E. P. B. NSP-interacting kinase, NIK: a transducer of plant defence signalling. *J. Exp. Bot.* **61,** 3839–3845 (2010).
6. Mariano, A. C. *et al.* Identification of a novel receptor- like protein kinase that interacts with a geminivirus nuclear shuttle protein. *Virology* **318,** 24–31 (2004).
7. Sakamoto, T. *et al.* The tomato RLK superfamily: phylogeny and functional predictions about the role of the LRRII-RLK subfamily in antiviral defense. *BMC Plant Biol.* **12,** 229 (2012).
8. Shiu, S. H. & Bleecker, A. B. Receptor-like kinases from *Arabidopsis* form a monophyletic gene family related to animal receptor kinases. *Proc. Natl Acad. Sci. USA* **98,** 10763–10768 (2001).
9. Chinchilla, D., Shan, L., He, P., de Vries, S. & Kemmerling, B. One for all: the receptor-associated kinase BAK1. *Trends Plant Sci.* **14,** 535–541 (2009).
10. Fontes, E. P. B., Santos, A. A., Luz, D. F., Waclawovsky, A. J. & Chory, J. The geminivirus NSP acts as virulence factor to suppress an innate transmembrane receptor kinase-mediated defense signaling. *Genes Dev.* **18,** 2545–2556 (2004).
11. Santos, A. A., Carvalho, C. M., Florentino, L. H., Ramos, J. J. O. & Fontes, E. P. B. Conserved threonine residues within the A-loop of the receptor NIK differentially regulate the kinase function required for antiviral signaling. *PLoS ONE* **4,** e5781 (2009).
12. Carvalho, C. M. *et al.* Regulated nuclear trafficking of rpL10A mediated by NIK1 represents a defense strategy of plant cells against virus. *PLoS Pathog.* **4,** e1000247 (2008).
13. Rocha, C. S., Santos, A. A., Machado, J. P. B. & Fontes, E. P. B. The ribosomal protein L10/QM-like protein is a component of the NIK-mediated antiviral signaling. *Virology* **380,** 165–169 (2008).
14. Oh, H. S., Kwon, H., Sun, S. K. & Yang, C.-H. QM, a putative tumor suppressor, regulates proto-oncogene c-Yes. *J. Biol. Chem.* **277,** 36489–36498 (2002).
15. Imafuku, I. *et al.* Presenilin 1 suppresses the function of c-Jun homodimers via interaction with QM/Jif-1. *J. Cell Biol.* **147,** 121–134 (1999).
16. Monteclaro, F. S. & Vogt, P. K. A Jun-binding protein related to a putative tumor suppressor. *Proc. Natl Acad. Sci. USA* **90,** 6726–6730 (1993).

Supplementary Information is available in the online version of the paper.

Acknowledgements This research was financially supported by the following grants from Brazilian government agencies: Conselho Nacional de Desenvolvimento Científico e Tecnológico (CNPq) grants 573600/2008-2 and 470287/2011-0 (to E.P.B.F.) and FAPEMIG grant CBB-APQ-00070-09 (to E.P.B.F.); and by the US National Institutes of Health grant 5R01-GM94428 (to J.C.). O.J.B.B. was supported by a Coordenação de Aperfeiçoamento de Pessoal de Nível Superior (CAPES) graduate fellowship; C.Z., K.V.G.L., J.P.B.M., I.P.C., B.C.G. and P.A.B.R. were supported by CNPq graduate fellowships; K.J.T.N., W.A.P. and M.D. were supported by postdoctoral fellowships from CNPq. A.A.S. was supported by postdoctoral fellowships from CAPES; and M.A.C.S. was the recipient of an undergraduate scholarship from CNPq. J.C. is an Investigator of the Howard Hughes Medical Institute.

Author Contributions C.Z. and J.P.B.M. co-wrote the manuscript and performed most of the experiments related to LIMYB isolation and characterization. K.V.G.L. performed the T474D-related experiments. K.J.T.N. performed qPCR for viral DNA. W.A.P. generated the RPL10 constructs and conducted plant transformation. O.J.B.B. and F.F.S. performed the bioinformatic analysis of the RNA-sequencing data and the statistical analysis of the data. M.D. performed the infectivity assays. B.C.G. conducted qRT–PCR. P.A.B.R. and I.P.C. performed the protein synthesis assays. V.A.P.L. performed complementation assays. G.S.-M. performed the bimolecular fluorescence complementation experiments. M.A.C.S. performed the tissue expression experiments. A.A.S. constructed the mutant proteins and designed the infectivity assays. J.C. conceived the experiments and edited the final draft. E.P.F.B. co-wrote the manuscript, designed the experiments and directed the project.

Author Information RNA-sequencing data have been deposited in the Gene Expression Omnibus under accession number GSE56922. Reprints and permissions information is available at www.nature.com/reprints. The authors declare no competing financial interests. Readers are welcome to comment on the online version of the paper. Correspondence and requests for materials should be addressed to E.P.B.F. (bbfontes@ufv.br).

METHODS

Plasmid constructs. The clone pK7F-NIK1T474D was described previously[11]. This clone harbours a *GFP* gene fused in frame after the last codon of the respective mutant cDNA under the control of the CaMV 35S promoter. In the mutant cDNA T474D, the threonine residue at position 474 within the activation loop of NIK1 was replaced with an aspartate residue. The clones rpL10AST-pDONR201 (pUFV608), rpL10ANS-pDONR201 (pUFV609), rpL10AST-pDONR207 (pUFV900) and rpL10ANS-pDONR207 (pUFV901), which harbour the RPL10A coding region either with (ST) or without (NS) a translational stop codon inserted into the entry vectors pDONR201 or pDONR207, have also been previously described[12]. The RPL10A coding region was transferred from these entry clones to the yeast expression vectors pDEST32 and pDEST22, generating the clones pBD-RPL10A (pUFV1422) and pAD-RPL10 (pUFV785) as GAL4 binding domain (BD) or activation domain (AD) fusions. For BiFC, the RPL10A coding region was transferred to the vectors SPY-NE-GW and SPY-CE-GW. The resulting clones, pSPYNE-RPL10A (pUFV1652) and pSPYCE-RPL10A (pUFV1653), harboured the RPL10A coding region fused to either the N-terminal (NE) region of YFP or the YFP C terminus (CE), respectively, under the control of the 35S promoter. The clones pK7F-L10 and pYFP-L10, which harbour RPL10A fused in frame with GFP after its last codon or with YFP before its first codon under the control of the 35S promoter, respectively, have been previously described[10].

The clone pYFP-NLS-L10, which harbours a YFP–L10 fusion with a nuclear localization signal (NLS) under the control of the 35S promoter, was constructed by first inserting the amplified coding region of RPL10A into the SacI site of the pGR vector. The resulting clone, pGR-L10, which contains the RPL10A coding region fused to a glucocorticoid receptor (GR) domain with an NLS at the 5′ end, was then used as the template for the amplification of the NLS-containing L10 fusion with specific primers. The resulting product was inserted by recombination into pDONR207 and transferred to 35S-YFP-casseteA-Nos-pCAMBIA1300, generating pYFP-NLS-L10.

For the induction of T474D expression, the mutant cDNA T474D was transferred by recombination from the pDON201-T474D entry vector to the destination vector pBAV150 (ref. 17). The resulting clone pBAV150-NIK1 T474D–GFP harbours the mutant T474D open reading frame (ORF) under the control of a dexamethasone-inducible promoter and fused to a C-terminal GFP tag.

***Arabidopsis* growth conditions and transformation.** The Columbia (Col-0) ecotype of *A. thaliana* was used as the wild-type control, and the *nik1* knockout line[10] was used for plant transformation. The *nik1* lines[10] were transformed with pK7F-NIK1T474D or pBAV150- NIK1 T474D-GFP using the floral dip method. Two independently transformed lines expressing the T474D transgene (T474D-4 and T474D-6) were selected for the infection assays. The transgenic lines ectopically expressing NIK1–GFP (*NIK1-5* and *NIK1-8*) or an inactive kinase, the double mutant of NIK1, and the G473V/T474A–GFP dead kinase (G473V/T474A-10 and G473V/T474A-8) have been previously described[11,12] (Supplementary Table 1).

RT–PCR and real-time RT–PCR analyses. Total RNA was extracted from *Arabidopsis* leaves using TRIzol (Invitrogen). RT–PCR assays were performed using gene-specific primers, as previously described[18]. For gene expression analysis by qRT–PCR, gene-specific primers were designed using Primer Express 3.0 (Life Technologies). Real-time RT–PCR assays were performed on an ABI7500 instrument (Life Technologies) using the SYBR Green PCR Master Mix (Life Technologies). The amplification reactions were performed as follows: 2 min at 50 °C, 10 min at 95 °C and 40 cycles of 94 °C for 15 s and 60 °C for 1 min. The variation in gene expression was quantified using the comparative Ct method ($2^{-\Delta\Delta Ct}$), and absolute gene expression was quantified using the $2^{-\Delta Ct}$ method. The values were normalized to endogenous actin and ubiquitin as control genes[11].

RNA sequencing and data analysis. The transgenic and wild-type lines were infected at the seven-leaf stage with CaLCuV, as described later. After 10 dpi or after 21 dpi, total RNA from systemically infected leaves, as diagnosed by PCR, and mock-inoculated leaves from wild-type, 35S::NIK1-5 and 35S::T474D-4 lines was isolated using TRIzol (Invitrogen). For the RNA-sequencing experiments, we used two biological replicates of a pool of ten plants at 10 dpi, when we detected high levels of viral DNA in systemic leaves but symptoms had not yet developed, or at 21 dpi, when symptoms were visible. The RNA-sequencing data were obtained using an Illumina Hi-seq 2000. The paired-end 100-bp protocol was used with the following quality filter parameters: 5 bases trimmed at the 3′ and 5′ ends of the reads, a minimum average quality of 30 phred score. The data were stored in a comma-separated value spreadsheet file, and differential gene expression (DGE) analysis was performed using the R/Bioconductor package edger[19]. The raw data were normalized using the TMM normalization factor[20]. The dispersion was estimated by the tagwise edger parameter. Differential expression was determined using the cut-off *P* value of 0.1 adjusted by the false discovery rate (FDR). The read mapping process was executed using the Bowtie program[21] with the cDNA data set retrieved from The *Arabidopsis* Information Resource (TAIR) database (http://www.arabidopsis.org), tenth release. Gene ontology classification was performed using the R/Bioconductor packages GSEABase and GOstats. Clustering analysis was performed using the R package pvclust (Hierarchical Clustering with P-Values via Multiscale Bootstrap Resampling) using Ward's method[22], and heatmaps were generated using gplots. The results were stored in a relational database created in PostgreSQL, and a web interface was created using PHP to allow the database to be accessed and navigated (http://arabidopsisnik.inctipp.ufv.br).

***In vivo* labelling of leaf proteins.** *Arabidopsis* seedlings (300 mg) were incubated with 1 ml of nutrient solution containing 30 μg ml^{-1} dexamathosone, 10 μg ml^{-1} cycloheximide, 10 μg ml^{-1} puromycin or 25 μg ml^{-1} chloramphenicol for 1 h, 4 h or 8 h. After the incubation period, 20 μCi of [^{35}S]Met (EasyTag Protein Labelling Mix, [^{35}S]-, 2 mCi (74 MBq), Perkin Elmer) was added for 1 h at room temperature. To quantitate the incorporation of [^{35}S]Met into protein, aliquots of protein extracts were placed in 10% (w/v) TCA and incubated on ice for 30 min. The samples were filtered onto glass microfibre filters, and the filters were washed three times with 5 ml cold 5% (w/v) TCA and two times with 5 ml 95% ethanol. After drying, the filters were counted with a scintillation counter.

PS fractionation. PSs were fractionated from 500 mg of 15-day-old *Arabidopsis* seedlings over sucrose gradients as described[23]. Fractions were collected manually from the top, and total RNA was extracted with phenol/chloroform/isoamyl alcohol, precipitated with isopropanol, and treated with DNase I. The specific transcripts were examined by northern blot analysis. For the infection assays, PSs from wild type, *NIK1-4*-overexpressing and T474D-6-overexpressing lines were isolated 10 dpi with infectious CaLCuV clones.

PS gradients of dexamethasone-inducible T474D seedlings were prepared from 8-day-old seedlings, treated or not with 30 μg ml^{-1} dexamathosone. After 8 h of dexamethasone treatment, the seedlings were dried, frozen and ground in liquid nitrogen. Cytoplasmic extracts were prepared from 350 mg of powder that were resuspended in the ice-cold extraction buffer. Cell debris was removed by centrifugation and 0.6 ml of the supernadant were loaded onto a 4.5 ml 15–55% sucrose density gradient and separated by ultracentrifugation. Fractions (16) of 310 μl were collected from the top. Fractions 2–7 correspond to density regions of complexes ≤80S (NPSs) and fractions 8–15 correspond to density regions containing small and large polysomes (PSs). Quantitation of NPSs and PSs from the absorbance profile was performed as described previously[24]. The quantitation of total RNA from the combined NPS and PS fractions was performed as described previously[25]. To quantify mRNA loading into PSs, total RNA isolated from combined NPS (2–7) and PS (9–15) fractions was extracted using Trizol (Invitrogen), precipitated with isopropanol and quantified by qRT–PCR, as described earlier. qRT–PCR on each fraction from the PS gradient of dexamethasone-inducible T474D seedlings was also performed for quantitation of the distribution of *AtWWP1* and *S39* transcripts after induction of T474D expression. Each sample was amplified with 1 cycle at 50 °C for 2 min, 95 °C for 10 min and 40 cycles at 95 °C for 15 s and 60 °C for 1 min. Values were normalized to actin.

CaLCuV inoculation and viral DNA accumulation. *A. thaliana* plants at the seven-leaf stage were inoculated with plasmids containing partial tandem repeats of CaLCuV DNA-A and DNA-B by biolistic delivery[26], and the course of infection was monitored as described previously[10]. We used an attenuated form of the virus in which the coat protein ORF in the CaLCuV DNA-A was interrupted by the introduction of a stop codon at amino acid position 47. The inoculated plants were transferred to a growth chamber and examined for symptom development (leaf necrosis, chlorosis, leaf epinasty, leaf curly, young leaf death and stunted growth). Total nucleic acids were extracted from systemically infected leaves, and viral DNA was detected by PCR with DNA-B CaLCuV-specific primers (566CLCVBFBR1v, 5′-GGCGTG GGGTATCTTACTC-3′, and 1253CLCVBRBR1c, 5′-GACATAGCATCGGACA TCC-3′) as well as the actin-specific primers as an endogenous control. In each experiment, 20 plants of each line (Col-0, *nik1* and *nik1*-expressing NIK1 mutant proteins) were inoculated with 2 μg of tandemly repeated DNA-A plus DNA-B per plant. The course of infection was examined using data from three independent experiments.

Viral DNA accumulation was measured by qPCR. The reactions were prepared in a final volume of 10 μl using the Fast SYBR Green Master Mix (Life Technologies) according to the manufacturer's instructions and analysed on a 7500 Real Time PCR System. Virus-specific primers were designed using Primer Express 3.0 (Life Technologies) and tested by conventional PCR using plasmids containing the complete DNA-B of each virus (10^6 copies per reaction). The genomic copies of CaLCuV were normalized against an internal control (18S rRNA) to consider template input variation between tubes. CaLCuV DNA was amplified with primers B-Fwd (5′-GGGCCTGGGCCTGTTAGT-3′) and B-Rvs (5′-ACGGAAGATGGG AGAGGAAGA-3′). In this case, the genomic unit refers to one copy of the DNA-B of CaLCuV. PCR reactions were run in parallel with primers 18S-Fwd (5′-TAA TTTGCGCGCCTGCTGCC-3′) and 18S-Rvs (5′-TGTGCTGGCGACGCATCA TT-3′) for the reference plant gene *18SRNA*. Standard curves were obtained by

regression analysis of the Ct values of each of the three replicates of a given dilution as a function of the log of the amount of DNA in each dilution. Standard curves containing viral DNA and host DNA served as references. Each sample was analysed in triplicate from at least two biological replicates.

Two-hybrid screening. The yeast reporter strain MaV203 (MATαleu2-3,112 trp1-901 his3200 ade2-101 gal4 gal80 SPAL10::URA3 GAL1::lacZ HIS3UAS GAL1::HIS3-LYS2 can1R cyh2R; Trp- Leu- Ura-) was transformed sequentially with pBD-L10 and 25 μg of the pEXAD502 cDNA library previously prepared[27] and approximately 5×10^6 transformants were screened for histidine protoprophy an β-galactosidase activity, as described[27,28].

LIMYB-based plasmid constructs. The At5g05800 cDNA (LIMYB), which was isolated based on its ability to bind to rpL10A in yeast, was amplified by PCR from the cDNA library vector using AT5G05800-specific primers, re-amplified with the primers AttB1-Fwd and AttB1-Rvs, and cloned by recombination into the entry vectors pDONR201 and pDONR207. The resulting products were then transferred to different destination vectors for expression in yeast (pDEST32 and pDEST 22) and plants (pK7FWG2, 35S-YFP-casseteA-Nos-pCAMBIA1300, pSPYNEGW and pSPYCEGW). The resulting clones, pBD-At5g05800ST (pUFV1903) and pAD-At5g05800ST (pUFV1480), enabled the expression of AT5G05800 (LIMYB) in yeast as GAL4 binding domain (BD) or activation domain (AD) fusions, respectively. The clone pAt5g05800-GFP (pUFV1395) harboured the AT5G05800 (LIMYB) coding region fused to the GFP N terminus under the control of the 35S promoter, whereas in pYFP-At5g05800 (pUFV1886), the At5g05800 coding region was fused to the YFP C terminus. In the resulting clones, pSPYNE-At5g05800 (pUFV1658) and pSPYCE-At5g05800 (pUFV1657), the At5g05800 cDNA was linked to the YFP NE and the YFP CE, respectively, under the control of the 35S promoter.

The HA epitope was fused to the At5g05800 C terminus using the triple Gateway system, which consisted of the vector p5′, in which the 35S (2×) promoter had been previously cloned, the clone pUFV1378 (At5g05800 cDNA without a translational stop codon in pDONR201) and the vector p3′, in which a HA (6×) epitope had been previously inserted. The At5g05800 cDNA was transferred by recombination into the destination vector pK7M34GW along with 2×35S promoter and the HA tail, yielding the clone p2×35S-At5g05800-6HA (pUFV1984), which enabled the expression of At5g05800 fused in frame to HA under the control of the 35S promoter in plants. The same triple Gateway system was used to place the LIMYB fused in frame with Cherry or GFP under the control of the LIMYB promoter.

Transient expression in *N. benthamiana* leaves. To determine the subcellular localization of the proteins, *N. benthamiana* leaves were agro-infiltrated with pAt5g05800-GFP, pYFP-At5g05800 and pYFP-NAC81 (ref. 29), while for the co-immunoprecipitation assays, they were agro-infiltrated with pL10-GFP and p2×35S-At5g05800-6HA. *Agrobacterium tumefaciens* strain GV3101 was used for agroinfiltration. *Agrobacterium* infiltration was performed in the leaves of 3-week-old *N. benthamiana*, as previously described[12].

Confocal microscopy. Approximately 72 h after agro-infiltration, 1-cm^2 leaf explants were excised, and the GFP and YFP fluorescence patterns were examined in epidermal cells with a ×40 or ×60 oil immersion objective and a Zeiss inverted LSM510 META laser scanning microscope equipped with an argon laser and a helium laser as excitation sources, as described[27].

Co-immunoprecipitation assays. The co-immunoprecipitation assay was performed using the μMACSTM Epitope Tag Protein Isolation Kit (MACS/Miltenyi Biotec) according to the manufacturer's instructions. Total protein extracts were prepared from *N. benthamiana* leaves that had been agro-infiltrated with pL10-GFP and/or p2×35S-At5g05800-6HA. At 48 h after infiltration, 200 mg of leaves were homogenized with 1 ml of lysis buffer (50 mM Tris-HCl pH 8.0, 1% (v/v) Nonidet P-40) and incubated for 2 h with anti-GFP magnetic beads (MACS/Miltenyi Biotec) at 4 °C under gentle agitation. After extensive washing of the magnetic beads, the bound proteins were eluted using 50 ml of elution buffer pre-warmed to 95 °C. The immunoprecipitated proteins were separated by 10% (w/v) SDS–PAGE and immunoblotted with anti-HA (Miltenyi Biotec, catalogue number 130-091-972) or anti-GFP (Miltenyi Biotec, catalogue number 130-091-833) monoclonal antibodies. The reacting antibodies were detected using Signal West Pico Chemiluminescent Substrate (Thermo Scientific) according to the manufacturer's instructions.

BiFC. *N. benthamiana* leaves were agro-infiltrated as previously described for the transient expression experiments using the following combinations of recombinant plasmids: pSPYNE-At5g05800 + pSPYCE-rpL10A; pSPYCE-At5g05800 + pSPYNE-rpL10A; pSPYNE-At5g05800 + pSPYCE empty vector; pSPYNE-rpL10A + pSPYCE empty vector; pSPYCE-At5g05800 + pSPYNE empty vector; pSPYCE-rpL10A + pSPYNE empty vector. After incubation for 72 h, the leaf sectors were examined by confocal microscopy. YFP was excited at 514 nm using an argon laser, and YFP emission was detected using a 560–615 nm filter. The stability of the CE and NE YFP regions was monitored by immunoblotting of transfected leaf protein extracts with a polyclonal anti-YFP serum.

***LIMYB*- or *RPL10A*-expressing lines and T474D-expressing *limyb* lines.** *Arabidopsis* Col-0 was transformed with pAt5g05800-GFP, generating the transgenic line LIMYB-1; with pYFP-At5g05800, generating the transgenic lines LIMYB-2 and LiMYB-3; and with pYFP-NLS-L10, generating the transgenic lines RPL10-1, RPL10-2 and RPL10-3. Homozygous seeds of the T-DNA insertion *limyb* mutants (Salk_032054C and Salk_082995C) were obtained from the *Arabidopsis* Biological Resource Center. The *limyb-32* mutant was transformed with the gain-of-function mutant T474D, generating the transgenic lines *limyb*/T474-1, *limyb*/T474D-2 and *limyb*/T474D-3. Primary transformants were selected using the appropriate antibiotic (50 μg ml^{-1} kanamycin or 30 μg ml^{-1} hygromycin), and the stable incorporation of the transgene in the plant genome was evaluated by PCR with gene-specific primers. The expression of the transgenes was monitored by qRT–PCR.

LIMYB promoter construct and GUS histochemical assay. Approximately 1 kb of the 5′ flanking sequences of NIK1, RPL10A and At5g05800 (LIMYB) were amplified from *Arabidopsis* genomic DNA using Taq Platinum and specific oligonucleotides and inserted into the cloning vector pCR8/GW/TOPO (Invitrogen). The promoter sequences were then transferred by recombination into the destination vector pMDC162. The resulting clones, pNIK1-MDC162, pL10A-MDC162 and pAt5g05800-MDC162 (pUFV 1892), harboured the respective promoter sequences of the three genes fused to the β-glucuronidase (GUS) reporter gene and were used to transform *Arabidopsis* Col-0 plants. GUS expression was assayed histochemically.

Luciferase reporter gene assay. The At1g29970 (RPL18A) promoter was isolated from *Arabidopsis* DNA by PCR and cloned into pDONR-P4-P1R, generating pUFV2155. The clone LUCF-term-pDON221 (pUFV 2132) harbours the firefly luciferase cDNA in the entry vector pDON221, whereas the clone 2×35S-RLUCF-pDONR-P2R-P3 (pUFV 2131) contains *Renilla* luciferase cDNA under the control of a 2× 35S promoter. The RPL18A promoter was transferred from pUFV2155 to the destination vector pK7m34GW (pUFV 1918), along with 2×35S-RLUCF-pDONR-P2R-P3 (pUFV 2131) and LUCF-term-pDON221 (pUFV 2132), by triple recombination. The resulting clone, prAt1g29970-Lucif-term-2X35S RLucif pH7M34GW (pUVF2231), harboured the firefly luciferase cDNA under the control of the rpL18A promoter, as well as the *Renilla* luciferase cDNA under the control of a 2× 35S promoter. The same procedure was used to clone the firefly luciferase cDNA under the control of the RPL28e, RPS13A and ubiquitin promoters for luciferase transactivation assays.

N. benthamiana leaves were agro-infiltrated with *A. tumefaciens* GV3101 strains carrying the following combinations of DNA constructs: At1g29970-Lucif-term-2×35S RLucif pH7M34GW; At1g29970-Lucif-term-2X35S RLucif pH7M34GW + AT5G05800NS-pK7FWG2; At1g29970-Lucif-term-2X35S RLucif pH7M34GW + AT5G05800NS-pK7FWG2 + rpL10ANS-pK7FWG2; and At1g29970-Lucif-term-2×35S RLucif pH7M34GW + rpL10ANS-pK7FWG2. Forty-eight hours after infiltration, 200 mg of leaf tissue was harvested for total protein extraction. Luciferase activity was assayed with the Dual-Luciferase Reporter Assay System (Promega) according to the manufacturer's instructions.

Protoplast preparation from *A. thaliana* leaves and transient expression assays. Protoplasts were prepared from 15-day-old *Arabidopsis* seedlings as previously described[30], except that digestion was initiated for 30 s under vacuum and then prolonged for 6 h with agitation at 80 r.p.m. The transient expression assays were performed by electroporating (250 V, 250 μF) 10 μg of the expression cassette DNA and 30 μg of the sheared salmon sperm DNA into 2×10^5–5×10^6 protoplasts in a final volume of 0.8 ml. The protoplasts were diluted into 8 ml of MS medium supplemented with 0.2 mg ml^{-1} 2,4-dichlorophenoxyacetic acid and 0.8 M mannitol at pH 5.7. After 36 h of incubation in the dark, the protoplasts were washed with 0.8 M mannitol plus 20 mM MES at pH 5.7 and frozen in liquid N_2 until further use.

Statistical analyses. All statistical analyses (including gene expression clustering, qRT–PCR and protein synthesis data) were performed in R.

Cluster analysis. Cluster analysis of the RNA-sequencing data was used to classify the treatments (mock-inoculated and infected wild type, T474D and NIK1) according to similarities in the profiles of genome-wide expression at 10 and 21 dpi. The uncertainty of clustering results caused by sampling variations was verified by the probability-based cluster analysis, which was implemented using the pvclust package of R software. In this context, the bootstrap (BP) and approximately unbiased (AU) probability are used to validate the reported cluster. The BP and AU values are the percentage that a given cluster appears in the bootstrap and multiscale bootstrap replicates, respectively.

RNA-sequencing differential gene expression analysis. The edgeR package of R/bioconductor software was used to carry out the gene expression analysis. This package assumes negative binomial distribution for the read counts, and the used normalization is given by the TMM (trimmed mean of *M* value) method. The significance of differential gene expression was reported in terms of *q* values (FDR-adjusted *P* values).

Enrichment analysis. Gene set enrichment analysis (GSEA) was used to uncover biological processes associated with sets of differentially expressed genes instead of

focusing on individual genes. This analysis was implemented in the GOstats package of R/bioconductor software by using the function GSEAGOHyperGParams, which uses the relationships among the gene ontology terms as extra information in the statistical inference of groups.

Percentage of protein synthesis analysis. Analysis of protein synthesis was based on the one-proportion one-sided (less) test using chi-squared distribution. The tested hypothesis was the 100% synthesized labelled protein for each treatment; thus, if a given treatment is significant, it indicates that the proportion (or percentage) is different from 100%.

Confidence interval analysis. Nonparametric bootstrap confidence intervals were used on our graphics to increase the accuracy of the confidence limits by an overlapping analysis[31]. This method was introduced as a nonparametric device for estimating standard errors and biases. It is an automatic algorithm for producing highly accurate confidence limits from a bootstrap distribution implemented with the 'boot' package in R software.

Phylogenetic analysis. MYB family sequences were retrieved from the Agris database (http://arabidopsis.med.ohio-state.edu). The alignment was performed by Maft aligner software[32], and the tree was built by Fasttree[33] software.

17. Vinatzer, B. A. *et al.* The type III effector repertoire of *Pseudomona syringae pv. syringae* B728a and its role in survival and disease on host and non-host plants. *Mol. Microbiol.* **62,** 26–44 (2006).
18. Delú-Filho, N. *et al.* A sucrose binding protein homologue from soybean affects sucrose uptake in transgenic tobacco suspension-cultured cells. *Plant Physiol. Biochem.* **38,** 353–361 (2000).
19. Robinson, M. D., McCarthy, D. J. & Smyth, G. K. EdgeR: a Bioconductor package for differential expression analysis of digital gene expression data. *Bioinformatics* **26,** 139–140 (2010).
20. Robinson, M. D. & Oshlack, A. A scaling normalization method for differential expression analysis of RNA-seq data. *Genome Biol.* **11,** R25 (2010).
21. Langmead, B. *et al.* Ultrafast and memory-efficient alignment of short DNA sequences to the human genome. *Genome Biol.* **10,** R25 (2009).
22. Ward, J. H. Jr. Hierarchical grouping to optimize an objective function. *J. Am. Stat. Assoc.* **58,** 236–244 (1963).
23. Kim, T. H., Kim, B. H., Yahalom, A., Chamovitz, D. A. & von Arnim, A. G. Translational regulation via 5′ mRNA leader sequences revealed by mutational analysis of the *Arabidopsis* translation initiation factor subunit eIF3h. *Plant Cell* **16,** 3341–3356 (2004).
24. Kawaguchi, R., William, A. J., Bray, E. A. & Bailey-Serres, J. Water deficit-induced translational control in *Nicotiana tabacum*. *Plant Cell Environ.* **26,** 221–229 (2003).
25. Kawaguchi, R., Girke, T., Bray, E. A. & Bailey-Serres, J. Differential mRNA translation contributes to gene regulation under non-stress and dehydration stress conditions in *Arabidopsis thaliana*. *Plant J.* **38,** 823–839 (2004).
26. Santos, A. A., Florentino, L. H., Pires, A. B. L. & Fontes, E. P. B. Geminivirus: biolistic inoculation and molecular diagnosis. *Methods Mol. Biol.* **451,** 563–579 (2008).
27. Florentino, L. H. *et al.* A PERK-like receptor kinase interacts with the geminivirus nuclear shuttle protein and potentiates viral infection. *J. Virol.* **80,** 6648–6656 (2006).
28. Carvalho, C. M. *et al.* A novel nucleocytoplasmic traffic GTPase identified as a functional target of the bipartite geminivirus nuclear shuttle protein. *Plant J.* **55,** 869–880 (2008).
29. Pinheiro, G. L. *et al.* Complete inventory of soybean NAC transcription factors: sequence conservation and expression analysis uncover their distinct roles in stress response. *Gene* **444,** 10–23 (2009).
30. Costa, M. D. L. *et al.* A new branch of endoplasmic reticulum-stress signaling and the osmotic signal converge on plant specific asparagine-rich proteins to promote cell death. *J. Biol. Chem.* **283,** 20209–20219 (2008).
31. DiCiccio, T. J. & Efron, B. Bootstrap confidence intervals. *Stat. Sci.* **11,** 189–228 (1996).
32. Katoh, K. & Standley, D. M. MAFFT multiple sequence alignment software version 7: improvements in performance and usability. *Mol. Biol. Evol.* **30,** 772–780 (2013).
33. Price, M. N., Dehal, P. S. & Arkin, A. P. FastTree 2—approximately maximum-likelihood trees for large alignments. *PLoS ONE* **5,** e9490 (2010).

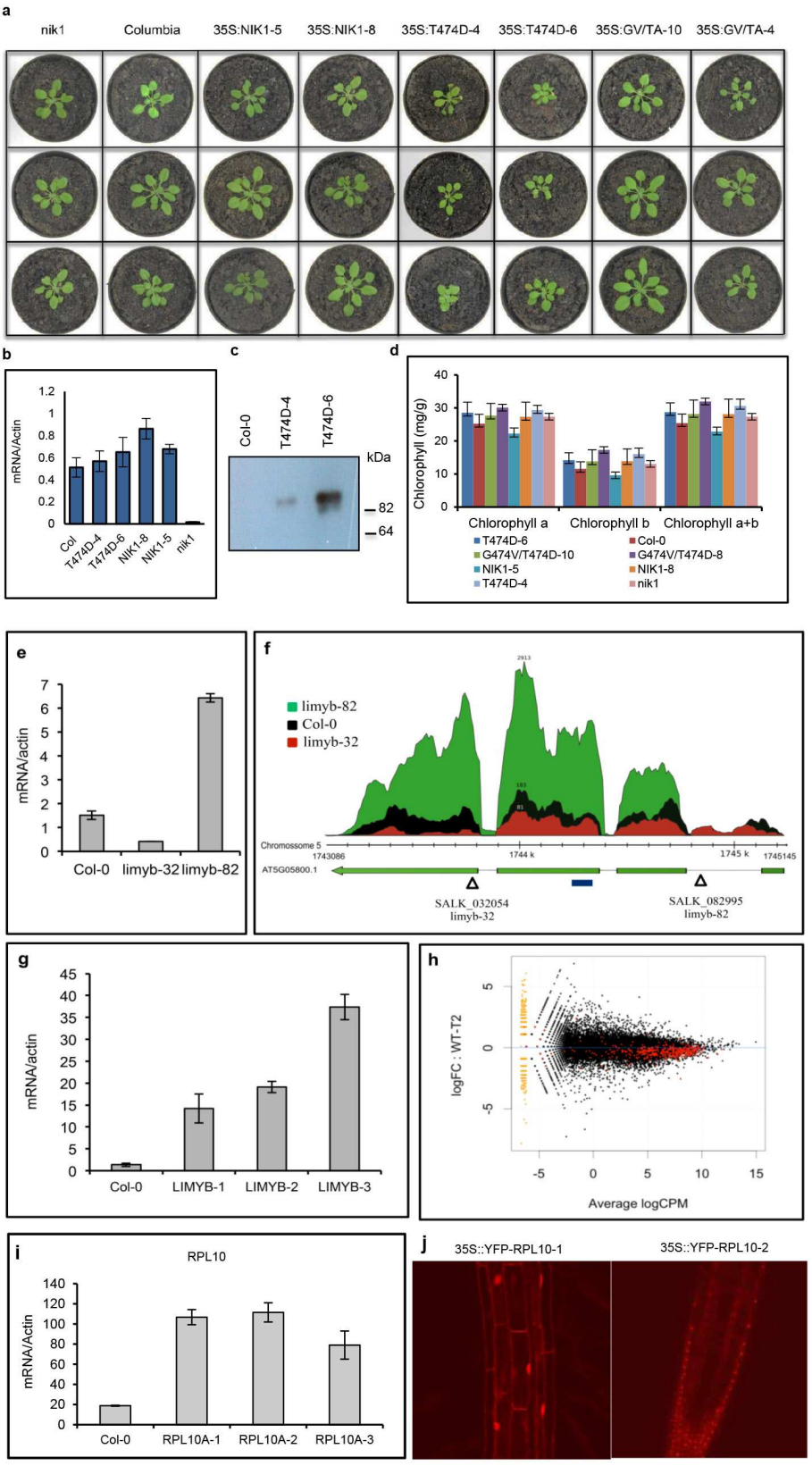

Extended Data Figure 1 | Characterization of the *Arabidopsis* transgenic lines. **a**, Phenotypes of wild-type (Col-0) and *nik1* plants transformed with NIK1 (NIK1-5 and NIK1-8), T474D (T474D-4 and T474D-6) or the double-mutant G4743V/T474A (inactive kinase, GV/TA-10 and GV/TA-4). Transgenic plants (R2 generation, $n = 15$) were grown in soil at 22 °C under short day conditions and photographed 2 weeks after planting. **b**, T474D transcript accumulation in transgenic lines (R2 generation). The expression of T474D or NIK1 in the leaves of independent transgenic lines was monitored by quantitative RT–PCR. Mean ± 95% confidence intervals ($n = 3$) based on bootstrap resampling replicates of three independent experiments. **c**, Accumulation of T474D–GFP in transgenic lines. Total protein was extracted from the leaves of independent transgenic lines (as indicated), immunoprecipitated and immunoblotted with an anti-GFP antiserum. **d**, Chlorophyll content of transgenic lines. Total chlorophyll, chlorophyll *a* and chlorophyll *b* were determined in leaf sectors of the indicated transgenic lines. Error bars, 95% confidence intervals ($n = 3$) based on bootstrap resampling replicates of four independent experiments. **e**, Transcript accumulation of *LIMYB* in T-DNA insertion mutant lines. *LIMYB* expression was monitored by qRT–PCR of RNA prepared from Col-0, *limyb-32* (SALk_032054) and *limyb-82* (SALK_082995) plants. Gene expression was calculated using the $2^{-\Delta Ct}$ method, and actin was used as an endogenous control. Error bars, 95% confidence intervals ($n = 3$) based on bootstrap resampling replicates of three independent experiments. **f**, Schematic representation of the *At5g05800* (*LIMYB*) locus in the chromosome 5 and RNA sequencing data. The *At5g05800* gene harbours three introns and four exons. Triangles show the positions of the T-DNA insertion in the *limyb-32* and *limyb-82* mutants, and the blue line indicates the position of the amplicon from **e**. The relative abundance of the mapped RNA hits in the *At5g05800* locus is shown in red in *limyb-32*, black in Col-0 and green in *limyb-82*. The accumulation of *LIMYB* transcripts was much lower in *limyb-32* and higher in *limyb-82* than in Col-0. Sequencing of the *limyb-32* and *limyb-82* transcripts revealed unprocessed intron sequences and premature stop codons that would have prevented the translation of a functional protein in these mutant lines. Therefore, *limyb-32* and *limyb-82* were confirmed as loss-of-function *limyb* mutant lines. **g**, *LIMYB* transcript accumulation in *LIMYB*-overexpressing lines (R2 generation). *LIMYB* expression in the leaves of independent transgenic lines was monitored by quantitative RT–PCR. Error bars, 95% confidence intervals ($n = 3$) based on bootstrap resampling replicates of three independent experiments. **h**, General downregulation of translational machinery-related genes in LIMYB-1 seedlings. The 'MA' plots show the log of the ratio of the expression levels against log concentration, and each dot represents a gene. This plot visualizes the contrast of LIMYB-1 and Col-0 seedlings. The smear of points on the left side indicates those genes that were observed in only one group of replicated samples, and the red points denote ribosomal and protein synthesis-related genes. CPM, counts per million; FC, fold change; WT, wild type. **i**, *RPL10* transcript accumulation in *RPL10*-overexpressing lines (R2 generation). The expression of an NLS-containing *RPL10* transgene in the leaves of independent transgenic lines was monitored by quantitative RT–PCR. Error bars, 95% confidence intervals ($n = 3$) based on bootstrap resampling replicates of three independent experiments. **j**, Nuclear localization of the NLS-containing YFP–RPL10 fusion in transgenic lines. Root tips from transgenic seedlings expressing the NLS-containing YFP–RPL10 fusion were directly examined under a laser confocal microscope. The figure shows representative confocal images from five independent biological replicates.

a

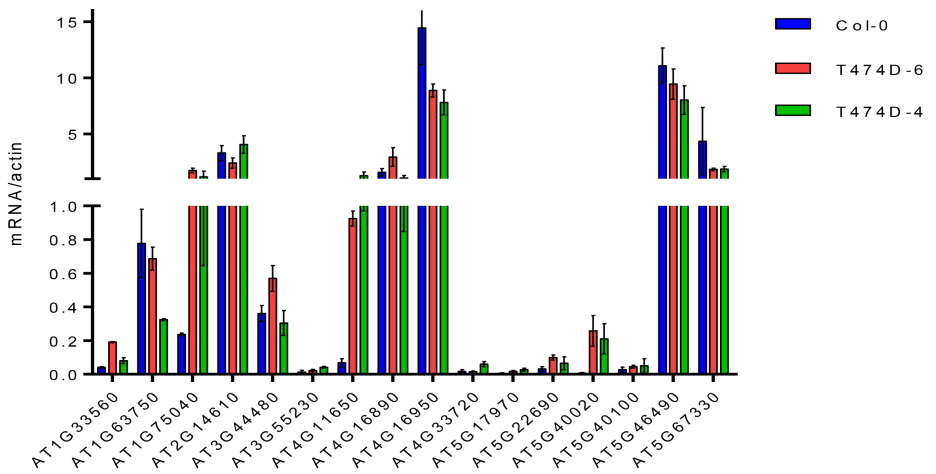

b

TAIR 10	log2 (Fold Change)	q-value (FDR)	Symbol	Description
AT2G14610.1	-2.0266	0.00166622880245705	PR1	Pathogenesis-related gene 1
AT4G11650.1	-1.4957	0.00338420995139227	OSM34	Osmotin 34
AT3G44480.1	-0.1045	0.763775753084199	RPP1, cog1	Disease resistance protein (TIR-NBS-LRR class)
AT4G16890.1	-0.0927	0.81956561493713	SNC1, BAL	Suppressor of NPR1
AT4G16950.1	-0.0397	0.923791385238997	RPP5	Disease resistance protein (TIR-NBS-LRR class)
AT4G33720.1	0.0	0.0	PR1	Pathogenesis-related 1 protein
AT5G17970.1	0.0	0.0		Disease resistance protein (TIR-NBS-LRR class)
AT5G40100.1	0.1313	1		Disease resistance protein (TIR-NBS-LRR class)
AT5G46490.1	0.2537	0.557766109000824		Disease resistance protein (TIR-NBS-LRR class)
AT5G67330.1	0.3322	0.497337654351076	NRAMP4	Natural resistance associated macrophage protein 4
AT3G55230.1	0.8647	0.293804289942712		Disease resistance-responsive (dirigent-like protein)
AT5G40020.1	1.1202	0.360825407950067		Pathogenesis-related thaumatin superfamily protein
AT1G63750.1	1.2229	0.209031413356128		Disease resistance protein (TIR-NBS-LRR class)
AT1G33560.1	1.3284	0.0253419904795418	ADR1	Disease resistance protein (CC-NBS-LRR class)
AT5G22690.1	1.8197	0.0106685101569183		Disease resistance protein (TIR-NBS-LRR class)
AT1G75040.1	2.8732	0.000722106289807284	PR-5	Pathogenesis-related gene 5

c

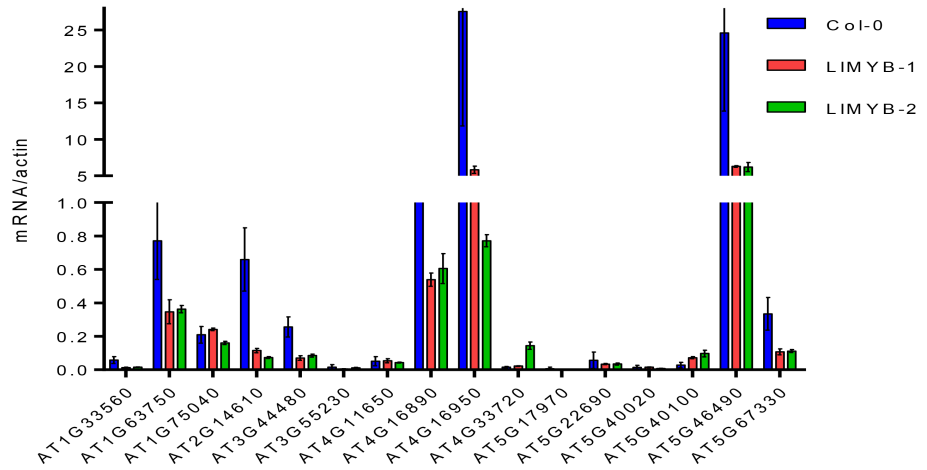

Extended Data Figure 2 | Expression of immune-system-related genes in T474D-overexpressing lines and in *LIMYB*-overexpressing lines. **a**–**c**, On the basis of our global comparison of EST sequences (Fig. 1a) and the role of NIK as an antiviral receptor, we asked whether the constitutive activation of NIK would elicit a defence response similar to that induced by geminivirus infection via the salicylic acid pathway or typical defence responses to virus. No significant gene enrichment was detected in the virus-induced gene silencing (GO:0009616) and viral defence response (GO:0051607) categories using the gene set enrichment analysis (GSEA) method (Supplementary Table 2). For the immune system category, gene enrichment was found in both up- and downregulated changes using the GSEA method. However, the typical markers of salicylic acid signalling, such as *PR1* and *SNC1*, were either non-differentially expressed or downregulated, and the expression of T474D did not enhance the salicylic acid level in the transgenic lines. Collectively, these results indicate that ectopic expression of T474D did not activate typical viral defences, such as salicylic acid signalling or gene silencing. **a**, **b**, Transcript accumulation of selected immune-system-related gene markers by RT–PCR (**a**) or RNA-sequencing in T474D-overexpressing lines (**b**). qRT–PCR of a representative sample confirmed an 80% match with the RNA-sequencing results. **c**, Transcript accumulation of the immune-system-related genes in LIMYB-overexpressing lines. The expression of the indicated genes in the leaves of independent transgenic lines was monitored by qRT–PCR. **a**, **c**, Mean ± 95% confidence intervals ($n = 3$) are shown, based on bootstrap resampling replicates of three independent experiments.

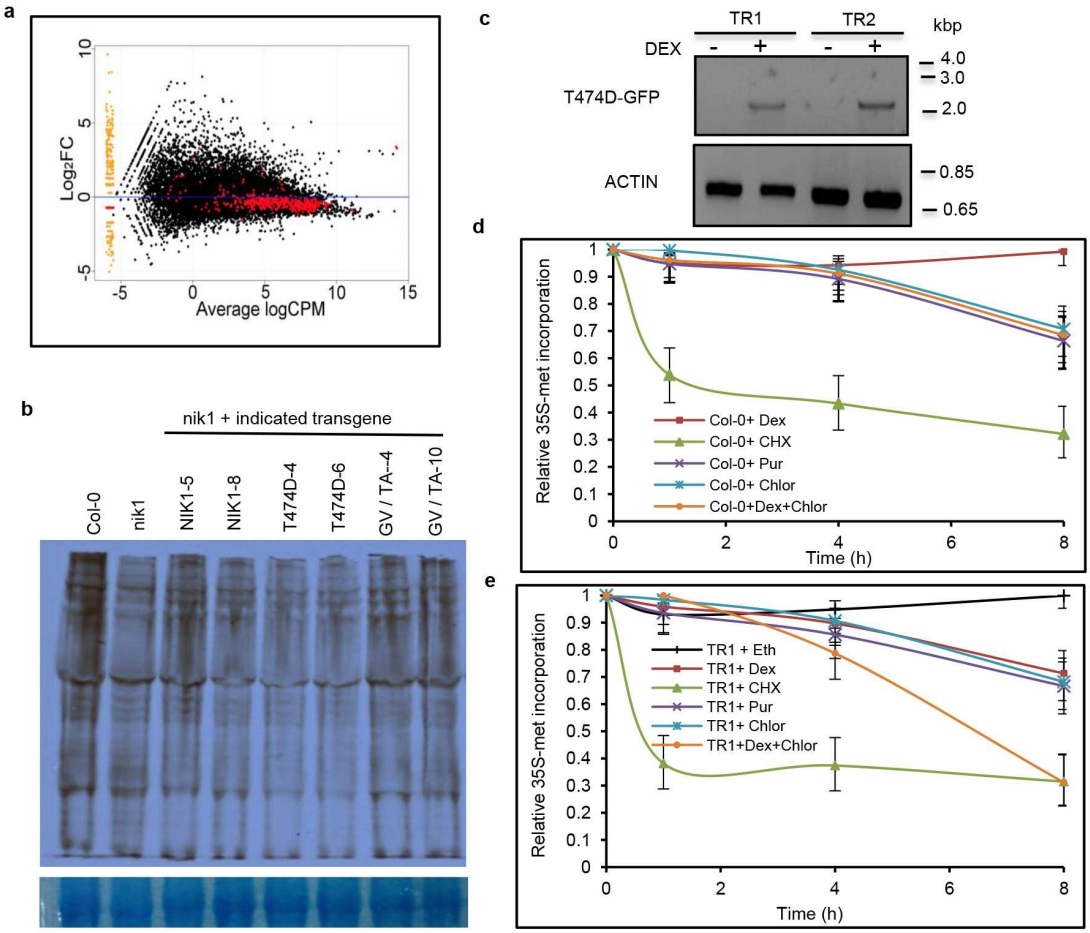

Extended Data Figure 3 | Ectopic expression of T474D-D downregulates translational-machinery-related genes and suppresses *de novo* protein synthesis. **a**, Representation of the translational-machinery-related genes differentially expressed in the T474D lines. The 'MA' plots show the log of the ratio of expression levels versus the log concentration, and each dot represents a gene. This plot represents the contrast between the T474D mock-inoculated lines and the Col-0 mock-inoculated lines. The red points denote ribosomal and protein synthesis-related genes (as shown in Supplementary Table 3). **b**, Downregulation of global translation by ectopic expression of T474D in *Arabidopsis*. The *in vivo* labelling of leaf proteins with [^{35}S]Met was performed in 20-day-old Col-0 plants and T474D transgenic lines. The total protein extracts were fractionated by SDS–polyacrylamide gel electrophoresis (SDS–PAGE), and the radioactive bands were quantified by densitometric analysis of the images obtained by autoradiography. The labelling percentage was normalized to the leaf chlorophyll content, and the protein loading on the gel was adjusted to the Coomassie-stained band of the large subunit of rubisco. **c**, Induction of T474D expression by dexamethasone (DEX) in *Arabidopsis* transgenic seedlings. The constitutive expression of T474D was associated with stunted growth in the transgenic lines (Extended Data Fig. 1a) and repression of global protein synthesis (Fig. 1b). These phenotypes precluded the use of an appropriate normalization method for protein loading in comparative gels of contrasting genotypes to estimate precisely the T474D-mediated protein synthesis inhibition in our assay. To overcome this limitation, we used a dexamethasone-inducible promoter to control the T474D expression in the transgenic lines. *Arabidopsis* seedlings independently transformed with a T474D–GFP fusion under the control of a dexamethasone-inducible promoter (TR1 and TR2) were treated with 30 μM dexamethasone for 8 h, and the induction of T474D–GFP expression was monitored by semi-quantitative RT–PCR. The dexamethasone-induced expression of T474D for 8 h led to a higher inhibition of *de novo* protein synthesis in the transgenic lines, as measured by TCA-precipitable radioactivity, which could be normalized to total protein (TR1 and TR2; Fig. 1c). **d**, Inhibition of *de novo* protein synthesis by protein synthesis inhibitors in Col-0, untransformed lines. We also compared the T474D-mediated suppression of translation with known global translation inhibitors, such as the cytosolic protein synthesis inhibitors cycloheximide and puromycin and the chloroplast translation suppressor chloramphenicol. *Arabidopsis* seedlings (10 days old) were treated with 10 μM cycloheximide (Cyclo), 10 μM puromycin (Pur), 25 μM chloramphenicol (Chlor) or 30 μM dexamethasone (Dex) for the indicated periods of time, and then they were pulse labelled with L-[^{35}S]Met for 60 min. Lysates of treated cells were measured by liquid scintillation counting and normalized to total protein. The relative [^{35}S]Met incorporation was normalized to wild-type (WT = 1) control without treatment. Means ± 95% confidence intervals ($n = 3$) based on bootstrap resampling replicates of three independent experiments are shown. **e**, Inhibition of *de novo* protein synthesis by inducible expression of T474D. Seedlings (10 days old) from the TR1 transgenic line were treated with dexamethasone and the protein synthesis inhibitors for the times as indicated in the figure, and then they were pulse labelled with L-[^{35}S]Met for 60 min. Lysates were processed as described in **d**. Means ± 95% confidence interval ($n = 3$) based on bootstrap resampling replicates of three independent experiments are shown. Cycloheximide was the most effective inhibitor of translation in both the wild-type and T474D-expressing lines. T474D expression inhibited global translation to the same extent as puromycin and caused a further inhibition in the level of chloramphenicol translational inhibition in a combined treatment. The increase in translational inhibition by combining T474D expression and chloramphenicol treatment may indicate that T474D inhibits cytosolic protein synthesis, which is consistent with the T474D-mediated downregulation of components of the cytosolic translational machinery (Supplementary Table 3).

a

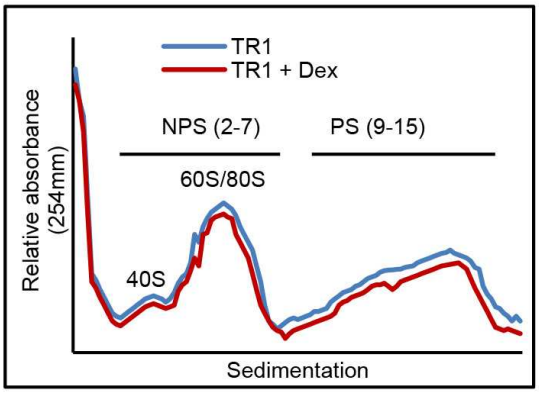

e

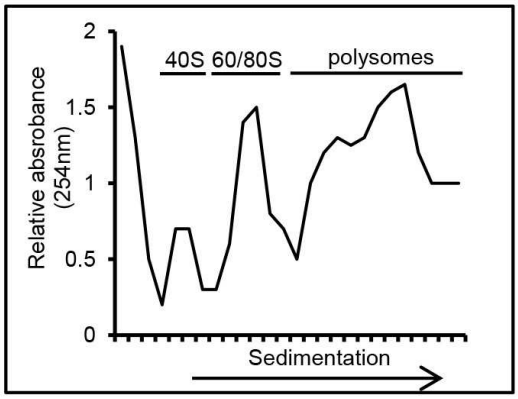

b

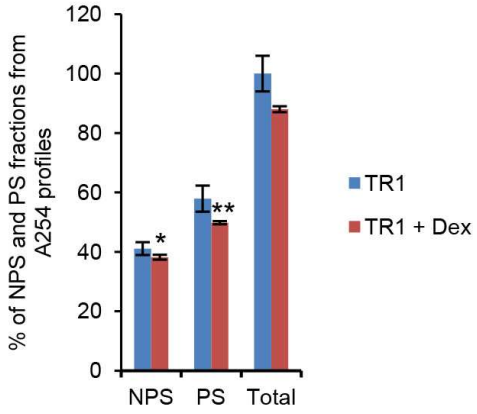

f

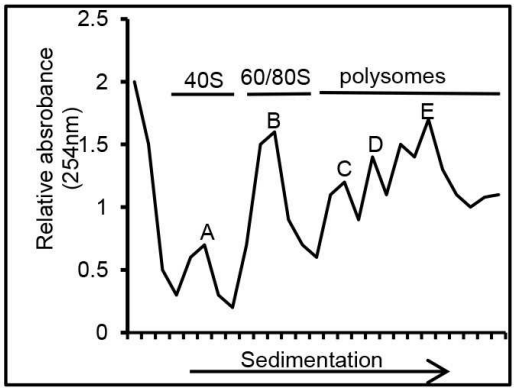

c

Relative RNA content in NPS and PS complexes

	NPS	PS	Total
TR1	0.45 ± 0.03	0.55 ± 0.02	100%
TR1+ Dex	0.39 ± 0.02	0.48 ± 0.02	87%

g

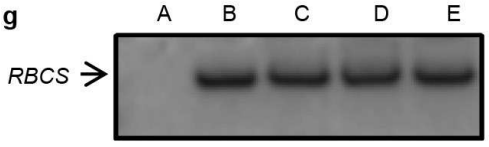

d

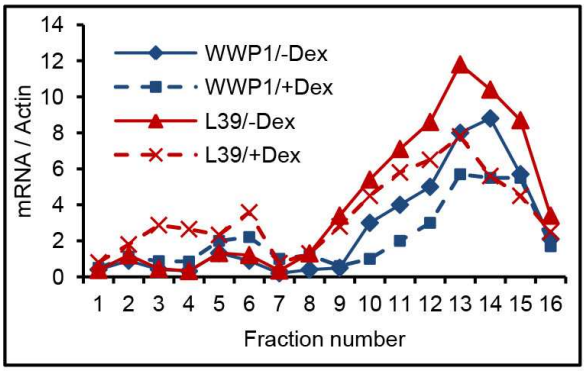

h

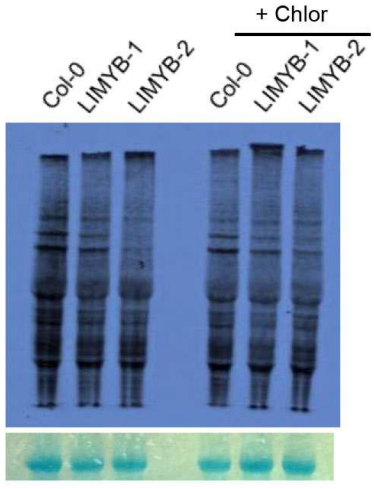

Extended Data Figure 4 | Isolation of PS fractions from *Arabidopsis* seedlings and LIMYB-mediated inhibition of protein synthesis. **a**, Ultraviolet absorbance profiles of the sucrose gradient used for RNA fractionation of dexamethasone (Dex)-inducible T474D transgenic lines. Sixteen fractions of 310 µl were collected. NPS RNA includes complexes ≤ 80S that fractionated in the top half of the gradient (fractions 2–7) and PS (polysome) represents complexes fractionated in the bottom of the gradient (fractions 9–15). **b**, Distribution (%) of NPS and PS fractions on polysome density gradients. The percentage of NPS or PS was calculated by integrating the areas under the corresponding peaks in the $A_{254\,nm}$ profile delimited by a gradient baseline absorbance (buffer density). Values are the average ± standard deviation (s.d.) of three biological replicates. NPS and PS fractions from T474D + Dex samples were significantly different from the corresponding fractions of the T474D samples by the *t*-test (greater). NPS, **P* value = 0.03725; PS, ***P* value = 0.009137 (*t*-test; greater). **c**, Relative RNA content in NPS and PS complexes. RNA was precipitated from NPS and PS density regions of sucrose gradients (as in **a**) and quantified. Relative NPS RNA and PS RNA contents from T474D and T474D + Dex samples were calculated in relation to the total NPS + PS content from T474D. Values for the relative NPS and PS RNA content are the average ± s.d. of three biological replicates and they were significantly different between the samples ($P < 0.01$, *t*-test). **d**, Distribution of specific mRNAs in the PS gradient fractions from extracts prepared from T474D seedlings treated (or not) with dexamethasone. The RNA on each fraction was reverse transcribed and aliquots amplified with specific primers for the indicated genes by qPCR. **e**, Ultraviolet absorbance profiles of the sucrose gradient used for the RNA fractionation of Col-0 seedlings. PSs from 15-day-old Col-0 seedlings were fractionated on a sucrose gradient, and the fractions were manually collected. **f**, Ultraviolet absorbance profiles of the sucrose gradient used for RNA fractionation from T474D seedlings. PSs from 15-day-old T474D-overexpressing seedlings were fractionated on a sucrose gradient, and the fractions were manually collected. **g**, Levels of the small subunit of rubisco (*RBCS*) mRNA per fraction. The levels of mRNA of *RBCS* were examined by northern blotting. This control was used to ensure the quality and distribution of a specific mRNA. **h**, Overexpression of LIMYB suppresses cytosolic translation. *In vivo* labelling of leaf proteins with [^{35}S]Met was performed in Col-0 and *LIMYB-1* transgenic seedlings in the presence and absence of chloramphenicol treatment. The total protein extracts were fractionated by SDS–PAGE, and the radioactive bands were quantified by densitometric analysis of the images obtained by autoradiography. The labelling percentage was normalized to the leaf chlorophyll content, and protein loading is shown by Coomassie staining of the radioactive gel.

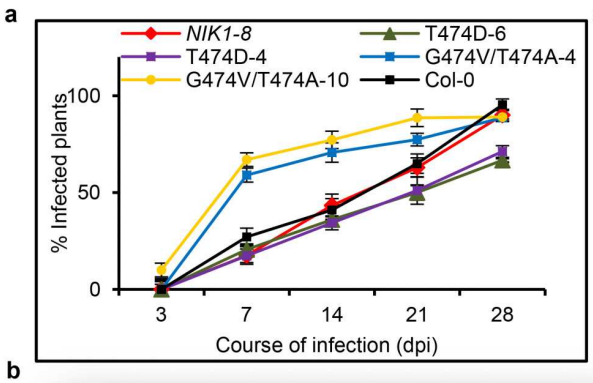

c

T474D infected – Col-0 infected (10 days)			
Viral Component	log2FC	q-value	NCBI Locus ID
A	0.9139909	1.381925e-01*	CLU65529
B	1.2348528	1.257184e-08	CLU65530
T474D infected – WT infected (21 days)			
Viral Component	log2FC	q-value	NCBI Locus ID
A	-4.534558	7.640602e-126	CLU65529
B	-3.682993	1.129406e-112	CLU65530

*Non significative according to Negative Binomial Exact Test (edgeR) by q-value (FDR) < 0.05

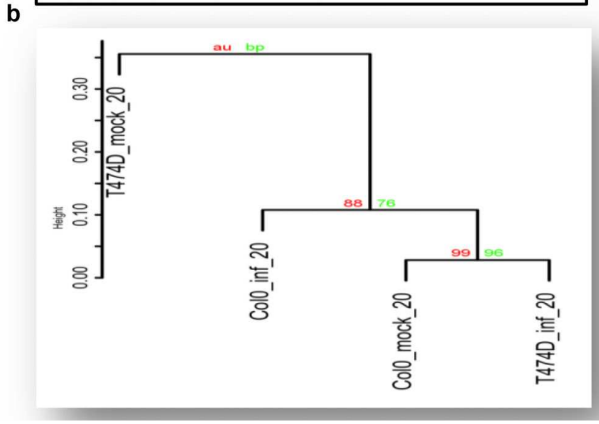

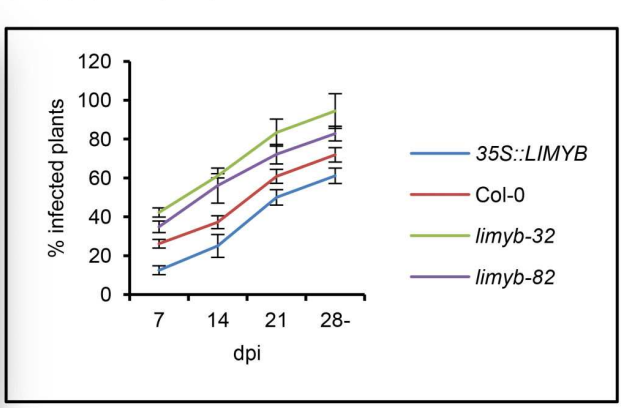

Extended Data Figure 5 | Ectopic expression of T474D and LIMYB confers tolerance to begomovirus infection. **a**, Delayed onset of infection in the T474D-4- and T474D-6-overexpressing lines. Ecotype Col-0 plants, as well as the T474D-4- and T474D-6-overexpressing lines, and the *NIK1-8* and G473V/T474A-overexpressing lines were infected with CaLCuV DNA by the biolistic method. The progression of the infection was monitored by PCR detection of viral DNA in the systemic leaves of the inoculated plants. The values represent the percentages of systemically infected plants at different dpi. Error bars, 95% confidence intervals ($n = 3$) based on bootstrap resampling replicates of four independent experiments. **b**, Upon symptom development, the T474D-induced transcriptome diverges from the infected Col-0 transcriptome. The mock-inoculated T474D-overexpressing lines exhibited a constitutively infected wild-type transcriptome at 10 dpi (Fig. 1a). Nevertheless, these T474D transgenic lines did not phenocopy the infected wild-type plants because they did not develop symptoms of viral infection. In fact, the wild-type plants displayed typical symptoms of CaLCuV infection at 21 dpi, such as leaf distortion, stunting with epinasty and chlorosis (Fig. 1e). The symptoms in the T474D-expressing lines at 21 dpi, however, were greatly attenuated, with no visible leaf distortion or chlorosis. To examine these phenotypes, we performed a Ward hierarchical clustering of the gene expression data (normalized by the trimmed mean of *M*-values (TMM) normalization method) from the *Arabidopsis* infection experiments at 21 dpi. The TMM normalization method assumes that the majority of genes are not differentially expressed, and it adjusts genes with larger read counts and lower variance on the logarithmic scale. The dendrogram provides two types of *P* values: AU (black) and BP (grey). The AU *P* value comes from multiscale bootstrap resampling, while the BP value represents normal bootstrap resampling. These *P* values were calculated by multiscale bootstrap resampling using the R-cran package pvclust with a cut-off of 0.05. These *P* values show the significance of the proximity of each gene expression experiment profile. The cluster analysis at 21 dpi indicated that when symptoms had developed in the infected Col-0 leaves, the T474D-induced transcriptome diverged from the infected Col-0 transcriptome. The mock T474D transcriptome formed a unique clade, while the infected T474D transcriptome was more closely related to the mock-inoculated Col-0 transcriptome. **c**, Reduced viral transcript accumulation in T474D-overexpressing lines at 21 dpi. RNA-sequencing data of viral gene transcripts in the systemic leaves of infected wild-type and T474D-overexpressing plants at 10 dpi and 21 dpi. **d**, The onset of infection is delayed in *LIMYB*-overexpressing lines. Ecotype Col-0 plants and *LIMYB*-overexpressing and *limyb* mutant lines were infected with CaLCuV DNA using the biolistic method. The progression of the infection was monitored by the PCR detection of viral DNA in the systemic leaves of the inoculated plants. The values represent the percentages of systemically infected plants at different dpi. Error bars, 95% confidence intervals ($n = 3$) based on bootstrap resampling replicates of four independent experiments.

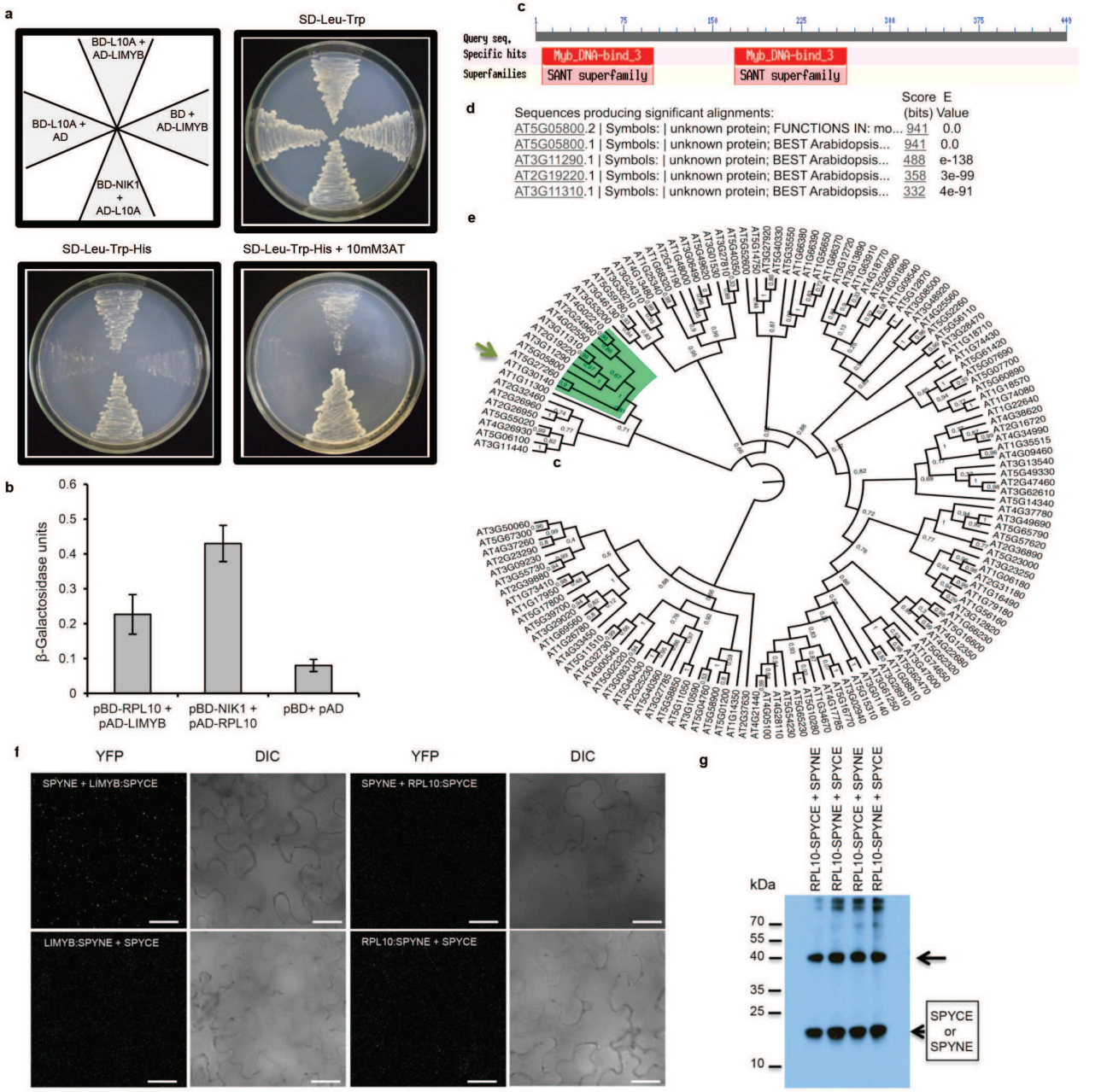

Extended Data Figure 6 | LIMYB, which belongs to the MYB domain-containing superfamily, interacts with RPL10 in the yeast two-hybrid system. **a**, LIMYB and RPL10 interact in yeast. LIMYB was expressed in yeast as a GAL4 activation domain (AD) fusion (pAD–LIMYB), and RPL10 was expressed as a GAL4 binding domain (BD) fusion (pBD–RPL10). The interactions between the tested proteins were examined by monitoring His prototrophy. **b**, The interactions were further confirmed by measuring the expression activity of the β-galactosidase reporter enzyme for the second reporter gene, β-galactosidase. The interaction between pAD–RPL10 and pBD–NIK1 was monitored as a positive control. Means ± 95% confidence intervals ($n = 3$) based on bootstrap resampling replicates of three technical replicates are shown. **c**, LIMYB harbours two MYB domains. The position of these MYB domains is indicated in the schematic representation of the LIMYB primary structure. **d**, Sequence identity of the closest related *LIMYB* (*At5g05800*) homologues. **e**, Dendrogram of MYB domain-containing proteins from *Arabidopsis*. The MYB family sequences were retrieved from the Agris database (http://arabidopsis.med.ohio-state.edu). The alignment was performed by Maft aligner software using full-length sequences, and the tree was built by Fasttree software (the bootstrap values are indicated close to the branch divisions). The arrow indicates *LIMYB* (*At5g05800*). **f**, **g**, The negative controls used in the BiFC analysis. **f**, Confocal fluorescent image of SPYNE + LIMYB:SPYCE, LIMYB:SPYNE + SPYCE, SPYNE + RPL10:SPYCE and RPL10:SPYNE + SPYCE, as indicated in the figure. We used a BiFC assay to determine whether RPL10 and LIMYB interact in the nuclei of plant cells. The formation of a RPL10–LIMYB complex occurred in the nuclei of transfected cells independent of the orientation of the LIMYB or RPL10 fusions (amino terminus or carboxy terminus of YFP; Fig. 2a), and the reconstituted fluorescent signal was much higher than that of the background (control panels with combinations of the protein fusions with empty vectors). The figure displays representative samples from three independent biological repeats. Scale bars, 20 μm. **g**, The C-terminal (SPYCE) and N-terminal region (SPYNE) of YFP accumulates detectably in co-transfected leaves. Total protein extracts from leaves co-transfected with the indicated constructs were immunoblotted with anti-YFP serum. The arrow indicates the position of RPL10–SPYCE and RPL10–SPYNE fusions, and arrowheads indicate the positions of the C-terminal (SYYCE) and N-terminal (SPYNE) regions of YFP.

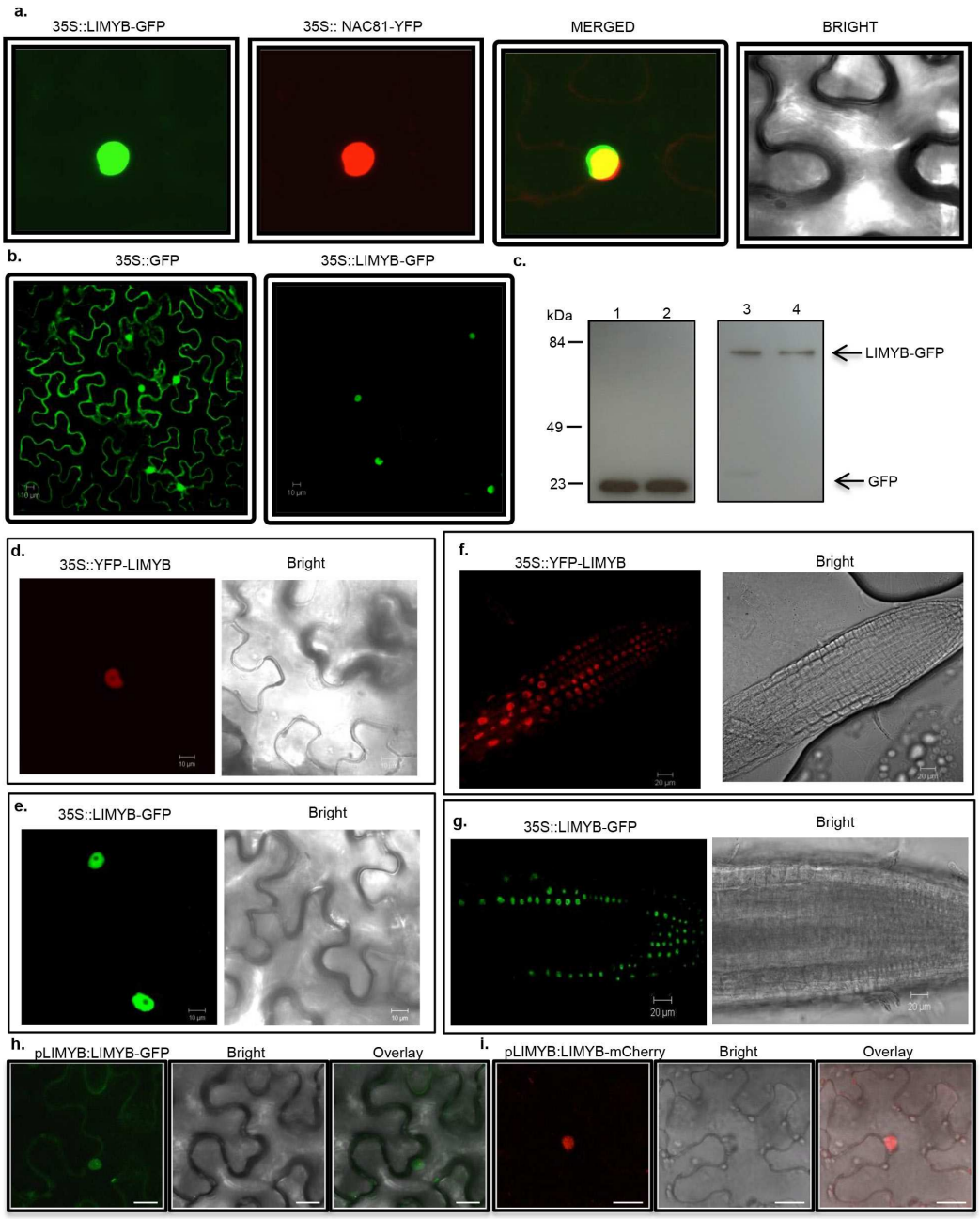

Extended Data Figure 7 | Nuclear localization of LIMYB. **a**, Colocalization of LIMYB with the nuclear marker gene *Glycine max* (*Gm*)*NAC81*. *N. benthamiana* leaves were co-infiltrated with *A. tumefaciens* carrying a 35S::LIMYB–GFP construct and a 35S::YFP–GmNAC81 construct. Forty-eight hours after infiltration, the subcellular localizations of the fluorescent fusion proteins were examined by confocal microscopy. The figure shows representative confocal images from two independent experiments. **b**, Confocal fluorescence image of transiently expressed GFP (left) or LIMYB–GFP (right) in epidermal cells of tobacco leaves. Scale bars, 10 μm. The figure shows representative confocal images from two independent experiments. **c**, Immunoblotting of transiently expressed LIMYB–GFP in epidermal cells of tobacco leaves. Total protein was extracted from agro-infiltrated *N. benthamiana* leaves containing the 35S::GFP (left lanes) or 35S::LIMYB–GFP (right lanes) constructs and immunoblotted with an anti-GFP monoclonal antibody to examine the stability of the fusion protein. The positions of molecular mass are shown in kDa. **d**, Confocal fluorescence image of transiently expressed GFP–LIMYB in epidermal cells of tobacco leaves. Scale bars, 10 μm. The figure shows representative confocal images from four independent experiments. **e**, Confocal fluorescence image of transiently expressed LIMYB–GFP in epidermal cells of tobacco leaves. Scale bars, 10 μm. The figure shows representative confocal images from four independent experiments. **f**, **g**, Confocal fluorescence image of root cells stably transformed with YFP–LIMYB or LIMYB–GFP. Root tips from transgenic seedlings expressing YFP–LIMYB (**f**) or LIMYB–GFP (**g**) were directly examined under a laser confocal microscope. Scale bars, 20 μm. The figures show representative confocal images from three biological replicas. Neither the fusion of YFP to the LIMYB N terminus nor GFP to its C terminus altered the nuclear localization of LIMYB in either agro-inoculated *N. tabacum* leaves or stably transformed *Arabidopsis* roots. **h**, **i**, Confocal fluorescent image of LIMYB fused to GFP or mCherry under the control of its own promoter. The figures show representative confocal images from two independent experiments. The fluorescence was also concentrated in the nucleus of transfected cells by expression of LIMYB–GFP or LIMYB–mCherry fusions under the control of the LIMYB endogenous promoter. Scale bars, 20 μm. Collectively, these results indicate that LIMYB was localized in the nucleus.

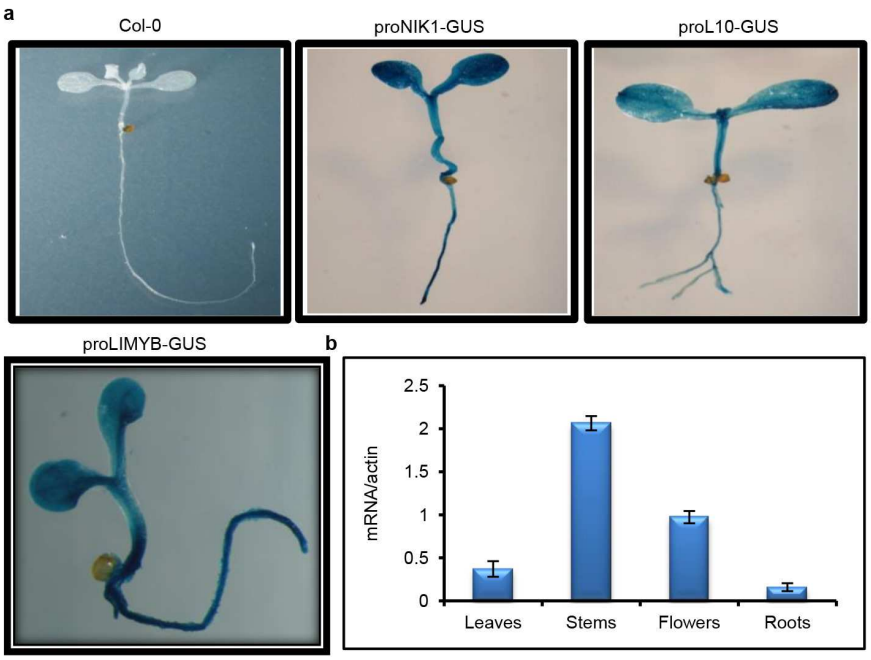

Extended Data Figure 8 | *LIMYB*, *RPL10* and *NIK1* display overlapping expression profiles. **a**, pLIMYB::GUS, pRPL10::GUS and pNIK1::GUS are ubiquitously expressed in seedling tissues. GUS reporter gene expression was histochemically monitored in 2-week-old seedling leaves and roots from transgenic lines harbouring a β-glucuronidase (*GUS*) reporter gene expressed from the LIMYB, RPL10 and NIK1 promoters. The figure shows representative GUS staining images of three seedlings per genotype. All three genes were ubiquitously expressed in all seedling tissues. **b**, Expression analysis of LIMYB in various plant organs. *LIMYB* expression was monitored by qRT–PCR of RNA prepared from leaves, roots, stems or flowers of Col-0 plants. Gene expression was calculated using the $2^{-\Delta Ct}$ method, and actin was used as an endogenous control. Error bars, 95% confidence intervals ($n = 3$) based on bootstrap resampling replicates of three independent experiments. LIMYB was also expressed in the leaves, roots, stems and flowers, indicating that *LIMYB*, *RPL10* and *NIK1* are co-expressed in several organs.

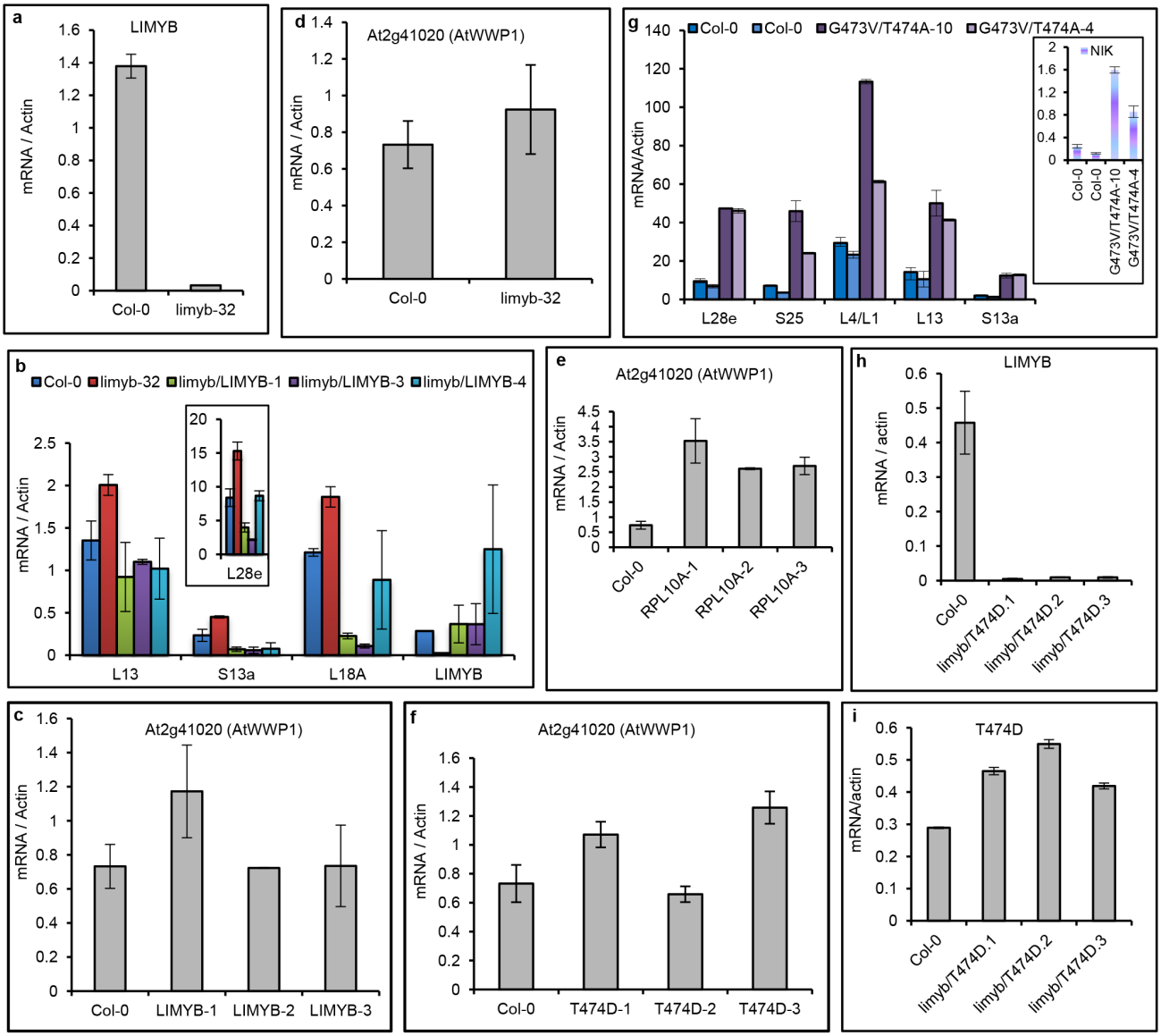

Extended Data Figure 9 | Controls for the regulation of RP gene expression experiments. **a**–**i**, Expression of the indicated genes in the leaves of independent transgenic lines was monitored by qRT–PCR. **a**, *LIMYB* expression in the *limyb-32* mutant was examined. **b**, *LIMYB* expression in *limyb-32* mutant restores wild-type expression of the RP genes. Expression of the *S13a*, *L18A* and *L28e* genes was monitored in three independently transformed *limyb-32* knockout plants with the *LIMYB* gene. **c**–**f**, Expression of the unrelated gene *AtWWP1* was monitored as a negative control in three independently transformed *LIMYB*-, *RPL10*- and T474D-overexpressing lines in addition to the *limyb-32* mutant. **g**, The double-mutant inactive kinase, G4743V/T474A, does not downregulate the RP genes. The transcript accumulation of the indicated RP genes was quantified by qRT–PCR in two independently transformed *nik1* knockout lines expressing the G4743V/T474A double mutant. **h**, **i**, Expression of *LIMYB* (**h**) and the transgene T474D (**i**) was monitored in the *limyb-32* lines, which were transformed with T474D. **a**–**i**, Means ± 95% confidence intervals ($n = 3$) based on bootstrap resampling replicates of three independent experiments are shown.

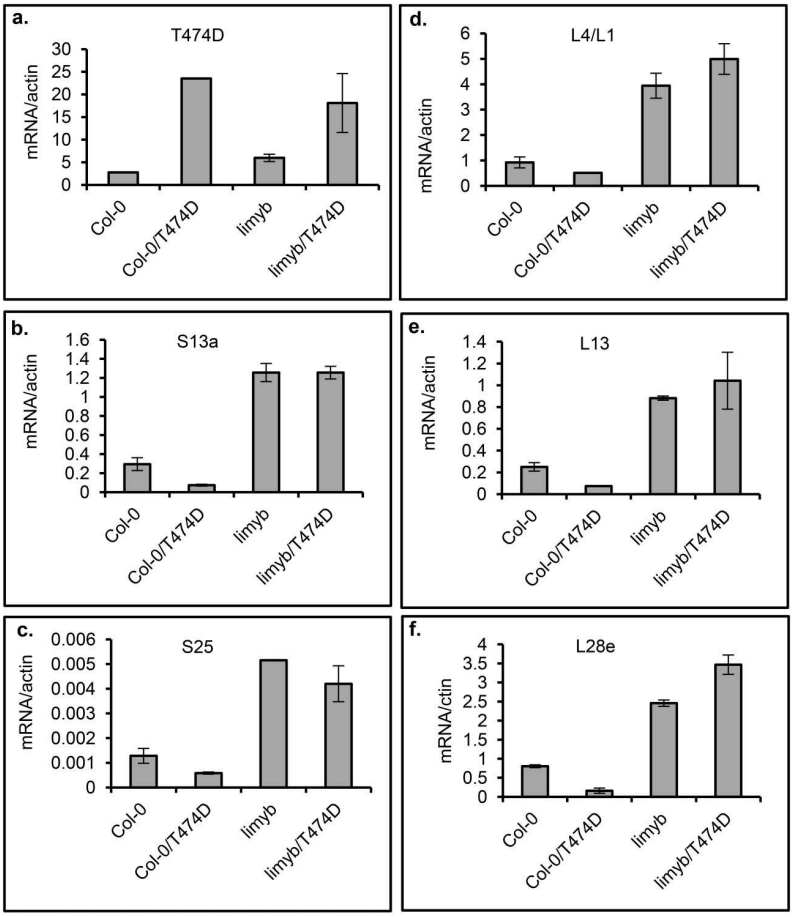

Extended Data Figure 10 | T474D requires LIMYB function to mediate the downregulation of translational machinery-related genes. **a**–**f**, A 35S::T474D–GFP construct was electroporated into protoplasts prepared from Col-0 and *limyb-32* seedlings, and the expression of the indicated RP genes was monitored by qRT–PCR of RNA prepared from untransfected and transfected protoplasts. Gene expression was calculated using the $2^{-\Delta Ct}$ method, and actin and ubiquitin were used as an endogenous control. Means ± 95% confidence intervals ($n = 3$) based on bootstrap resampling replicates of three independent experiments are shown.

Plant Biotechnology Journal

Plant Biotechnology Journal (2015), pp. 1–12 doi: 10.1111/pbi.12349

Sustained NIK-mediated antiviral signalling confers broad-spectrum tolerance to begomoviruses in cultivated plants

Otávio J.B.Brustolini[1,2,†], Joao Paulo B. Machado[1,2,†], Jorge A. Condori-Apfata[2], Daniela Coco[1,2], Michihito Deguchi[1,2], Virgílio A.P. Loriato[1,2], Welison A. Pereira[2], Poliane Alfenas-Zerbini[2], Francisco M. Zerbini[2], Alice K. Inoue-Nagata[2,4], Anesia A. Santos[1,2], Joanne Chory[5], Fabyano F. Silva[3] and Elizabeth P.B. Fontes[1,2,*]

[1]*Departamento de Bioquímica e Biologia Molecular, Bioagro, Viçosa, MG, Brazil*

[2]*National Institute of Science and Technology in Plant–Pest Interactions, Bioagro, Viçosa, MG, Brazil*

[3]*Departamento de Zootecnia, Universidade Federal de Viçosa, Viçosa, MG, Brazil*

[4]*Embrapa Vegetables, Brasília, DF, Brazil*

[5]*Howard Hughes Medical Institute and Plant Biology Laboratory, The Salk Institute for Biological Studies, La Jolla, CA, USA*

Received 3 July 2014;
revised 30 December 2014;
accepted 6 January 2015.
**Correspondence* (Tel +55 31 3899 2948;
fax +55-31-38992864
email bbfontes@ufv.br)
[†]These authors contributed equally to this work.

Keywords: NIK, NSP-interacting kinase, nuclear shuttle protein, tomato-infecting begomoviruses, begomovirus, leucine-rich repeats receptor-like kinase.

Summary

Begomovirus-associated epidemics currently threaten tomato production worldwide due to the emergence of highly pathogenic virus species and the proliferation of a whitefly B biotype vector that is adapted to tomato. To generate an efficient defence against begomovirus, we modulated the activity of the immune defence receptor nuclear shuttle protein (NSP)-interacting kinase (NIK) in tomato plants; NIK is a virulence target of the begomovirus NSP during infection. Mutation of T474 within the kinase activation loop promoted the constitutive activation of NIK-mediated defences, resulting in the down-regulation of translation-related genes and the suppression of global translation. Consistent with these findings, transgenic lines harbouring an activating mutation (T474D) were tolerant to the tomato-infecting begomoviruses ToYSV and ToSRV. This phenotype was associated with reduced loading of coat protein viral mRNA in actively translating polysomes, lower infection efficiency and reduced accumulation of viral DNA in systemic leaves. Our results also add some relevant insights into the mechanism underlying the NIK-mediated defence. We observed that the mock-inoculated T474D-overexpressing lines showed a constitutively infected wild-type transcriptome, indicating that the activation of the NIK-mediated signalling pathway triggers a typical response to begomovirus infection. In addition, the gain-of-function mutant T474D could sustain an activated NIK-mediated antiviral response in the absence of the virus, further confirming that phosphorylation of Thr-474 is the crucial event that leads to the activation of the kinase.

Introduction

Begomoviruses (whitefly-transmitted geminiviruses) cause severe diseases of high economic impact in a variety of agriculturally relevant crops in tropical and subtropical areas (Rojas *et al.*, 2005). Current climate changes are expected to further alter the whitefly distribution across the globe, posing a major threat to agriculture worldwide. The threat is particularly strongly for tomato plants, which are inflicted by a variety of emergent species of tomato-infecting begomoviruses. Previous attempts to develop pathogen-derived resistance using begomovirus DNA sequences in transgenic plants have failed to achieve immunity, resistance or tolerance, even though a delay of infection and/or attenuation of symptoms were frequently observed (Day *et al.*, 1991; Hashmi *et al.*, 2011; Hong and Stanley, 1996; Kunik *et al.*, 1994; Lin *et al.*, 2012; Noris *et al.*, 1996; Stanley *et al.*, 1991). The only exception was a single common bean transgenic line expressing a siRNA that targets the replication protein from BGMV (*bean golden mosaic virus*), which has been shown to be immune to this begomovirus (Aragão and Faria, 2009). However, it has been extremely difficult to engineer broad-spectrum resistance against tomato-infecting begomoviruses through a similar RNA silencing strategy (Lucioli *et al.*, 2008). One explanation for the failure of siRNA tomato transgenic lines to resist begomovirus infection is the emergence of new species of tomato-infecting begomoviruses that evolve rapidly through recombination or pseudo-recombination, which produces divergent genome sequences, giving the virus an advantage over its host's recognition system (Albuquerque *et al.*, 2012; Castillo-Urquiza *et al.*, 2008; Galvão *et al.*, 2003). More recently, transgenic tomato lines expressing peptide aptamers, which bind efficiently to and inhibit the begomovirus replication protein (Rep), have been shown to display enhanced tolerance to *Tomato yellow leaf curl virus* or *Tomato mottle virus* (Reyes *et al.*, 2013). Thus, the Rep-binding peptide octamers may serve as an efficient strategy for engineering transgenic tomato plants that are resistant to diverse begomoviruses. Likewise, expression of the single-stranded DNA binding protein virE2 from Agrobacterium in

Please cite this article as: Brustolini ,O.J.B., Machado, J.P.B., Condori-Apfata, J.A., Coco, D., Deguchi, M., Loriato, V.A.P., Pereira, W.A., Alfenas-Zerbini, P., Zerbini, F.M., Inoue-Nagata, A.K., Santos, A.A., Chory, J. Silva, F.F. and Fontes, E.P.B. (2015) Sustained NIK-mediated antiviral signalling confers broad-spectrum tolerance to begomoviruses in cultivated plants. *Plant Biotechnol. J.*, doi: 10.1111/pbi.12349

tobacco has been shown to reduce *Mungbean yellow mosaic virus* DNA accumulation, although the spectrum of the resistance has not been established (Sunitha *et al.*, 2011).

Begomoviruses are single-stranded DNA viruses with a monopartite or bipartite genome configuration. For the bipartite begomoviruses, the proteins required for replication (Rep and REn), transactivation of viral genes (TrAP), the suppression of RNAi defence functions (TrAP and AC4) and encapsidation of viral DNA (CP) are encoded by the DNA-A component, whereas the nuclear shuttle protein (NSP) and intercellular movement protein (MP) are encoded by DNA-B (Rojas *et al.*, 2005). NSP facilitates the traffic of viral DNA from the nucleus to the cytoplasm and acts in concert with MP to move the viral DNA to the adjacent, uninfected cells. The mechanistic model for viral DNA intracellular trafficking holds that NSP binds to newly replicated viral DNA in the nuclei of infected cells and utilizes the nuclear export machinery to move the viral DNA to the cytoplasm (Carvalho *et al.*, 2008a,b; Gafni and Epel, 2002). Consistent with this model, NSP contains a HIVRev-like or TFIIA-like leucine-rich nuclear export signal (NES) that can be functionally replaced by TFIIIA NES in both nuclear export and infectivity (Ward and Lazarowitz, 1999). NSP is found within the nuclei of transfected plant, insect and yeast cells, but is relocated to the cell periphery when co-expressed with viral movement protein (MP, Carvalho *et al.*, 2008b; Sanderfoot and Lazarowitz, 1995, 1996; Sanderfoot *et al.*, 1996; Zhang *et al.*,2001). The fundamental role of NSP in virus movement predicts that this viral protein may interact with host factors in different subcellular compartments. Accordingly, NSP has been shown to interact with an *Arabidopsis thaliana* nuclear acetylase, designated nuclear shuttle protein interactor (AtNSI) and a cytosolic GTPase that facilitates the release of the viral DNA-NSP complex from the nuclear pores to the cytosol, designated NIG (NSP-interacting GTPase). NSP also interacts with plasma membrane receptor-like kinases, designated NsAKs (NSP-activating kinases) from Arabidopsis and NIKs (NSP-interacting kinases) from tomato, soya bean and Arabidopsis (Carvalho *et al.*, 2008b; Florentino *et al.*, 2006; Mariano *et al.*, 2004; McGarry *et al.*, 2003). In Arabidopsis, NSP interacts with three members of the LRR-receptor-like kinase (RLK) family, NIK1, NIK2 and NIK3, which have been shown to be authentic serine/threonine kinases with biochemical properties consistent with a receptor signalling function (Fontes *et al.*, 2004).

NIK was recently discovered as a component of the antiviral plant immune system (Carvalho *et al.*, 2008c; Fontes *et al.*, 2004). The viral NSP binds to the kinase domain of NIK to suppress its activity and increase begomovirus pathogenicity (Fontes *et al.*, 2004). The current model for NIK activation holds that upon begomovirus infection, NIK oligomerizes and transphosphorylates the kinase domain on a key threonine residue at position 474 (T474; Carvalho *et al.*, 2008c; Rocha *et al.*, 2008; Santos *et al.*, 2009). This phosphorylation-dependent activation of NIK leads to the phosphorylation of a downstream component, the ribosomal protein L10A (RPL10), which in turn translocates to the nucleus, where it interacts with LIMYB to fully down-regulate translation machinery-related genes, leading to host translation suppression that affects the translation of begomovirus mRNAs (Carvalho *et al.*, 2008c; Zorzatto *et al.*, 2015). To counteract this mechanism, the viral NSP binds to the kinase domain of NIK and prevents phosphorylation of T474, leading to the suppression of the kinase activity and establishing an environment that is more favourable to begomovirus infection. Accordingly, the loss of NIK function enhances the susceptibility of NIK null alleles to begomovirus infection, whereas the overexpression of Arabidopsis (At) NIK1 in begomovirus-infected tobacco leaves titrates the virally produced NSP inhibitor and the molar excess of NIK overcomes NSP-mediated inhibition (Santos *et al.*, 2010). Likewise, enhanced accumulation of AtNIK1 in tomato plants attenuates begomovirus infection. However, the effectiveness of the NIK-mediated signalling pathway against begomovirus infection is limited because the viral NSP functions as a NIK suppressor and because activation of the pathway seems to be dependent on the onset of infection.

To increase the effectiveness of the NIK-mediated pathway against virus infection, we prepared a gain-of-function AtNIK1 mutant (T474D) by replacing a threonine residue at position 474 with an aspartic acid residue (a phosphomimic). We have previously shown that this mutation leads to hyperactivation of the kinase activity, with a 1.5-fold increase in substrate phosphorylation activity and an enhanced capacity to relocate RPL10 to the nucleus (Santos *et al.*, 2009). In this study, we used the gain-of-function mutant from Arabidopsis to generate an antiviral strategy to fight tomato-infecting begomoviruses and to gain insights into the activation of the NIK-mediated defence response. We showed that the antiviral signalling activity of a constitutively activated NIK receptor from the cruciferous plant *Arabidopsis thaliana* is retained after its transfer to the solanaceous plant tomato (*Solanum lycopersicum*), making the tomato transgenic lines more resistant to different species of begomovirus.

Results

NSP-NIK complex formation is barely detected *in vivo* by BiFC

Proteins that shuttle between the nucleus and the cytoplasm are concentrated within the nucleus because the rate of nuclear import exceeds that of export. In fact, NSPs from several begomoviruses ectopically expressed in transfected cells are nuclear localized (Carvalho *et al.*, 2008b; Sanderfoot and Lazarowitz, 1995; Sanderfoot *et al.*, 1996). Likewise, the ectopically expressed NSPs from CaLCuV, ToYSV and ToSRV colocalized with the nuclear marker AtWWP1 in the nuclei of *N. benthamiana* epidermal cells (Figure S1). This preferential nuclear localization of NSP when transiently expressed in leaf cells compromises the use of the BiFC (bimolecular fluorescence complementation) assay and co-immunoprecipitation of ectopically expressed proteins in efficiently detecting interactions between NSP and membrane proteins *in planta*. Accordingly, our attempts to examine interactions between NSP from CaLCuV and NIK *in vivo* by BiFC resulted in a very low frequency of transfected cells displaying any reconstituted fluorescence on the plasma membrane (Figure 1a), although it was greater than the background levels (right panels). In addition, the formation of an NSP-NIK1 complex occurred *in vivo* independently of the orientation of the NSP or NIK1 fusions (N-terminus or C-terminus of YFP; Figure 1a). These results confirmed that NSP interacts with NIK *in vivo*, but they also demonstrated that the detection of NIK-NSP complex formation *in planta* clearly depends on the saturation of the nuclear import machinery by high expression of NSP, which is limited when driven by the BiFC vectors. Therefore, the efficiency of detection of NSP-NIK interactions *in planta* by transient expression of NSP is extremely dependent on the opportunistic low concentration of NSP in the cell periphery, which very often is below the level of detection.

The hyperactive AtNIK1 mutant T474D bypasses NSP inhibition from tomato-infecting begomoviruses

Because of the low detection level of NSP interactions with plasma membrane proteins in transient expression assays, we assayed whether NSP from a tomato-infecting begomovirus interacts with the kinase domain of NIK from Arabidopsis through a yeast two-hybrid assay, which has been shown to efficiently detect interactions between host and begomovirus proteins (Carvalho *et al.*, 2008b; Florentino *et al.*, 2006; Fontes *et al.*, 2004; Mariano *et al.*, 2004). We showed that, similar to the NSP from the Arabidopsis-infecting begomovirus CaLCuV (*Cabbage leaf curly virus*), which interacts with the NIK immune receptors in yeast and *in planta* (Fontes *et al.*, 2004; Figure 1a), NSP from the tomato-infecting begomovirus ToYSV (*Tomato yellow spot virus*) interacted stably with the kinase domain of NIK from Arabidopsis in yeast (Figure 1b). Yeast transformed with the empty vector (pAD-GAL4) and BD-NIK was used as a negative control, and yeast co-transformed with BD-NIK and AD-NSPCaLCuV was used as a positive control (Fontes *et al.*, 2004). These interactions were further confirmed by monitoring β-galactosidase activity in yeast protein extracts (Figure 1c). Replacing T474 with aspartate did not prevent NSP binding (Figure 1b) but impaired the NSP-mediated inactivation of kinase activity (Figure 1d). These results suggest that the hyperactive NIK T474D mutant is a more effective target for engineering resistance against begomovirus.

Activation of the NIK-mediated signalling pathway triggers a typical response to begomovirus infection

We prepared tomato plants expressing different amounts of T474D (AtNIK1 mutant), which exhibit enhanced accumulation of the protein (Figure S2). In the first generation, some transgenic lines displayed shorter roots and stunted growth compared to wild type, but this phenotype did not persist over the subsequent generations. In fact, the development, overall physiological performance and horticultural traits of T474D-2-, T474D-5- and T474D-6-overexpressing lines were similar to those of wild-type plants and AtNIK1-expressing transgenic lines (NIK1-4; 15) for more than three generations (from R1 to R3) under normal greenhouse conditions. During the vegetative phase, the transgenic lines and wild-type control displayed similar plant height and biomass accumulation, as measured by shoot and root dry weight (Figures S3a–d). The net CO_2 assimilation rate (A), transpiration rate (E), stomatal conductance to water vapour (g_s) ration and internal to ambient CO_2 concentration ratio (C_i/C_a) of fully expanded leaves did not differ significantly among the transgenic lines and wild-type control (Figure S3e–h). Fully ripened tomatoes were harvested and analysed for colour, morphology, total soluble solids (brix) and nutritional quality (Figure S4). The ripe fruits of the transgenic lines were bright red (Figure S4a) and displayed an overall shape (Figure S4a), colour (Figure S4d), size (Figure S4e) and nutritional value (Figure S4c, f, g) similar to those of the wild-type control. The fruit yield (Figure S4b, i) and the overall development of the reproductive phase (Figure S4h, i) of the transgenic lines were similar to those of wild-type plants grown under normal greenhouse conditions.

To examine whether the virus infection alone triggered NIK-mediated defence signalling, the transgenic lines T474D-6 and NIK1-4 were challenged with infectious clones of the begomovirus ToYSV. Using RNA deep sequencing, we compared the virus-induced and NIK1 or T474D mutant transcriptomes. The hierarchical clustering via the multiscale bootstrap resampling method was employed to obtain clusters from normalized treatments data sets (Figure 2a). These global comparisons of the expressed sequences among the mock-treated and infected wild type (WT), NIK and T474D lines showed that the transcriptomes of the infected wild-type and mock-inoculated T474D lines were more closely related, as these samples clustered together. These transcriptomes differed greatly from the NIK mock-inoculated transcriptome, confirming that the gain-of-function T474D mutant may be activated in a constitutive manner that allows it to support a sustained NIK-mediated response. In addition, a sustained NIK-mediated response may lead to a 'priming' state that further enhances the response to begomovirus infection in T474D- and NIK-overexpressing leaves; the virus-induced transcriptomes of these samples cluster together and differ from the T474D mock-inoculated transcriptome (Figure 2a). The values of the approximately unbiased *P*-value (au) and the bootstrap probability (bp) were significant using a threshold of 0.05. Therefore, this analysis clearly uncovered a strong similarity between the general gene expression profile of the mock T474D and infected WT plants, suggesting that activation of the NIK-mediated signalling pathway in tomato triggers a typical response to begomovirus infection similar to that in Arabidopsis (Zorzatto *et al.*, 2015). Consistent with this finding, upon trimming the mock T474D–mock WT differentially expressed (DE) genes off of all treatments, the effect of viral infection seemed to be titrated off, and each T474D mock-, NIK mock- and WT mock-inoculated treatment grouped together with the infected counterpart (Figure 2b). Taken together, these results suggest that the gain-of-function mutant T474D can sustain an activated NIK-mediated antiviral response in the absence of the virus and that the activation of the NIK-mediated signalling pathway triggers a typical response to begomovirus infection. However, the T474D-induced infection response represents only a subset of the transgenic response because a residual effect of the transgene promoted the separation of the genotypes in the cluster analysis.

Constitutive activation of AtNIK (T474D) in tomato plants causes a general down-regulation of translation machinery-related genes and impairs translation

To determine the global gene expression variation of the infected WT and the mock-inoculated overexpressing NIK and T474D tomato plants, we analysed the following combinations: infected WT–mock WT, mock NIK-OX–mock WT and mock T474D–mock WT, using the differential gene expression (DGE) methods edgeR/TMM, edgeR/TC, DESeq and baySeq. The differentially expressed (DE) genes were stored using SQL tables at the PostgreSQL relational database (http://inctipp.bioagro.ufv.br/tomatodb/), which listed the corresponding $\log_2$FC (fold change) and *P*-value corrected by FDR (q-value) for all DE genes. We performed a gene enrichment analysis using the GSEA methods based on biological process from the GO data. Many enriched categories were found using *P*-value cut-off of <0.05 (http://tomatodb.inctipp.ufv.br). Because of the poor annotation of the tomato genome regarding some GO categories, we changed the *P*-value cut-off to <0.01 and only accepted the GO categories that had been labelled by at least three DGE methods (Table S1). A strong bias arose from some poorly annotated GO categories in the enrichment analysis, which led to the recognition of some significant groups in spite of their very low number of genes (*P*-value <0.01). Thus, we only

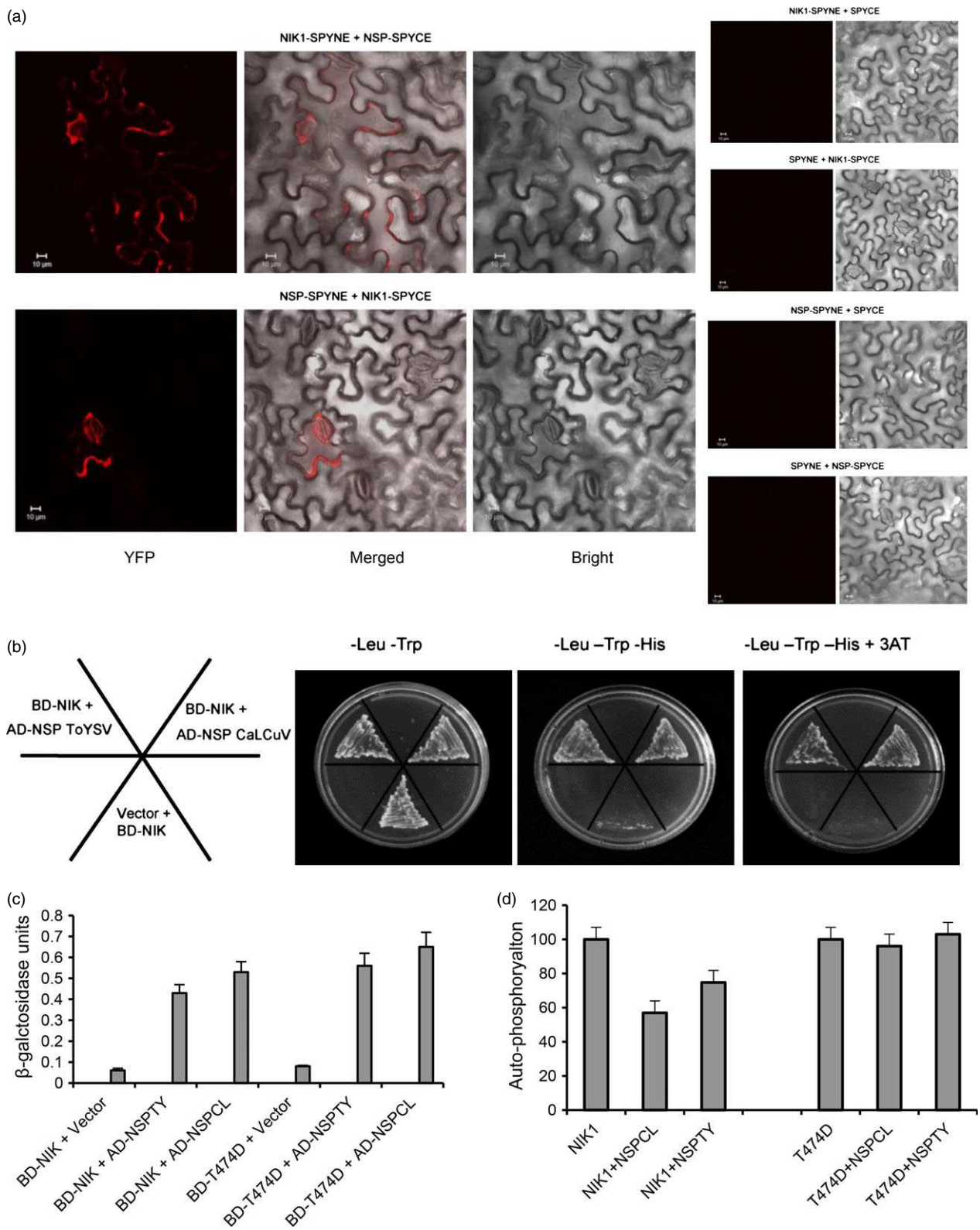

considered the groups with more than three genes (Table S1). The enriched categories for the contrast mock T474D–mock WT, which included the highest number of enriched GO categories, are shown in Figure 2. Among all the analysed combinations, the enriched category GO:0006412 (translation) from the mock T474D–mock WT combination displayed the most significant *P*-value (average *P*-value 4.69e-07; Table S1). This category is represented by components of the translational machinery,

Figure 1 T474D, a hyperactive AtNIK1 mutant, bypasses NSP inhibition and yet binds to ToYSV NSP. (a) *In vivo* interaction between NSP from CaLCuV and AtNIK1 by BiFC analysis. Fluorescence (YFP), bright and merged confocal images were taken of epidermal cells of tobacco leaves co-expressing NIK1-YFPC (NIK1-SPYCE) +NSP-YFPN (NSP-SPYNE) or NIK1YFPN (NIK1-SPYNE) + NSP-YFPC (NSP-SPYCE) fusion proteins in the presence of HC-Pro suppressor, 2 h after agro-infiltration with the indicated DNA constructs. Negative controls are shown on the right. Scale bars = 10 μm. (b) and (c) Interactions of ToYSV NSP with AtNIK1 and T474D. NSPs from CaLCuV (NSPCL, control) and ToYSV (NSPTY) were expressed in yeast as GAL4 activation domain (AD) fusions (AD-NSP ToYSV and AD-NSP CaLCuV), and the kinase domains of AtNIK1 (NIK) and T474D were expressed as GAL4 binding domain (BD) fusions (BD-NIK). Interactions between the tested proteins were examined by monitoring His prototrophy (b) and confirmed by measuring the activity (mean ± SD, $n = 3$) of the β-galactosidase reporter enzyme corresponding to the second reporter gene β-Gal (c). Error bars represent the confidence interval ($\alpha = 0.05$) of three technical replicates. (d) ToYSV NSP inhibits AtNIK1 autophosphorylation, but does not suppress T474D kinase activity. The kinase domain of AtNIK1 (NIK1) or T474D was expressed as a GST fusion and incubated with [γ-32P]ATP in the presence or absence of GST-NSP. Phosphorylated proteins were quantified by counting the scintillation of the excised protein bands. Autophosphorylation activity in the presence of NSP was expressed as the percentage of the total activity of NIK1 or T474D alone. Error bars represent the confidence interval ($\alpha = 0.05$) of three technical replicates from two independent experiments.

including ribosomal genes and other components of protein synthesis, such as translational initiation and elongation factors and molecular chaperones. To determine whether down-regulation of the translation machinery-related genes directly resulted from T474D expression, we plotted all the annotated genes attributed to GO:0006412 (translation) in a smear-plot as red dots (Figure S5). In the T474D mock–WT mock combination, the translation-related genes (red dots) tended to be down-regulated, because their log2FC values were clearly concentrated below zero. In contrast, this trend was not shared by the down-regulated GO:0006629: lipid metabolic process-enriched category in the mock T474D–mock WT combination; these genes were highly dispersed without any tendency for up- or down-regulated profiles (Figure S5, see red dots). These results indicate that merging the DGE data as the average of at least three DGE methods may have underestimated the number of translation-related DE genes in the T474D mock–WT mock combination. Constitutive activation of AtNIK1 in Arabidopsis has also been shown to promote the down-regulation of translation-related genes, which is reflected by the suppression of global translation (Zorzatto *et al.*, 2015).

To confirm that protein synthesis was impaired by the constitutive activation of AtNIK in the T474D tomato lines, we labelled leaf proteins *in vivo* with [^{35}S]Met in control plants and T474D overexpression lines (Figure 3a). There was a significant decrease (25% in T474D-5, 22.5% in T474D-6 and 19.6% in T474D-2; $P < 0.05$) in the amount of newly synthesized protein in T474D-overexpressing leaves compared with the amounts found in wild-type and NIK-overexpressing leaves. We observed a slight variation in the T474D-mediated inhibition of translation during development, as the reduction of translation was 18.1% (T474D-2), 16.8% (T474D-5) and 15.5% (T474D-6) when the incorporation of [^{35}S]Met into total proteins was measured in 28-day-old leaves (Figure 3b). Our data indicated that the gain-of-function mutant T474D from Arabidopsis functions similarly in tomato plants as it causes a general down-regulation of translation machinery-related genes and affects translation in transgenic tomato lines. This suppression of translation might underlie at least part of the molecular mechanism involved in NIK-mediated antiviral defences.

Constitutive activation of NIK confers broad-spectrum tolerance to tomato-infecting begomoviruses

We next examined whether the constitutive activation of NIK was effective at controlling begomovirus infection. To this end, four independent T474D-overexpressing transgenic lines (T474D-9, T474D-6, T474D-5 and T47D-2), a wild-type (untransformed) line and the NIK-overexpressing lines NIK1-4 and NIK1-6 (Carvalho *et al.*, 2008c) were inoculated with tandemly repeated ToYSV DNA-A and DNA-B (Andrade *et al.*, 2006) using biolistic delivery, and the plants were assayed for symptoms of infection and the accumulation of viral DNA, as detected by PCR and qPCR. The wild-type plants displayed typical symptoms of ToYSV infection, such as leaf curling and yellow spots all over the leaves (>10 spots/cm^2; Figure 4a). Consistent with a previous observation (Carvalho *et al.*, 2008c), the NIK-overexpressing line NIK1-4 displayed attenuated symptoms (less accentuated leaf distortion and a lower number of yellow spots per leaf area, <6 spots/cm^2). The symptoms in the T474D-overexpressing lines, however, were even more attenuated, with few spots per leaf area (varying among the lines) and no visible leaf curling (see T474D-2 and T474D-5 lines, Figure 4a, b). The T474D-6 transgenic line displayed typical tolerance to begomoviruses, as it did not develop symptoms (Figure 4a, d), but we detected viral DNA accumulation in both inoculated and systemically infected leaves (Figure 4e). The symptomless ToYSV infections of the T474D-6 line were associated with a delayed course of infection (Figure 4f), a lower rate of infection (DPI50, days postinoculation to infect 50% of plants; Figure 4g), and a lower accumulation of viral DNA in the systemically infected leaves, as shown by qPCR (Figure 4h).

Likewise, in the T474D-2 and T474D-5 lines, the progress and rate of infection were delayed compared with those of the wild-type control lines and the NIK1-overexpressing lines (Figure 4f, g). In the case of ToYSV, which showed high levels of accumulation in all samples analysed, both the T474D-2 and T474D-6 lines displayed lower viral DNA accumulation levels in the systemically infected leaves, although the high dispersion of the data among the samples prevented us from ascertaining the statistical significance of these findings (Figure 4h). Collectively, these results indicate that the T474D-overexpressing lines are more tolerant to ToYSV infection as compared to AtNIK1-overexpressing lines and wild-type lines.

Tomatoes are usually infected by a variety of rapidly evolving species of tomato-infecting begomoviruses and engineering broad-spectrum resistance to these viruses in crops constitutes a relevant trait to achieve durable resistance against begomoviruses. These transgenic lines were also challenged with the tomato-infecting begomovirus ToSRV (*Tomato severe rugose virus*), which displays a highly divergent genomic sequence from ToYSV sequence (Albuquerque *et al.*, 2012). ToSRV infection caused severe leaf distortion in wild-type leaves but not in the T474D-6 overexpressing line (Figure 5a). In these T474D-overexpressing lines, the viral DNA accumulation in the systemic leaves from ToSRV infections was significantly lower at 14 and 21 DPI ($P < 0.05$; Figure 5b, c). These results indicate that the ectopic

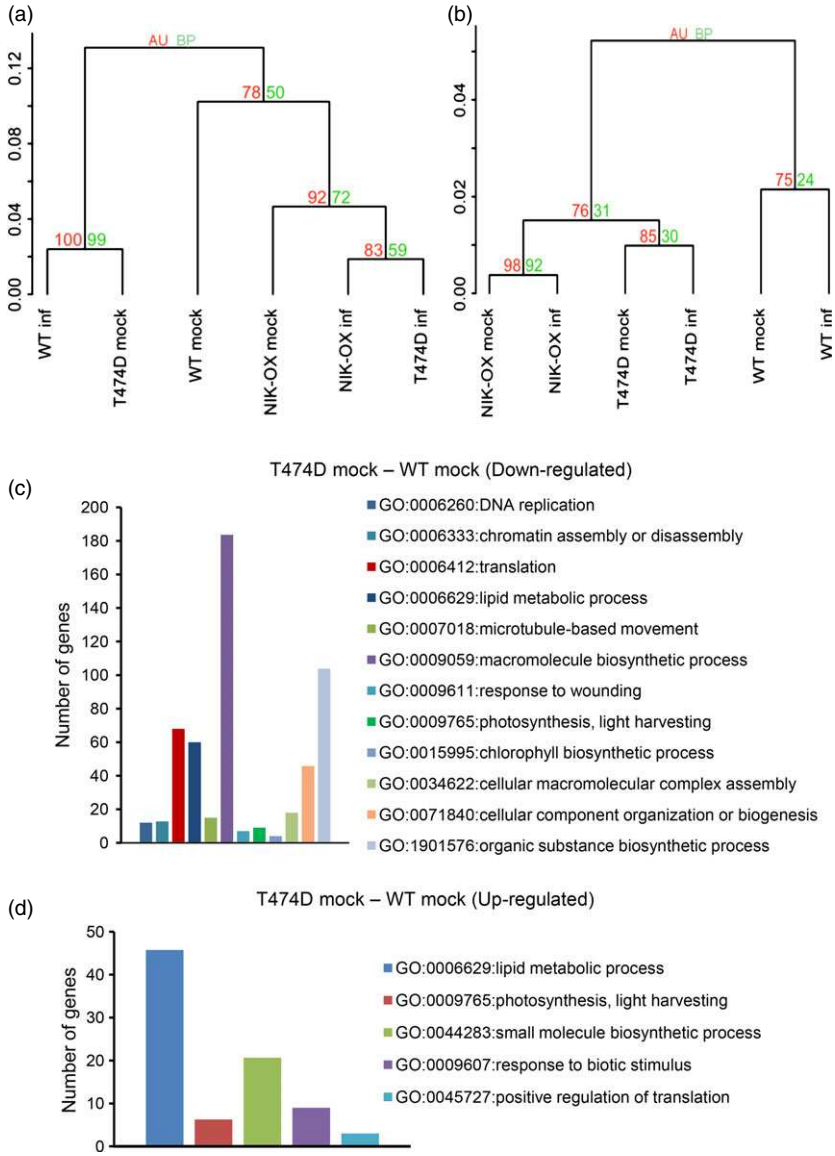

Figure 2 Transcriptomic analyses of mock-inoculated and infected (inf) T474D, NIK-OX and wild-type lines (a) Mock-inoculated T474D-overexpressing lines display a constitutive infected wild-type (WT) transcriptome. Clustering analysis was performed using the R package pvclust (hierarchical clustering with *P*-values via multiscale bootstrap resampling) using the TMM normalization method and the Ward agglomerative clustering method. The dendrogram provides two types of *P*-values: AU (approximately unbiased – red, from multiscale bootstrap resampling) and BP (bootstrap probability – green, normal bootstrap resampling). The AU *P*-value comes from multiscale bootstrap resampling, and the BP value represents normal bootstrap resampling. These *P*-values were calculated by Multiscale Bootstrap Resampling using the R-cran package pvclust with a cut-off of 0.05. These *P*-values show the significance of the proximity of each GE experiment profile. NIK-OX indicates NIK-overexpressing lines. (b) Elimination of the mock T474D–mock WT DE genes from the raw data minimizes the gene expression variation as a result of virus infection. The hierarchical clustering of the gene expression (GE) data was performed as described in Figure 2, except that the DE genes of mock T474D–mock WT were removed from the raw data from all treatments prior to the clustering analysis. The red numbers indicate unbiased *P*-values (au), and the green ones indicate bootstrap probabilities. (c) and (d) Bar graphs of the enriched down- (c) and up-regulated (d) categories based on biological process from the gene ontology (GO) database. Using at least four DGE methods, the enriched GO categories were determined by at least three DGE methods and included more than three genes (Table S1).

expression of T474D in tomato confers tolerance to heterologous species of tomato-infecting begomoviruses, which are phylogenetically separated within the two major groups of begomoviruses found in Brazil (Albuquerque *et al.*, 2012). The performance of the T474D-overexpressing lines upon begomovirus infection further confirmed that the T474D mutant protein could mount a sustained NIK-mediated antiviral defence in the absence of viral infection. The constitutive activation of T474D and its ability to bypass viral NSP inhibition likely account for the tolerance to begomovirus infection displayed by the transgenic lines.

Begomovirus infection does not affect resistance-related proteins and defence-related genes in the T474D-overexpressing lines

NIK belongs to the LRRII-RLK subfamily and shares high sequence conservation and a similar receptor configuration with the

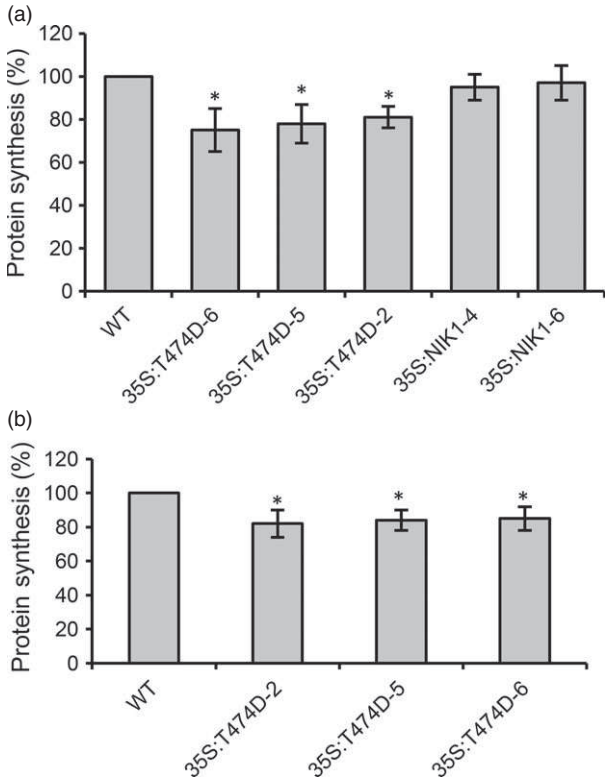

Figure 3 Ectopic expression of the T474 mutant receptor down-regulates global protein synthesis in leaves of 10 days (a) old and 28 days old (b) tomato plants. Equal fresh weights of tomato leaves (300 mg) were incubated with 50 μg/mL chloramphenicol and 20 μCi of [35S]methionine for 3 h at room temperature. Incorporation of [35S]Met into protein was measured in the TCA-precipitated total protein (mean ± SD, $n = 3$, $P < 0.05$) from wild-type and T474D transgenic lines. Asterisks indicate significant differences from the wild-type control ($P < 0.05$, Student's *t*-test).

well-characterized PAMP recognition co-receptor BRI1-associated receptor kinase 1 (BAK1; Sakamoto *et al.*, 2012; Shiu and Bleecker, 2001). To understand whether the pre-activation of the NIK-mediated antiviral response in the T474D-expressing lines would prime typical BAK1-mediated defence responses, such as PTI or SA signalling marker genes, in response to geminivirus infection, we compared the transcriptome changes in infected WT–mock WT vs infected T474D–mock T474D. We detected eight resistance protein-related genes (R genes) that were up-regulated by ToYSV infection in the T474D lines, but not in the WT lines (Table S2). However, significant gene enrichment was not detected for the R gene category, gene silencing category, or abiotic stress response gene category, which includes the immune system category and the response to SA marker genes, using the gene set enrichment analysis (GSEA) method (Table S3). We also compared the ToYSV infection-induced transcriptome of T474D lines with that recently described for the tolerant TYLCV-resistant tomato breeding line CLN2777A (Chen *et al.*, 2013). None of the 40 defence-related genes up-regulated in CLN2777A in response to TYLCV infection were T474D up-regulated genes, although we found some similarities when functional terms were used as the basis for comparison (Table S4). Collectively, these results indicate that typical viral defences, such as activation of SA signalling, gene silencing or the immune system, may not account for the resistant mechanism of the T474D lines. These lines may invoke an alternative mechanism for T474D protection against begomovirus infection.

The enhanced tolerance to begomovirus displayed by the T474D-expressing lines may be associated with the translational control branch of the NIK-mediated antiviral responses

The mock T474D–mock WT combination identified genes affected by T474D expression in the absence of virus infection. These data clearly showed that expression of the T474D mutant in tomato led to a significant down-regulation of translation-related genes and impaired translation, a phenotype associated with the translational control branch of the NIK-mediated antiviral signalling pathway, which has recently been described in Arabidopsis (Zorzatto *et al.*, 2015). Because T474D expression caused a global down-regulation of protein synthesis, we determined whether viral RNA translation was impaired in the T474D-expressing lines. We investigated whether we could detect viral RNA transcripts in actively translating polysome fractions that had been separated from nonpolysomal fractions on sucrose gradients (Figure S6). The polysomal fractions were prepared from infected leaves at 10 DPI, when the accumulation of viral mRNA in transgenic and wild-type leaves was similar (Figure 6b). We observed a significant reduction in the polysome loading of viral mRNA (coat protein mRNA) in systemically infected leaves of the T474D-6-overexpresing line compared to infected wild-type and NIK1-overexpressing leaves (Figure 6a, b). The accumulation of total virus transcripts in all infected lines was confirmed in our RNA sequencing data. These results indicated that the begomovirus was not capable of sustaining high levels of viral mRNA translation in the T474D-6-expressing lines, indicating that suppression of global protein synthesis may effectively protect plant cells against DNA viruses.

Discussion

Begomoviruses are one of the largest and most successful groups of plant viruses and cause severe diseases in major crops worldwide, inflicting significant economic losses in many dicotyledonous crops. The tomato-infecting begomoviruses have become an even greater threat to tomato cultivation due to the emergence of new species along with the recent introduction into South America of a new biotype of the whitefly vector Bemisia tabaci, which colonizes tomato plants with high efficiency (Albuquerque *et al.*, 2012; Castillo-Urquiza *et al.*, 2008; Galvão *et al.*, 2003). Current climate changes are expected to further alter the whitefly distribution across the globe, posing a serious threat to agriculture worldwide. Here, we described a novel strategy to control begomovirus infection. By constitutively activating NIK-mediated antiviral signalling, we succeeded in developing a tolerant tomato crop. Tomatoes are usually inflicted by diverse begomoviruses, making engineered tolerant/resistant lines even more difficult to develop. Importantly, the T474D-overexpressing tomato transgenic lines were tolerant to ToYSV and ToSRV, which display highly divergent genomic sequences and hence are phylogenetically separated within the two major groups of begomoviruses found in Brazil (Albuquerque *et al.*, 2012). The NIK-mediated strategy was also effective in conferring tolerance to CaLCuV in the model plant Arabidopsis (Zorzatto *et al.*, 2015). These observations indicate the potential of a sustained NIK-mediated defence pathway to confer broad-spectrum tolerance to begomoviruses in distinct plant species.

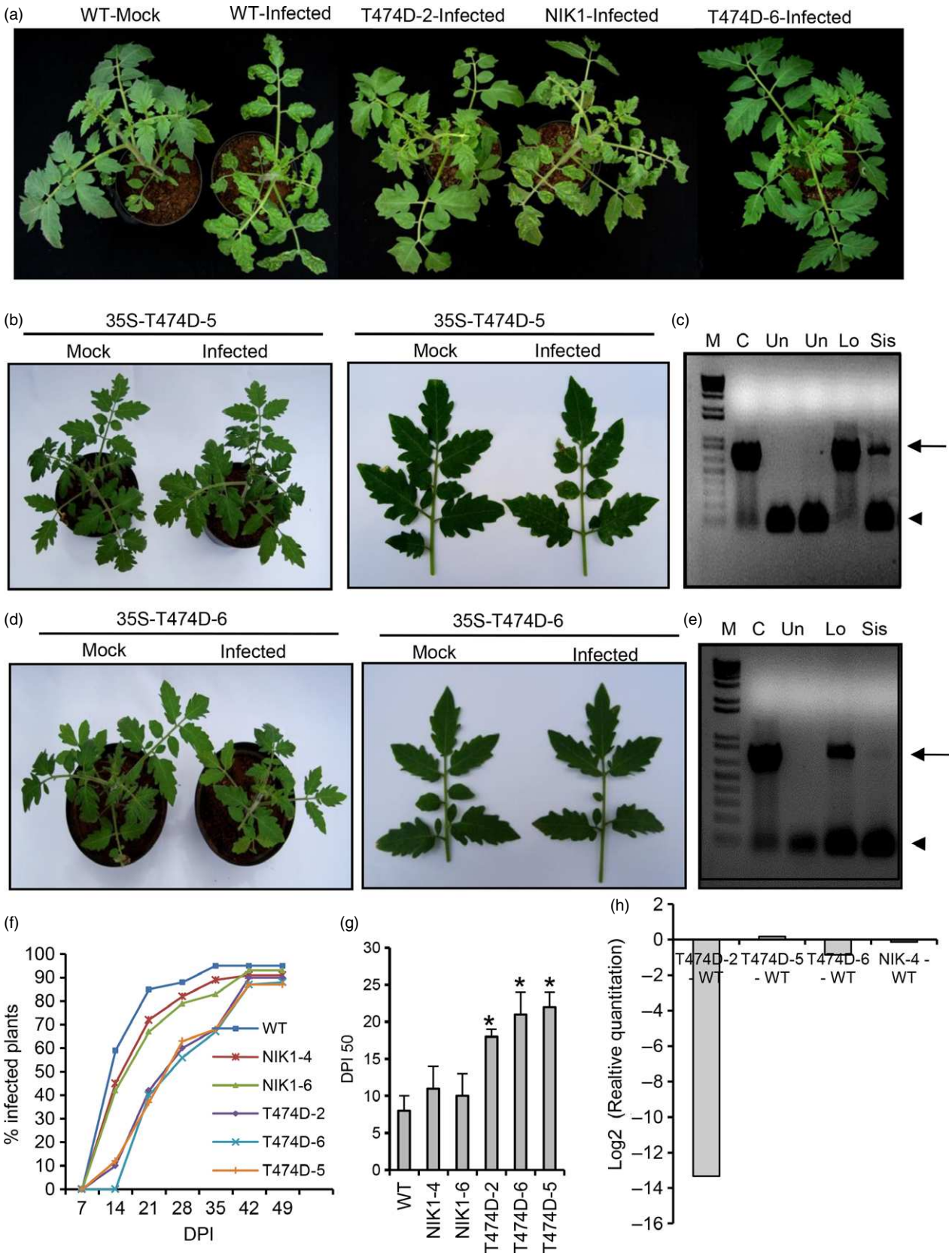

The current mechanistic model for the activation of the NIK-mediated antiviral signalling pathway holds that upon an unknown stimulus, the NIK LRR extracellular domain undergoes oligomerization with itself or another receptor, allowing the intracellular kinase domains to transphosphorylate and activate one another. The activation of NIK by phosphorylation on the

Figure 4 Ectopic expression of T474D in tomato confers tolerance to ToYSV infection. (a) Ectopic expression of T474D in tomato plants attenuates the development of symptoms upon ToYSV infection. Tandemly repeated ToYSV DNA-A and DNA-B sequences were introduced into the indicated lines by biolistic inoculation. Photographs were taken at 21 days postinoculation (DPI). (b) Symptoms associated with ToYSV infection in the 35S-T474D-5 line. Photographs were taken at 21 DPI. (c) Viral DNA accumulation in the infected leaves of the T474-5 line. Total DNA was isolated from infected plants at 21 DPI, and PCR was performed with viral DNA-B-specific primers and actin-specific primers (as an internal control) in the same reaction. Lo indicates inoculated and Sys denotes systemic leaves. 'Un' indicates mock-inoculated leaves. The gel shows representative samples of WT and the 35S::T474D-5 transgenic line. The upper band (1.2 kb, arrow) is the amplified genomic fragment from actin, and the lower band (0.5 kb, arrowhead) is the viral DNA fragment. (d) and (e) The line 35S-T474D-6 displayed tolerance to ToYSV infection. The T474D-6 line was infected with ToYSV, and photographs were taken at 21 DPI. Viral DNA accumulation was detected by PCR in inoculated ('Lo') and systemic ('Sys') leaves. (f) The course of infection was delayed in T474D lines. The indicated lines were infected with ToYSV by the biolistic method, and the course of infection was monitored by PCR amplification of viral DNA. In each experiment (three biological replicates), 20 plants of each line were inoculated. Values represent the percentage of systemically infected plants at different DPI. (g) Infection efficiency in T474D-overexpressing lines. The infection efficiency is expressed as the DPI required to infect 50% of the plants (mean ± SD of three replicates). Asterisks indicate significantly different means ($P < 0.05$, Student's *t*-test). (h) Viral DNA accumulation in T474D-overexpressing lines, as determined by quantitative PCR at 28 DPI. The fold variation (±SD, $n = 3$ biological replicates) is shown as log2-scaled copy units of the viral genome. Viral DNA accumulation was determined in systemic leaves at 28 DPI.

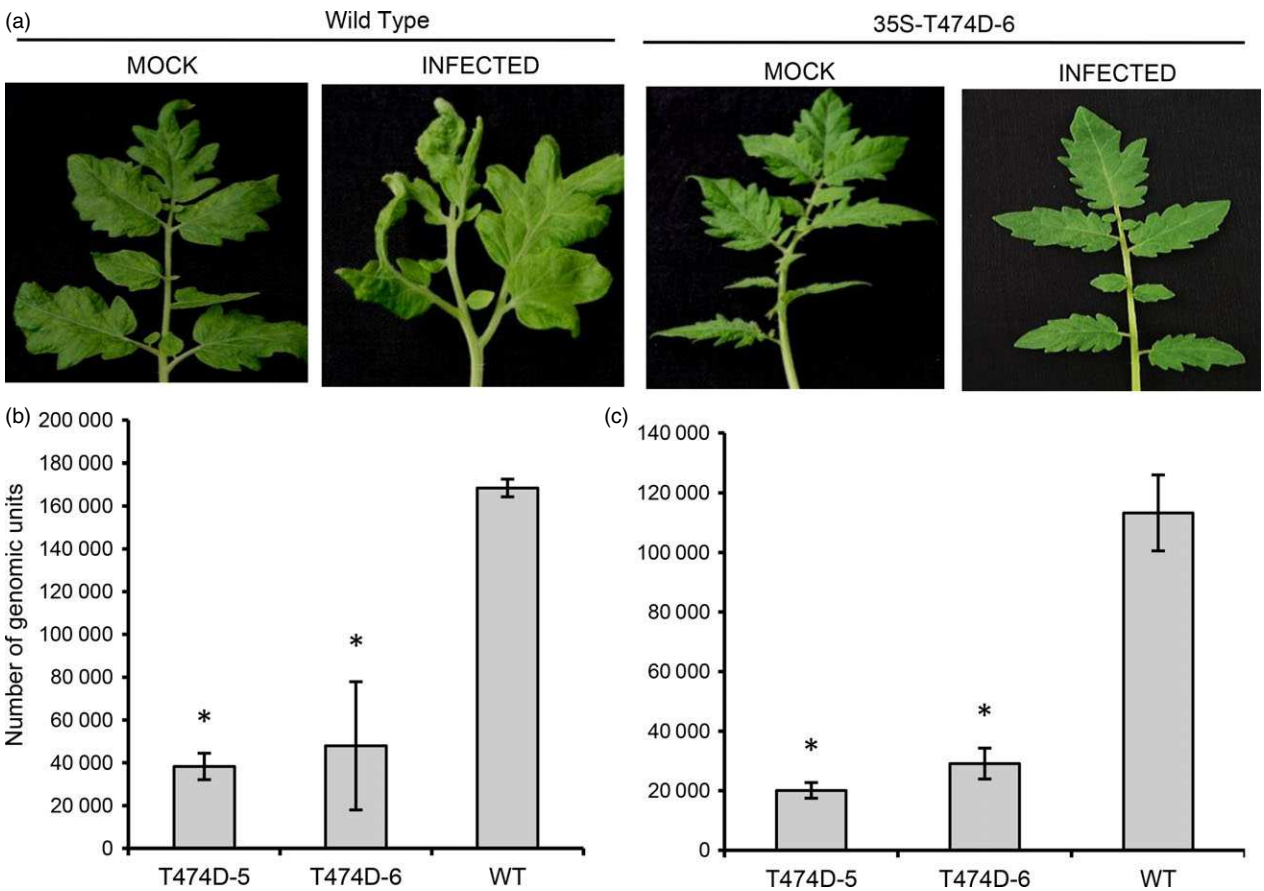

Figure 5 The T474D-6 overexpressing line is also tolerant to ToSRV infection. (a) Symptoms associated with ToSRV infection in the 35S-T474D-6 line. The T474D-6 line was infected with ToSRV, and photographs were taken at 21 DPI. (b) and (c) Viral DNA accumulation in the T474D-6- and T474-5-overexpressing lines at 14 DPI (b) and 28 DPI (c). Prior to performing real-time PCR, infected leaves were diagnosed by standard PCR. Subsequently, total DNA extracted from systemically infected leaves at 14 DPI (b) or 28 DPI (c) was used as a template for quantitative PCR using ToYSV DNA-A-specific primers. The fold variation (±SD, $n = 3$ biological replicates) is shown as copy units of the viral genome. The asterisks indicate significant differences with $P < 0.05$ according to a Student's *t*-test.

crucial threonine residue at position 474 leads to the regulated relocation of RPL10 to the nucleus where it interacts to LIMYB to fully down-regulate translation-related genes (Zorzatto *et al.*, 2015). Our current data add a number of relevant insights to the understanding of this layer of defence. First, a comparison between the transcriptomes induced by virus infection in wild-type lines and by ectopic expression of the T474D gain-of-function mutant in transgenic lines indicated that activation of the NIK-mediated signalling pathway triggers a typical response to virus infection. This interpretation is supported by the observation that mock-inoculated T474D-overexpressing lines showed a constitutively infected wild-type transcriptome (Figure 2a). Furthermore, the elimination of the mock T474D DE genes from the raw data of all treatments further indicates that the expression profile induced

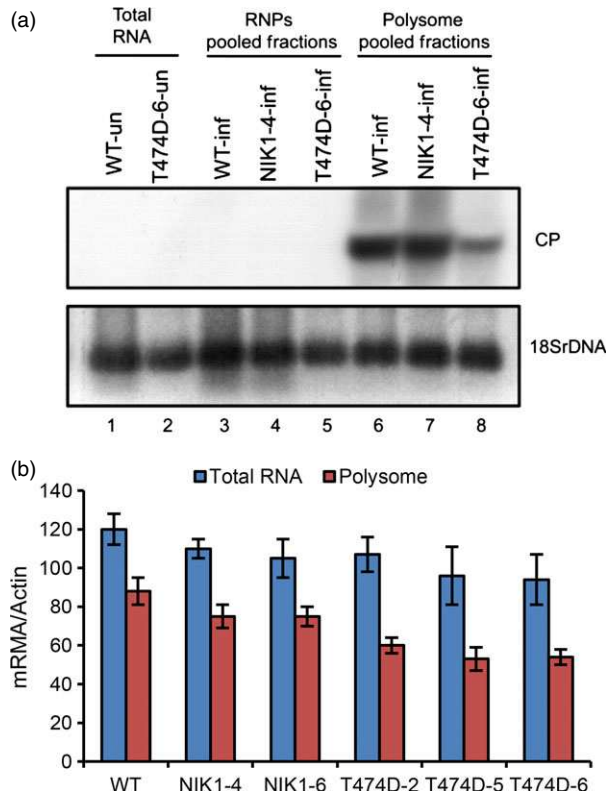

Figure 6 Polysome loading of viral mRNA is reduced in systemically infected leaves in the T47D-6-overexpressing lines. (a) Polysome loading of coat protein (CP) mRNA from ToYSV DNA-A in systemically infected leaves of WT, NIK-overexpressing and T47D-6-overexpressing lines. Polysomes from infected WT, NIK1-4-overexpressing and T474D-6-overexpressing lines were isolated from systemic leaves at 10 days postinoculation with tandem copies of DNA-A and DNA-B of ToYSV, as shown in Fig. S6. RNPs refer to a 40S-enriched fraction. Polysome-bound RNA from pooled fractions was extracted with phenol/chloroform/isoamyl alcohol, precipitated with isopropanol, blotted and probed with the coat protein DNA (CP) and 18S rDNA. The identity of the polysome-pooled fraction was confirmed by treatment with 25 mM EDTA prior to the sucrose gradient (data not shown), which releases the mRNA from the polysomes. (b) Quantitation of polysome-associated coat protein viral transcripts in T474D-overexpressing lines by qRT-PCR. Polysomes from infected WT, NIK1-4-overexpressing and T474D-6-overexpressing lines were isolated 10 days postinoculation with infectious ToYSV clones. Polysome-bound RNA from pooled fractions was extracted with phenol/chloroform/isoamyl alcohol, precipitated with isopropanol and quantified by qRT-PCR. Values were normalized to the expression of actin. Error bars represent SD from three measurements.

by the T474D mutant greatly mimics the response to viral infection, as the mock- and infection-induced transcriptomes from each genotype clustered together with high significance (Figure 2b). Second, our data are consistent with the notion that the gain-of-function mutant T474D can sustain an activated NIK-mediated antiviral response in the absence of the virus, further confirming that phosphorylation on Thr-474 is the crucial event that leads to the activation of the kinase. In fact, expression of the T474D mutant potentiated the NIK-mediated response, as it would be expected from expression of a constitutively activated defence receptor NIK. Accordingly, the ectopic expression of the T474D gain-of-function mutant was more effective against begomovirus infection than overexpression of the NIK defence receptor in the tomato transgenic lines.

The experiments presented here shed light on the response underlying NIK-mediated antiviral defences. We showed that constitutive activation of NIK in the T474D lines impaired global translation, and such activation might constitute an excellent strategy for fighting begomovirus infection in host cells. We have also demonstrated recently that constitutive activation of NIK1 and overexpression of LIMYB in Arabidopsis down-regulate translation machinery-related genes, suppress translation and confer tolerance to begomovirus infection (Zorzatto *et al.*, 2015). Because begomoviruses rely completely on the plant translation machinery and cannot circumvent host translational regulation, a global repression of translation is expected to significantly affect virus infection, as observed in the T474D-overexpressing lines. In fact, by directly assessing viral transcripts, we showed that the loading of coat protein mRNA into actively translating polysomes was significantly reduced in systemic infected leaves of T474D-overexpressing plants compared to WT and NIK1-overexpressing lines (Figure 6). This result indicates that the suppression of global protein synthesis may effectively protect plant cells against DNA viruses.

Based on our data, it is clear that the level of translational inhibition mediated by constitutive activation of NIK1 did not impact development in tomato under greenhouse conditions. In the first generation, however, some transgenic lines displayed shorter roots that regained normal biomass and growth in the subsequent generations. As a possible explanation for this phenotype, the T474D-mediated translation inhibition would have maintained the transgenic lines under a constant perception of stress, which, in turn, promoted acclimation to maintain normal growth under greenhouse conditions. We also found that T474D-mediated translation inhibition persisted in different developmental stages of the transgenic lines but to different extents. At later stages of development (28-day-old leaves), we observed a 7% reduction in the level of translation inhibition compared to that of seedlings. This difference in the efficiency of global translation inhibition mediated by ectopic expression of the T474D mutant receptor may reflect an adjustment of transgenic lines towards adaptation at later stages. However, it is very intriguing that ectopic expression of T474D did not impact tomato development despite 19–25% suppression of global translation at earlier stages of development. Therefore, the intrinsic capacity to withstand the deleterious effect from the suppression of global translation must be considered in attempts to transfer the T474D-mediated defence strategy to other agronomically relevant crops.

Experimental procedures (a detailed description of experimental procedures is provided as supporting information)

Tomato transformation and RNA sequencing experiment

The clone pK7F-NIK1T474D has been previously described (Santos *et al.*, 2009). It harbours a GFP gene fused in-frame after the last codon of the mutant cDNA T474D under the control of the CaMV 35S promoter. In the mutant cDNA T474D, the threonine residue at position 474 within the activation loop of NIK1 was mutated to an aspartate residue. Leaf discs from *in vitro*-grown tomato plants (*Solanum lycopersicum*, cultivar Moneymaker) were transformed with pK7F-NIK1T474D via

Agrobacterium-mediated plant transformation (strain LBA4404), as previously described (Carvalho *et al.*, 2008c). The transgenic lines T474D-2, T474D-5 and T474D-6 were selected for further analysis. We also used the previously described NIK1-overexpressing lines NIK1-4 and NIK1-6 (Carvalho *et al.*, 2008c) for infection assays and RNA-seq analysis. NIK1-4 and NIK1-6 lines harbour the Arabidopsis NIK cDNA fused to a GFP cDNA under the control of the CaMV 35S promoter. The transgenic and wild-type lines were infected at the six-leaf stage with ToYSV-[MG-Bi2], as described below in the infectivity assay. At 10 days postinoculation (dpi), total RNA was isolated using TRIzol for the RNA sequencing experiments. The Illumina RNA sequencing data were obtained using a Genome Analyzer in the Fasteris facilities. A systematic comparison in our tomato data set of five representative normalization methods with and without the correction factors for CG-content and gene length was performed using the Bioconductor packages edgeR (Robinson *et al.*, 2010), DESeq (Yang *et al.*, 2013), and EDASeq (Risso *et al.*, 2011). For differential gene expression (DGE) analysis, we subjected the normalized data provided by the counting table to the most common negative binomial methods present in R/Bioconductor software, such as edgeR (Robinson *et al.*, 2010), DESeq (Anders and Huber, 2010) and baySeq (Hardcastle and Krystyna, 2010). The RNA-seq data were submitted to NCBI-GEO, http://www.ncbi.nlm.nih.gov/geo/info/linking.html, accession number GSM932558.

Infectivity assays

The transgenic and wild-type lines were infected at the six-leaf stage with either ToYSV-[MG-Bi2] or ToSRV infectious clones by biolistic delivery. In each experiment, 20 plants of each line were inoculated with 2 μg of tandemly repeated DNA-A plus DNA-B per plant and grown in a greenhouse under natural light, 70% relative humidity and approximately equal day and night lengths. Viral DNA was quantified by qRT-PCR, and coat protein viral mRNA was quantified by qRT-PCR from polysome-associated RNA prepared from T474D, NIK1 and wild-type infected leaves at 10 dpi.

Acknowledgements

This research was financially supported through the following grants from Brazilian Government Agencies: CNPq grants 483659/2012-6, 573600/2008-2, 447578/2014-6 (to E.P.B.F.), FAPEMIG grant CBB-APQ-00070-09 (to E.P.B.F.). O.J.B.B. and D.C were supported by CAPES graduate fellowships; J.P.B.M. was supported by a CNPq graduate fellowship; M.D. and W.A.P. were supported by postdoctoral fellowships from CNPq; A.A.S. was the recipient of a postdoctoral fellowship from CAPES.

Conflict of interest

The authors declare no conflict of interest.

References

Albuquerque, L.C., Varsani, A., Fernandes, F.R., Pinheiro, B., Martin, D.P., de Tarso, O.F.P., Lemos, T.O. and Inoue-Nagata, A.K. (2012) Further characterization of tomato-infecting begomoviruses in Brazil. *Arch. Virol.* **157**, 747–752.

Anders, S. and Huber, W. (2010) Differential expression analysis for sequence count data. *Genome Biol.* **11**, R106.

Andrade, E.C., Manhani, G.G., Alfenas, P.F., Calegario, R.F., Fontes, E.P.B. and Zerbini, F.M. (2006) Tomato yellow spot virus, a tomato-infecting begomovirus from Brazil with a closer relationship to viruses from Sida sp., forms pseudorecombinants with begomoviruses from tomato but not from Sida. *J. Gen. Virol.* **87**, 3687–3696.

Aragão, F.J. and Faria, J.C. (2009) First transgenic geminivirus-resistant plant in the field. *Nat. Biotechnol.* **27**, 1086–1088.

Carvalho, C.M., Machado, J.P.B., Zerbini, F.M. and Fontes, E.B.P. (2008a) NSP-Interacting GTPase: a cytosolic protein as cofactor for nuclear shuttle proteins. *Plant Signal. Behav.* **3**, 752–754.

Carvalho, C.M., Fontenelle, M.R., Florentino, L.H., Santos, A.A., Zerbini, F.M. and Fontes, E.P.B. (2008b) A novel nucleocytoplasmic traffic GTPase identified as a functional target of the bipartite geminivirus nuclear shuttle protein. *Plant J.* **55**, 869–880.

Carvalho, C.M., Santos, A.A., Pires, S.R., Rocha, C.S., Saraiva, D.I., Machado, J.P., Mattos, E.C., Fietto, L.G. and Fontes, E.P.B. (2008c) Regulated nuclear trafficking of rpL10A mediated by NIK1 represents a defense strategy of plant cells against virus. *PLoS Pathog.* **4**, e1000247.

Castillo-Urquiza, G.P., Beserra, J.E. Jr, Bruckner, F.P., Lima, A.T., Varsani, A., Alfenas-Zerbini, P. and Zerbini, F.M. (2008) Six novel begomoviruses infecting tomato and associated weeds in Southeastern Brazil. *Arch. Virol.* **153**, 1985–1989.

Chen, T., Lv, Y., Zhao, T., Li, N., Yang, Y., Yu, W., He, X., Liu, T. and Zhang, B. (2013) Comparative transcriptome profiling of a resistant vs. susceptible tomato (*Solanum lycopersicum*) cultivar in response to infection by tomato yellow leaf curl virus. *PLoS ONE*, **8**, e80816.

Day, A.G., Bejarano, E.R., Buck, K.W., Burrell, M. and Lichtenstein, C.P. (1991) Expression of an antisense viral gene in transgenic tobacco confers resistance to the DNA virus tomato golden mosaic virus. *Proc. Natl Acad. Sci. USA*, **88**, 6721–6725.

Florentino, L.H., Santos, A.A., Fontenelle, M.R., Pinheiro, G.L., Zerbini, F.M., Baracat-Pereira, M.C. and Fontes, E.P.B. (2006) A PERK-like receptor kinase interacts with the geminivirus nuclear shuttle protein and potentiates viral infection. *J. Virol.* **80**, 6648–6656.

Fontes, E.P.B., Santos, A.A., Luz, D.F., Waclawovsky, A.J. and Chory, J. (2004) The geminivirus NSP acts as virulence factor to suppress an innate transmembrane receptor kinase-mediated defense signaling. *Gene Dev.* **18**, 2545–2556.

Gafni, Y. and Epel, B.L. (2002) The role of host and viral proteins in intra- and intercellular trafficking of geminiviruses. *Physiol. Mol. Plant Pathol.* **60**, 231–241.

Galvão, R.M., Mariano, A.C., Luz, D.F., Alfenas, P.F., Andrade, E.C., Zerbini, F.M., Almeida, M.R. and Fontes, E.P.B. (2003) A naturally occurring recombinant DNA-A of a typical bipartite begomovirus does not require the cognate DNA-B to infect *Nicotiana benthamiana* systemically. *J. Gen. Virol.* **84**, 715–726.

Hardcastle, T.J. and Krystyna, A.K. (2010) baySeq: empirical Bayesian methods for identifying differential expression in sequence count data. *BMC Bioinformatics*, **11**, 422.

Hashmi, J.A., Zafar, Y., Arshad, M., Mansoor, S. and Asad, S. (2011) Engineering cotton (*Gossypium hirsutum* L.) for resistance to cotton leaf curl disease using viral truncated AC1 DNA sequences. *Virus Genes*, **42**, 286–296.

Hong, Y. and Stanley, J. (1996) Virus resistance in *Nicotiana benthamiana* conferred by African cassava mosaic virus replication-associated protein (AC1) transgene. *Mol. Plant Microbe Interact.* **9**, 219–225.

Kunik, T., Salomon, R., Zamir, D., Navot, N., Zeidan, M., Michelson, I., Gafni, Y. and Czosnek, H. (1994) Transgenic tomato plants expressing the tomato yellow leaf curl virus capsid protein are resistant to the virus. *Biotechnology*, **12**, 500–504.

Lin, C.Y., Tsai, W.S., Ku, H.M. and Jan, F.J. (2012) Evaluation of DNA fragments covering the entire genome of a monopartite *begomovirus* for induction of viral resistance in transgenic plants via gene silencing. *Transgenic Res.* **21**, 231–241.

Lucioli, A., Sallustio, D.E., Barboni, D., Berardi, A., Papacchioli, V., Tavazza, R. and Tavazza, M. (2008) A cautionary note on pathogen-derived sequences. *Nat. Biotechnol.* **26**, 617–619.

Mariano, A.C., Andrade, M.O., Santos, A.A., Carolino, S.M.B., Oliveira, M.L., Baracat-Pereira, M.C., Brommonshenkel, S.H. and Fontes, E.P.B. (2004)

Identification of a novel receptor- like protein kinase that interacts with a geminivirus nuclear shuttle protein. *Virology*, **318**, 24–31.

McGarry, R.C., Barron, Y.D., Carvalho, M.F., Hill, J.E., Gold, D., Cheung, E., Kraus, W.L. and Lazarowitz, S.G. (2003) A novel Arabidopsis acetyltransferase interacts with the geminivirus movement protein NSP. *Plant Cell*, **15**, 1605–1618.

Noris, E., Accotto, G.P., Tavazza, R., Brunetti, A., Crespi, S. and Tavazza, M. (1996) Resistance to tomato yellow leaf curl geminivirus in *Nicotiana benthamiana* plants transformed with a truncated viral C1 gene. *Virology*, **224**, 130–138.

Reyes, M.I., Nash, T.E., Dallas, M.M., Ascencio-Ibáñez, J.T. and Hanley-Bowdoin, L. (2013) Peptide aptamers that bind to geminivirus replication proteins confer a resistance phenotype to TYLCV and ToMoV infection in tomato. *J. Virol.* **87**, 9691–9706.

Risso, D., Schwartz, K., Sherlock, G. and Dudoit, S. (2011) GC-content normalization for RNA-Seq data. *BMC Bioinformatics*, **12**, 480.

Robinson, M.D., McCarthy, D.J. and Smyth, G.K. (2010) edgeR: a Bioconductor package for differential expression analysis of digital gene expression data. *Bioinformatics*, **26**, 139–140.

Rocha, C.S., Santos, A.A., Machado, J.P.B. and Fontes, E.P.B. (2008) The ribosomal protein L10/QM-like protein is a component of the NIK-mediated antiviral signaling. *Virology*, **380**, 165–169.

Rojas, M.R., Hagen, C., Lucas, W.J. and Gilbertson, R.L. (2005) Exploiting chinks in the plant's armor: evolution and emergence of geminiviruses. *Annu. Rev. Phytopathol.*, **43**, 361–394.

Sakamoto, T., Deguchi, M., Brustolini, O.J.B., Santos, A.A., Silva, F.F. and Fontes, E.P.B. (2012) The tomato RLK superfamily: phylogeny and functional predictions about the role of the LRRII-RLK subfamily in antiviral defense. *BMC Plant Biol.* **12**, 229.

Sanderfoot, A.A. and Lazarowitz, S.G. (1995) Cooperation in viral movement: the geminivirus BL1 movement protein interacts with BR1 and redirects it from the nucleus to the cell periphery. *Plant Cell*, **7**, 1185–1194.

Sanderfoot, A.A. and Lazarowitz, S.G. (1996) Getting it together in plant virus movement: cooperative interactions between bipartite geminivirus movement proteins. *Trends Cell Biol.* **6**, 353–358.

Sanderfoot, A.A., Ingham, D.J. and Lazarowitz, S.G. (1996) A viral movement protein as a nuclear shuttle: the geminivirus BR1 movement protein contains domains essential for interaction with BL1 and nuclear localization. *Plant Physiol.* **110**, 23–33.

Santos, A.A., Carvalho, C.M., Florentino, L.H., Ramos, H.J. and Fontes, E.P.B. (2009) Conserved threonine residues within the A-Loop of the receptor NIK differentially regulate the Kinase function required for antiviral signaling. *PLoS ONE*, **4**, e5781.

Santos, A.A., Lopes, K.V.G., Apfta, J.A.C. and Fontes, E.P.B. (2010) NSP-interacting kinase, NIK: a transducer of plant defence signalling. *J. Exp. Bot.* **61**, 3839–3845.

Shiu, S.H. and Bleecker, A.B. (2001) Receptor-like kinases from Arabidopsis form a monophyletic gene family related to animal receptor kinases. *Proc. Natl Acad. Sci. USA*, **98**, 10763–10768.

Stanley, J., Frischmuth, T. and Ellwood, S. (1991) Defective viral DNA ameliorates symptoms of geminivirus infection in transgenic plants. *Proc. Natl Acad. Sci. USA*, **87**, 6291–6295.

Sunitha, S., Marian, D., Hohn, B. and Veluthambi, K. (2011) Antibegomoviral activity of the agrobacterial virulence protein VirE2. *Virus Genes*, **43**, 445–453.

Ward, B.M. and Lazarowitz, S.G. (1999) Nuclear export in plants: use of geminivirus movement proteins for a cell-based export assay. *Plant Cell*, **11**, 1267–1276.

Yang, E.-W., Girke, T. and Jiang, T. (2013) Differential gene expression analysis using coexpression and RNA-Seq data. *Bioinformatics*, **29**, 2153–2161.

Zhang, S.C., Wege, C. and Jeske, H. (2001) Movement proteins (BC1 and BV1) of Abutilon mosaic geminivirus are cotransported in and between cells of sink but not of source leaves as detected by green fluorescent protein tagging. *Virology*, **290**, 249–260.

Zorzatto, C., Machado, J.P.B., Lopes, K.V.G., Nascimento, K.J.T., Pereira, W.A., Brustolini, O.J.B., Reis, P.A.B., Calil, I.P., Deguchi, M., Martins, G.S., Gouveia, B.C., Loriato, V.A.P., Silva, M.A.C., Silva, F.F., Santos, A.A., Chory, J. and Fontes, E.P.B. (2015) NIK-mediated translation suppression functions as a plant antiviral immunity mechanism. *Nature*, doi: 10.1038/nature14171.

Supporting information

Additional Supporting information may be found in the online version of this article:

Data S1 Supporting Experimental Procedures – detailed description of experimental procedures.
Figure S1 NSP from CaLCuV and ToYSV concentrates in the nucleus when ectopically expressed in N. benthamiana leaves.
Figure S2 Overexpression of T474D mutant receptor in tomato leaves.
Figure S3 Characterization of the T474D-overexpressing lines during the vegetative phase.
Figure S4 Fruit quality and yield of the T474D-overexpressing lines.
Figure S5 Representation of the translational machinery-related genes in the down-regulated changes.
Figure S6 Isolation of polysomal fractions from tomato seedlings.
Table S1 Enriched biological process categories from the GO database using the GSEA method.
Table S2 Resistance protein-related genes differentially expressed in infected T474D (infected T474D-mock T474D).
Table S3 Gene Enrichment Analysis.
Table S4 Functional overlap of DE defence-related genes up-regulated in CLN2777 (resistant) by 3, 5, and 7 dpi and in T474D infected by 10 dpi.

Supporting information- Experimental Procedures

Sustained NIK-mediated antiviral signaling confers broad-spectrum tolerance to begomoviruses in cultivated plants

Otávio J.B.Brustolini [a,b*], Joao Paulo B. Machado[a,b*], Jorge A. Condori-Apfata [b], Daniela Coco [a,b], Michihito Deguchi[a,b], Virgílio A. P. Loriato[a,b], Welison A. Pereira, Poliana Alfenas-Zerbini [b], Francisco M. Zerbini [b], Alice K. Inoue-Nagata[b,d], Anesia A. Santos [a,b], Joanne Chory[e], Fabyano F. Silva[c], Elizabeth P.B. Fontes [a,b,&]

[a]Departamento de Bioquímica e Biologia Molecular [b]National Institute of Science and Technology in Plant-Pest Interactions, Bioagro, [c]Departamento de Zootecnia, Universidade Federal de Viçosa, 36570.000, Viçosa, MG, Brazil. [d]Embrapa Vegetables, Brasília, DF 70359-970, Brazil. [e]Howard Hughes Medical Institute and Plant Biology Laboratory, The Salk Institute for Biological Studies, La Jolla, California 92037, USA

[*]These authors contributed equally to this work

[&]For correspondence:

Elizabeth B. P. Fontes, Departamento de Bioquímica e Biologia Molecular/Bioagro, National Institute of Science and Technology in Plant-Pest Interactions, Universidade Federal de Viçosa, 36570.000, Viçosa, MG, Brazil, pone +55 31 3899 2948 [&]email bbfontes@ufv.br

Yeast strain and two-hybrid assays. The NSP ORF was amplified from ToYSV DNA-B using PCR with the appropriate linkers and introduced through recombination into the entry vector pDONR201 to generate pDON-NSP-ToYSV, also designated as pUFV1323; the NSP ORF was subsequently transferred to the pDEST22 vector. The resulting clone pAD-NSP-ToYSV, also designated pUFV1370 or AD-NSPTY (Figure 1B), contained the GAL4 DNA-activating domain fused to the NSP-ToYSV sequence. Sequences encoding the mutant (T474D) kinase domain of NIK were transferred from pDON-T474D (Santos et al., 2009) to pDEST32 to yield pBD-T474D or BD-T474D (Figure 1B). The clones pAD-NSP-CaLCuV (AD-NSPCL, in Figure 1B) and pBD-KDNIK (BD-NIK in Figure 1B) have been previously described (Fontes et al., 2004).

The yeast two-hybrid assays were performed as previously described (Florentino et al., 2006). The yeast reporter strain AH109 (MATa, Trp1-901, leu2-3, 112, ura3-52, his3-200, gal4Δ, LYS2::$GAL1_{UAS}$-$GAL1_{TATA}$-HIS3, MEL1 $GAL2_{UAS}$-GAL_{TATA}::MEL_{UAS}-$MEL1_{TATA}$-lacZ,) was cotransformed with AD-NSP fusions and pBD-NIK1 or pBD-T474D. The interactions were monitored by the ability of the reporter strain to grow on media lacking leucine, tryptophan, uracil and histidine, but supplemented with 25 mM 3-aminotriazole for 7 days at 30 ^{0}C. The interactions were further confirmed by measuring β-galactosidase activity in yeast extracts using o-nitrophenyl β-D-galactopyranoside substrate, as described previously (Uhrig et al., 1999).

Phosphorylation assay. To create plasmids for E. coli expression, the mutant NIK1 C-terminal kinase domain or intact NIK (KD, encoding amino acids 298–638) were amplified from the appropriate mutated clone, introduced by recombination into the entry vector pDONR201 and then transferred to the bacterial expression vector pDEST15, resulting in GST fused to mutant kinase domains, designated pGST-KDNIK1T474A or pGST-KDNIK1. The E. coli-expressed and purified KDNIK1T474D and KDNIK1recombinant proteins were incubated alone or with NSP from CaLCuV, ToYSV or ToSRV at 25°C for 45 min in 30 μL of kinase buffer containing 18 mM HEPES pH 7.4, 10 mM $MgCl_2$, 10 mM $MnSO_4$, 1 mM DTT, 10 μM ATP and 5 μCi [γ-^{32}P]ATP. Phosphoproteins were resolved by SDS-PAGE.

The gel was stained with Coomassie brilliant blue to verify protein loading, dried, and subjected to autoradiography. Incorporated radioactivity in protein bands was quantified by phosphoimaging and protein loading by densitometry using the Multi Gauge V3.0 software (Fujifilm).

Bimolecular fluorescence complementation (BiFC) analysis. For biochemical complementation of fluorescent fragments of yellow fluorescent protein (YFP), NSP and NIK were fused to the N-terminus (N) or C-terminus (C) of the reporter gene. Then, constructs expressing NSP-YFPC, NSP-YFPN, NIK-YFPC and NIK-YFPN in different combinations were co-agroinfiltrated in tobacco leaves in the presence of the suppressor of silencing HC-Pro according to a previously described protocol (Carvalho et al., 2008c). YFP fluorescence was observed by confocal microscopy.

Tomato transformation. The clone pK7F-NIK1T474D has been previously described (Santos et al., 2009). It harbors a GFP gene fused in-frame after the last codon of the mutant cDNA T474D under the control of the CaMV 35S promoter. In the mutant cDNA T474D, the threonine residue at position 474 within the activation loop of NIK1 was mutated to an aspartate residue. Leaf discs from in vitro-grown tomato plants (Solanum lycopersicum, cultivar Moneymaker) were transformed with pK7F-NIK1T474D via Agrobacterium-mediated plant transformation (strain LBA4404). The transformed shoots were selected on MS medium supplemented with 6-benzylaminopurine (500 $mg.L^{-1}$), cefotaxime (300 $mg.L^{-1}$), and kanamycin sulfate (50 $mg.L^{-1}$). The regenerated shoots were rooted, transferred into soil and grown under standardized greenhouse conditions to generate seeds. The transgenic lines were confirmed using PCR. The analysis of transgene expression was performed by RT-PCR and real-time RT-PCR using transgene-specific primers, and actin was used as an endogenous control to normalize all values. The transgenic lines 35S:NIK1-4 and 35S:NIK1-6 have been previously described (Carvalho et al., 2008c). They harbor the Arabidopsis NIK cDNA fused to a GFP cDNA under the control of the CaMV 35S promoter.

RT-PCR and real-time RT-PCR analyses. Total RNA was extracted from tomato leaves using TRIzol (Invitrogen). The reverse transcription (RT)-PCR assays were performed with 2 µg of total RNA, 0.5 mM of poly-dT and 1 U of M-MLV reverse transcriptase (Invitrogen Life Technologies, Inc.) as previously described (Delu-Filho et al., 2000). The PCR reaction was performed using virus-specific primers. The PCR comprised 30 cycles of 45 s at 94 °C, 30 s at 55 °C and 2 min at 72 °C. The real-time RT-PCR reactions were performed on an ABI7500 instrument (Applied Biosystems, Foster City, CA) using the SYBR Green PCR Master Mix (Applied Biosystems) as previously described (Costa et al., 2008). The amplification reactions were performed as follows: 2 min at 50°C, 10 min at 95°C and 40 cycles of 94°C for 15 sec and 60°C for 1 min. To confirm the quality and primer specificity, we verified the size of amplification products using 1.5% agarose gel electrophoresis and analyzed the Tm (melting temperature) of the amplification products in a dissociation curve performed on the ABI7500 instrument. Actin was used as an endogenous control to normalize all values in the real-time RT-PCR assays. Gene expression was quantified using the $2^{\Delta C}$T method. The fold variation of gene expression was quantified using the comparative Ct method: $2^{-(\Delta CtTreatment - \Delta CtControl)}$.

Immunoblot analysis. Total protein was extracted from the leaves of wild-type and T474D-overexpressing tomato transgenic seedlings as previously described (Cascardo et al., 2000). Following SDS-PAGE, the proteins were transferred from 10% SDS-polyacrylamide gels to nitrocellulose membranes by electroblotting. The membranes were blocked in NaCl/Tris containing 0.05% v/v Tween-20 and 5% w/v non-fat dry milk, and they were subsequently incubated with rabbit anti-GFP at a 1:10,000 dilution for 2 h at room temperature. The bound antibody was detected using alkaline-phosphatase-conjugated goat anti-rabbit IgG serum in conjunction with nitroblue tetrazolium/5-bromo-4-chloro-3-indolyl phosphate detection reagents (Bio-Rad).

RNA sequencing method and data analysis. The transgenic and wild-type lines were infected at the six-leaf stage with ToYSV-[MG-Bi2], as described below in infectivity assay. After 10 days post-inoculation,

total RNA from systemically infected leaves, as diagnosed by PCR, and mock-inoculated leaves from wild-type, 35S::NIK1-4 and 35S::T474D lines was isolated using TRIzol (Invitrogen). For the RNA sequencing experiments we used two biological replicates of a pool of 10 plants at 10 days after inoculation when we detected high levels of viral DNA in systemic leaves but symptoms were not visible as yet. The experimental design was 6 treatments as follow: mock-inoculated (mock WT, mock NIK1-OX, mock T474D) lines and infected (inf WT, inf NIK1-OX, inf T474D) lines with 2 repetitions. The RNA sequencing Illumina data was obtained using a Genome Analyzer in the Fasteris facilities. The GEX-NIaIII protocol was used with the following quality filter parameters: maximum of 1 base below a quality of 5 in the first 30 bases, a minimum average quality of 10, no "N" calls allowed and not more than 35 identical bases (low information reads). The data were stored in a comma-separated values (csv) spreadsheet file.

A systematic comparison in our tomato data set of five representative normalization methods with and without the correction factors for CG-content and gene length was performed using the Bioconductor packages edgeR (Robinson et al., 2010), DESeq (Yang et al., 2013), and EDASeq (Risso et al., 2011). We have also adopted as a comparative experimental design a pairwise comparison and a false discover rate (FDR) p-value adjustment with the cutoff < 0.05. Four of those normalization methods were implemented on the edgeR, such as total count (TC), upper quartile (UQ) (Bullard et al., 2010), relative log expression (RLE) (Anders and Huber, 2010) and trimmed mean of M values (TMM) (Robinson and Oshlack, 2010); the fifth was the normalization method implemented direct in DESeq package. The GC-content and gene length correction factors were performed by the Bioconductor package EDASeq (Risso et al., 2011). For differential gene expression (DGE) analysis, we employed the normalized data provided by the counting table to the most common negative binomial methods present in R/Bioconductor software, such as edgeR (Robinson et al., 2010), DESeq (Anders and Huber, 2010) and baySeq (Hardcastle et al., 2010). The parameter of dispersion was estimated by the tagwise program. Differential expression was determined using the FDR adjusted cutoff p-value of 0.05. The read mapping process was executed using the Bowtie program (Langmead et al., 2009) with the cDNA data set retrieved from the International Tomato

Annotation Group (ITAG - http://solgenomics.net/organism/Solanum_lycopersicum/genome), second release. Gene ontology classification was performed using the R/Bioconductor packages GSEABase and GOstats. The entire annotation data set from ITAG/Phytozome (http://www.phytozome.net) was stored in the relational database PostgreSQL 9.3 (http://www.postgresql.org). To detect gene set enrichment from our RNA-seq DE data, we used the GSEA method provided by the R/Bioconductor GSEABase package based on the Gene Ontology (GO) database (Ashburner et al., 2000). Clustering analysis was performed using the R package pvclust (Hierarchical Clustering with P-Values via Multiscale Bootstrap Resampling) using Ward's method (Ward, 1963), and heatmaps were generated using gplots. The results were stored in a relational database created in PostgreSQL, and a web interface was created using PHP to allow the database to be accessed and navigated (http://tomatodb.inctipp.ufv.br). The RNA-seq data of T474D lines were submitted to NCBI-GEO, http://www.ncbi.nlm.nih.gov/geo/info/linking.html, accession number GSM932558.

In vivo labeling of leaf proteins. Tomato seedlings (300 mg) were incubated with 1 mL of nutrient solution containing 50 µg/ml chloramphenicol and 20 µCi of [35S]methionine (EasyTag Protein Labeling Mix, [^{35}S]-, 2mCi (74MBq), Perkin Elmer) for 3 h at room temperature. To quantitate incorporation of [^{35}S]methionine into protein, aliquots of protein extracts were placed in 10% (w/v) TCA and incubated on ice for 30 min. The samples were filtered onto glass microfiber filters and the filters were washed three times with 5 ml of cold 5% (w/v) TCA and two times with 5 ml of 95% ethanol. After drying, the filters were counted with a scintillation counter.

Polysome fractionation. Polysomes were fractionated over sucrose gradients as described (Wang et al., 2003). Briefly, 500 mg of 15-day-old tomato seedlings were ground in liquid nitrogen and 1 mL of extraction buffer (0.2 M Tris-HCl, pH 8.0, 50 mM KCl, 25 mM MgCl2, 1% Triton X-100, 400 units/mL of RNasin and 50 mg/mL of cycloheximide). After centrifuging for 10 min, the supernatant was loaded onto a 10-mL 15% to 50% sucrose gradient and spun in a Beckman SW41Ti rotor at 135,000 g for 3.5 h.

Fractions were collected manually from the bottom, and total RNA was extracted with phenol/chloroform/isoamyl alcohol, precipitated with isopropanol, and treated with DNase I. The specific transcripts were amplified from RNA of T474D, NIK1 and wilt-type infected lines using qRT-PCR.

Infectivity assays. For the infectivity assays, we used T2 transgenic plants harboring the T474D mutant gene construct, which were derived from four independently regenerated kanamycin-resistant plants (35S::T474D-2, 35S::T474D-5, 35S::T474D-6 and 35S::T474D-9). We also used the previously described transgenic lines expressing AtNIK1 under the control of the CaMV 35S promoter, 35S::NIK1-4 and 35S::NIK1-6 (Carvalho et al., 2008c). The transgenic and wild-type lines were infected at the six-leaf stage with either ToYSV-[MG-Bi2] or ToSRV by biolistic delivery using tandemly repeated viral DNA-A and DNA-B and a microprojectile bombardment model PDS-1000/He accelerator (BIORAD) at 900 psi. In each experiment, 20 plants of each line were inoculated with 2 µg of tandemly repeated DNA-A plus DNA-B per plant and grown in a greenhouse under natural conditions of light, 70% relative humidity and approximately equal day and night lengths. Total nucleic acid was extracted from the systemically infected leaves (young leaves), and viral DNA was detected by PCR using DNA-A and DNA-B begomovirus-specific primers (PBL1v 2040, GCCTCTGCAGCARTGRTCKATCTTCATACA, and PCRC1, CTAGCTGCAGCATATTTACRARWATGCCA, or PAL1v1978, GCATCTGCAGGCCCACATYGTCTTYCCNGT, and PAR1c496, AATACTGCAGGGCTTYCTRTACATRGG) at 10 days post-infection.

Quantitation of viral DNA in infected plants. Viral DNA accumulation was measured by quantitative PCR (qPCR). The reactions were prepared in a final volume of 10 µl using the Fast SYBR Green Master Mix (Applied Biosystems) according to the manufacturer's instructions and analyzed on a 7500 Real Time PCR System (Applied Biosystems). Virus-specific primers were designed using Primer Express 3.0 (Applied Biosystems) and tested by conventional PCR using plasmids containing the complete DNA-A of each virus (10^6 copies per reaction). The following primer sequences were used: ToSRVFwd,

CACGTGCCCACATCGTCTT, and ToSRVRev, GGCCGGAACGACCTATTA-3', or ToYSVFwd, CCACGATTTTAAAGCTGCATTCT, and ToYSVRev, CAATCCTGGTGAGGGAGTCAGT. For viral DNA quantitation, standard curves were prepared using serial dilutions of these clones (10^0 to 10^6 copies of viral genome per reaction). The genomic unit refers to one copy of the DNA-A of ToYSV or ToSRV. Standard curves were obtained by regression analysis of the Ct values of each of the three replicates of a given dilution in relation to the log of the amount of DNA in each dilution. For the absolute quantitation of the number of viral DNA molecules in the different treatments, 100 ng of total DNA from the infected plants was used in the qPCR reactions containing virus-specific primers. Each sample was analyzed in triplicate from at least two biological replicates.

Physiological measurements of tomato transgenic lines. Photosynthetic CO2 assimilation (A), transpiration rate (E), and stomatal conductance (gs) measurements were performed with a portable open-flow gas exchange system (LICOR 6400, Li-COR, Lincoln, Nebraska, USA) under ambient CO2 concentrations (370 ± 10 µmol mol-1) and temperature conditions under artificial, saturating PAR (1,000 umol photons m^{-2} s^{-1} at the leaf level).

Estimation of total carotenoids, lycopene, and β-carotene. Total carotenoids from fully ripened tomato fruits were extracted with cold acetone and petroleum ether, as described by Rodriguez-Amaya et al. (1976). The extract (30 µL) was separated by HPLC using reversed phase C18 column (Phenomenex Gemini, 250 x 4,6 mm, 5 µm) and a C18 guard column (Phenomenex ODS, 4 mm x 3 mm) on a Shimadzu, SCL 10AT VP HPLC system coupled to a DAD detector (Shimadzu, SPD-M10A) and operating at a flow rate of 1.7 mL/min. The mobile phase buffer used was methanol:ethyl acetate:acetonitrile (70:20:10, v/v/v). The chromatograms were obtained at 450 nm and integrated using the software Multi System Class Vp 6.12. Lycopene and β-carotene were quantified from HPLC profile

by using a purified lycopene standard (Sigma Chemical Co.) and a β-carotene standard purified from carrots.

References

Anders, S. and Huber ,W. (2010) Differential Expression Analysis for Sequence Count Data. *Genome Biol.,* **11**, R106.

Ashburner, M. C., Ball, J., Blake, J.A., Botstein, D., Butler, H., Cherry, J.M., Davis, A.P. Dolinski, K., Dwight, S.S., Eppig, J.T., Harris, M.A., Hill, D.P., Issel-Tarver, L., Kasarskis, A., Lewis ,S., Matese, J.C., Richardson, J.E., Ringwald, M., Rubin, G.M. and Sherlock, G. (2000) Gene Ontology: Tool for the Unification of Biology. The Gene Ontology Consortium. Nat. Genet., **25**, 25–29.

Bullard, J.H., Purdom, E., Hansen, K.D. and Dudoit, S. (2010). Evaluation of Statistical Methods for Normalization and Differential Expression in mRNA-Seq Experiments. *BMC Bioinformatics,* **11,** 94.

Cascardo JCM, Almeida RS, Buzeli RAA, Carolino SMB, Otoni WC and Fontes E.P.B. (2000) The phosphorylation state and expression of soybean BiP isoforms are differentially regulated following abiotic stresses. J. Biol. Chem., **275,** 14494–14500.

Costa, M.D.L., Reis, P.A.B., Valente, M.A.S., Irsigler, A.S.T., Carvalho, C.M., Loureiro, M.E., Aragão, F.J., Boston, R.S., Fietto, L.G. and Fontes, E.P.B**.** (2008) A new branch of endoplasmic reticulum-stress signaling and the osmotic signal converge on plant specific asparagine-rich proteins to promote cell death. J. Biol. Chem., **283**, 20209–20219.

Delú-Filho, N., Pirovani, C.P., Pedra, J.H.F., Matrangolo, F.S.V., Macêdo, J.N.A., Otoni, W.C. and Fontes, E.P.B. (2000) A sucrose binding protein homologue from soybean affects sucrose uptake in transgenic tobacco suspension-cultured cells. Plant Physiol. Biochem., **38**, 353–361.

Florentino, L.H., Santos, A.A., Fontenelle, M.R., Pinheiro, G.L., Zerbini, F.M., Baracat-Pereira, M.C. and Fontes, E.P.B**.** (2006) A PERK-like receptor kinase interacts with the geminivirus nuclear shuttle protein and potentiates viral infection. J. Virol., **80**, 6648–6656.

Hardcastle, T.J. and Krystyna, A.K. (2010) baySeq: Empirical Bayesian Methods for Identifying Differential Expression in Sequence Count Data. BMC Bioinformatics, **11**, 422.

Langmead, B., Trapnell, C., Pop, M. and Salzberg, S.L. (2009) Ultrafast and memory-efficient alignment of short DNA sequences to the human genome. Genome Biol., **10**, R25.

Risso, D., Schwartz, K., Sherlock, G. and Dudoit, S. (2011) GC-Content Normalization for RNA-Seq Data. *BMC Bioinformatics,* **12**, 480.

Robinson, M.D., McCarthy, D.J. and Smyth, G.K. (2010) edgeR: a Bioconductor package for differential expression analysis of digital gene expression data. Bioinformatics **26,** 139–140.

Robinson, M.D. and Oshlack, A. (2010) A scaling normalization method for differential expression analysis of RNA-seq data. Genome Biol., **11**, R25.

Uhrig, J.F., Soellick, T.-R., Minke, C.J., Philipp, C., Kellmann, J.-W. and Schreier, P.H. (1999) Homotypic interaction and multimerization of nucleocapsid protein of tomato spotted wilt topovirus: identification and characterization of two interacting domains. Proc. Natl Acad. Sci. USA **96**, 55–60.

Wang, W., Scali, M., Vignani, R., Spadafora, A., Sensi, E., Mazzuca, S. and Cresti, M. (2003) Protein extraction for two-dimensional electrophoresis from olive leaf, a plant tissue containing high levels of interfering compounds. Electrophoresis **24,** 2369–2375.

Ward, JH. (1963). Hierarchical Grouping to Optimize an Objective Function. J. Am. Stat. Assoc., **58,** 236–244.

Yang, E.-W., Girke T., and Jiang T. (2013). Differential Gene Expression Analysis Using Coexpression and RNA-Seq Data. Bioinformatics, 29, 2153-2161.

Supporting information - Figures S1-S6

Sustained NIK-mediated antiviral signaling confers broad-spectrum tolerance to begomoviruses in cultivated plants

Otávio J.B.Brustolini [a,b*], Joao Paulo B. Machado[a,b*], Jorge A. Condori-Apfata [b], Daniela Coco [a,b], Michihito Deguchi[a,b], Virgílio A. P. Loriato[a,b], Welison A. Pereira, Poliana Alfenas-Zerbini [b], Francisco M. Zerbini [b], Alice K. Inoue-Nagata[b,d], Anesia A. Santos [a,b], Joanne Chory[e], Fabyano F. Silva[c], Elizabeth P.B. Fontes [a,b,&]

[a]Departamento de Bioquímica e Biologia Molecular [b]National Institute of Science and Technology in Plant-Pest Interactions, Bioagro, [c]Departamento de Zootecnia, Universidade Federal de Viçosa, 36570.000, Viçosa, MG, Brazil. [d]Embrapa Vegetables, Brasília, DF 70359-970, Brazil. [e]Howard Hughes Medical Institute and Plant Biology Laboratory, The Salk Institute for Biological Studies, La Jolla, California 92037, USA

[*]These authors contributed equally to this work

[&]For correspondence:

Elizabeth B. P. Fontes, Departamento de Bioquímica e Biologia Molecular/Bioagro, National Institute of Science and Technology in Plant-Pest Interactions, Universidade Federal de Viçosa, 36570.000, Viçosa, MG, Brazil, pone +55 31 3899 2948 [&]email bbfontes@ufv.br

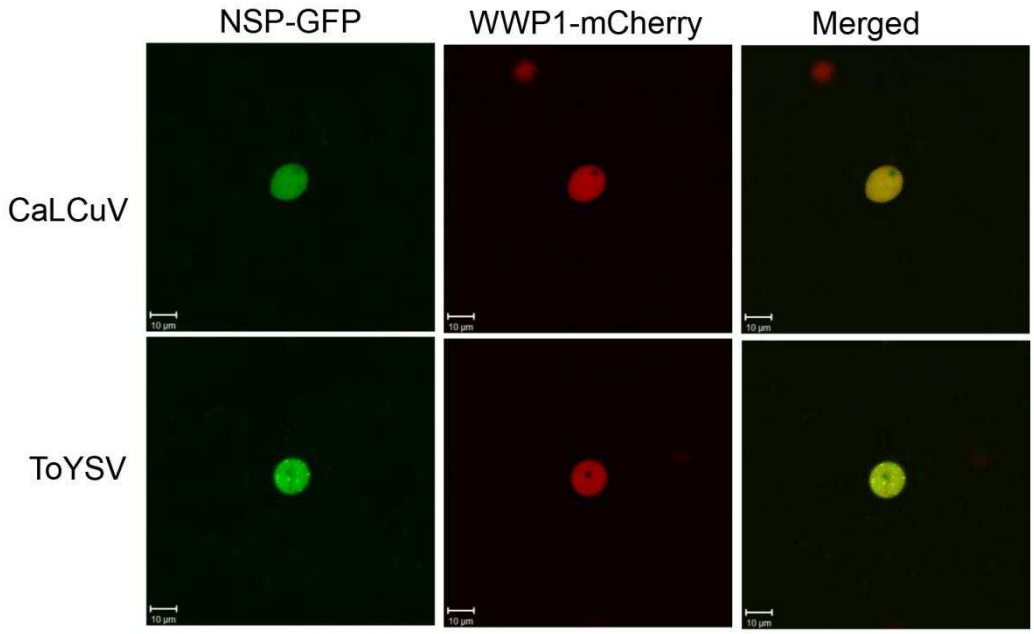

Figure S1. NSP from CaLCuV and ToYSV concentrates in the nucleus when ectopically expressed in N. benthamiana leaves. N. benthamiana leaves were co-infiltrated with A. tumefaciens carrying a 35S::NSP-GFP construct from CaLCuV or ToYSV together with a 35S::AtWWP1-mCherry construct. After 48 h post-infiltration, the subcellular localizations of the fluorescent fusion proteins were examined by confocal microscopy.

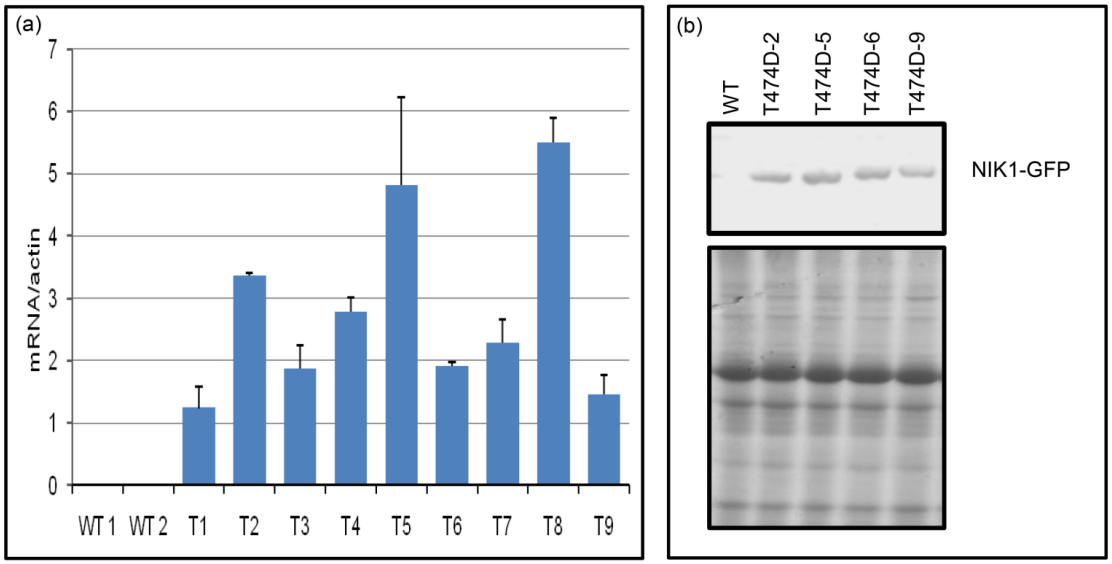

Figure S2. Overexpression of T474D mutant receptor in tomato leaves.
(a) T474D transcript accumulation in primary transformants. The expression of T474D in the leaves of several independent transgenic lines was monitored by quantitative RT-PCR. Values of expression were calculated using the $2^{-\Delta Ct}$ method with actin as an endogenous control. Values represent the mean ± SD of three replicates. **(b)** Accumulation of T474D-GFP in transgenic lines. Total protein was extracted from the leaves of independent transgenic lines (as indicated), fractionated by SDS-PAGE (bottom) and immunoblotted with an anti-GFP antiserum.

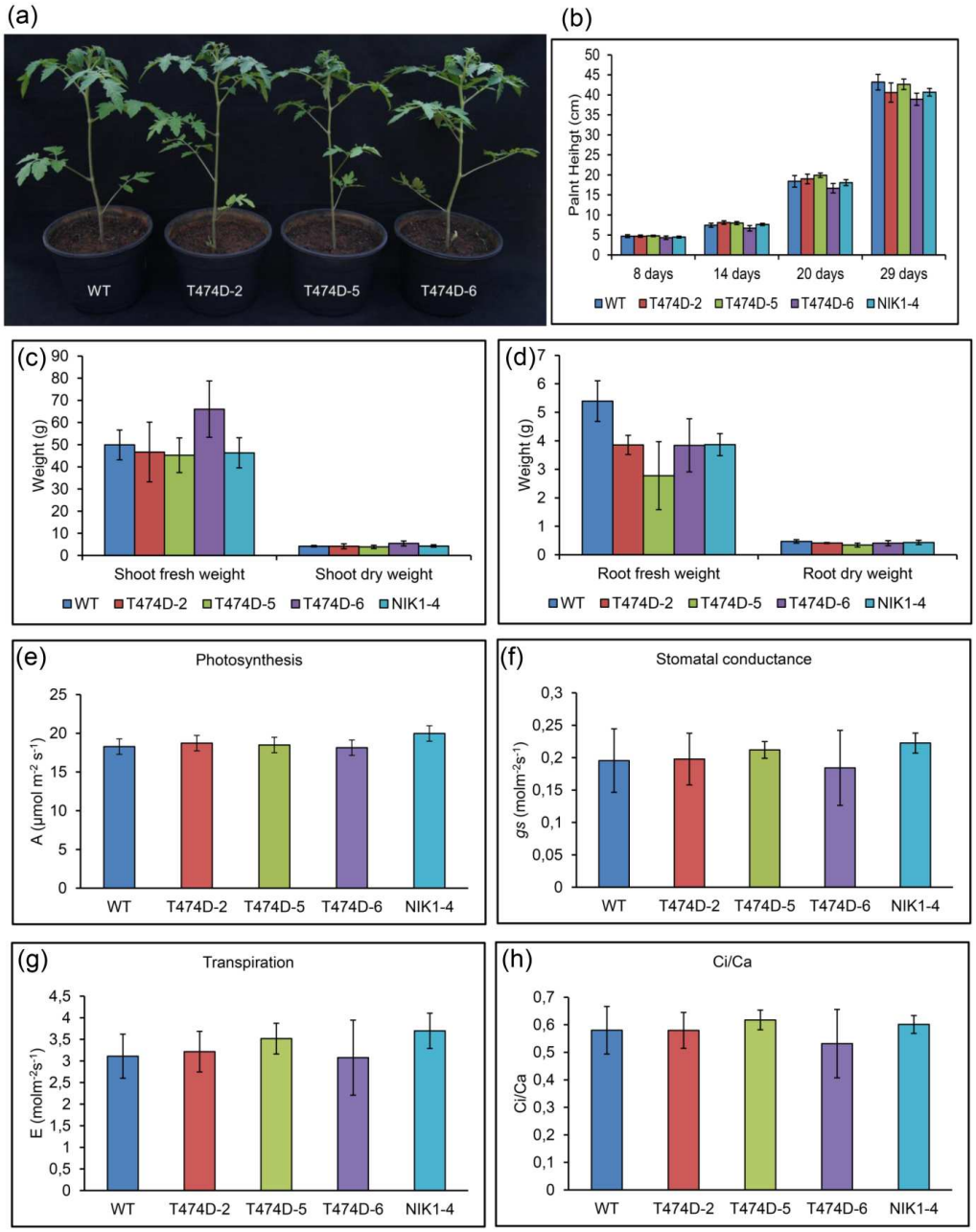

Figure S3. Characterization of the T474D-overexpressing lines during the vegetative phase.
(a), **(b)**, **(c)** and **(d)** Developmental phenotypes associated with overexpression of the T474D gain-of-function mutant in the R3 generation of tomato transgenic lines. **(a)** The images are plants of T474D-2, T474D-5, T474D-6 and wild-type lines grown for 30 days under normal greenhouse conditions. The transgenic lines are visibly undistinguishable from the wild-type plant. The indicated day correspond to the period of time after transferring germinated seedlings to the soil. **(b)**. Plant height of wild-type line and T474D-2, T474D-5, T474D-6 and NIK1-4 transgenic lines grown for 8, 14, 20 or 29 days in the greenhouse. The indicated days correspond to the period of time after transferring germinated seedlings to the soil. Values represent the mean ± IC (α=0,05) of 11 biological replicates and did not differ between wild-type and transgenic lines in each period of the measurement. **(c)** Shoot fresh and dry weight and **(d)** root fresh and dry weight of wild-type and transgenic lines (as indicated) grown for 30 days in greenhouse. Values represent the mean ± IC (α=0,05) of three biological replicates. (e-h) Physiological measurements of transgenic lines. The net CO_2 assimilation rate (A), transpiration rate (E),stomatal conductance to water vapor (g_s) and internal-to-ambient CO_2 concentration ratio (C_i/C_a) of fully expanded leaves of wild-type, T474D-2, T474D-5 and T474D-6 transgenic lines were measured by the LI-6400 infrared (IR) gas analyzer at growth irradiance. The error bars represent the confidence interval (α = 0.05) of measurements from five individual plants.

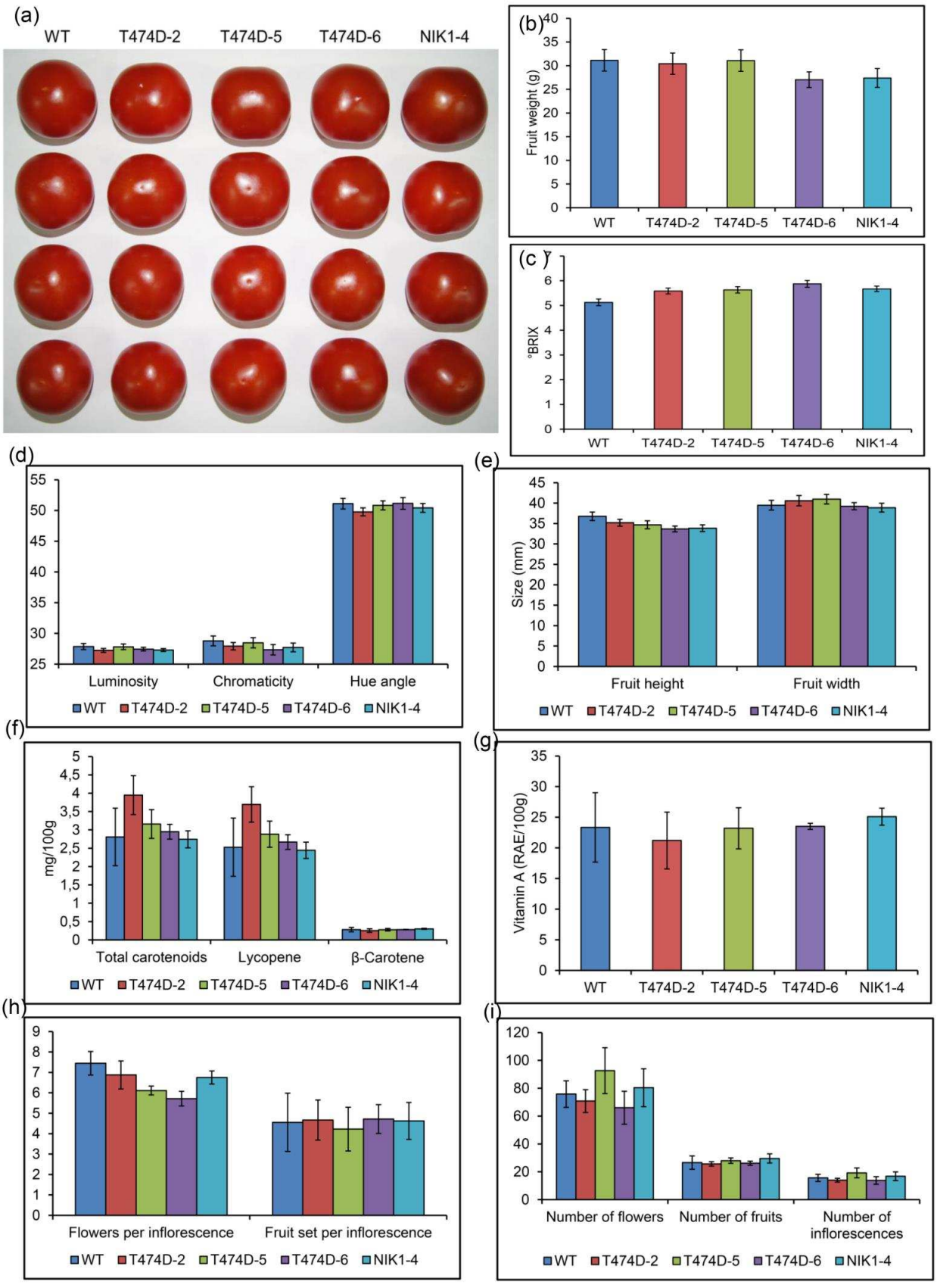
(a)
WT
T474D-2
T474D-5
T474D-6
NIK1-4
(b)
Fruit weight (g)
0
5
10
15
20
25
30
35
40
WT
T474D-2
T474D-5
T474D-6
NIK1-4
(c)
°BRIX
0
1
2
3
4
5
6
WT
T474D-2
T474D-5
T474D-6
NIK1-4
(d)
25
30
35
40
45
50
55
Luminosity
Chromaticity
Hue angle
WT
T474D-2
T474D-5
T474D-6
NIK1-4
(e)
Size (mm)
0
5
10
15
20
25
30
35
40
45
Fruit height
Fruit width
WT
T474D-2
T474D-5
T474D-6
NIK1-4
(f)
mg/100g
0
0,5
1
1,5
2
2,5
3
3,5
4
4,5
5
Total carotenoids
Lycopene
β-Carotene
WT
T474D-2
T474D-5
T474D-6
NIK1-4
(g)
Vitamin A (RAE/100g)
0
5
10
15
20
25
30
35
WT
T474D-2
T474D-5
T474D-6
NIK1-4
(h)
0
1
2
3
4
5
6
7
8
9
Flowers per inflorescence
Fruit set per inflorescence
WT
T474D-2
T474D-5
T474D-6
NIK1-4
(i)
0
20
40
60
80
100
120
Number of flowers
Number of fruits
Number of inflorescences
WT
T474D-2
T474D-5
T474D-6
NIK1-4

Figure S4. Fruit quality and yield of the T474D-overexpressing lines **(a)** Morphology and color of fresh ripe tomato fruits from T474D-overexpressing lines. The ripe fruit of the transgenic lines were bright red and were classified as small round, varying in size as indicated in the figure. **(b)** Fruit weight. Error bars, 95% confidence intervals (n=5) based on bootstrap resampling replicates from 160 fruits. **(c)** Content of soluble solids of tomato fruits from T474D-, NIK1-overexpressing lines and wild-type. Fully ripened tomato fruits were also analyzed for total soluble solids (TSS), which were not different between the transgenic lines and wild-type. Total soluble solids were determined using a manual refractometer model ATC103 (BIOBRIX). The tomato sample was squashed manually and about three or four drops were transferred to the refractometer. Results were expressed as degrees of Brix. Error bars, 95% confidence intervals (n=3) based on bootstrap resampling replicates from 85 fruits. **(d)** Skin color of tomato fruits. Skin coloration was analyzed according to luminosity (L), chromaticity (C) and hue angle (H) parameters (two readings per fruit), by means of reflectometry in a colorimeter brand KONICA MINOLTA. Values represent the mean ± IC (α=0,05) of 53 fruits. **(e)** Fruit Size. Fully ripened tomato fruits were also analyzed for size. Values represent the mean ± IC (α=0,05) of 160 fruits. **(f)** Content of carotenoids. Total carotenoids, lycopene and β-carotene were determined by HPLC. Values represent the mean ± IC (α=0,05, n=3) from three biological replicates. **(g)** Vitamin A content. The vitamin A content is expressed as recommended by the Institute of Medicine (2001), in which 1 retinol activity equivalent (RAE) corresponds to 1 μg of retinol, 12 μg of β-carotene and 24 μg of other pro-vitamin carotenoids. Values represent the mean ± IC (α=0,05, n=3) from three biological replicates. **(h)** and **(i)**. Developmental and yield performance of wild type and transgenic lines. The number of days to flowering (30-31 days) did not differ among transgenic lines and wild-type control. The number and size of inflorescence as well as fruit yield were measured. Values represent the mean ± IC (α=0,05) of seven biological replicates.

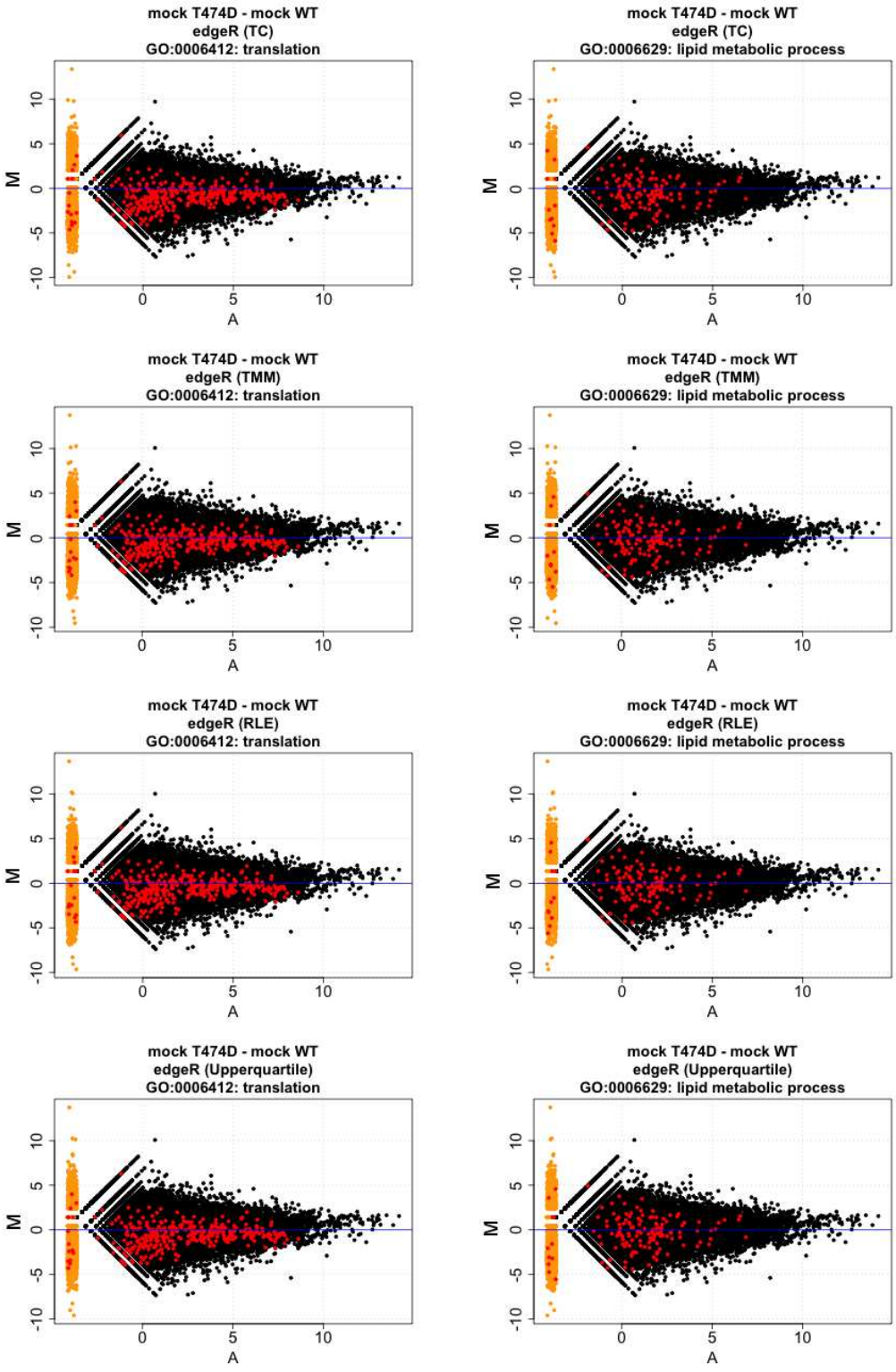

Figure S5. Representation of the translational machinery-related genes in the down-regulated changes. The 'MA' plots show the log of the ratio of expression levels against log-concentration, and each dot represents a gene. These plots are from the contrast mock T474D-mock WT and the normalization method used is shown on the top of the plots. The smear of points on the left side indicates genes that were observed in only one group of replicated samples, and the red points denote the translation related genes (GO:0006412) or lipid metabolic process-related genes (GO:0006629). For the translation related genes, the density of the red dots is concentrated below zero, whereas for the lipid metabolic process-related genes, the red dots are spread to the overall dispersion.

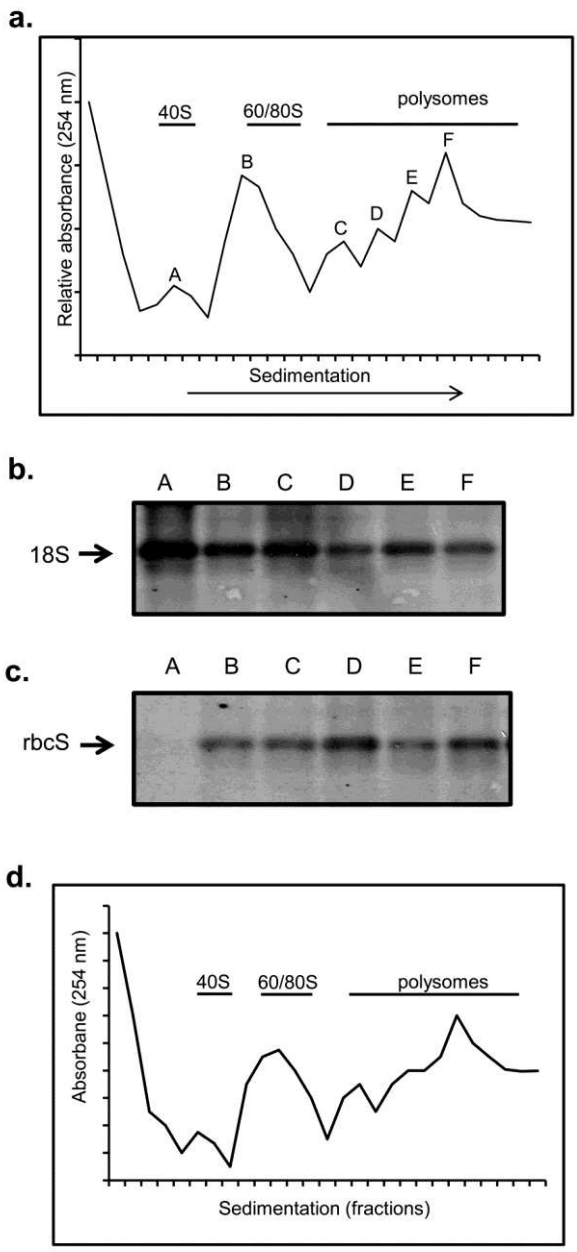

Figure S6. Isolation of polysomal fractions from tomato seedlings.
(a) UV absorbance profiles of the sucrose gradient used for RNA fractionation from infected T474D-overexpressing lines. Polysomes from infected T474D-overexpressing lines at 10 DPI were fractionated on a sucrose gradient, and the fractions were manually collected. **(b)** Distribution of 18S rRNA on the sucrose gradient. Total RNA from the fractions, as indicated in A by the letters, was extracted with phenol/chloroform/isoamyl alcohol, precipitated with isopropanol, blotted and probed with 18S rDNA. The result indicates the distribution of the 40S small subunit. The higher concentration of 18S in fraction A indicates a 40S-enriched fraction. The heavier fractions are monosomes (RNPs) and polysomes. **(c)** Levels of rbcS mRNA per fraction. The levels of the small subunit of rubisco (rbcS) mRNA were examined by northern blotting. This control was used to ensure the quality and distribution of a specific mRNA. **(d)** UV absorbance profiles of the sucrose gradient used for RNA fractionation of the infected wild type leaves at 10 DPI. Polysomes from wild type leaves at 10 DPI were isolated as in (a). The pooled fractions were used for RNA extraction and for the amplification of specific resistance-like gene transcripts. The bars indicate actin and rbcS transcripts.

Table S1. Enriched biological process categories from the GO database using the GSEA* method

Infected WT – mock WT (UP-regulated)			
Enriched Categories	**DGE** methods: number of genes / number of genes in the GO group (p-value)**	**AN***	**Average p-value**
GO:0006073: cellular glucan metabolic process	edgeR/RLE: 4/93 (0.007615) edgeR/upper: 4/93 (0.008759) baySeq: 7/93 (0.006532)	5	0.007635
GO:0009765: photosynthesis, light harvesting	edgeR/RLE: 3/33 (0.002581) edgeR/upper: 3/33 (0.002895) baySeq: 4/33 (0.007371)	3	0.004282
Infected WT – mock WT (DOWN-regulated)			
Enriched Categories	**DGE methods: number of genes / number of genes in the GO group (p-value)**	**AN**	**Average p-value**
GO:0006629: lipid metabolic process	edgeR/TMM: 19/592 (1.79e-05) edgeR/TC: 22/592 (0.0004238) edgeR/RLE: 16/592 (8.847e-05) edgeR/upper: 7/343 (0.009761)	16	1.77E-04
GO:0006633: fatty acid biosynthetic process	edgeR/TMM: 5/69 (0.00087) edgeR/TC: 5/69 (0.006144) edgeR/RLE: 5/69 (0.0004101) edgeR/upper: 5/69 (0.0001461) DESeq: 2/69 (0.006187)	5	0.00275
GO:0009611: response to wounding	edgeR/TMM: 5/22 (3.054e-06) edgeR/TC: 5/22 (2.732e-05) edgeR/RLE: 5/22 (1.351e-06) edgeR/upper: 5/22 (4.486e-07) DESeq: 3/22 (6.617e-06)	5	7.76E-06
GO:0032787: monocarboxylic acid metabolic process	edgeR/TMM: 5/96 (0.003758) edgeR/RLE: 5/96 (0.001836) edgeR/upper: 5/96 (0.000681)	5	0.002091
GO:0044283: small molecule biosynthetic process	edgeR/TMM: 8/217 (0.002388) edgeR/RLE: 7/217 (0.003716) edgeR/upper: 7/217 (0.001046)	7	0.002383
GO:0046394: carboxylic acid biosynthetic process	edgeR/TMM: 8/189 (0.0009954) edgeR/RLE: 7/189 (0.001713) edgeR/upper: 7/189 (0.000462)	7	0.0010568
GO:0055114: oxidation-reduction process	edgeR/TMM: 29/1645 (0.004426) edgeR/RLE: 25/1645 (0.00631) edgeR/upper: 21/1645 (0.006762)	25	0.005833
Mock NIK-OX – mock WT (UP-regulated)			
Enriched Categories	**DGE methods: number of genes / number of genes in the GO group (p-value)**	**AN**	
GO:0046148: pigment biosynthetic process	edgeR/TMM: 3/28 (0.006671) edgeR/TC: 3/28 (0.004615) edgeR/RLE: 3/28 (0.0075) edgeR/upper: 3/28 (0.003001)	3	0.0038946
Mock NIK-OX – mock WT (DOWN-regulated)			
Enriched Categories	**DGE methods: number of genes / number of genes in the GO group (p-value)**	**AN**	**Average p-value**
GO:0009611: response to wounding	edgeR/TMM: 3/22 (0.001621) edgeR/TC: 3/22 (0.003048) edgeR/RLE: 3/22 (0.001937) edgeR/upper: 3/22 (0.002832)	3	0.0023595
GO:0043648: dicarboxylic acid metabolic process	edgeR/TMM: 3/27 (0.002961) edgeR/TC: 3/27 (0.005512) edgeR/RLE: 3/27 (0.003528) edgeR/upper: 3/27 (0.005128)	3	0.0042822
GO:0044262: cellular carbohydrate	edgeR/TMM: 7/214 (0.00841) edgeR/TC: 8/214 (0.00833) edgeR/upper: 8/214 (0.007165)	8	0.007968

metabolic process			

Mock T474D – mock WT (UP-regulated)

Enriched Categories	DGE methods: number of genes / number of genes in the GO group (p-value)	AN	Average p-value
GO:0006629: lipid metabolic process	edgeR/TMM: 47/592 (0.007967) edgeR/RLE: 46/592 (0.003633) edgeR/upper: 45/592 (0.007517) baySeq: 45/343 (5.446e-06)	46	0.00478
GO:0009765: photosynthesis, light harvesting	edgeR/TMM: 6/33 (0.008713) edgeR/upper: 6/33 (0.006678) DESeq: 5/33 (0.005769) baySeq: 8/33 (0.001161)	7	0.00558
GO:0009607: response to biotic stimulus	edgeR/TMM: 9/58 (0.009423) edgeR/upper: 8/58 (0.007652) baySeq: 10/58 (0.004553)	9	0.007209
GO:0044283: small molecule biosynthetic process	edgeR/TMM: 21/217 (0.009161) edgeR/RLE: 20/217 (0.008819) edgeR/upper: 21/217 (0.004946)	21	0.007642
GO:0051247: positive regulation of protein metabolic process	edgeR/TMM: 3/7 (0.00502) edgeR/RLE: 3/7 (0.004125) edgeR/upper: 3/7 (0.004283)	3	0.004476

Mock T474D – mock WT (DOWN-regulated)

Enriched Categories	DGE methods: number of genes / number of genes in the GO group (p-value)	AN	Average p-value
GO:0006260: DNA replication	edgeR/TMM: 12/87 (0.001556) edgeR/RLE: 12/87 (0.003899) edgeR/upper: 12/87 (0.00235)	12	0.0026
GO:0006270: DNA replication initiation	edgeR/TMM: 2/2 (0.002646) edgeR/TC: 2/2 (0.007579) edgeR/RLE: 2/2 (0.003304) edgeR/upper: 2/2 (0.002919)	2	0.004112
GO:0006275: regulation of DNA replication	edgeR/TMM: 2/2 (0.002646) edgeR/TC: 2/2 (0.007579) edgeR/RLE: 2/2 (0.003304) edgeR/upper: 2/2 (0.002919) DESeq: 2/2 (0.00171)	2	0.00363
GO:0006323: DNA packaging	edgeR/TMM: 12/77 (0.0005285) edgeR/RLE: 12/77 (0.001394) edgeR/upper: 12/77 (0.0008159)	12	0.004509
GO:0006333: chromatin assembly or disassembly	edgeR/TMM: 12/80 (0.0007529) edgeR/TC: 15/80 (0.003447) edgeR/RLE: 12/80 (0.001953) edgeR/upper: 12/80 (0.001154)	13	0.001826
GO:0006334: nucleosome assembly	edgeR/TMM: 12/77 (0.0005285) edgeR/RLE: 12/77 (0.001394) edgeR/upper: 12/77 (0.0008159)	12	0.000913
GO:0006412: translation	edgeR/TMM: 53/579 (2.923e-05) edgeR/TC: 110/579 (1.131e-15) edgeR/RLE: 67/579 (2.465e-08) edgeR/upper: 59/579 (1.62e-06) DESeq: 51/579 (2.342e-07)	68	4.69E-07
GO:0006629: lipid metabolic process	edgeR/TMM: 56/592 (6.552e-06) edgeR/TC: 82/592 (1.355e-05) edgeR/RLE: 61/592 (5.595e-06) edgeR/upper: 58/592 (6.822e-06) DESeq: 43/592 (0.0002239)	60	0.000645
GO:0007018: microtubule-based movement	edgeR/TMM: 14/60 (1.519e-06) edgeR/TC: 19/60 (3.965e-07) edgeR/RLE: 16/60 (1.667e-07) edgeR/upper: 15/60 (4.582e-07) DESeq: 11/60 (2.969e-05)	15	4.07E-04
GO:0009059: macromolecule biosynthetic process	edgeR/TC: 250/2200 (1.178e-06) edgeR/RLE: 156/2200 (0.00198) edgeR/upper: 145/2200 (0.004376)	184	6.45E-03
GO:0009611: response to wounding	edgeR/TMM: 7/22 (8.009e-05) edgeR/TC: 7/22 (0.001975) edgeR/RLE: 7/22 (0.0001609) edgeR/upper: 7/22 (0.0001092) DESeq: 7/22 (1.977e-05)	7	0.00251
GO:0009765: photosynthesis,	edgeR/TMM: 9/33 (3.03e-05) edgeR/TC: 9/33 (0.001575) edgeR/RLE: 9/33 (7.225e-05) edgeR/upper: 9/33 (4.459e-05) DESeq: 9/33 (5.25e-06)	9	0.00237

light harvesting			
GO:0015995: chlorophyll biosynthetic process	edgeR/TMM: 4/13 (0.003425) edgeR/RLE: 4/13 (0.005109) edgeR/upper: 4/13 (0.00409)	4	0.000421
GO:0022607: cellular component assembly	edgeR/TMM: 17/153 (0.002249) edgeR/RLE: 17/153 (0.006862) edgeR/upper: 17/153 (0.003725)	17	0.00428
GO:0034622: cellular macromolecular complex assembly	edgeR/TMM: 17/131 (0.0003895) edgeR/TC: 21/131 (0.004471) edgeR/RLE: 17/131 (0.001345) edgeR/upper: 17/131 (0.0006802)	18	0.001721
GO:0044249: cellular biosynthetic process	edgeR/TMM: 163/2634 (0.004014) edgeR/TC: 296/2634 (2.09e-07) edgeR/RLE: 187/2634 (0.0005531) edgeR/upper: 172/2634 (0.002566)	205	0.00178
GO:0071824: protein-DNA complex subunit organization	edgeR/TMM: 12/77 (0.0005285) edgeR/RLE: 12/77 (0.001394) edgeR/upper: 12/77 (0.0008159)	12	9,13E-04
GO:0071840: cellular component organization or biogenesis	edgeR/TMM: 39/488 (0.004133) edgeR/TC: 62/488 (0.001511) edgeR/RLE: 42/488 (0.005659) edgeR/upper: 40/488 (0.005529)	46	0.00421
GO:1901576: organic substance biosynthetic process	edgeR/TMM: 173/2717 (0.0007624) edgeR/TC: 60/517 (0.002539) edgeR/RLE: 43/517 (0.003325) DESeq: 139/2717 (0.002492)	104	0.00228

*GSEA - Gene set enrichment analysis
**DGE – Differential gene expression
***AN – Average number

Table S2. Resistance protein-related genes differentially expressed in infected T474D (infected T474D-mock T474D)

Up-regulated resistance protein-related genes				
ITAG	**LOG2FC**	**Q-VALUE**	**GO**	**DESCRIPTION**
Solyc02g032050.1.1	1,620578758	0,040756495		Disease resistance-responsive (dirigent-like protein) family protein
Solyc05g042090.1.1	4,907459511	5,24E-06	GO:0043531,GO:0006915, GO:0005524	NB-ARC domain-containing disease resistance protein
Solyc07g008590.1.1	1,572643749	0,005472267	GO:0005515	disease resistance family protein / LRR family protein
Solyc07g008620.1.1	2,208276596	2,04E-06	GO:0005515	disease resistance family protein / LRR family protein
Solyc08g081780.1.1	1,470947445	0,002867545		Disease resistance-responsive (dirigent-like protein) family protein
Solyc12g044190.1.1	3,942547883	1,63E-12	GO:0043531,GO:0006915, GO:0005524	LRR and NB-ARC domains-containing disease resistance protein
Solyc12g097010.1.1	1,982314928	0,001087781	GO:0005515	disease resistance protein (TIR-NBS-LRR class), putative
Down-regulated resistance protein-related genes				
ITAG	**LOG2FC**	**Q-VALUE**	**GO**	**DESCRIPTION**
Solyc05g054340.2.1	-1,752069826	0,000112318	GO:0043531,GO:0006915, GO:0005524	NB-ARC domain-containing disease resistance protein
Solyc07g061940.2.1	-1,119795309	4,23E-03	GO:0000287,GO:0030976, GO:0003824	chlorsulfuron/imidazolinone resistant 1

Table S3. Gene Enrichment Analysis*

(edgeR TMM T474D infected – T474D mock)					
Biological Process	**Total**	**Downregulated genes**	**P-value**	**Upregulated genes**	**P-value2**
ITAG 2.3 (Number of genes)	**34727**	**758**		**1115**	
Response to Salicylic Acid (GO:0009751)	**404**	**6**	**0,87703**	**9**	**0,903966**
Defense response to pathogen (GO:0042742 + GO:0050832)	**1038**	**14**	**0,981838**	**36**	**0,34073**
Defense response to virus (GO:0051607)	**115**	**1**	**0,921305**	**2**	**0,887503**
Virus induced gene silencing (GO:0009616)	**198**	**1**	**0,987503**	**6**	**0,613786**
Resistance like proteins	**450**	**2**	**9,99E-01**	**7**	**0,990446**

* Data were retrieved from http://amigo.geneontology.org/amigo/term/GO:0009607 (Reponse to biotic stress GO:0009607). These groups are presented at: Source ITAG 2.3

** Statistical test based on hypergeometric distribution probability with significance of < 0.01

Response to Salicylic Acid (GO:0009751)

Up-regulated genes: 9

ITAG	*log2FC*	*q-value*	*Functional Description*
Solyc10g008930.1.1	5,415037799	1,99E-09	Thioredoxin superfamily protein
Solyc09g006010.2.1	1,606710467	0,0161833	pathogenesis-related gene 1
Solyc03g044710.2.1	3,15063541	0,0003967	phospholipase A 2A
Solyc12g009770.1.1	1,685177219	0,0496567	receptor like protein 33
Solyc09g074270.2.1	2,0162989	0,0409224	alpha/beta-Hydrolases superfamily protein
Solyc03g095770.2.1	1,483341855	2,15E-05	WRKY DNA-binding protein 70
Solyc08g062930.1.1	1,371314257	0,0409224	calmodulin-binding family protein
Solyc12g008960.1.1	2,706815715	0,0132704	calmodulin-binding family protein
Solyc06g073080.2.1	4,773135868	0,0138776	2-oxoglutarate (2OG) and Fe(II)-dependent oxygenase superfamily protein

Down-regulated genes: 6

ITAG	*log2FC*	*q-value*	*Functional Description*
Solyc07g044860.2.1	-1,77385935	0,0228224	photosystem II subunit P-1
Solyc04g076280.2.1	-1,48304437	0,0001254	K-box region and MADS-box transcription factor family protein
Solyc06g066370.2.1	-1,15176408	0,0030149	WRKY DNA-binding protein 33
Solyc04g079240.2.1	-2,21696865	0,0155383	phospholipase A 2A
Solyc02g065400.2.1	-1,3369428	0,0231291	photosystem II subunit O-2
Solyc11g072540.1.1	-1,23909901	0,0056528	Transducin/WD40 repeat-like superfamily protein

Defense response to pathogen (GO:0042742 + GO:0050832)

Up-regulated genes: 36

ITAG	*log2FC*	*q-value*	*Functional Description*
Solyc01g088400.2.1	2,557050285	2,19E-08	Fatty acid hydroxylase superfamily
Solyc10g008930.1.1	5,415037799	1,99E-09	Thioredoxin superfamily protein
Solyc08g082850.2.1	1,30014893	0,001843	general control non-repressible 3
Solyc11g022590.1.1	4,206634007	3,18E-30	kunitz trypsin inhibitor 1
Solyc09g006010.2.1	1,606710467	0,0161833	pathogenesis-related gene 1
Solyc03g044710.2.1	3,15063541	0,0003967	phospholipase A 2A
Solyc03g122140.2.1	2,157982473	0,0248087	Aldolase-type TIM barrel family protein
Solyc01g006320.2.1	2,558595875	0,0147839	Late embryogenesis abundant (LEA) hydroxyproline-rich glycoprotein family
Solyc06g074030.1.1	2,074839924	7,25E-05	Polynucleotidyl transferase, ribonuclease H-like superfamily protein
Solyc06g084090.2.1	4,159211076	0,0020422	histone H2A 11
Solyc03g095770.2.1	1,483341855	2,15E-05	WRKY DNA-binding protein 70
Solyc09g092580.2.1	6,390790185	7,31E-05	cytochrome P450, family 83, subfamily B, polypeptide 1
Solyc12g096520.1.1	2,734468692	0,0130991	HOPW1-1-interacting 2
Solyc08g062930.1.1	1,371314257	0,0409224	calmodulin-binding family protein
Solyc12g008960.1.1	2,706815715	0,0132704	calmodulin-binding family protein
Solyc07g066470.2.1	2,115154845	0,0007068	hydroxymethylbilane synthase
Solyc06g073080.2.1	4,773135868	0,0138776	2-oxoglutarate (2OG) and Fe(II)-dependent oxygenase superfamily protein
Solyc04g014900.2.1	2,261184884	0,0002135	Leucine-rich receptor-like protein kinase family protein
Solyc01g088400.2.1	2,557050285	2,19E-08	Fatty acid hydroxylase superfamily
Solyc10g008930.1.1	5,415037799	1,99E-09	Thioredoxin superfamily protein
Solyc09g006010.2.1	1,606710467	0,0161833	pathogenesis-related gene 1
Solyc03g044710.2.1	3,15063541	0,0003967	phospholipase A 2A

Solyc07g008590.1.1	1,572643749	0,0054723	disease resistance family protein / LRR family protein
Solyc07g008620.1.1	2,208276596	2,04E-06	disease resistance family protein / LRR family protein
Solyc09g083440.2.1	1,655610795	0,0032739	Serine protease inhibitor, potato inhibitor I-type family protein
Solyc09g084480.2.1	3,754166988	2,17E-28	Serine protease inhibitor, potato inhibitor I-type family protein
Solyc05g055540.1.1	1,917007619	0,0497139	Major facilitator superfamily protein
Solyc10g055810.1.1	1,398374292	1,58E-08	basic chitinase
Solyc10g068350.1.1	1,594933688	0,0028495	basic chitinase
Solyc10g074460.1.1	2,699915542	0,0002217	basic chitinase
Solyc06g035960.2.1	1,79310431	0,0107374	AMP-dependent synthetase and ligase family protein
Solyc03g095770.2.1	1,483341855	2,15E-05	WRKY DNA-binding protein 70
Solyc09g074270.2.1	2,0162989	0,0409224	alpha/beta-Hydrolases superfamily protein
Solyc08g062930.1.1	1,371314257	0,0409224	calmodulin-binding family protein
Solyc12g008960.1.1	2,706815715	0,0132704	calmodulin-binding family protein
Solyc06g073080.2.1	4,773135868	0,0138776	2-oxoglutarate (2OG) and Fe(II)-dependent oxygenase superfamily protein

Down-regulated: 14

ITAG	***log2FC***	***q-value***	***Functional Description***
Solyc07g044860.2.1	-1,77385935	0,0228224	photosystem II subunit P-1
Solyc12g011330.2.1	-1,27585231	0,0467073	Signal transduction histidine kinase, hybrid-type, ethylene sensor
Solyc04g079240.2.1	-2,21696865	0,0155383	phospholipase A 2A
Solyc06g066370.2.1	-1,15176408	0,0030149	WRKY DNA-binding protein 33
Solyc01g099780.2.1	-2,06643518	0,0001809	translationally controlled tumor protein
Solyc02g065400.2.1	-1,3369428	0,0231291	photosystem II subunit O-2
Solyc04g012160.2.1	-1,3460686	0,0008015	Protein kinase superfamily protein
Solyc04g080960.2.1	-1,6180677	1,01E-08	Papain family cysteine protease
Solyc04g078140.2.1	-1,16116624	0,0130819	cytochrome B5 isoform D

Solyc03g115820.2.1	-1,34281829	1,17E-05	D-ribulose-5-phosphate-3-epimerase
Solyc07g044860.2.1	-1,77385935	0,0228224	photosystem II subunit P-1
Solyc04g079240.2.1	-2,21696865	0,0155383	phospholipase A 2A
Solyc06g066370.2.1	-1,15176408	0,0030149	WRKY DNA-binding protein 33
Solyc08g079230.1.1	-2,8867094	0,0017567	Bifunctional inhibitor/lipid-transfer protein/seed storage 2S albumin superfamily protein

Defense response to virus (GO:0051607)

Up-regulated genes: 2

ITAG	*log2FC*	*q-value*	*Functional Description*
Solyc10g006200.2.1	1,587426078	0,029986	dicer-like 1
Solyc03g044710.2.1	3,15063541	0,0003967	phospholipase A 2A

Total number of Up-regulated genes: 1115
Total number of the group: 115
Hipergeometric probabilist for gene enrichment: 0.887503

Down-regulated genes: 1

ITAG	*log2FC*	*q-value*	*Functional Description*
Solyc04g079240.2.1	-2,21696865	0,0155383	phospholipase A 2A

Total number of Up-regulated genes: 758
Total number of the group: 115
Hipergeometric probabilist for gene enrichment: 0.921305

Virus induced gene silencing (GO:0009616)

Up-regulated: 6

ITAG	*log2FC*	*q-value*	*Functional Description*
Solyc10g006200.2.1	1,587426078	0,029986	dicer-like 1
Solyc06g065450.2.1	2,753475097	3,31E-06	forkhead-associated (FHA) domain-containing protein
Solyc08g082040.2.1	2,067544001	0,0267454	Protein of unknown function (DUF3133)
Solyc04g015030.2.1	3,168099422	3,03E-18	farnesylated protein 3
Solyc04g076850.2.1	0,591435042	0,00391	indole-3-acetic acid inducible 9
Solyc04g076850.2.1	0,591435042	0,00391	indole-3-acetic acid inducible 9

Down-regulated: 1

ITAG	*log2FC*	*q-value*	*Functional Description*
Solyc07g062300.2.1	-2,53317561	0,0247331	NHL domain-containing protein

Resistance protein-related genes

Up-regulated: 7

ITAG	*log2FC*	*q-value*	*Functional Description*
Solyc02g032050.1.1	1,620578758	0,0407565	Disease resistance-responsive (dirigent-like protein) family protein
Solyc05g042090.1.1	4,907459511	5,24E-06	NB-ARC domain-containing disease resistance protein
Solyc07g008590.1.1	1,572643749	0,0054723	disease resistance family protein / LRR family protein
Solyc07g008620.1.1	2,208276596	2,04E-06	disease resistance family protein / LRR family protein
Solyc08g081780.1.1	1,470947445	0,0028675	Disease resistance-responsive (dirigent-like protein) family protein
Solyc12g044190.1.1	3,942547883	1,63E-12	LRR and NB-ARC domains-containing disease resistance protein
Solyc12g097010.1.1	1,982314928	0,0010878	disease resistance protein (TIR-NBS-LRR class), putative

Total number of Up-regulated genes: 1115

Total number of the group: 450
Hipergeometric probabilist for gene enrichment: 0.990446

Down-regulated: 2

ITAG	***log2FC***	***q-value***	***Functional Description***
Solyc05g054340.2.1	-1,75206983	0,0001123	NB-ARC domain-containing disease resistance protein
Solyc07g061940.2.1	-1,11979531	0,0042344	chlorsulfuron/imidazolinone resistant 1

Total number of Up-regulated genes: 758
Total number of the group: 450
Hipergeometric probabilist for gene enrichment: 0.999491

Table S4. Functional overlap DE defense-related genes up-regulated in CLN2777 (resistant) by 3, 5, and 7 dpi and in T474D infected by 10 dpi

ITAG	LOG2FC	Q-VALUE	GO	DESCRIPTION	FUNCTIONAL TERM
Solyc12g006910.1.1	1,437488357	0,000256891		cadmium tolerance 1	cadmium tolerance
Solyc06g065570.2.1	1,099197794	0,003977388	GO:0008080,GO:0016747, GO:0008152	Acyl-CoA N-acyltransferases (NAT) superfamily protein	acyltransferase
Solyc08g078120.1.1	1,119007505	0,012176808		Acyl-CoA N-acyltransferase with RING/FYVE/PHD-type zinc finger protein	acyltransferase
Solyc09g008520.2.1	1,292201253	3,46E-02	GO:0005515	Acyl-CoA N-acyltransferase with RING/FYVE/PHD-type zinc finger domain	acyltransferase
Solyc11g017250.1.1	1,751107855	0,002179764	GO:0016746,GO:0008152, GO:0008415	2-oxoacid dehydrogenases acyltransferase family protein	acyltransferase
Solyc06g074030.1.1	2,074839924	7,25E-05	GO:0005634	Polynucleotidyl transferase, ribonuclease H-like superfamily protein	ribonuclease
Solyc04g011430.2.1	2,132076671	0,034795837	GO:0016881	ubiquitin carrier protein 7	ubiquitin
Solyc09g017980.1.1	2,641368759	0,038145499	GO:0004221,GO:0006511	ubiquitin-specific protease 20	ubiquitin
Solyc10g081500.1.1	1,288849101	9,39E-05	GO:0005515,GO:0005198	protein kinases;ubiquitin-protein ligases	ubiquitin
Solyc12g099030.1.1	0,891122674	0,010381067	GO:0005515,GO:0003735, GO:0006412,GO:0005622, GO:0005840	ubiquitin 6	ubiquitin
Solyc11g013110.1.1	1,451913705	0,001383335	GO:0016491,GO:0016706, GO:0055114	flavonol synthase 1	flavonol synthase 1
Solyc02g088830.2.1	1,546356738	0,022099189		hydroxyproline-rich glycoprotein family protein	hydroxyproline-rich glycoprotein

Solyc10g078160.1.1	1,187143132	0,048966799		hydroxyproline-rich glycoprotein family protein	hydroxyproline-rich glycoprotein
Solyc08g080620.1.1	3,108395737	1,23201E-09		osmotin 34	osmotin
Solyc05g006730.2.1	2,355051524	0,018046248	GO:0005515	Glutathione S-transferase family protein	Glutathione S-transferase
Solyc03g115120.1.1	2,264334786	1,91E-02	GO:0031072	DNAJ heat shock N-terminal domain-containing protein	heat shock
c04g005900.2.1	1,560832185	0,040388262	GO:0005515	F-box/RNI-like superfamily protein	F-box